SEPTEMBER 1980
ENVIRONMENTAL SCIENCE & TECHNOLOGY
ES&T

Indoor air pollution

1023

“ERT IS OUR FASTEST, SUREST ROUTE TO THE PERMITS WE NEED.”

Arrowsmith knows that, as the complexity of environmental permitting continues to increase, it is essential to work with the people who know the regulations from the ground up and how to keep your costs down. ERT is a step ahead on all of the changing regulations with the methods and technology to take you through the complex permitting process faster and at lower *real* cost. At the beginning of each project, ERT takes an in-depth look at your requirements to identify your specific problems and to develop the most direct route to solve them, eliminating costly false starts or questionable data which could mean disruptive delays. Whether your environmental problem is air, water, toxic substances, solid waste, or new source permitting, ERT is the firm to call for every manager who recognizes the value of doing the job right the first time. For free literature on environmental permitting or for immediate assistance with your specific environmental problems, call or write E. Reston, ERT, 696 Virginia Road, Concord, MA 01742, (617) 369-8910, Ext. 316.

ERT is the nation’s leading full-service environmental consulting firm, with offices in Atlanta, Boston, Chicago, Ft. Collins, Houston, Los Angeles, Pittsburgh, and Washington, D.C.

ERT *a step ahead*

CIRCLE 6 ON READER SERVICE CARD

ห้องสมุด กรมวิทยาศาสตร์บริการ

ES&T

CONTENTS

Volume 14, Number 9, September 1980

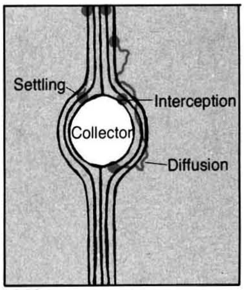

1052

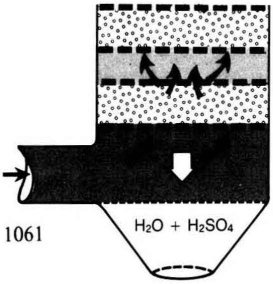

1061

1067

OUTLOOK

1023
Indoor air quality. Pollutant concentrations are often higher indoors than out, raising questions about personal exposures and past epidemiological studies.

1028
Incinerator processes. Scientists look at higher-temperature effects on hazardous wastes.

1030
Groundwater strategies. Alternatives for protection, contaminant containment, and possible cleanup methods.

1037
Adsorption on carbon. In an interview, Dr. Georges Belfort discusses interactions between solute, solvent, and sorbent.

REGULATORY ALERT

1051
Benzene regulations. ERT legal counsel Michael Deland, Esq., discusses the Supreme Court invalidation of OSHA standards.

FEATURES

1052
Small particles in water. Charles R. O'Melia, the Johns Hopkins University, Baltimore, Md.

1061
Trace metal catalysis. Michael R. Hoffman, California Institute of Technology, Pasadena, Calif.

1067
Burning coal cleaner with gas. Benjamin Schlesinger, American Gas Association, Arlington, Va.

RESEARCH

1089
Removal and recovery of organic pollutants from aquatic environment. 2. Removal and recovery of dodecylbenzenesulfonate from aqueous solution by cross-linked poly(*N*-benzyl-4-vinylpyridinium halide). Nariyoshi Kawabata* and Toshio Morigaki

A BVP resin was found to have an excellent capacity for DBS adsorption and was scarcely affected by the presence of inorganic salts.

1094
Resistance to photochemical decomposition of polycyclic aromatic hydrocarbons vapor-adsorbed on coal fly ash. W. A. Korfmacher, E. L. Wehry, G. Mamantov, and D. F. S. Natusch*

Results suggest that the photosensitivity of an adsorbed polynuclear hydrocarbon is strongly dependent upon the nature of the adsorbing surface.

1099
Covalent binding of aromatic amines to humates. 1. Reactions with carbonyls and quinones. George E. Parris

Variables affecting rate and extent of reactions of aromatic amines and humates are discussed in terms of possible modes of adduct formation.

1106
Sorption of iodide on copper. Zia Haq, G. Michael Bancroft*, William S. Fyfe, Gordon Bird, and Vincent J. Lopata

The kinetics, mechanism, and thermodynamics of iodide sorption on copper are elucidated with the use of surface-sensitive probes.

Environmental Science & Technology

Published monthly by the American Chemical Society from 20th and Northampton Sts., Easton, Pa. 18042. Executive Offices: Editorial Headquarters, 1155 16th St., N.W., Washington, D.C. 20036. Advertising office: 25 Sylvan Road South, Westport, Conn. 06880. Second-class postage paid at Washington, D.C., and at additional mailing offices.

SUBSCRIPTION PRICES 1980: Members, 1 year $16.00, 3 years $48.00. Nonmember personal, 1 year $20.00; 3 years $48.00. Institutions, 1 year $64.00. Foreign postage. $7.00 per year. Air freight rates per year available on request. Single issue prices: current year $5.50; prior year $6.00. Back volume price: $68.00. Foreign postage additional. **Phone orders** can be placed for printed, microfiche, and microfilm editions by calling **toll free,** the Sales Office at (1) (800) 424-6747 from anywhere in the continental U.S. Can use Visa or Master Charge. Mail orders c/o ACS Washington address. Claims for missing numbers will not be allowed if loss was due to failure of notice of change of address to be received in the time specified; if claim is dated (a) North America, more than 90 days beyond issue date; (b) all other foreign, more than one year beyond issue date; or if the reason given is "missing from files." Hard copy claims are handled at the ACS Columbus address.

SUBSCRIPTION SERVICE: Send all new and renewal subscriptions with payment to: Office of the Controller, 1155 16th St., N.W., Washington, D.C. 20036. All correspondence and telephone calls regarding changes of address, claims for missing issues, subscription service, the status of records and accounts, air mail and air freight rates should be directed to: Manager, Membership and Subscription Services, American Chemical Society, P.O. Box 3337, Columbus, Ohio 43210. Telephone (614) 421-7230. On changes of address, include both old and new address with ZIP code accompanied by a recent mailing label. Allow six weeks for change to become effective.

MICROFILM AND MICROFICHE. Inquiries re: servicing, orders, products, contact Microforms, ACS Washington, or call (202) 872-4554.

Servicing of orders for printed editions of single issues or back volumes should be directed to Special Issues Sales at the ACS Washington address or call (202) 872-4365.

Credits: 1017, *ES&T*'s Julian Josephson; 1018, UPI

Cover: Illustration by Ger Quinn

ESTHAG 14(9) 1013-1150 (1980)
ISSN 0013-936X

1111
Elemental distribution in coal fly ash particles. Lee D. Hansen* and Gerald L. Fisher

Methods are developed for determining quantitative relative concentrations of elements in the aluminosilicate matrix and nonmatrix of coal fly ash.

1118
Sulfate in diesel exhaust. Timothy J. Truex, William R. Pierson*, and Douglas E. McKee

A controlled-condensation sampling procedure is used to determine the chemical speciation of vehicle SO_4^{2-} emissions.

1121
Effects of barium fuel additive and fuel sulfur level on diesel particulate emissions. Timothy J. Truex, William R. Pierson*, Douglas E. McKee, Mordecai Shelef, and Richard E. Baker

Results suggest that a barium fuel additive has a significant effect during the carbonaceous particulate formation process.

1124
The fate of selected herbicides in a terrestrial laboratory microcosm. Jay D. Gile*, James C. Collins, and James W. Gillett

The transport and metabolism of simazine, bromacil, trifluralin, and 2, 4,5-T in a TMC were determined.

1129
Partitioning of No. 2 fuel oil in controlled estuarine ecosystems. Sediments and suspended particulate matter. Patrick J. Gearing*, Juanita N. Gearing, Richard J. Pruell, Terry L. Wade, and James G. Quinn

Results on the interaction of oil hydrocarbons with suspended particulate matter and sediments are presented.

1136
Biogeochemistry of benzanthracene in an enclosed marine ecosystem. Kenneth R. Hinga*, Michael E. Q. Pilson, Richard F. Lee, John W. Farrington, Kjell Tjessem, and Alan C. Davis

A radiotracer label is used to monitor the fate of benz(*a*)anthracene and its metabolites in a closed marine ecosystem.

NOTES

1143
Correlation of microbial degradation rates with chemical structure. N. Lee Wolfe*, Doris F. Paris, William C. Steen, and George L. Baughman

Structure reactivity relationships are established for the microbial degradation of selected organic compounds.

1145
Mutagenicity of textile dyes. Mendel Friedman*, Martin J. Diamond, and James T. MacGregor

Testing of 28 textile dyes raises significant questions about the possible mutagenic hazards associated with dye production and use.

1147
Aromatic amines in and near the Buffalo River. Charles R. Nelson and Ronald A. Hites*

Results suggest that leaching of waste chemicals from a dye manufacturing plant may be partially responsible for tumors observed in fish.

CORRESPONDENCE

1149
Measurement of gaseous hydrogen chloride emissions from municipal refuse energy recovery systems in the United States. Edward J. Kaplin

* To whom correspondence should be addressed.

This issue contains no papers for which there is supplementary material in microform.

DEPARTMENTS

Published by the
AMERICAN CHEMICAL SOCIETY
1155 16th Street, N.W.
Washington, D.C. 20036
(202) 872-4600

Please send *research* manuscripts to Manuscript Reviewing, *feature* manuscripts to Managing Editor.

For author's guide and editorial policy, see the January 1980 issue, page 45, or write Katherine I. Biggs, Manuscript Reviewing Office ES&T. A sample copyright transfer form, which may be copied, appears on page 102 of the January 1980 issue.

Environmental concerns? We can help you comply— from planning to filing.

Whether you have one or many environmental concerns, we can help you. We're the Rockwell International Environmental Monitoring & Services Center (EMSC), a team of professionals addressing the full spectrum of environmental requirements. We have offices coast to coast, and are familiar with the national and regional issues that often influence your environmental programs.

During the many years the EMSC has been in business, we've built a reputation for service backed by expertise. Experience is our most important asset — and your assurance of thoroughness when we assist you in the planning, analysis, or implementation of your program. Since we understand not only the environmental, but the fiscal constraints of a project as well, we can act as an effective arm of your organization.

Whether yours is a current or future problem, whether you have a requirement for planning a new facility or for a generalized study, we can help. We are prepared to stand by you with proof that the requirements of cognizant agencies are met.

For full information on how we can service your needs, contact Dr. Bob Yelin, Environmental Monitoring & Services Center, Environmental & Energy Systems Division, Rockwell International, 2421 West Hillcrest Drive, Newbury Park, CA 91320. Phone: (805) 498-6771.

Rockwell International

...where science gets down to business

CIRCLE 11 ON READER SERVICE CARD

ES&T CURRENTS

WASHINGTON

Generators of hazardous wastes have been named for the first time in a government suit. The defendants are charged with having contributed wastes containing chlorinated hydrocarbons and heavy metals to 2 dump sites near Baton Rouge, LA. Wastes stored in pits at the 55-acre Brooklawn site, still in use, have been deliberately pumped into Bayou Baton Rouge, according to the EPA. Flooding and leaks have also led to discharges. At the second site, a protective covering intended to prevent releases has eroded since the site was closed in 1974. The government claims that the defendants "knew or should have known about the questionable and dangerous disposal practices," and is seeking fines of $10 000 and an order to clean up the sites. In the past the EPA has gone after waste haulers and site operators only. Named in the action were Dow Chemical, Ethyl, Uniroyal, Shell Chemical, Exxon Chemical, Allied Chemical, Rubicon Chemical, Copolymer Rubber and Chemical, American Hoechst, and U.S.S. Chemical.

The proposal to list ammonia as a toxic pollutant may be withdrawn, the EPA now says. Listing would have the effect of blocking waivers to the "best available control technology" requirement on dischargers; without listing, waivers may be granted for economic reasons or if local water quality already meets EPA requirements. Over 200 comments have been filed on the proposal, and almost all have been critical—though according to the EPA, most have also misunderstood the implications of listing. The proposal is being reviewed; a final decision is expected by the beginning of this month.

The 1981 CO standard for automobiles should be reconsidered, according to a National Academy of Sciences panel. The 1977 amendments to the Clean Air Act require a limit of 3.4 g/mi of CO by 1981. But the panel found that reducing emissions to that level from the 1980 limit of 7.0 gpm would result in a 2% loss in fuel efficiency and would cause increased stalling; furthermore, the panel cited data from the California Air Resources Board indicating that the 7-gpm standard would be sufficient to result in compliance with the ambient air standard for CO. The EPA should grant waivers of up to 2 years to smaller manufacturers, the panel also concluded, since they rely heavily on suppliers for parts and are experiencing delays.

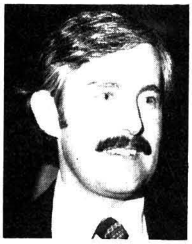

EPA's Gage

The EPA plans to eliminate in-house publication of its research papers. At the July meeting of the agency's Science Advisory Board, Assistant Administrator Stephen J. Gage reported that 47 linear feet of this "gray literature" was published last year. The EPA will now stress publication of its research results in the open, peer-reviewed literature.

The design of 7 solar cogeneration projects will be supported by DOE. The selected proposals will study the use of solar-heated steam or air to generate electricity, with the waste heat going to industrial processes, such as sugar milling and copper smelting, or to space heating and cooling. Cogeneration offers higher efficiency than single-use systems and can thus reduce the amount and cost of solar collection equipment. DOE expects to share the costs of detailed design and construction in a later phase of the program; completion dates in 1985–86 are anticipated.

A major study of regional air pollution has just been completed by the EPA, 6 other U.S. agencies, and the Canadian government. The month-long, $2-million project tracked the formation, movement, and chemical transformation of air pollution plumes in the Northeast with instrumented aircraft, balloons, and ground measurements. Pollutants measured in the "Persistent Elevated Pollution Episodes" study included ozone, aerosols, sulfates, and nitrates; meteorological factors, such as turbulence, were also monitored. "Although we know a great deal about the formation of aerosol sulfates during pollution episodes," said Dr. Francis Pooler of the EPA's Environmental Sciences Research Laboratory, "we don't know much about the formation of other compounds that go into atmospheric aerosols. We hope that this summer's study will answer a lot of questions in that area."

Advanced wastewater treatment may be too costly and of too little effect to be justified, says a General Accounting Office report. Noting that states do not generally consider costs in setting water quality standards, and that standards are often based on questionable scientific data, the GAO concludes that "a number of costly advanced waste treatment plants may have little effect on water quality." The report recommends amending the Clean Water Act to require some consideration of costs and benefits.

STATES

Volcanic ash from Mt. St. Helens poses no health threat to the general public, the Washington State De-

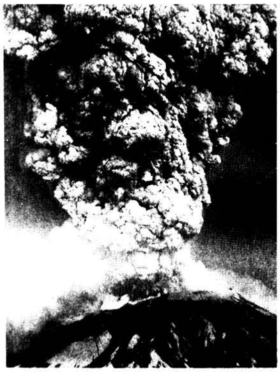

Mt. St. Helens

partment of Labor and Industries has concluded. But loggers and agricultural workers may be exposed to high levels of the ash, which is resuspended in the air when trees are felled and when ash-covered fields are harvested. The ash contains 3–10% crystalline silica, and the DLI is concerned that exposed workers may face increased risks of contracting silicosis.

Disposal of coal ash will be studied in New York, announced James L. Larocca, chairman of the state's Energy Research and Development Authority. "In order for the state and its utilities to further plan for conversion to coal, we must continue to gather information on the best options for disposal of wastes generated by coal utilization," Larocca said in announcing the 8-month, $71 000 project. Options being considered include disposal in ponds and quarries, and forming the ash into blocks which would be used to create artificial ocean reefs. By 1994, the state's utilities are expected to use coal for 45% of their fuel needs; this will mean an annual production of 4 million tons of ash.

Illinois reports improvement in O_3 and CO, but deterioration in SO_2, NO_2, and particle levels during 1979. Ozone levels were in particular much improved over the previous 3 years; none of the 43 stations in the state's air monitoring network registered levels above 0.2 ppm. On the other hand, particles and SO_2, which had been decreasing in previous years, suffered a reverse. The statewide average particle concentration was $74\ \mu g/m^3$, up from $70\ \mu g/m^3$ in 1978; SO_2 was 0.012 ppm, up from 0.010 ppm.

The New England states have agreed to a uniform manifest for hazardous wastes. Under the Resource Conservation and Recovery Act, due to take effect Nov. 19, states must require generators, transporters, and disposers of hazardous wastes to keep track of shipments through a system of manifests. The uniform system will simplify the procedure for shipments that cross state lines. The EPA's Region I has meanwhile indicated that only Rhode Island and Vermont among the 6 will have their complete state hazardous waste plans approved by the Nov. 19 effective date. Connecticut's plan will likely be approved early next year, while Massachusetts's may be 2 years away. The EPA will administer the RCRA rules in states whose plans have not been approved.

Washington state has purchased a waste dump site on the Hanford Reservation, a federal area currently used for disposal of radioactive waste. The 640-acre portion bought by the state will be used for hazardous chemical waste only. "Washington will be one of the first states in the nation to have a central location for the disposal and treatment of hazardous chemical wastes generated by our state's industries," said Governor Dixy Lee Ray. "Acquisition of this site will help prevent disposal of these wastes haphazardly." The state had been relying on a dump site in Oregon.

RESEARCH AWARDS

EPA scientists received Scientific and Technological Achievement Awards from the agency for their outstanding contributions to scientific research supporting the nation's efforts to control pollution. Scientists from the Environmental Research Center at Research Triangle Park, N.C., who received monetary awards include: **Dr. Basil Dimitriades,** for formulating procedures for analyzing ozone, hydrocarbons, and nitrogen oxide relationship; **Mr. Robert K. Stevens** and **Dr. Thomas G. Dzubay,** who shared a $5000 award for documentation of advanced procedures for sampling and analyzing particulate pollutants; **Mr. Ronald K. Patterson** and **Dr. Jack Wagman,** who shared a $2500 award for research on causes of reduced visibility in urban areas; **James D. Mulik** for ion chromatography research; **Mr. Joseph P. F. Lambert** and **Mr. Frank W. Wilshire,** who shared a $500 award for developing a method for the direct analysis of particulate matter collected routinely on glass-fiber filters. Award selections were made by the EPA Science Advisory Board, a group of more than 70 outside experts. The board was established under congressional mandate to counsel the agency on scientific and technical aspects of environmental issues.

MONITORING

At what rate do airborne lead and sulfates deposit to crops? To try to answer that question, Herman Sievering of Governors State University (IL) took measurements at each of 4 levels of a 1000-ft tower at the Boulder (CO) Atmospheric Observatory. Each reading was 1 min long, and the 1000-ft round trip in an open-cage elevator had to be finished in 20 min. The readings measured minute lead and sulfate particles. Sievering said that once the crop deposition rate is known, it can be combined with the concentration of pollutant particles at any location to ascertain the quantity being absorbed by crops.

TECHNOLOGY

One of the nuclear waste disposal research tasks at Argonne National Laboratory is to find means of incorporating high-level wastes into crystalline ceramics by processes usable on a production scale. Another goal is to determine the mineral composition that can best withstand temperatures as high as 575 °F, with pressures to 5000 psi during immersion in groundwater ranging from pure to brine. Other projects involve characterizing the molecular structure of the ceramic material, with and without nuclear wastes inside, and the material's ability to withstand internal radiation damage from radionuclides.

A means of improving the cost-effectiveness of fluidized-bed coal combustors is another effort at Argonne. The key is to improve the performance of the limestone or dolomite "stones" that react with SO_x from coal burning. Normally, 300–600 lb of "stones" are needed per ton of coal to meet EPA emission standards. Also, about 20–30% of the stones are actually reacted.

Calibration Gas Mixtures

Three Decisions Have to Be Made

DECISION NO. 1
THE RIGHT APPROACH

Even a simple listing of mixture components can require decisions. Mixture accuracy, component compatibility, background impurities and pressure levels are some of the factors to be considered. Matheson has the experienced personnel at each location to provide the right approach for your application.

DECISION NO. 2
THE RIGHT CYLINDER

To many, this means only the material of construction or internal cylinder treatment. At Matheson, this question means much more. Safety, pressure-volume relationship, chemical properties of the components, storage and portability, in addition to material of construction and internal cylinder treatment are all inter-related and vary with your requirements—Matheson's 30 years of experience in gas mixtures will provide the right cylinder decision.

DECISION NO. 3
THE RIGHT REGULATOR

Matheson has more than 100 different pressure regulators from which to choose exactly the right regulator for your mixture. The selection of the wrong regulator can change your mixture by adding impurities and/or reducing component concentrations. Our experience takes the guess work out of regulator decisions.

When you need a gas mixture—the decision is simple—let Matheson be your supplier.

Matheson has prepared a brochure on mixtures and the factors affecting them. It's valuable information for instrument users. Use the Reader Service No. for your free copy.

Matheson®

Lyndhurst, N.J. 07071
Whitby, Ontario, Canada L1N 5R9
B 2431 Oevel, Belgium

Manufactured and Distributed Worldwide

CIRCLE 8 ON READER SERVICE CARD

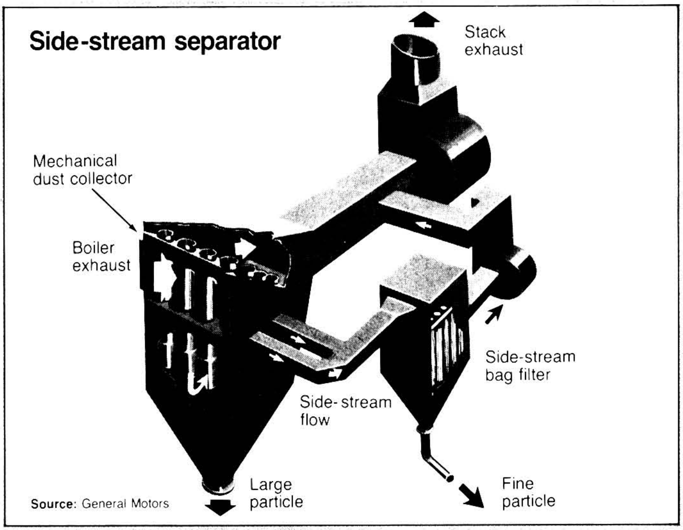

Side-stream separator

Source: General Motors

However, sprinkling the used stones with water converts calcium sulfate to hydroxide; subsequent drying produces calcium oxide and also makes more stone surface accessible to SO_2. The stones become sufficiently porous so that as much as 86% of the calcium can be reacted with coal SO_2.

Perhaps earth materials can attenuate polybrominated biphenyl (PBB) and hexachlorobenzene (HCB) concentrations through absorption and immobilization, if they are in aqueous solution. However, when PBB and HCB were dissolved in organic solvents, no measurable adsorption by soils occurred, according to R. A. Griffin and S. F. J. Chou of the Illinois Institute of Natural Resources. Even in aqueous solutions, HCB showed more adsorbability than did PBB. Also, organic solvents caused desorption of PBB and HCB from soil materials. In all solvents, water or organic, PBB and HCB were strongly adsorbed by carbonaceous "Ambersorb XE-348" adsorbent. But they were found to resist biodegradation.

Particulate emissions from coal-fired boilers can be further reduced through a side-stream separator developed by General Motors' Fisher Body Division (Warren, MI). Particulate control is boosted by up to 50%, according to Fisher Body engineers. In conventional particle collectors, fine particles, often higher up in the system, could escape. However, in this system, the fines are drawn off through side ducts and collected in relatively small filter bags. Blasts of compressed air force the collected fines into an accumulation bin.

INDUSTRY

EPA's "bubble" policy restrictions are being challenged in court by the Chemical Manufacturers Association (Washington, DC). CMA supports the concept that places a whole plant beneath an imaginary "bubble" and calls for *total* emissions to be kept to a certain required level. However, EPA has refused to delegate to New Jersey the authority to apply the "bubble" concept, insisting, instead, that the state obtain EPA approval for each individual use of the concept. CMA argues that EPA has no statutory authority to refuse to allow a state to implement its "bubble" plan as long as minimum requirements of the law are met.

The fight to restore funding cuts from the solar budget of fiscal year 1981 is being carried on by the Solar Energy Industries Association (Washington, DC). SEIA believes that funds should be restored for certain programs designed to move solar energy "off the drawing boards and into public use." Other restorations called for involving the Barstow, CA, "power-tower" project, wind conversion, ocean thermal systems, photovoltaics, and international programs. Failure to restore the funds could cause project delays and force the U.S. to pull out of certain international programs, SEIA warns.

Development of a proprietary coal desulfurization process is the aim of a 2-year, $420 000 contract awarded by the DOE to Research-Cottrell, Inc. and Rutgers University. The idea is to advance a process patented by Research-Cottrell that converts the sulfur in coal to soluble forms by selective oxidation. These soluble materials are then removed, while the coal's heating value is unaffected. Rutgers will perform the work under the direction of Research-Cottrell.

A recommended general industrial method to convert cellulosic wastes to alcohols and fuel was given to *ES&T* by Leonard Bruno, General Manager of American Enzyme Corp. (Brown Deer, WI). Among steps Bruno listed were maceration to the smallest possible size, and a 30% slurry in water, boiled, then cooled and digested by cellulase enzyme. Next comes addition of amyloglocosidase enzyme at 190–200 °F. Resulting hexoses and pentoses are fermented with *Saccharomyces* and *Torlua.* The final mash is distilled in a benzene azeotrope vapor as close as possible to 164.3 °F to get the purest, highest-proof alcohol for use as fuel or feedstock, Bruno said.

AWWA President Shine

Three changes in the Safe Drinking Water Act (SDWA) are advocated by the American Water Works Association (Denver, CO). AWWA President Donald Shine called for passage of House Resolution 4509, which would require contaminant regulation only when substances "pose an unreasonable risk" to human health. The resolution also would require EPA to set performance standards, rather than specify treatment techniques, and would make EPA justify costs with projected benefits of regulations. Shine said that so amending the SDWA would largely resolve problems AWWA has with the act.

Water Treatability. Come to the experts the experts come to.

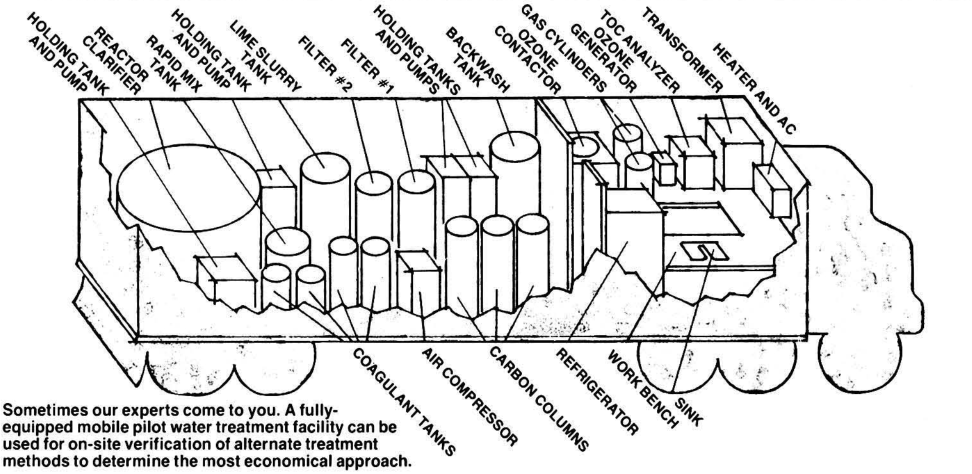

Sometimes our experts come to you. A fully-equipped mobile pilot water treatment facility can be used for on-site verification of alternate treatment methods to determine the most economical approach.

Some of the most knowledgeable people in the field — including those who make the rules — consult with our Environmental Services Department for answers about industrial waste water pollutants and treatability.

That's because Monsanto has "written the book" on the analysis and treatment of waste waters through experimentation and experience. As a result, we have outstanding personnel and facilities to provide current, cost-effective solutions to water pollution problems.

In our centrally-located laboratories (where analysis is a basic function) we can analyze site-collected samples, perform a preliminary treatability study, and interpret results to select process steps promising the most cost-effective treatment system. We then can use our mobile pilot treatment system on-site to verify that process selection. Finally, we can recommend or assist with program implementation. And since we manufacture no products involved in the recommended process, we can be totally impartial in that recommendation.

To solve your water pollution problems efficiently and economically, come to the experts the experts come to. Monsanto Research Corporation. For typically fast response, clip and mail the coupon below. Today.

For more information about Water Treatability services or other environmental problem solving, mail coupon to:
Monsanto Research Corporation, Environmental Services, Dept. ES-9,
Station B, Box 8, Dayton, Ohio 45407. Phone 513/268-3411

Name________________ Title__________

Company____________ Address____________

City & State________________ Zip______

Monsanto

Monsanto Research Corporation

CIRCLE 17 ON READER SERVICE CARD

Find, identify, measure, count and record pollutants with Zeiss.

For all microscope techniques illustrated below and for many others used in pollution analysis Zeiss has the instrument you need.

Fully automatic camera microscopes. Photomicroscope III with automatic flash and data recording system for 35 mm photomicrography; Ultraphot IIIb for both fully automatic photomicrography and photomacrography, 35 mm and 4x5″ formats.

Inverted camera microscope ICM 405. Fully automatic, inverted camera microscope for transmitted and reflected light with integrated 35 mm and 4x5″ cameras. Ultra-stable.

Standard and WL microscopes. Exceptional versatility and Zeiss quality optics at competitive prices.

Universal microscope. The most universal microscope for routine and research applications. The automatic attachment camera MC 63 takes 35 mm or 4x5″ (including Polaroid®), and provides highly resolved, exceptionally bright images.

Stereo and dissecting microscopes. High resolution, flat field, long working distances.

Specimen-saving transmission electron microscope EM 109. New high-performance (3.44Å) EM, instantly ready for use. Three unique innovations: outside-the-vacuum camera system, specimen-saving focusing system, ultra-clean vacuum system.

Nationwide Service.

The great name in optics

ZEISS

West Germany

CIRCLE 15 ON READER SERVICE CARD

Carl Zeiss, Inc., 444 5th Avenue, New York, N.Y. 10018 (212) 730-4400. Branches: Atlanta, Boston, Chicago, Houston, Los Angeles, San Francisco, Washington, D.C. In Canada: 45 Valleybrook Drive, Don Mills, Ontario, M3B 2S6. Or call (416) 449-4660.

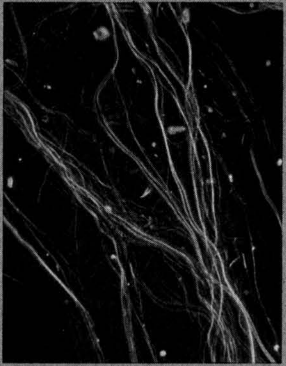

1: Chrysotile asbestos. Phase contrast 220x.

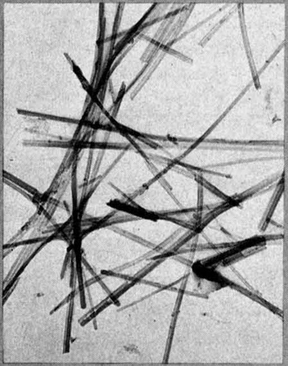

2: Chrysotile asbestos. Electron micrograph 9,500x.

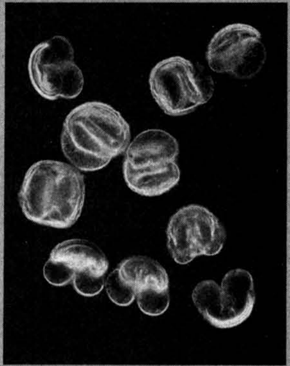

3: Pine pollen. Darkfield 220x.

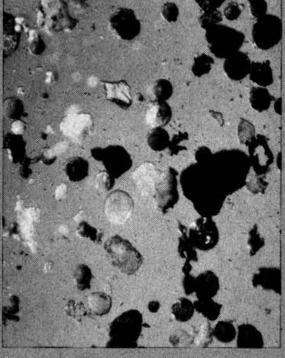

4: Fly ash. Combination of slightly uncrossed polarizers and reflected light 35x.

5: Fly ash. Nomarski Differential Interference Contrast 620x.

6: Detergent residue. Fluorescence 90x.

Photos 1, 2, 3, 4, and 6 by John G. Delly, Senior Research Microscopist, McCrone Research Institute.
Photo 5 by Dr. Robert F. Smith, Director of Biomedical Communications, New York State College of Veterinary Medicine, Cornell University.

ES&T
OUTLOOK

Indoor air pollution

The discovery that pollutant concentrations are often higher indoors than out raises questions about energy conservation and casts into doubt much of the air pollution epidemiology done to date

One day last fall James L. Repace, an EPA employee in the Office of Policy Analysis, carried with him through his day's activities a portable monitor for respirable particles. He recorded the highest concentrations of the day not while walking in downtown Washington, nor while commuting during the rush hour, nor while driving behind a smoky diesel truck, but while cooking dinner that evening in his well-ventilated kitchen. The second highest levels were in the smoking section of the cafeteria at Goddard Space Flight Center, which he visited at lunchtime.

Repace's observations add just one more piece to a puzzle whose outline is already discernable: Indoor concentrations of pollutants often equal or exceed outdoor concentrations—and outdoor concentrations may have little to do with the true exposures to pollution we are all experiencing.

The high indoor particle concentrations Repace recorded are in no way flukes. NO_2, traced to gas combustion in stoves, has been found indoors at twice the outdoor level; CO in offices, garages, and hockey rinks is routinely in excess of the 8-h EPA standard; hydrocarbons from myriad sources appear in high concentrations; and radioactive radon gas, emitted naturally from a variety of building materials—and even by soil—has been detected indoors at levels that exceed ambient by factors of 2–20.

Add to this the fact that an estimated 90% of the average person's time is spent indoors, and indoor pollution emerges as a health threat that seems to make outdoor pollution pale by comparison.

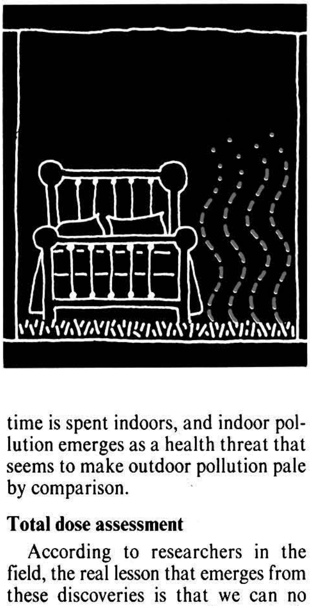

Total dose assessment

According to researchers in the field, the real lesson that emerges from these discoveries is that we can no longer use measurements from a single "microenvironment" as an indicator of the population's exposure to pollution. Ambient concentrations are an uncertain measure of personal exposure, and air quality standards framed in terms of ambient concentrations alone may be woefully inadequate to their mission of protecting public health. The key word, though, is "alone."

"The indoor environment is an entity by itself," said Demetrios Moschandreas of Geomet Technologies, Inc. (Gaithersburg, Md.), who has been involved in indoor air pollution studies since 1976. "But that does not mean ignore outdoor levels. We will miss the essence if we decide that we have spent all this money needlessly [on outdoor pollution] and now we have to spend twice as much on indoors. You have to consider the whole thing. That is why I go back to the total exposure concept—and total exposure is just that, total."

John D. Spengler of the Harvard University School of Public Health made a similar point: "The objective of our measurements is to find the exposure of the population to pollutants. The important thing about indoor pollutant measurements is sorting people out into exposure groups."

Determining when, where, and how exposure occurs is the key not only to limiting exposure, but even to understanding the fundamental effects of pollution correctly. Ultimately, Spengler said, "we're trying to get the right measure to associate with health effects." For example, is it long-term average, short-term average, or peak exposures that are most important? Where can fixed samplers be placed, and how many will be needed, to provide an accurate indication of personal exposure for a given segment of the population? And what are the key variables—such as use of gas stoves—that determine personal exposure? These are the questions that have been raised by recognition of in-

Personal exposure to respirable particles

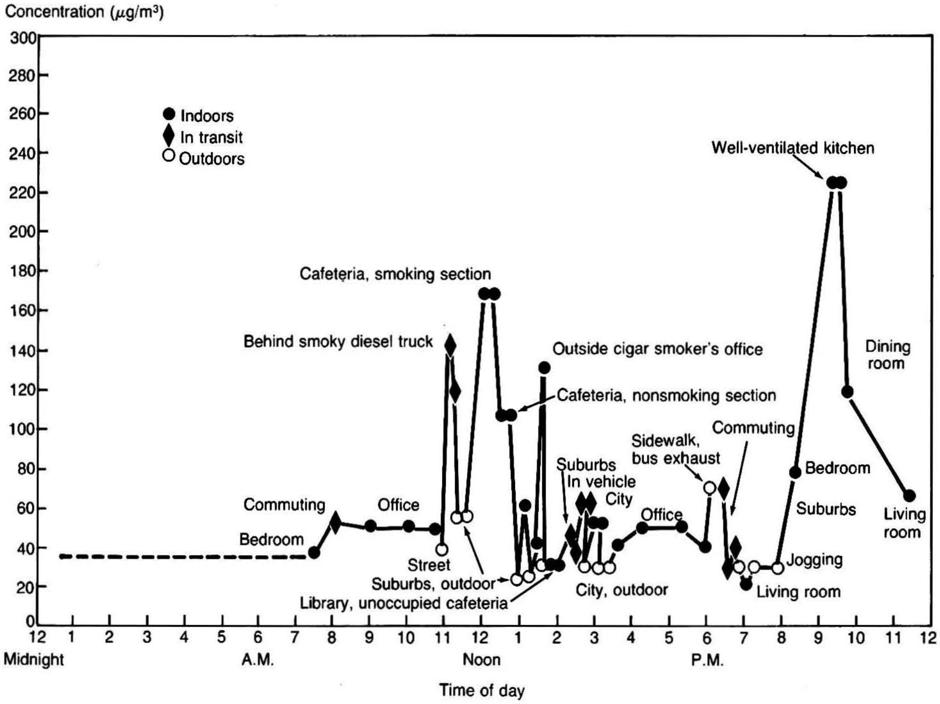

James L. Repace's exposure to respirable particles, as recorded by a portable monitor which he carried with him on Oct. 16, 1979.

door pollution, and that may be answered by further study of indoor pollution.

Shockers steal the show

But maintaining this perspective is difficult in the face of the undeniably disturbing revelations about indoor pollution. Some have been real horror stories.

In the course of a continuing epidemiological study involving six cities and some 20 000 subjects, Spengler conducted indoor and outdoor measurements in 73 houses. In those with gas cooking, NO_2 was measured repeatedly, and for as long as hours at a time, at over 500 $\mu g/m^3$. Annual mean values in kitchens with gas stoves may well exceed the ambient air standard of 100 $\mu g/m^3$. And the effects are noticeable.

"For nonoccupational groups, children for instance, you see two populations," Spengler explained. "The gas-cooking population is having a higher mean exposure than the electric-cooking population." And according to Spengler and others, that difference is associated with increased respiratory disease and decreased lung volume in the gas-cooking group.

Respirable particles can reach astounding concentrations indoors, particularly where there is smoking going on. Repace sampled particle levels in a variety of indoor environments and found consistently higher levels where there was smoking; typical values were 70–900 $\mu g/m^3$ of respirable particles in environments ranging from restaurants to church bingo games to a hospital waiting room. The grand prize went to an office building conference room, which tipped the scales at 2000 $\mu g/m^3$. The ambient standard calls for the 24-h average not to exceed 260 $\mu g/m^3$ more than once a year.

Formaldehyde has received much attention from the complaints of sickness, sometimes severe, that have followed on the installation of urea-formaldehyde foam insulation in houses. And according to Craig D. Hollowell of the Lawrence Berkeley Laboratory, "formaldehyde is just the tip of the iceberg of the issue of organics. We have found a large number of organic compounds" indoors, particularly in office buildings where carpeting, paneling, construction adhesives, and cleaning compounds contribute a whole grab bag of substances to the air.

Another shocker is benzo[a]pyrene. "BaP is elevated indoors and that is something that should concern people a great deal," said Moschandreas, who reported a concentration of 11.4 ng/m³ in one home which had a fireplace going. Wood-burning stoves and smoking can also jack up indoor levels of this "most unchallenged carcinogen," according to Moschandreas.

But the most frightening component of indoor air may be radioactive radon gas. Radon is emitted naturally by anything that contains radium-226—and that includes concrete, brick, stone, even the soil under building foundations. Radon decays to give rise to four "daughter" elements, all radioactive as well; these tend to stick to airborne particles which may then be inhaled. The dose of alpha radiation that the lung tissue receives when these inhaled daughters decay has been closely linked with lung cancer incidence in uranium miners exposed to high concentrations.

Hollowell's group has estimated that, at present, indoor exposure to radon daughters may account for as many as 1000–20 000 lung cancer deaths each year in the U.S.

Tightening up on energy—and air

Much of the attention that indoor air quality has received of late has arisen from concern over the effects of energy conservation measures, such as weather-stripping and caulking, that reduce ventilation rates. With a reduction in ventilation comes an increase in the indoor concentration of any pollutant with an indoor source. The two Department of Energy programs designed to cut building energy use—the Building Energy Performance Standards (BEPS) and the Residential Conservation Service (RCS)—have in particular forced the issue to a head.

But many researchers are quick to point out that the problem is not new. "The indoor environment was dirty before energy conservation came along," said Moschandreas. And Hollowell said, "Energy conservation programs have sensitized many people, but there was a problem even before you looked at energy conservation."

What *is* new is awareness of the problem, though in retrospect it is hard to understand how it could have taken so long to come about. Since about 1970 the EPA had been funding some work on indoor air quality, but at a very low level. "EPA looked at the problem as 'outdoor will determine indoor levels,'" said Moschandreas.

In 1976 the EPA sought proposals for a major study; the contract went to Moschandreas' group at Geomet; and, as Moschandreas put it, "they found out otherwise." Hollowell had meanwhile become interested in the indoor environment, in particular the role of emissions generated by gas combustion indoors. He pursued the matter with the Atomic Energy Commission, and subsequently with the Energy Department's building conservation section.

Energy conservation is what woke up the EPA policy people. When the DOE proposals were reviewed by the EPA last year, Repace "realized right away that both the RCS and the BEPS would have tremendous indoor air quality implications. There was a serious air quality problem and it was about to get worse," he said.

The EPA entered into negotiations with DOE in an effort to put some limits on the RCS program. "In the midst of our negotiations," Repace continued, "Maxine Savitz [assistant secretary for conservation and solar at DOE] sent a letter to [EPA Administrator] Costle requesting the establishment of indoor air quality standards. As far as I was concerned, this was a very significant development. At that point we felt we could justify a big program, and that it was needed—it was of national importance."

Outside the agency, however, the view of how much will be done tends to be pessimistic. Hollowell, and to a lesser degree Spengler, claimed that the EPA is reluctant to touch the issue at all. Spengler cited arguments raised within the agency and by environmental groups that recognition of indoor air pollution would weaken the case for ambient standards, which have been hard fought for. And Hollowell suggested that the Geomet study and a National Academy of Sciences study commissioned by the agency were more an attempt to show that the EPA was doing something rather than part of an effort to truly take on the problem. It was the Savitz letter that goaded the EPA into taking charge as much as it has, Hollowell said: "It's become an issue that the EPA can no longer ignore."

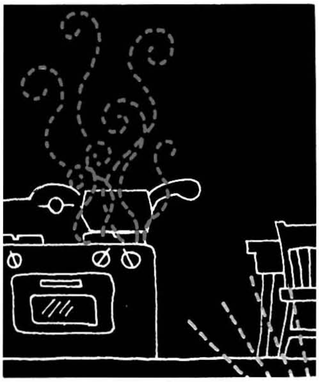

Pollutant concentrations in a gas kitchen

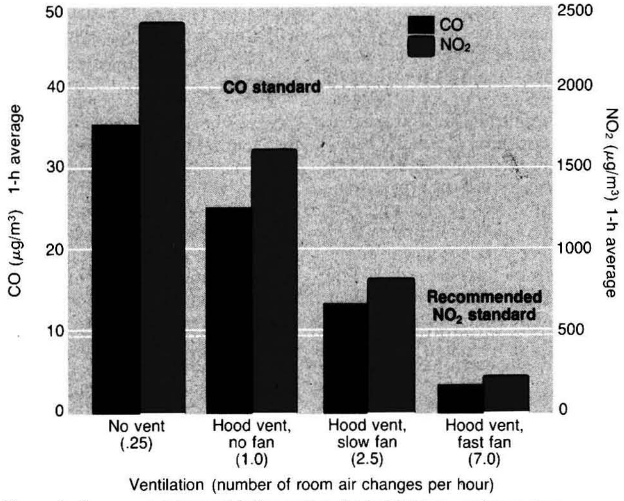

Concentrations were measured in the center of a test kitchen, under varying ventilation conditions, while a gas oven was operated at 350 °F.

Source: C. D. Hollowell

Legal and political barriers

But even if the EPA does make the decision to tackle the issue, it faces some genuine obstacles. The so-called "industry argument"—that ambient standards may be weakened—is only one of them.

A more serious problem is that the EPA probably lacks legal authority to deal with indoor pollution, though the point is disputed. A clear mandate could come from an amendment to the Clean Air Act, an action that will be urged on Congress by a General Accounting Office report that was in preparation at press time.

There will no doubt be many "turf" problems as well, of which the EPA-DOE dispute over energy conservation is only the first. The Occupational Safety and Health Administration, the Consumer Product Safety Commission, the Department of Health and Human Services, and the Department of Housing and Urban Development are all already in the act in one way or another.

Finally, there is certain to be opposition from groups, such as the house builders, who would be affected by any eventual regulations and who will raise the "spectre of the government telling

Indoor, outdoor, and personal concentrations

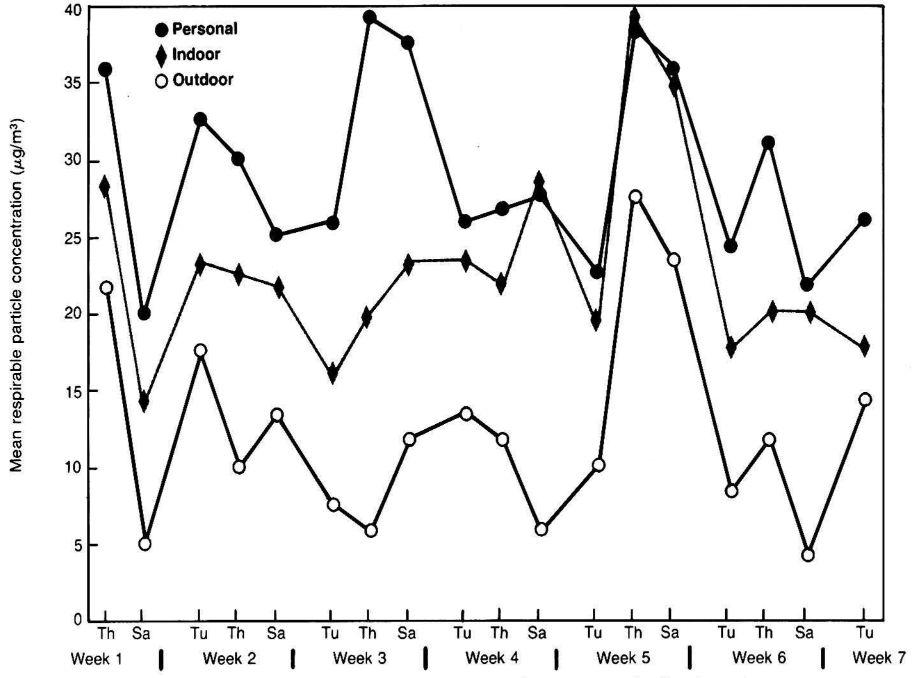

Daily average concentrations for the entire group of 46 subjects in the Topeka study

Source: J. D. Spengler

people what to do indoors," as Repace put it.

But Repace once again tends toward the optimistic, dismissing these obstacles and declaring, "It is completely obvious to me that we will need indoor air quality standards." The extent to which his view is shared by his superiors is unclear.

Repace simply shrugs off the "industry argument." "If people are going to take your argument and use it against you, you can't stop them. And, to a certain extent, they have a point. But first of all, background levels indoors come from outdoors. Secondly, we know from a very large number of studies, you have acute cause and effect with factory emissions—people do die." And he made a point that both Spengler and Moschandreas emphasized when asked whether outdoor standards were important: "Some people spend the great bulk of their time outdoors." Spengler added that if it is peak exposures that determine the health effects, spending even a short time outdoors in the presence of high concentrations could be harmful.

As for worries over the EPA's telling people what to do, Repace said, "That is a very naive view. Controls can be implemented through changes in building codes rather than in personal behavior."

Airing views

In the meantime—and it may be a long meantime before these problems are sorted out—the EPA is seeking to have the RCS program limit its tightening up of residential buildings so that ventilation rates are not reduced below one complete air change per hour. The EPA has argued that the program intends to cut the average exchange rate in half, a move that would more than double indoor radon concentrations and would result in as many as 20 000 additional radon-induced lung cancer deaths per year. DOE argues that that is a gross overestimate, since the program would only reach 25–30% of the houses in the country and would only tighten them up by 25%, not 50%. Furthermore, they claim, the average ventilation rate is already below 1.0 exchange per hour. An agreement between the two agencies is expected shortly on the residential conservation program, but it will be a long time before there is any agreement on what the actual risks are. According to Hollowell, it will be a long time before we even know what the risks are.

"You just can't do it today," he said. "Setting a standard is not the way to go. But we're going to have to come up with some sort of trigger level" which will set off corrective action to reduce exposure.

Reduced ventilation unquestionably increases concentrations. Experiments by Hollowell's group have shown a direct relation between concentrations of CO, NO_2, and formaldehyde, produced by a gas oven, and ventilation rates in a test kitchen. Detailed measurements of radon in one house, under varying ventilation conditions, show a similar relation. And Hollowell has concluded that, for most cases, "an air exchange rate of 0.5 ach [air changes per hour] is required in order to maintain radon concentrations below 4 nCi/m^3, the maximum permissible given by health guidelines." Some energy-efficient houses have ventilation rates as low as 0.1 ach.

Air-to-air heat exchangers, which draw in fresh air through one duct while expelling indoor air in an adjacent duct, heat the incoming air and reduce the energy cost of ventilation; this may provide one, at least partial, solution. Control strategies for radon may include filters that remove airborne particles which carry the radon daughters. But according to Hollowell, "the whole control technology field needs a lot of work."

A monkey wrench in epidemiology

The control technology field isn't the only one. The finding of indoor sources and high indoor levels of pollutants has cast a shadow on past epidemiology, which attempted to relate health effects with outdoor levels only.

"The effects that you do see could be occurring at lower levels" than would appear from these studies, said Spengler. A typical epidemiological study might compare matched populations in two different cities, one with high outdoor concentrations of a pollutant and one with low outdoor concentrations; differences in morbidity and mortality between the two groups would then be ascribed to the different degrees of pollution. But indoor pollution can introduce several possible distortions. If, for example, a city with high outdoor levels of NO_2 used predominantly electric stoves while a city with low outdoor levels used gas stoves, actual personal exposures in both cities might be very similar. A study which looked only at outdoor levels would conclude that higher NO_2 concentrations had little effect on health. A systematic bias the other way is also possible, leading to an overestimate of the health effects.

Even if there is no systematic bias, however, the variation in indoor exposures introduces a "random variable" which reduces the sensitivity of the study. Hollowell asked the question on everyone's mind: "How can one do an epidemiology study and forget the indoor environment?"

Personal monitoring

Spengler sees this as a compelling reason by itself to study the indoor environment. "If it's a confounding factor in outdoor epidemiology, it's worth some investment—that's independent of it being a health problem of itself."

The ultimate aim for health studies on large populations, according to Spengler, is to see whether it is possible to "take one or two key variables, such as the presence or absence of gas stoves, and characterize the exposure of the whole population." In pursuit of this aim, Spengler has begun some personal exposure monitoring in conjunction with the Harvard Six City Study. Measurements made by portable samplers carried by the subjects are correlated with the subject's activities—recorded in a log—and with measurements taken at fixed locations indoors and out. One of these experiments, carried out in Topeka, Kans., shows some telling results: If outdoor concentrations of NO_2 and stove type are considered, 77% of the variance in recorded personal exposures can be explained; if only outdoor concentrations are considered, only 22% of the variance is explained. Spengler is in the process of extending these studies to the other cities of the Six City Study.

But expanding such a study to the point that it is more than a series of spot measurements—Spengler's Kansas study involved only 23 subjects—will be expensive and will be limited by available instruments. "Trying to develop low-cost, reliable, portable—if we could, even personal—monitors is the issue," said Hollowell. Both Hollowell and Spengler have had to design and build their own devices. The problem is not a lack of knowledge of how to measure these pollutants. ("Everything's available as far as principle of operation," said Spengler.) But instrument manufacturers have not yet found it worthwhile to produce units for the specific applications required. And portability and low cost are only a part of the issue: "The methods used to measure the same pollutants outdoors will likely encounter new interferences indoors," according to Spengler. Spengler ran into one such case when he attempted to use a commercial NO_2 monitor indoors. Everything was fine until house painters arrived on the scene; as soon as they started work, the meter went off scale.

An expensive study

There is a growing sentiment that a large study is needed. As Moschandreas said, "One house does not focus on the big problem. We are not there yet. We cannot make general conclusions." Whether the money will be available for the "comprehensive, statistically valid study" that Moschandreas envisions is another matter.

At present it seems that $3-4 million may be budgeted by the EPA for fiscal year 1982. In the meantime, the DOE indoor air quality program at Lawrence Berkeley will continue at a budget of about half that, as it has for several years; and $2 million is being made available to the EPA immediately through a two-year agreement with the National Institute for Occupational Safety and Health. NIOSH's

interest is in having 24-h exposure profiles developed for workers in the electronics and biosynthesis industries; the EPA expects to learn something about general indoor exposures to radon, formaldehyde, respirable particles, and asbestos in the course of the work.

Indoor atmospheric chemistry

More is needed than a large survey of indoor concentrations. What is in the air in the first place is still a major unknown, particularly in the case of organics. "Organics from building materials is still an area that has not really been explored," said Hollowell. "I don't think we really understand what all the sources are"—or even what the identities of all the compounds are.

How indoor pollutants interact is also an unknown. Compared with the outdoor environment, said Spengler, "you're injecting into the air totally different characteristics of temperature, humidity, and other pollutants." Ammonia, produced by humans, should be higher indoors, for example, and could react with sulfates or sulfuric acid. The question is: What is the chemical species that ends up inside?

"The other thing that's missing is quantification of removal rates," Spengler continued. "You have tremendously more surface area indoors; you have much more opportunity for surface reactions." Particle deposition rates, room-to-room air-transfer rates, and ventilation rates need to be known better too.

No one is underestimating the size of the task. "I see a need for a major program that should take somewhere from three to five years," said Moschandreas. And there is an understanding that all available resources will need to be tapped. "None of us can do the whole thing," he said.

—Stephen Budiansky

Incinerator research abuilding

Scientists are taking a basic look at the incineration process in their laboratories and designing lab-scale reactors to study what is happening to hazardous materials in the decomposition process

Historically, the use of incineration or other thermal decomposition processes of managing hazardous wastes has been uneconomical, mainly because of the very low cost of alternatives—land disposal, biological treatment using microorganisms and enzymes, and physical/chemical treatment. Indeed, until now incineration has been more of an art than a science. But things are slowly changing in this field.

Toxic organic wastes pose a severe threat to the well-being of people throughout the world. One method for the safe and permanent disposal of these wastes, that is, eliminating their existing and future effects, is high-temperature incineration. But the thermal decomposition characteristics of wastes must be better understood before large-scale incineration can be safely conducted.

A laboratory-scale thermal decomposition analytical system (TDAS) was described in a paper by D. S. Duvall, W. A. Rubey, and J. A. Mescher of the University of Dayton Research Institute (Dayton, Ohio) at a session on this topic at the 73rd annual meeting of the Air Pollution Control Association, held in late June in Montreal, Canada. The system has been used for studies of the destruction of PCBs, PBBs, and "Hex" industrial wastes (*ES&T*, May 1980, p. 508).

This laboratory system provides precisely controlled thermal exposures in a narrow-bore (0.97-mm) quartz tube reactor. Then thermal decomposition products pass into an adsorptive, cryogenic (if needed) trap where they are collected, and where any chemical reactions are quenched. Subsequently, the products are thermally desorbed and subjected to high-resolution gas chromatographic separation and mass spectrometric identification. By conducting these decompositions at different temperatures, the investigators are able to obtain a profile of the thermal decomposition properties of an organic substance.

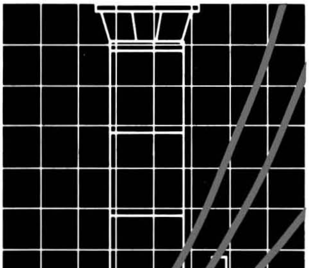

Available at the University of Dayton Research Institute, this system provides information needed for optimizing conditions for waste degradation, such as exposure temperature, residence time, and whether inert or oxidative atmospheres are involved. Knowledge of the formation of toxic or highly stable intermediates can provide further guidance in specifying conditions for the ultimate disposal of organic waste.

For example, K. C. Lee et al., in a paper at last year's APCA meeting (Cincinnati, Ohio), determined the residence time data for 15 compounds. They showed that above a relatively low critical temperature, a compound's destruction proceeds by a first-order reaction mechanism in the presence of a large excess of oxygen.

In a paper by P. A. Fredette, T. J. Schultz, and B. W. Dominiak of the Midland-Ross Corp. (Toledo, Ohio), it was said that over the past 10 years the concept of "pyrolysis afterburner" (pyrolysis followed by fume incineration) has been successfully demonstrated and has led to the development of process and equipment for the thermal disposal of hazardous chemicals, including fluorinated and chlorinated compounds, mustard and nerve agents, styrene tar, rubber wastes, API separator bottoms, and pharmaceutical sludges.

Pyrolysis implies heating in the absence of air to degrade the material thermally to a volatile gaseous portion and a residual solid comprised of fixed carbon and ash. By adding inexpensive reactive compounds to the wastes and allowing them to react with elements such as sulfur and chlorine, it is possible to form nonvaporizing or very low vaporizing solid compounds of these elements.

These researchers have shown that chemical constituents, such as chlorine, sulfur, and phosphorus, can be retained with the ash during the pyrolysis process. The degree of effectiveness varies with the type and concentration of additives utilized. The researchers claim that the results of their tests permit the mixing of several dissimilar waste streams in such a way as to permit two thermally reactive constituents to combine in the pyrolysis step.

Their experimental laboratory system used an electrically heated Lindberg oven modified as a muffle furnace, which permitted the pyrolysis process to take place in an inert nitrogen atmosphere. The gas outlet on the muffle furnace was connected to a gas

ENJOY YOUR OWN MONTHLY COPY OF

Environmental Science & Technology

1980

Toll Free: New Orders: (800) 424-6747

	U.S.	Foreign**
ACS Members*	☐ $16.00	☐ $23.00
Nonmembers-Personal	☐ $20.00	☐ $27.00
Nonmembers-Institutional	☐ $64.00	☐ $71.00

☐ Bill Me ☐ Bill Company ☐ Payment Enclosed
(Make payable to American Chemical Society)

Charge my ☐ Master Charge ☐ VISA

Card # ______ Interbank # ______
(Master Charge only)

Exp. Date ______

Signature ______

Name ______

Position ______

Your Employer ______

Address ☐ Home ☐ Business ______

City ______ State ______ Zip ______

Employer's Business ☐ Manufacturing ☐ Academic ☐ Government ☐ Other ______

If manufacturing, type of products produced ______

*Subscriptions at ACS member rates are for personal use only.
**Payment must be made in U.S. Currency, by international money order, UNESCO coupons, U.S. bank draft, or through your book dealer.

Allow 60 days for your first copy to be put in the mail. 9998G

MAIL THIS POSTAGE FREE CARD TODAY

ENJOY YOUR OWN MONTHLY COPY OF
Environmental Science & Technology
1980
Toll Free: New Orders: (800) 424-6747
U.S. Foreign**
ACS Members* ☐ $16.00 ☐ $23.00
Nonmembers-Personal ☐ $20.00 ☐ $27.00
Nonmembers-Institutional ☐ $64.00 ☐ $71.00
☐ Bill Me ☐ Bill Company ☐ Payment Enclosed
(Make payable to American Chemical Society)
Charge my ☐ Master Charge ☐ VISA
Card # ______ Interbank # ______
(Master Charge only)
Exp. Date ______
Signature ______
Name ______
Position ______
Your Employer ______
Address ☐ Home ☐ Business ______
City ______ State ______ Zip ______
Employer's Business ☐ Manufacturing ☐ Academic ☐ Government ☐ Other ______
If manufacturing, type of products produced ______
*Subscriptions at ACS member rates are for personal use only.
**Payment must be made in U.S. Currency, by international money order, UNESCO coupons, U.S. bank draft, or through your book dealer.
Allow 60 days for your first copy to be put in the mail. 9998G
MAIL THIS POSTAGE FREE CARD TODAY

NO POSTAGE
NECESSARY
IF MAILED
IN THE
UNITED STATES

BUSINESS REPLY CARD
FIRST CLASS PERMIT NO. 10094 WASHINGTON, D. C.

POSTAGE WILL BE PAID BY ADDRESSEE

AMERICAN CHEMICAL SOCIETY
Attn: Gayle Hebron
1155 Sixteenth Street, N.W.
Washington, D. C. 20036

NO POSTAGE
NECESSARY
IF MAILED
IN THE
UNITED STATES

BUSINESS REPLY CARD
FIRST CLASS PERMIT NO. 10094 WASHINGTON, D. C.

POSTAGE WILL BE PAID BY ADDRESSEE

AMERICAN CHEMICAL SOCIETY
Attn: Gayle Hebron
1155 Sixteenth Street, N.W.
Washington, D. C. 20036

The thermal decomposition analytical system (TDAS)

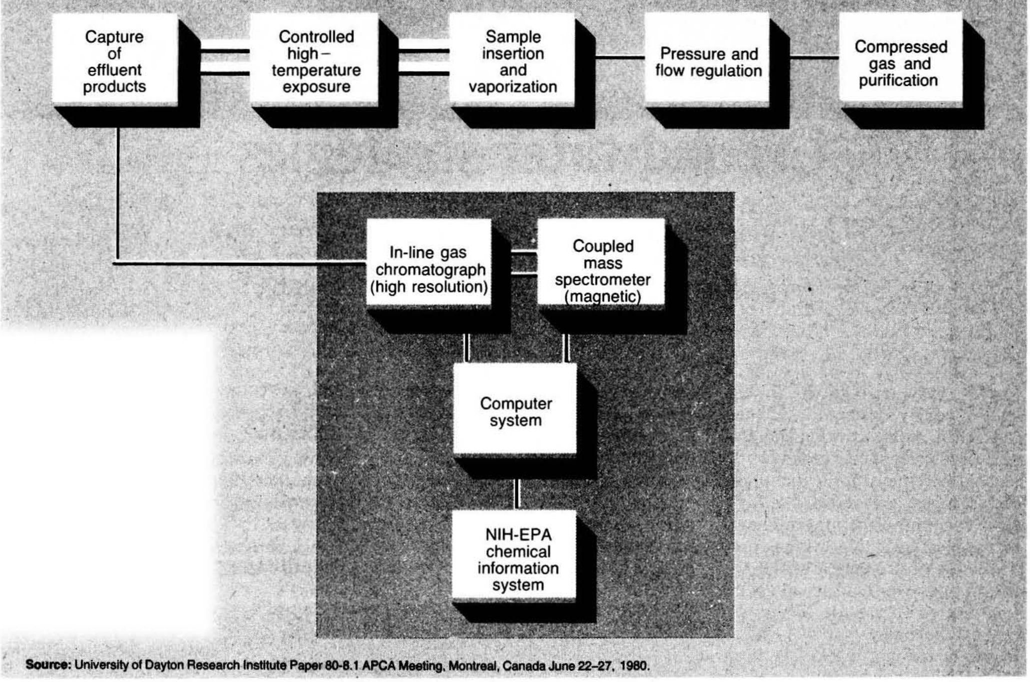

Source: University of Dayton Research Institute Paper 80-8.1 APCA Meeting, Montreal, Canada June 22–27, 1980.

cooler. To remove the acidic gases before venting, the cooled effluent gases were passed through water and a caustic scrubbing system.

Leo Weitzman of the U.S. EPA (Cincinnati, Ohio) said that EPA has embarked upon a major research program on incineration that includes further development of TDAS. This system permits one to establish the required thermal degradation characteristics for a material's destruction, that is, the minimum temperature and residence time conditions needed to achieve satisfactory destruction.

One question facing the EPA is: If a given waste can be burned successfully in incinerator A, can it be burned safely in incinerator B? Weitzman mentioned a potential definition of incinerator similarity as: "Two geometrically similar incinerators of different capacity are deemed similar if, when burning the same type of waste, they produce the same level of destruction and their stack gases and residues, respectively, have the same composition."

The three Ts of incinerator are time, temperature, and turbulence. Two units should behave in the same manner if their heat-transfer characteristics and turbulence conditions are the same. Dimensionless analysis—a technique of reducing the heat-transfer and flow conditions to a series of dimensionless numbers which, when they are equal for the two systems, indicate that similarity of this property—has been shown to be a satisfactory method of dealing with such systems. Examples of such dimensionless numbers are Reynolds and Mach numbers for fluid flow or Prandtl and Nusselt numbers for heat transfer. Of course, there are many other dimensionless numbers.

It is known, for example, that similarity of fluid flow in two geometrically similar systems is achieved if the Reynolds numbers are the same in both systems, assuming that the fluid is incompressible and gravitational forces are small. In the event that these assumptions do not apply, then the Mach number and Froude number must also be determined.

It has also been shown that to demonstrate similarity in convective heat flux between a flowing fluid and a surface, the Nusselt number must be reproduced. The relationship, Nusselt $- f$ (Reynolds, Prandtl), can be derived through dimensionless analysis, or by examination of the Navier-Stokes and the energy equations, according to Weitzman.

For example, in a rotary kiln, similarity may require equivalent Reynolds, Biot, and Nusselt numbers in different zones of the kiln. Because of material restrictions, and of contradictory demands that may be presented by each mechanism (for example, high velocity for equivalent mixing vs. low velocity for equivalent residence time), full similarity may not be achieved. Analytical and experimental work is under way in order to determine which parameters most influence the similarity of emissions.

The difficulty in the use of these dimensionless numbers comes in choosing the proper dimension for the system to use. For example, which length dimension determines the desired Reynolds numbers for two incinerators?

Although the state of the art of incinerator scale-up is very crude at this time, the EPA's new experimental program involves construction and testing of a model of an existing incinerator. The model will have approximately one-twentieth the capacity of the full-size unit. The objective of this program will be to develop criteria to be used for comparing data from one incinerator to another and to establish similarity criteria for incinerators.

—Stanton Miller

Groundwater strategies

They could involve several alternative regulatory and technical approaches to aquifer protection. Perhaps, even cleanup methods may evolve in the future

In early July, on National Broadcasting Company's program "Meet the Press," EPA Administrator Douglas Costle specifically named groundwater as one of the principal priorities of his agency's more concentrated efforts toward environmental improvement. A main objective is to provide appropriate levels of protection to the nation's groundwater in order to assure that projected future use of that resource can be made.

Right or wrong, EPA has been characterized as having pursued groundwater programs which were fragmented and lacking in authority, resources, and knowledge. Be that as it may, the agency is now making concerted efforts to evolve long-range groundwater management plans; its Office of Drinking Water (ODW) is leading the effort. Another federal organization involved in groundwater is the Water Resources Division of the U.S. Geological Survey (USGS), presently headed by Eugene Patten.

A three-phase effort

The EPA effort to develop a groundwater protection strategy consists of three phases. Phase I, now completed, called for assembling information on water use, contamination, federal/state laws and programs, and the groundwater protection state of the art. That phase also involved putting together a roster of knowledgeable individuals, Victor Kimm, EPA's deputy assistant administrator for water supply, explained to a seminar, "Federal Protection of Groundwater: A Pervasive Regulatory Force." That seminar was organized by Executive Enterprises, Inc. (New York, N.Y.), and was held in Arlington, Va., in late May.

Phase II involved workshops comprising these representatives of government, business/industry, and professional and environmental advocacy groups. The workshops, held in late June, analyzed the issues and recommended alternative policies.

Phase III will be the strategy-determination phase. A draft strategy reflecting the views emerging from the workshops will be reviewed in hearings, to be held nationwide in October and November, and will be published by EPA next January.

The final strategy will provide:

- a clear statement of problems and issues being addressed, with a greater national understanding of groundwater issues
- a national program with fully defined federal and state roles

USGS groundwater programs

For fiscal year 1978, the USGS Water Resources Division budget was \$148 million, of which \$60 million were allocated to the groundwater resource and its environment. Of the latter figure, about \$20 million were devoted to groundwater quality and pollution. The number of groundwater projects was 600, of which 175 covered waste, pollution, and quality. The three major categories concentrated on the federal program, the federal–state cooperative program, and critical national water problems.

Funding for many of the programs has increased since fiscal year 1978, although dollar figures were not available as this went to press. Almost all of the programs are extant.

Under the federal program, important elements are:

- data collection and analysis
- national water data exchange (computerized information base)
- interagency coordination of water data activities (federal and state; state participation is voluntary)
- regional groundwater appraisals
- core program of hydrologic research, covering quality, quantity, planning/management, and environmental impacts
- hydrologic investigations on public lands, emphasizing impacts of coal, shale, and phosphate operations, as well as spring and well inventories
- regional aquifer systems analyses, including adequacy evaluation for environmental and waste management
- investigations for many other federal agencies, including EPA and CEQ.

The federal–state cooperative program concerns itself with:

- cooperative studies
- coal hydrology (including mining impacts)
- water use.

Listed under critical national water problems are:

- coal hydrology (especially new, or enlarged mining operations)
- nuclear energy hydrology (waste burial sites)
- oil shale hydrology
- underground heat storage
- groundwater recharge
- subsurface waste storage.

- a comprehensive EPA policy to apply to all programs concerned with groundwater
- tighter relationships among cognizant federal, state, and local government bodies
- a short-term action plan, as well as plans for dealing with groundwater problems over the long term.

Two scenarios

EPA's Kimm told the Arlington seminar that two possible major scenarios may emerge from groundwater strategy development. Strategy I would call for protecting almost all groundwater to the same extent. Strategy II would provide for varying levels of protection, based on some mechanism of local choice. Other, though less likely, scenarios may consist of a concept of nondegradation, that is, prevention of *any* further contamination. Another possibility might be treating contaminated groundwater at the point of use, rather than preventing contamination.

The principal regulatory approach under Strategy I would focus on point sources, with uniform requirements based on technology that addresses hazardous waste sites, landfills, and injection wells. There may be case-by-case variations granted, depending on engineering and hydrogeological conditions. Also, limited exceptions might be granted for sole-source aquifers or exempted aquifers.

On the other hand, Strategy II could be based on allowing degradation in some areas, to be offset by very strict controls in others. There might be a groundwater classification system of, say, three or four categories. These categories, from highest to lowest level of protection, may be based on desired use and social importance of the groundwater. The regulatory framework could vary from state to state.

Also under Strategy II, siting would be a major element of control for new point sources, with nondegradation (no new sources) appropriate for the highest protection classification, such as drinking water. Levels of control would rely on the outcome of the planning process, which would include public participation. Control of point and nonpoint sources would be integrated, and numerical groundwater quality standards, while allowed, would not necessarily be required.

Resource losses

Aside from RCRA, SDWA, and, to a lesser extent, CWA, which require EPA to develop regulatory strategies and regulations for groundwater protection, there are other reasons why such strategies are needed. Among them is a loss of groundwater resources, ascribable to contamination, as listed in a Library of Congress Report. Loss listings cover a period from about 1950 to the beginning of this year—a 30-year time span.

The report mentions about 1360 well closings brought about by 128 incidents of toxic groundwater contamination. They are broken down as follows:

- metals contamination, 619 wells
- organic chemical contamination, 242 wells, including 170 from trichloroethylene used to emulsify septic tank grease
- pesticide contamination, 201 wells
- industrial waste contamination, 185 wells
- landfill leachate contamination, 64 wells
- chlorides, 26 wells
- nitrates, 23 wells

Incidents of toxic well contamination could present even more of a problem in the immediate future if the prediction of Robert Goyer, deputy director of the National Institute of Environmental Health Sciences, is borne out. The source would be toxic chemical waste dumps. Goyer called for toxicological studies to establish health effects from chemicals identified in those dumps. However, he observed that toxicological data are available on less than 50% of the chemicals identified so far, and that many of the wastes are poorly defined residues.

The well closing figures above were published in "Resource Losses from Surface Water, Groundwater, and Atmospheric Contamination: A Catalog," available in very limited quantities at the Committee on Environment and Public Works, U.S. Senate, Washington, D.C. 20510. Possibly, the committee will order a second printing.

Note: CWA = Clean Water Act
RCRA = Resource Conservation and Recovery Act
SDWA = Safe Drinking Water Act

For those concerned with groundwater regulations and science, the seminars presented by Geraghty & Miller, "The Fundamentals of Ground Water Quality Protection," are offered from time to time. The next will be held in Pittsburgh, Pa., next month. Contact Richard Miller, American Ecology Services, Inc., Dept. G, 127 E. 59th St., New York, N.Y. 10022; (212) 371-1620.

Technical efforts needed

The Arlington seminar and other discussion and publication media have brought out possible ideas for groundwater protection and contamination control from the regulatory standpoint. But the implementation of existing and forthcoming regulations will entail great technical and financial effort. Many aspects of what will be involved were discussed at a seminar, "The Fundamentals of Ground Water Quality Protection," organized by Geraghty & Miller, Inc. (G&M, Syosset, N.Y.). About 200 people came to that mostly technical seminar which was held in Chicago, Ill., in mid-May.

One topic addressed at the Chicago seminar dealt directly with an important aspect of groundwater protection—containment of plumes of contaminated groundwater. James Geraghty, Jr., G&M's president, defined a plume of contamination as "a body of contaminated fluid in the zone of saturation"; it may be present in one or more aquifers. Its source may still be extant or may have ceased years ago, and it would be caused by human activity at or below the land surface.

The contamination plume normally follows the direction of groundwater flow, but may deviate from that path somewhat because of differences in contaminant densities. The plume widens and thickens as it migrates, and some contaminants in the plume may move faster than others. They may also be in liquid phases that are different from that of the groundwater. Contaminant attenuation can be effected through adsorption on subterranean material, dispersion, diffusion, or natural ion exchange.

Containment

Geraghty explained that contaminant plume containment can comprise three principal concepts:

- complete blockage of plume migration, both horizontally and vertically
- partial blockage, that is, reducing the rate of plume migration, which may be the only workable solution in some cases
- removal of the plume through excavation or pumping out.

Most regulators would specify on-site containment, Geraghty said; but this could pose administrative and legal problems since the land involved can be sold or subdivided.

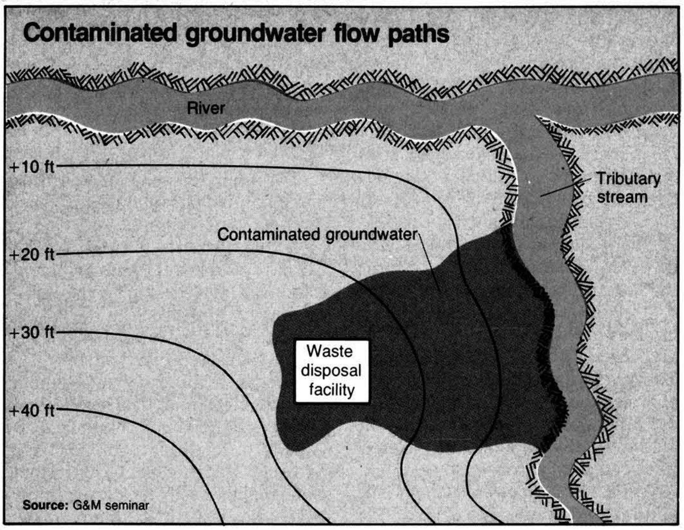

Contaminated groundwater flow paths

Source: G&M seminar

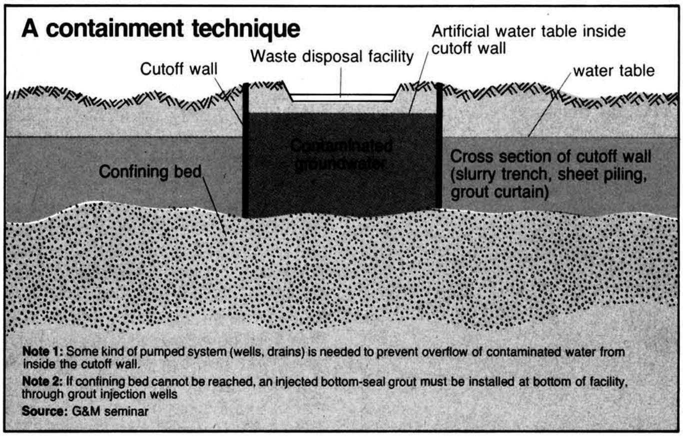

A containment technique

Note 1: Some kind of pumped system (wells, drains) is needed to prevent overflow of contaminated water from inside the cutoff wall.

Note 2: If confining bed cannot be reached, an injected bottom-seal grout must be installed at bottom of facility, through grout injection wells

Source: G&M seminar

Excavation or pumping out may involve digging a pit or installing pumping wells to remove the plume completely. But these approaches also can present problems. For instance, what does one do with contaminated materials removed from underground? Also, excavation may be too costly, or environmentally disruptive, or "just plain impossible" in many cases. Pumping out, while theoretically possible in many cases, is rarely totally successful and, with two-phase liquid contamination problems, is normally infeasible, Geraghty said.

Another containment technique calls for in-situ, or installed, clays with permeabilities of 10^{-7} cm/s or less. Most regulations assume that such low permeabilities provide total containment. Is it indeed provided?

First of all, Geraghty pointed out that in the final analysis, all clays or artificial barriers "eventually leak." Moreover, given the weight of overburden above the containment barrier, and the resulting pressure head, leakage could accelerate. In addition, the excavation and construction necessary to install impoundment walls or "floors" may be extremely expensive, if at all feasible. In fact, Geraghty noted, it is not feasible to emplace an artificial impermeable floor beneath a plume. Even if complete impoundment were possible, continuous withdrawal of fluid would be necessary for facilities actively discharging into groundwater.

Other complete containment approaches comprise blocking contaminant migration with drains; pumping from wells; injecting contaminants into

Groundwater regulatory strategies

	Advantages	**Disadvantages**
Strategy I: Protect (almost) all groundwater to the same extent	Simple to administer Similar in concept to successful air, and surface water pollution control programs	Average level of protection would be too little in some areas, too much in others Does not consider siting as a control measure Neglects nonpoint sources
Strategy II: Provide varying levels of protection, based on some mechanism of social choice	Allows tailoring of programs to local conditions; forces weighing of social values involved Takes advantage of siting controls Integrates point and nonpoint source controls	Places much greater burden on state and local authorities from the standpoint of both resources and institutional capacity Many states could not do it now Previous programs along these lines have had bad mixed results Lack of criteria for federal oversight; if states do not do an adequate job, can "feds" move in?

Source: Presentation by EPA's Victor Kimm to "Federal Protection of Groundwater: A Pervasive Regulatory Force" seminar.

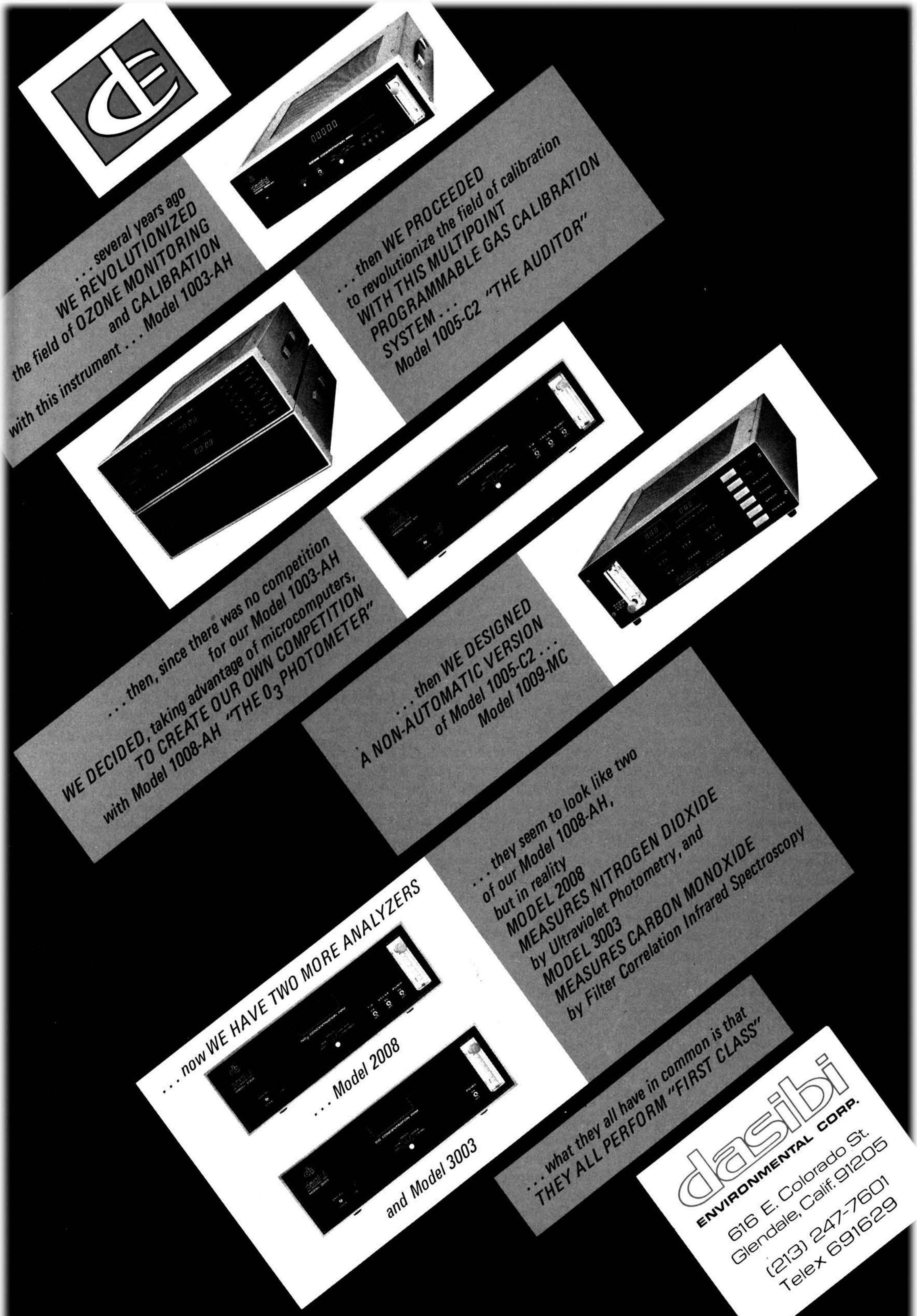

Comparative installation costs of selected containment systems

Methods	Examples of dimensions	Range in cost (thousands of dollars)	Remarks
Bentonite slurry trench	1700 ft long and 60 ft deep	500–840	Mainly used for shallow unconsolidated aquifers
Grout curtain	1700 ft long and 60 ft deep	800–2000	Mainly used for shallow unconsolidated aquifers
Sheet piling	1700 ft long and 60 ft deep	650–960	Mainly used for shallow unconsolidated aquifers
Bottom seal	10-acre area and 4 ft thick	1100–4200	Difficult to accomplish; results uncertain; unconsolidated aquifers only
Well points	900-ft-long array	20–30	Limited by suction lift of 20–30 ft; unconsolidated aquifers only
Pump-back well	100 ft deep	10–30	Suitable for all aquifers at all depths
Deep injection well	5000 ft deep	500–1000	Suitable only where confined salty aquifers present at depth
Injection of fixatives	10-acre area	50–100	Immobilizes only some contaminants; results unpredictable

Source: G&M seminar

deep, nonpotable aquifer zones; and reducing or immobilizing contaminants with biological or chemical agents.

Partial containment practices could involve installing a clay roof (used at Love Canal) to prevent rainfall infiltration or leachate from reaching the saturated zone. This method does little or nothing against contaminants already in the saturated zone; moreover, these clay coverings eventually would fail without perpetual care.

Installations

A typical containment installation is a cutoff wall surrounding a slurry trench. Such a trench could be excavated to about 50 ft with backhoes or 90 ft with draglines, with horizontal dimensions of 1700 ft in length and width. The trench is dug to the top of the confining bed beneath the aquifer. The excavated trench is filled with a slurry of water and bentonite. When the desired depth is reached, a mixture of soil (or cement) and bentonite is installed.

A trench wall costs \$3.50–5/vertical ft^2, installable at rates of 1000–3000 vertical ft^2/d. If there are four walls, say, 1700 × 60 ft each, installed at \$4.25/vertical ft^2, the total cost is in excess of \$1.74 million.

The foregoing assumes excavation down to a confining bed, a formation through which groundwater passes with very great difficulty or not at all. If it is not possible to reach the bed, then the bottom needs to be sealed with a grout curtain of cement, silicone rubber, epoxy resins, lime, fly ash, or some other essentially impermeable material, depending upon the permeability of the surrounding soil. In some cases, the grout is injected through pipes. Adding grout, of course, increases the cost. Geraghty noted that adding grout may slow contamination seepage materially, but not stop it entirely, since, as noted before, "everything eventually leaks." Normal maximum feasible grout injection depth is 50–60 ft.

Other installations or approaches encompass sheet piling cutoff walls (to 100 ft down), floor seals, wellpoint systems (with special screening; limited to about 25 ft), drains, biological or chemical fixatives (newer approach needing considerable "shakedown"), and deep injection wells. The injection well approach involves gravity drainage of contaminant plume material or pumping to the surface with subsequent reinjection, depending upon geohydrological conditions. These deep wells must be fully isolated hydraulically from fresh potable groundwater.

Remedial measures

The effort to decontaminate groundwater is in its very early stages, but attempts are being made. Also, nature itself sometimes renders an "assist" by adsorbing certain contaminants to a sufficient degree as to reduce their mobility and concentration. Various underground materials may act as adsorbents, such as certain types of clay. Also, microbial action may help break toxic organics down to simpler, nontoxic forms. However, the extent to which these natural processes work needs to be better defined and quantified.

Human efforts might also lend a hand. For instance, waste-specific measures may be taken. Heavy metals could be insolubilized with alkalis or sulfides. Cyanides can be destroyed with oxidizing agents. Fluorides may be precipitated with calcium ions. Reducers could handle hexavalent chromium, and render it insoluble.

If organic wastes, either dissolved in water or in separate phase, are present, they might be treated with bacteria injected in quantity into the aquifer. But there are problems with both chemical and biological treatment. For instance, how does one guarantee that complete mixing of the treatment reagent(s) occurred in the aquifer? How well would bacteria degrade aquifer contaminants in situ? How can one be sure that enough reagents or biological agents were added to neutralize the contaminants, but not enough to cause contamination of their own or contamination through undesirable side reactions? To answer these questions, intensive monitoring would be needed.

Another approach might be to pump up the contaminated groundwater, treat it at the surface, and either recharge the aquifer or use the treated water, say, as industrial makeup water. Pumping, in turn, would bring uncontaminated groundwater into the pumping well's cone of influence, thereby reducing contaminant concentration. But will this approach bring up sufficient contaminated water, and, through the underground dilution process, reduce contaminant levels in the groundwater to within whatever the EPA or state standards happen to be? Moreover, if the contaminated groundwater is pumped up for treatment, will there be enough clean water in the aquifer itself to effect the necessary in situ dilution? Or will more contaminated fluid flow into the well's cone of influence?

These and many other questions

bedevil the efforts of those seeking to restore contaminated groundwater. It may also be that some contaminated aquifers cannot be rehabilitated no matter what is done.

Some specific remedies

Near Regina, Sask., Canada, an underground pipe break caused a loss of 6800–21 000 L of PCB- and chlorobenzene-containing transformer oil. The clay formations into which these substances seeped were heavily fractured. High PCB levels were found throughout 6–8 m of this clay; and it could migrate as an oil because of the clay's low sorptive capacity. There was a clear threat to groundwater used for both domestic and industrial purposes.

The recommended remedy included removing 10 000–20 000 m^3 of soil contaminated with these substances. Further information on this episode and countermeasures are available in Publication No. NRCC 17586 from Publications, National Research Council of Canada, Ottawa, Ontario KlA OR6, Canada. The price is $5.

Another case involved contaminated water at the U.S. Rocky Mountain Arsenal (RMA) near Denver, Colo. The problem involved toxic organic chemicals, especially diisopropyl methylphosphonate (DIMP, a by-product of nerve gas manufacture) and dicyclopentadiene (DCPD, used to produce pesticides). Impoundment of the contaminated water was accomplished as early as 1957 in a basin lined with a waterproof membrane. Nevertheless, as late as the mid-1970s, Colorado health officials detected DIMP and DCPD in surface and groundwaters off-post, and served RMA with a Cease and Desist Order in 1975.

These substances had to be removed from water prior to discharge. The most promising methods appeared to be anionic-exchange resins and activated carbon, Carl Loven, chief of RMA's Process Development and Evaluation Division, said. Anionic-exchange resins, while very efficient, proved to be uneconomical. The choice narrowed down to powdered or granular activated carbon (GAC), and GAC was the final choice.

RMA pilot-tested "virgin" and reactivated GAC with a five-column system provided by Calgon Corp. (Pittsburgh, Pa). Four of the columns were filled with GAC, and the fifth with coal and sand filter media.

Loven said that the amount required to treat 1000 gal was 0.877 lb of reactivated GAC. He noted that it greatly outperformed "virgin" GAC, perhaps because of the greater percentage of larger pores in the reactivated carbon, and the large (180.17) molecular weight of DIMP. But both types of carbon reduced DIMP levels from 4000 ppb to less than 5 ppb (lower detection limit) with an empty-bed contact time of 30 min.

The arsenal also constructed a subsurface barrier to block contaminated groundwater flow. This barrier was built by filling a 3-ft-wide, 1500-ft-long trench dug 25-ft down to a clay shale layer. The barrier material consisted of soil and impermeable bentonite clay.

This barrier construction was a pilot project that has operated successfully for two years, Loven told *ES&T*. It is now being expanded to 6800 ft, the length needed for total contaminated groundwater containment treatment. However, attempts are being made to control the "sources" of these migratory contaminants to avoid "perpetual operation" of the barrier systems, Loven said.

Prevention is better

In essence, technologies could be developed to treat contaminated groundwater in situ or at the surface. Metals, for example, may be insolubilized or handled by physical or chemical means, as might anions. Organics could be stripped by aeration, if volatile; oxidized with air, oxygen, or ozone; adsorbed on carbon, polymers, or resins; or decomposed by waste-specific microorganisms. Probably, better cleanup can be achieved at the surface after the water is pumped up, rather than when the water is in its original ground formation.

Other approaches entail the physical containment of a contaminated groundwater plume by methods described previously. A main problem is that even with extensive and dense monitoring networks, it may be difficult or even impossible to tell what contaminant went where. For instance, cations may migrate in groundwater at one speed, anions at another, water-soluble organics at yet another speed, and separate-phase liquid organics in ways characteristic to them.

In other words, groundwater contamination and cleanup is a formidable task, perhaps uneconomical, or even technically infeasible in many cases. The idea is, then, through protection mechanisms such as industrial zoning, potential contamination episode response, strict chemical storage rules, sewer leakage repair, and other means, to prevent contaminants from reaching aquifers in the first place.

—Julian Josephson

MSA INSTRUMENTS in the NEWS

COMBUSTION CONTROL • HEALTH & SAFETY • ENVIRONMENTAL • PROCESS

On-stack oxygen analyzer saves fuel while measuring emissions.

MSA's new Model 803 Oxygen Analyzer was designed to solve many of the practical operating problems that you face in accurate monitoring of hot, dirty flue gases.

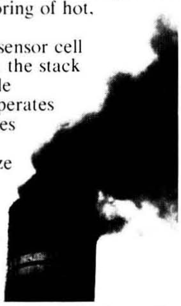

The Model 803 sensor cell mounts directly on the stack for shortest possible sampling line. It operates hot to keep all gases above their dew points and minimize plugging. The stabilized fuel cell sensor measures oxygen—not an effect of oxygen—so it produces a high-level signal. It analyzes 0.1% to 21% O_2. The lower the oxygen concentration, the better the readability on its logarithmic scale.

Users of the Model 803 Oxygen Analyzer have commented on its fast response to changes in furnace operating conditions. And its close matchup between oxygen readings and theoretical calculation of O_2 content gave them fuel savings that paid for the analyzer quickly.

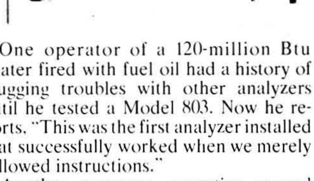

One operator of a 120-million Btu heater fired with fuel oil had a history of plugging troubles with other analyzers until he tested a Model 803. Now he reports, "This was the first analyzer installed that successfully worked when we merely followed instructions."

Another company, operating several marine-style 20,000-lb steam boilers, liked the demonstration of the 803 so well that they kept the demonstration model and ordered another for full evaluations.

If you need a dependable, accurate oxygen analyzer that stays out of trouble and saves you fuel, get details on the Model 803.

CIRCLE 31

Factory cuts fuel bill for dryer in half by monitoring combustible solvents.

The printing and dyeing operation in a fabric finishing plant involved the removal of mineral spirits from the cloth in a gas-heated dryer. Insurance regulations called for control of solvent vapor below 15% LEL. To achieve this level, the operator was forced to change air in the dryer as often as four times a minute—wasting fuel and heat.

An MSA instrument specialist studied the problem, came up with a two-point combustible gas analyzer system with sensors mounted in strategic monitoring points. The MSA instrument system monitors and measures the concentrations of combustible vapors so accurately that the dryer can be operated safely at much higher solvent concentrations. That translates directly to fuel savings.

The analyzer was set up to provide an audible alarm at 20% LEL; if the vapor concentration reaches 25% LEL, it automatically shuts off the gas, starts the fan, and increases the amount of makeup air to reduce vapor concentration. Result: The plant is a safer place to work. The insurance firm has since increased the allowable top limit to 30% LEL. The company saved half of its annual fuel bill for operating the dryers, and savings have already paid for the MSA instrument system. The plant is planning a similar installation in its finishing department.

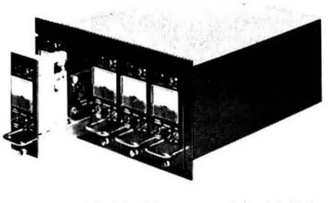

CIRCLE 32

New carbon monoxide indicator joins the MSA portable instrument line.

MSA now offers a battery-operated CO indicator that will work a full shift between charges. The Portable Carbon Monoxide Indicator, Model 70, provides over eight hours of detection of airborne CO in the 0-100 parts per million (ppm) range or 0-500 ppm range.

The Model 70 helps you keep track of "the silent killer" in garages, loading docks, coke plants, open-hearth furnaces, manufacturing plants, refineries and similar locations. When CO concentrations reach preset TLV levels, the instrument provides a visual alarm, plus an audible alarm if you wish. The alarm point can be set at any desired level.

For compliance records, the Model 70 CO Indicator is calibrated for use with a 1-volt recorder, or it can be adapted easily to other recorders.

Recharging is by 115-volt ac source or from a 12-volt battery. Maintenance on this solid-state unit is simple. A calibration check kit is available for reproducible testing and certification.

Ask your MSA instrument specialist for more details or write for literature.

CIRCLE 33

Questions about OSHA limits on hazards?

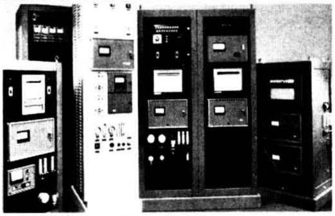

MSA has some answers.

Your workplace atmosphere must meet OSHA regulations on over 500 gas, vapor and dust hazards whose TLVs (Threshold Limit Values) have been determined.

MSA has the spot and continuous monitoring instruments to help you detect most of the hazards on the official list.

One way to start on your hazardous-atmosphere monitoring problems is to discuss them with an MSA field representative.

CIRCLE 34

Make sure/check MSA

Call us (we're in the Yellow Pages). Or circle the appropriate Reader Service Number. MSA Instrument Division, 600 Penn Center Boulevard, Pittsburgh, PA 15235.

Adsorption on carbon: solvent effects on adsorption

The interactions between solute, solvent, and sorbent, including Georges Belfort's adaptation of the solvophobic theory to include solvent effects in the equilibrium adsorption process, are discussed

The first part of this article described the overall process of adsorption, emphasizing the steps of adsorption, the important factors affecting adsorption, and the physicochemical character of activated carbon itself. The various well-known and not-so-well-known equilibrium theories of adsorption were presented, as well as theories for predicting competitive adsorption. One major limitation of the theories is that they all originally derived from gas- and vapor-phase adsorption and thereby *a priori* ignored the presence of the solvent during adsorption of solute. Also, they all need single-solute isotherm data to predict multisolute competitive adsorption. Other empirical mathematical equations represent the data without attempting to establish a physical model.

In this part, the first attempts to include the presence of the solvent and its surface tension, suggested by Traube nearly 100 years ago in the equilibrium adsorption formalism, are discussed. A semiempirical quasi-theoretical approach based on partial solubility parameters called the net adsorption energy approach is presented. Then a general comprehensive solution interaction approach, originally developed by Sinanoğlu and co-workers and recently adapted to the adsorption of organic homologues from dilute aqueous solutions by Belfort, is presented.

Ranking adsorption capacity

Since hydrophobic interactions are thought to play a dominant role in activated carbon adsorption of nonpolar (or nonpolar moieties of) solutes, a short introduction on the origin of these interactions is presented after discussing the significance of ranking adsorption capacity and describing other correlation attempts.

> *Such organic substances as alcohol, fatty acids, aldehydes, ketones, amines, and other organic nonelectrolytes or weak electrolytes, lower surface tension to a greater degree as the length of the carbon chain increases in the homologous series.*
>
> I. Traube, 1880s

Since the ultimate objective is to develop a predictive theory for preferential adsorption in the aqueous phase, it is natural to ask why it is necessary to rank adsorption capacity of different organics either alone or, more importantly, in competition with other organics. Belfort provided an answer to this question, "Because most real systems have more than one organic solute (multisolute) in the feed solution, the preference of adsorption for, competition between, and chromatographic elution by different solutes are clearly related to the process removal efficiency. In a larger sense, they are also related to the ability of the process to produce an acceptable effluent quality that meets the imposed standards. By developing a formalism to predict ranking of adsorption capacity for different organics in competition, a better understanding of these complications should result."

Previous correlation attempts

By using the same type of adsorbent and identical solution conditions, different workers have attempted to correlate single-solute adsorptive capacity with molecular weight, solubility, functionality, and position of substitution. The results indicate the following general trends. Capacity for adsorption will:

- increase with molecular weight as a homologous series is ascended
- decrease with solute polarity and solubility
- decrease for the position of substitution for hydroxy and amino-benzoic acids in the order ortho, para, and meta
- decrease with branching.

Many exceptions to these trends are at present unexplained.

Dr. Georges Belfort
"We are obviously aware of the wide significance of our results."

Despite all the attempts at correlating the extent of adsorption with these variables, not one parameter has emerged in predicting the dominant effect of adsorption. In fact, the most recent attempts at correlating the extent of adsorption with specific single-solute parameters (R. J. Martin and K. S. Al-Bahrani, *Water Research,* Vol. 10, 1976, p. 731; Vol. 11, 1977, p. 991; Vol. 12, 1978, p. 879) or with nonspecific surrogate parameters, such as TOC, UV, emission fluorescence scanning, fixed wavelength fluorescence (Brodtman and co-workers, 1976 ACS National Meeting, Miami Beach, Fla., 1978), were unsuccessful in obtaining meaningful correlations.

Dr. Belfort believes that a comprehensive fundamental theory incorporating all the variables (i.e., multidimensional approach) is needed to successfully describe the extent of adsorption. It is probably not reasonable to expect a one-dimensional approach to provide a consistent predictive correlation. Because of the complex interrelationships between the single variables mentioned above, a cloudy picture with partial success has emerged from the literature. Using the fundamental multidimensional approach of the solvophobic thermodynamic theory, Dr. Belfort already has been able to correlate the extent of adsorption with polar, steric, and/or nonpolar parameters that describe solute/solvent interaction forces (*ES&T,* Vol. 13, No. 8, 1979, pp. 939–46).

Some confusion has arisen with respect to hydrophobic interactions. Dr. Belfort explained that "several people have misunderstood the origin of these (hydrophobic) interactions and have coined the term *hydrophobic bonds,* which could incorrectly imply the existence of attractive forces associated with such a bond. Why nonpolar hydrocarbonaceous group, moieties, or surfaces often find themselves associated in aqueous solution has been steadfastly explained by Hildebrand as follows: There is no *hydrophobia* between the hydrocarbonaceous surfaces and water, just not enough *hydrophilia* to pry apart the hydrogen bonds of water. Like entropy is a measure of disorder, so the hydrophobic effect is a measure of *negative hydrophilia.*" This phenomenon has been used by Belfort and others to explain why many dissolved organic compounds with nonpolar moieties or regions are more easily adsorbed on activated carbon than more polar organic compounds, everything else being equal.

Solubility parameter approach

Hildebrand and co-workers developed (J. H. Hildebrand and R. L. Scott, "The Solubility of Nonelectrolytes," 3rd ed., Dover, N.Y., 1964; "Regular Solutions," Prentice-Hall, Englewood Cliffs, N.J., 1962) the solubility parameter theory, which predicts that the solvency increases as the solubility parameter, δ, of the solvent approaches that of the solute.

Hildebrand suggested that for relative nonpolar solutes (i) and solvents (j), their interaction energy was mostly dispersive and proportional to the number of electrons in i (n_i) and to the polarizabilities of the electrons of i (α_i) and j (α_j). With the assumption that n_i is approximately proportional to the molar volume of i ($\bar{v}_i$) and the definition that the total solubility parameters [δ_T^i and δ_T^j] are proportional to polarizabilities (α_i and α_j) respectively, a molar interaction energy, E_{ij}, can be defined for breaking all the i–j bonds. Conceptually, this bond disruption process is analogous to the vaporization of i from j:

$$j - i - j = j - j + i \qquad (1)$$

where half as many bonds are formed as are broken. The energy change ΔE_v for this reaction is given by:

$$\Delta E_v = 2E_{ij} - E_{jj} \qquad (2)$$

The major thermodynamic relations for this theory are summarized in Table 1. Quoting Belfort, "The undeniable simplicity of this theory is expressed through the simple relationship of Equation 5, where the total solubility parameters are expressed through the vaporization energy (or via an empirical relationship between vaporization energy and boiling point) and molar volume (molecular weight divided by density)."

Snyder describes in his recent review article (CHEMTECH, Vol. 10, No. 3, 1980, pp. 188–93) various ways in which the Hildebrand treatment can be "patched up" to include polar solvents such as water. Thus, Hansen, and later Karger and Snyder, refined the solubility parameter theory and extended the possible solvent-solute interactions from mainly nonspecific dispersion (London) forces to dipole interactions (permanent and induced) and to hydrogen bonding. The partial solubility parameter relations are shown in Table 2.

"McGuire and Suffet, using the separable formalism of the partial solubility parameters, defined a net adsorption energy for the adsorption of solute from a dilute solution onto a sorbent," Belfort said. This net adsorption energy is expressed for low surface coverages in McGuire et al.'s paper (*J. Am. Water Works Assoc.*, Vol. 70, 1978, pp. 565–72) as:

$$E_T^A = E_{is}^A - E_{js}^A - E_{ij}' \qquad (9)$$

where E_{is}^A is the energy of the affinity of the solute i for the surface phase, s; E_{js}^A is the energy of the affinity of the solvent j for surface phase, s; and E_{ij}' is the energy associated with the affinity of the solute for the solvent phase. Belfort quoted from McGuire et al.'s paper, "The component energy terms are calculated using component values of the δ_T of the organic compounds (Table 3)."

"Using this quasi-theoretical approach, McGuire and Suffet have been able to qualitatively rank adsorption capacity with net adsorption energy for widely differing organic compounds," Belfort continued. "Much work is still needed to firm up both relative and absolute quantitative estimates of several of the partial solubility parameters. For example, arbitrary relative values for the acid and basic solubility hydrogen bonding parameters are assigned to compounds of different

Nomenclature

A = Molecular surface area, Å^2
B = Interatom potential correction factor
D = Clausius–Mosotti function, see Table 5
$\mathcal{D}$ = Function of static dielectric constant, Clausius–Mosotti function at high frequency
E_{ij} = Molar interaction energy, kcal mol^{-1}
E_{is}^A = Energy of affinity for surfaces, kcal mol^{-1}
E' = Energy of affinity of solute for solvent, kcal mol^{-1}
$-f(Q', Q'')$ = Results from the integration of the interaction over the first discrete solvation layer
ΔG_{cav}^{net} = Standard free energy of cavity formation, see Equation 21a, kcal mol^{-1}
$\Delta G_{(gas)}^{assoc}$ = Standard free energy change for the association reaction in the gas phase, kcal mol^{-1}
$\Delta G_{(solvent)}^{assoc}$ = Standard free energy change for the association reaction in the solvent, kcal mol^{-1}
ΔG_{es}^{net} = Standard free energy change of solute–solvent electrostatic interaction, kcal mol^{-1}
ΔG_{mix}^{net} = Standard free energy of mixing process, kcal mol^{-1}
ΔG_{red}^{net} = Standard free energy of reduction due to presence of solvent, kcal mol^{-1}
$\Delta G_{(solvent\ effect)}^{net}$ = Difference of solvent- and gas-phase free energy change (Equation 19), kcal mol^{-1}
ΔG_{vdw}^{net} = Standard free energy of solute–solvent van der Waals interaction, kcal mol^{-1}
k^H = Henry's law constant, atm
K_f = Freundlich adsorption capacity at unity solution concentration, mol g^{-1}
K_{soln} = Equilibrium constant for solute–carbon adsorption process
n = Refractive index
N = Avogadros number, molecules mol^{-1}
P = Pressure, atm.
p_i = Partial pressure, atm
$\bar{p}_i$ = Adsorption capacity
$\mathcal{P}$ = Function of polarizability and molecular volume
Q_m' = Adsorption capacity, g mol g^{-1}
$Q^o b$ = Langmuirian adsorption capacity or Henry's constant at infinite dilution, Lg^{-1}
R = Gas constant, J (mol-K)$^{-1}$
R_i = Molecular diameter, Å
$\bar{v}$ = Molar volume, cm^3
W = Entropy and energy correction for the interfacial tension between solute and solvent
x_i = Mole fraction of i in solution
X = Liquid mole fraction
Y = Vapor mole fraction
α = Polarizability, Å^3
δ = Interfacial tension, ergs/cm^2
δ_T = Total solubility parameter
δ_J = Partial solubility parameter of species i and interaction j
Δ = Function of ionization potential (Table 5), eV
ϵ = Static dielectric constant of solvent
ϵ_0 = Permittivity constant, C^0 (J-M)$^{-1}$
Θ = Dilute solute adsorption constant (Equation 22), kcal mol^{-1}
κ^e = Curvature correction fitting parameter for surface tension, (Table 5)
ν = Molecular volume, Å^3
σ = London parameter, Å
ω = Accentric factor
μ = Dipole moment, Debyes

solubility without theoretical justification. In addition, the partial polar parameter is not calculated directly but is obtained by subtracting the partial dispersion and hydrogen bonding solubility parameters from an estimated total solubility parameter."

Belfort believes that with additional refinements to the method and better estimates of the partial solubility parameters for different compounds, the solubility parameter approach should be evaluated first with similar (homologous) and later with different organic compounds for the adsorption from solution. Only after such a comprehensive study, he believes, will this approach be on firm ground. "McGuire and Suffet's contribution," Belfort maintained, "has been to emphasize the importance of the solute, solvent, and sorbent interactions in the liquid phase. This should not be underestimated."

Other more general limitations with the modified (partial) solubility parameter approach still remain, according to Belfort, especially for semipolar organic compounds and the very polar water solvent.

Even with the refinements described earlier, Belfort quoted Snyder, "(the) solvents which comprise alcohols and water give poor agreement with theory due to self-association and deviations from regular solution behavior."

In spite of these limitations, Belfort believes that the solubility parameter or net adsorption energy approach that McGuire and Suffet have adapted for the aqueous adsorption of organics onto activated carbon, provides a useful semiquantitative screening method for estimating the relative adsorption capacity (rank order) of different organics.

Comprehensive solution interaction

It has been known for nearly a hundred years (see Traube's quotation) that solvent and sorbent properties play an important role during the adsorption of organics from dilute aqueous solutions onto solid surfaces. Belfort pointed out that 50 years ago Holmes and McKelvey (*J. Phys. Chem.*, Vol. 32, 1928, p. 1522), in a particularly elegant experiment, showed how the order of adsorption of a homologous series of alkyl fatty acids was reversed when a polar sorbent (silica gel) and nonpolar solvent (toluene) were replaced by a nonpolar sorbent (carbon) and a polar solvent (water).

In this discussion, the thermodynamic basis for the equilibrium adsorption process incorporating the presence and influence of the solvent is presented.

TABLE 1

Major thermodynamic relations for the solubility parameter approach

Process	Interaction energy	Equation no.
Net electrostatic attraction of solute (i) and solvent (j)	$E^{\circ}_{ij} = n_i \alpha_i \alpha_j$	(3)
Disruption of solute (i) and solvent (j) bonds per mole i	$E_{ij} = \bar{v}_i \delta^i_T \delta^j_T$	(4)
Vaporization of solute (i) from solvent (j)	$\Delta E_v = 2E_{ij} - E_{jj}$	(2)
Vaporization of pure (i)	$\Delta E_v = 2E_{ii} - E_{ii}$ $= E_{ii} = \bar{v}_i (\delta^i_T)^2$	(5)

Source: L. Snyder, "Solutions to solution problems–1," CHEMTECH, Vol. 9, 1979, pp. 750–54.

TABLE 2

Partial solubility parameter relations

Interaction	Equation	Equation no.	Definition
Total	$\delta_T^2 \equiv \delta_d^2 + \delta_p^2 + \delta_h^2$ (Definition)	(6)	—
Dispersion	δ_d^2	—	—
Polar	$\delta_p^2 \equiv \delta_0^2 + 2\delta_{in}\delta_d$ (Definition)	(7)	δ_0 = Permanent dipole component δ_{in} = Induced dipole component
Hydrogen bonding	$\delta_h^2 \equiv 2\delta_a\delta_b$ (Definition)	(8)	δ_a = Acidic (proton donor strength component) in hydrogen bonding δ_b = Basic (proton acceptor strength component) in hydrogen bonding

Source: B. L. Keller and L. R. Snyder, "The Use of Solubility Parameters in Predicting Chromatographic Retention and Elutropic Strength," In "Gas Chromatography," R. Stock, Ed., London Institute of Petroleum, 1971.

TABLE 3

Major relations and assumptions for the net adsorption energy approach

Process	Interaction energy	Equation no.	Assumptions
Net adsorption of solute/solvent onto surface	$E^A_T = E^A_{is} - E^A_{js} - E'_{ij}$	(9)	—
Solute (i)–surface (s) interaction	$E^A_{is} = \bar{v}_j(\delta^i_d \delta^s_d)$	(10)	Dispersion forces dominate
Solvent (j)–surface (s) interaction	$E^A_{js} = \bar{v}_j(\delta^j_d \delta^s_d)$	(11)	Dispersion forces dominate
Solute (i)–solvent (j) interaction	$E'_{ij} = \bar{v}_i(\delta^i_a \delta^j_b + \delta^j_a \delta^i_b)$	(12)	Hydrogen bonding dominates

Source: Michael J. McGuire, "The Optimization of Water Treatment Unit Process for the Remova. of Trace Organic Compounds with an Emphasis on the Adsorption Membranes," Thesis in partial fulfillment of the requirements for the degree of Ph.D., Drexel University, Published by Xerox University Microfilms, Ann Arbor, Mich., 1977.

A number of theoretical expressions have been proposed to estimate the effect of a solvent on reaction kinetics or equilibria. Since the dominant, though not the only, interactions for the adsorption of nonpolar (or nonpolar moieties of) solutes onto activated carbon are hydrophobic (see Part 1), a theoretical approach successfully describing these interactions is desirable. Most theoretical approaches are based on a thermodynamic analysis for the transfer of solute from water to a nonpolar liquid (C. Tanford, *J. Am. Chem. Soc.*, Vol. 84, 1962, p. 4240; *Science*, Vol. 200, 1978, p. 1012; "The Hydrophobic Effect," Wiley-Interscience, N.Y., 1973). Other expres-

FIGURE 1

Illustration of the individual terms involved in the solvent effect (concept after Sinanoğlu)[a]

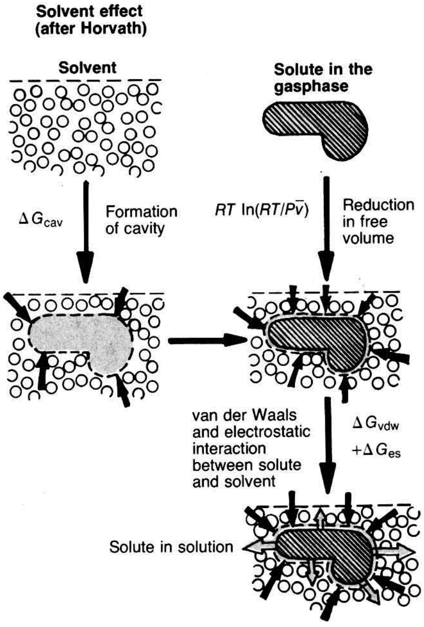

[a] Reprinted from C. Horvath and W. Melander, *American Laboratory*, Vol. 10, No. 10, 1978, p. 22. Copyright 1978 by International Scientific Communications, Inc.

sions deal with the influence of the dielectric constant of the solvent on reaction rates or equilibria. Statistical thermodynamic analysis of aqueous solutions has also been used in this regard. Although these approaches provide useful insight, they are either incomplete or not readily applicable to the problem at hand.

Solvophobic theory. Belfort and Altshuler thus have invoked a general thermodynamic treatment for describing the effect of various solvents on reaction rate constants and equilibria. The solvophobic theory was developed by Sinanoğlu and co-workers (for an excellent review of the theory, see O. Sinanoğlu, "Solvent Effects on Molecular Associations," In "Molecular Associations in Biology," B. Pullman, Ed., pp. 427–45, Academic Press, New York and London, 1968) and tested to estimate the effect of solvents on several types of reactions, including isomerization, association, and conformational changes. In principle, the theory employs readily available physicochemical data without the use of adjustable parameters.

Besides Belfort's adaptation of the solvophobic theory to adsorption (*ES&T,* Vol. 13, No. 8, 1979, pp. 939–46; "Selective Adsorption of Organic Homologues onto Activated Carbon from Dilute Aqueous Solutions: Solvophobic Interaction Approach-II," presented before the Division of Environmental Chemistry Symposium, ACS 179th National Meeting, Houston, Tex., March 23–28, 1980), Horvath and co-workers previously adapted this theory to the hydrophobic effect in reversed-phase chromatography (C. Horvath and W. Melander, *Am. Lab.,* Vol. 10, No. 10, 1978, pp. 17–36; C. Horvath, W. Melander, and I. Molnar, *J. Chromatog.,* Vol. 125, 1976, pp. 127–56). More recently, however, Melander and Horvath have also recognized the potential of the solvophobic approach to the adsorption of organic substances from dilute aqueous solutions by nonpolar adsorbents. In a forthcoming chapter, they review the thermodynamics of hydrophobic adsorption without testing the theory with experimental adsorption data ("Thermodynamics of Hydrophobic Adsorption," In "Activated Carbon Adsorption of Organics from the Aqueous Phase, Vol. I," I. H. Suffet and M. J. McGuire, Eds., Ann Arbor Science Publishers, Inc., Ann Arbor, Mich., 1980, Chapter 3, pp. 65–89). Their approach, as indicated by Belfort in his earlier paper, is similar to that used by Horvath et al. for reversed-phase liquid chromatography.

In solvophobic treatment, the effect of the solvent on the association reaction under consideration is obtained by subtracting the standard free energy change for the reaction in solution minus that in the gas phase under a unitary standard state ($x^{\circ}_{k} \equiv 1$, $p^{\circ}_{k} \equiv 1$ atm ideal gas). Using the equations summarized in Table 4, we get:

$$\Delta G^{\text{net}}_{\text{(solvent effect)}} = \Delta G^{\text{assoc}}_{\text{(solvent)}} - \Delta G^{\text{assoc}}_{\text{(gas)}} = RT \ln \left[\frac{k^{\text{H}}_{\text{SiC}}}{k^{\text{H}}_{\text{Si}} k^{\text{H}}_{\text{C}}}\right] \quad (19)$$

In order to conceptualize the solvent effect, Sinanoğlu proposed that the dissolution process takes place in two steps as illustrated in Figure 1. First, a hole or cavity needs to be prepared in the solvent to accommodate the solute molecule; second, after the solute is placed into the cavity, it interacts with the solvent. As shown in Figure 1, a total standard unitary free energy change can be assigned to each of these steps, for species k. Belfort pointed out, "Conceptually, this hypothetical process is the reverse of the solubility parameter approach in which bond disruption analogous to vaporization is proposed."

The energy associated with the formation of the cavity, ΔG_{cav}, is proportional to the surface area of the solute molecule and the corrected macroscopic surface tension of the solvent to take into account the highly curved rather than flat surface of the solute molecule. The value of this surface tension, which has been obtained and used in the solvophobic theory, can differ considerably from its usual value. Sinanoğlu has developed empirical curves relating the surface tension correction with cavity size for nonpolar and polar liquids.

Transferring a solute molecule from the gas phase into the solvent is accompanied by an entropy reduction. This free volume reduction has been termed the cratic term and is calculated directly from $RT \ln (RT/P\bar{v})$. The energies related to cavity formation and free volume change both have the same sign.

After the solute is placed into the prepared cavity, it will interact with the solvent. This energy of interaction, ΔG_{int}, comprises:

- van der Waals interactions due to dispersion forces, ΔG_{vdw}, which are roughly proportional to the molecular surface area

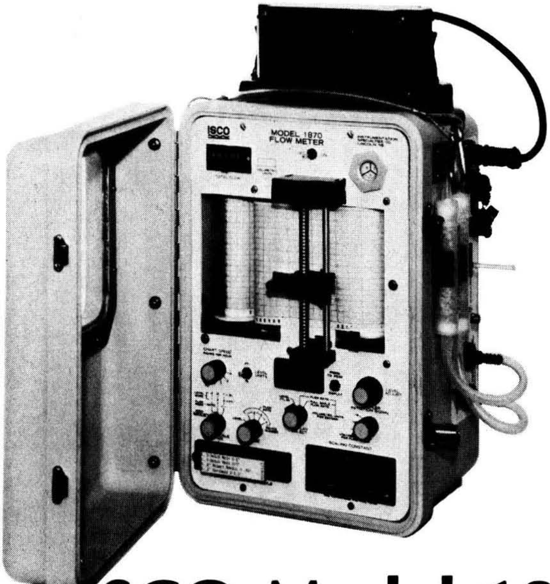

The ISCO Model 1870

All the features you demand in an open channel flow meter... And then some.

ACCURACY

When measuring flow in an open channel, accuracy is important, and you get it with the ISCO Model 1870. A sensitive electronic pressure transducer specially selected for minimal temperature coefficient provides a maximum level measurement error of ±0.75 percent full scale. A microprocessor based module provides level-to-flow conversion with an error of less than 0.05 percent.

VERSATILITY

The plug-in module can be programmed and reprogrammed for four different primary devices. With additional modules and the ability to program them for any primary device or other open channel application, the adaptability of the Model 1870 is limitless. Liquid level can be recorded, or flow rate can be recorded and totalized in any volumetric unit. Operable on 12VDC battery or 117VAC line power, the Model 1870 adapts to either temporary or permanent installations.

DURABILITY

The Model 1870's electronics, based on highly reliable CMOS integrated circuitry, are housed in a fully-gasketed, high-impact case that will withstand moisture and accidental submersion. The Nicad battery with long recharge life will not freeze or spill acid.

CONVENIENCE

The self-contained Model 1870 features an externally accessible battery and can be mounted practically anywhere, in any position — not necessarily over or even close to the flow stream. Flow or level data is continuously recorded on an easy-to-read 4-inch strip chart with a fiber tip pen.

VALUE

Feature for feature, you won't find a better flow meter than the Model 1870. Or a better value. ISCO gives you everything you demand in an open channel flow meter. And then some!

ISCO

3621 N.W. 36th Street
Lincoln, Nebraska 68524 U.S.A.

Phone toll free
(800) 228-4373

CIRCLE 23 ON READER SERVICE CARD

TABLE 4

Thermodynamic basis for defining the solvent effect for adsorption

Concentration	Aqueous phase	Gas phase
Adsorption reaction[a]	$S_i + C \rightleftarrows S_iC$ (13)[b] $x_{S_i} x_C x_{S_iC}$	$p_{S_i} p_C p_{S_iC}$
Equilibrium condition	$\Delta G = 0$ (14a)	$\Delta G = 0$ (14b)
Unitary standard state	$\overset{\circ}{x}_k \equiv 1$ (15a)	$\overset{\circ}{p}_k \equiv 1$ atm (15b) (ideal gas)
Free energy		
Single species free energy	$G_k = G_k^{\circ} + RT \ln x_k$ (16a)	$G_k = G_k^{\circ} + RT \ln p_k$ (16b)
Standard free energy change	$\Delta G^{\circ} = -RT \ln K_{soln}$ (17a) (unitary) $= G^{\circ}_{S_iC} - G^{\circ}_{S_i} - G^{\circ}_C$ (17c)	$\Delta G^{\circ}_{gas} = -RT \ln K_{gas}$ (17b)
Equilibrium contact	$K_{soln} = \dfrac{x_{S_iC}}{x_{S_i} x_C}$ (18a)	$K_{gas} = \dfrac{p_{S_iC}}{p_{S_i} p_C}$ (18b)

[a] Assume S_i is not a polymer and that dilute conditions and Henry's law apply, $K_k^H = p_k/x_k$ for k^{th} species.

[b] Equation numbers given are in the brackets. For the reversible associated adsorption reaction, S_i is the adsorbate, molecules of type i; C is the activated carbon surface; S_iC is the associated (sorbed) complex.

Source: Oktay Sinanoğlu, "Solvent Effects on Molecular Associations," In "Molecular Associations in Biology," B. Pullman, Ed., Academic Press, N.Y., 1968, pp. 427–45.

TABLE 5

Expressions defining the unitary free energy change for the interaction processes [a]

Interaction process	Free energy designation	Expression	Equation no.
Cavity formation	$\Delta G^{net}_{cav,i}$	$\kappa_i^e A_i \gamma_{w,i}(1-W)N$	(21a)
Solvent–solute interaction			
van der Waals	$\Delta G^{net}_{vdw,i}$	$-f(Q'Q'')B_i \Delta_i D_i D$	(21b)
Electrostatic	$\Delta G^{net}_{es,i}$	$-\dfrac{N}{2}\dfrac{\mu_i^2}{\nu_i}\mathcal{D}\mathcal{P}$	(21c)

[a] This table was taken from Georges Belfort's "Selective Adsorption of Organic Homologues onto Activated Carbon from Dilute Aqueous Solutions. Solvophobic Interaction Approach–II," presented before the Env. Chem. Symp. ACS 179th National Meeting, Houston, Tex., March 23–28, 1980. The table, however, was compiled from T. Halicioğlu's Ph.D. thesis entitled "Solvent Effect on the Reaction Rates and Equilibria," Yale University, University Microfilms, Inc., Ann Arbor, Mich., 1969.

- the electrostatic interactions, ΔG_{es}, which are partly dependent on the dipole moment of the solute and the dielectric constant of the solvent. These energies are usually opposite in sign to the energies associated with cavity formation and of the free volume change.

Belfort said that two additional corrective energy terms may also be necessary. For the case of polymer molecules, Henry's law dependence of free energy and entropy on the mole fraction is no longer valid, necessitating an additional energy term, ΔG_{mix}. Sinanoğlu (*Adv. Chem. Phys.*, Vol. 12, 1967, pp. 283-326) has shown that the interaction energy may be reduced by the presence of the solvent with respect to its gas-phase value (ΔG_{red}). This is especially possible for the interaction energy of the adsorbed complex in Equation 13, S_iC. In polymer-polymer interactions, for example, the London dispersion forces are reduced by 15-30% due to the presence of water, according to Sinanoğlu et al. ("Solvent Effects on van der Waals Dispersion Attractions Particularly in DNA," In "Electronic Aspects of Biochemistry," B. Pullman, Ed., Academic Press, N.Y., 1964, pp. 301-11).

For the association process (Table 4, Equation 13), such as (activated carbon) adsorption of organics from dilute aqueous solutions, the individual free energies as shown in Figure 1 are evaluated for each species, k, and summed to obtain a net free energy change associated with the solvent effect. Thus:

$$\Delta G_j^{net} = \Delta G_{j,S_iC} - (\Delta G_{j,S_i} + \Delta G_{j,C}) \quad (20)$$

where j is the type of interaction described above, such as the cavity, van der Waals, and electrostatic terms. The net solvent effect is given by:

$$\Delta G^{net}_{(solvent\ effect)} = \Delta G^{net}_{cav} + \Delta G^{net}_{vdw} + \Delta G^{net}_{es} + \Delta G^{net}_{mix} + \Delta G^{net}_{red} - RT \ln (RT/P\bar{v}) \quad (21)$$

Each of these terms can be calculated with a knowledge of the physicochemical properties of each species using detailed expressions from the literature. In Table 5, taken from Belfort's adsorption paper, the cavity $\Delta G^{net}_{cav,i}$ and interaction terms ($\Delta G^{net}_{vdw,i}$ and $\Delta G^{net}_{es,i}$) are defined for species i.

A varient of Figure 2 was originally published by Horvath and Melander (*Am. Lab.*, Vol. 10, No. 10, 1978, pp. 17-36) to illustrate the surface area reduction and how the forces discussed above for a single solute act for an association process, such as the reversible binding of the solute by the stationary phase in reversed-phase chromatography. Belfort suggested that this figure is equally applicable to the adsorption process. It clearly illustrates (with arrows) the balance of opposing interactions resulting from the solvent effect and its influence on the dominant nonpolar interaction between solute and sorbent.

The major thermodynamic relations for calculating the solvophobic interactions for adsorption in solution are summarized in Table 6. In addition, the overall standard unitary free energy for the association adsorption reaction is related directly through the equilibrium constant to the experimental adsorption capacity coefficient, $\bar{p}_i$. This coefficient is obtained from the isotherm data and characterizes the extent of adsorption for solute i. In fact, it equals Y_i/X_i, or Henry's constant for adsorption, and is obtained from various models that reduce to Henry's law at infinite dilution:

$$(\lim_{X_i \to 0} Y_i/X_i).$$

See Part 1 of this series for additional discussion on which models obey Henry's law. For those models that do not obey Henry's law, such as the Freundlich equation, Belfort pointed out, "Several researchers have arbitrarily chosen some convenient X_i to obtain a corresponding Y_i for comparison of the extent of adsorption of different (organic) solutes. This approach lacks a theoretical basis and

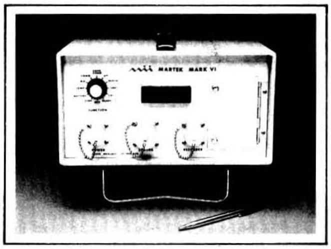
MARTEK MARK VI

How to get a handle on your waste phenol problem.

Ever since the EPA cited phenol as a major pollutant, manufacturers have used traditional methods of eliminating this material from their waste streams. Two of the most popular—oxidation and carbon adsorption—involve high operating costs and produce sludge or secondary pollutants in the process.

Fortunately, there is a proven way to reclaim waste phenol. Amberlite® polymeric adsorbents are not only selective for phenol but regenerable in place using common solvents such as methanol or dilute caustic soda. Phenol from the regenerant solution can then be recycled to the process stream.

Current applications include the use of Amberlite XAD-4 to recover phenolics from bisphenol "A" waste water and Amberlite XAD-7 to recover phenol from brine. Unlike adsorption with activated carbon, there are almost no adsorbent losses on regeneration. And getting a recoverable chemical as a bonus helps to amortize modest system costs.

For technical information on the use of Amberlite polymeric adsorbents for phenol recovery, circle the reader service number or contact Rohm and Haas Company, Marketing Services W80-3, Independence Mall West, Philadelphia, PA 19105.

ROHM AND HAAS
PHILADELPHIA, PA. 19105
A World Leader in Water Treatment

CIRCLE 21 ON READER SERVICE CARD

FIGURE 2

Surface area reduction of amphiphilic solute adsorbed onto activated carbon surface[a]

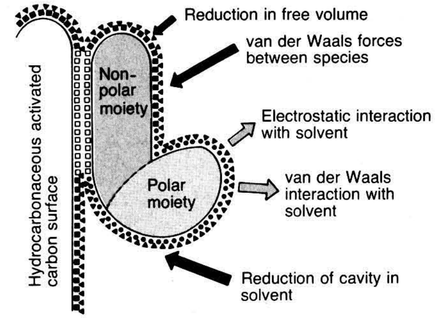

[a] Adapted from C. Horvath and W. Melander, *American Laboratory*, Vol. 10, No. 10, 1978, p. 22. Copyright 1978 by International Scientific Communications, Inc.

TABLE 6

Major thermodynamic relations for calculating the solvophobic interactions for adsorption

Process	Equation	Equation no.
Reversible association of solute (S_i) with sorbent (C).	$S_i + C \rightleftharpoons S_iC$	(13)
Overall standard unitary free energy change for the association in solution	$\Delta G^{assoc}_{(solvent)} = \Delta G^{net}_{(solvent\ effect)} + \Delta G^{assoc}_{(gas)}$	(19)
Equilibrium adsorption for association reaction[a]	$\Delta G^{assoc}_{(solvent)} = RT \ln \bar{p}_i + \Theta$	(22)
Net solvent effect	$\Delta G^{net}_{(solvent\ effect)} = \Delta G^{net}_{cav} + \Delta G^{net}_{int} + \Delta G^{net}_{mix} + \Delta G^{net}_{red} - RT \ln (RT/P\bar{v})$	(21)

[a] Where $\bar{p}_i$ is the adsorption capacity coefficient for solute i; $\Theta = RT \ln[C]$ is a constant for dilute solute adsorption and a given activated carbon; $\bar{p}_i = [C]K_{soln} = [S_iC]/[S_i] = Y_i/X_i$, where Y_i is the amount of solute i adsorbed per unit weight of carbon at equilibrium concentration X_i in solution.

Source: Georges Belfort, "Selective Adsorption of Organic Homologues onto Activated Carbon from Dilute Aqueous Solutions. Solvophobic Interaction Approach–II," presented before the Env. Chem. Symp., ACS 179th National Meeting, Houston, Tex., March 23–28, 1980.

often makes it difficult to compare data between laboratories in which different regions of X_i are studied."

Equations 19, 20, and 21 are used to calculate the overall standard free energy change for the association adsorption reaction in solution:

$$\Delta G^{assoc}_{(solvent)} = \Delta G^{assoc}_{(gas)} + [\Delta G_{cav} + \Delta G_{vdw} + \Delta G_{es} + \Delta G_{mix} + \Delta G_{red}]^{net}_{S_iC-(S_i+C)} - RT \ln (RT/P\bar{v}) \quad (23)$$

where $\Delta G^{assoc}_{(solvent)}$ is related to the experimental adsorption capacity, $\bar{p}_i$, through Equation 22 in Table 6. At this juncture two approaches could be taken. Dr. Belfort explained, "The first approach is to assume that $\Delta G^{assoc}_{(gas)}$ and the cratic term are relatively constant for similar solutes (reasonable for a homologous series) and that the terms in the square brackets for C are constant for a specific activated carbon. The other terms in the square bracket for S_iC and S_i then represent both the adsorbed solute complex/solvent and free solute/solvent interactions. Correlations of parameters that describe these interactions with measured adsorbability were presented in our first paper on solvent effects on adsorption (*ES&T*, Vol. 13, No. 8, 1979, pp. 939–46)."

Belfort continued, "The second approach, which is analogous to that used by Horvath and co-workers at Yale for HPLC, is to substitute the detailed mathematical expression into Equation 23 and, after making several simplifying assumptions, to relate $\Delta G^{assoc}_{(solvent)}$ through the equilibrium constant to the measurable adsorption capacity, $\bar{p}_i$, for different solutes or carbons. Resultant correlations can be used to highlight the dominant interactions. This approach was followed in our second paper in the series on solvent effects on adsorption." See Table 7 for the comprehensive and simplified solvophobic relations that result from this approach. The major assumptions of the model were also listed. For nonpolymers, ΔG^{net}_{mix} can be neglected, while ΔG^{net}_{red} can vary about 15–30% of ΔG^{net}_{vdw} but is probably fairly constant for a homologous series.

In applying the solvophobic theory to cis-trans isomerization of azobenzene in several solvents, Halicioğlu and Sinanoğlu (*Ann. N.Y. Acad. Sci.*, Vol. 158, 1969, pp. 308–17) calculated each of the terms in Equation 24 without the use of an adjustable parameter. In most cases, they found that the solvation or *inverse volume forces* (fourth term on the right side of Equation 24) and the *surface forces* (fifth term on the right side of Equation 24) both strongly affect the molecular association equilibrium or rate constants. The treatment indicates that these two solvent effects usually oppose each other. These trends have also been confirmed by East German scientists Birnstock et al., who determined the influence of solvents on the conformational structure of several organic compounds (F. Birnstock, H-J Hofmann, and H-J Kohler, *Theoret. Chem. Acta* (*Berl.*), Vol. 42, 1976, pp. 311–23). For small solute molecules, the solvation or *inverse volume forces* may dominate; however, as the relative size of the solute molecules increases, *surface forces* may predominate.

Belfort continued, "Although the individual interaction terms can in principle be calculated with the physicochemical properties of the system, it is a very complicated procedure. That the theory can be simplified and still retain its powerful predictive capability is the important point. For relatively large solute molecules in comparison with the size of water molecules, Equations 25 and 26 reduce to the very simple relationships between logarithm of extent of adsorption ($\ln \bar{p}_i$) and the solute molecular surface area (A_{S_i}). Thus, for aqueous adsorption dominated by hydrophobic interactions, all we need to predict adsorption capacity is the total solute molecular surface area."

Molecular cavity surface area. The overall approach taken by Belfort and his group is summarized in Figure 3. Correlations between extent of adsorption ($\ln \bar{p}_i$) and the comprehensive solvophobic model ($\Delta G^{assoc}_{(solvent)}$), the

TABLE 7

Comprehensive and simplified predictive solvophobic relations for correlating adsorption

Model	Application	Relation [a]	Equation no.	Assumptions
Comprehensive	General	$RT \ln \bar{p}_i = \Delta G^{\text{assoc}}_{(\text{gas,vdw})} - \Theta$ $- \Delta G_{\text{vdw},S_i} + \frac{N(\lambda - 1)}{2\lambda} \frac{\mu^2_{S_i}\mathcal{D}\mathcal{P}}{\nu_{S_i}}$ $- N\gamma \Delta A - N\gamma \bar{v}^{2/3}(\kappa^e - 1)$ $\times A_{S_i}/\bar{v}_{S_i}{}^{2/3} - RT \ln RT/(P\bar{v})$	(24)	(i) Nonpolar carbon ($\mu_C = 0$) $\Delta G^{\text{assoc}}_{(\text{gas})} = \Delta G^{\text{assoc}}_{(\text{gas,vdw})}$ (ii) Solute could be polar ($\mu_{S_iC} = \mu_{S_i}$) (iii) Dilute solute concentration ($\Delta G_{\text{vdw},S_iC} = \Delta G_{\text{vdw},C}$) (iv) Solute molecules larger than solvent molecules ($W_i = 0$)
Simplified	Same solvent and carbon for *different solutes*	$RT \ln \bar{p}_i = K_1' + K_2' \frac{\mu^2_{S_i}}{\nu_{S_i}} - N\gamma g A_{S_i}$ Inverse volume force Surface force	(25)	(i) K_1' is a constant equal to all the terms in Eq. 23 but not shown in Eq. 24 (ii) A_{S_i} = constant (V_{S_i}) for quasi-spherical solutes (iii) $\Delta A = gA_{S_i}$, g = constant
Simplified	Same solute and solvent for *different sorbents* (*carbon*)	$RT \ln \bar{p}_i = K_3' - K_4' A_{S_i}$	(26)	(i) Same as (i) directly above for Eqs. 23 and 25

Source: Georges Belfort, "Selective Adsorption of Organic Homologous onto Activated Carbon from Dilute Aqueous Solutions. Solvophobic Interaction Approach–II," Presented before the Env. Chem. Symp., ACS 179th National Meeting, Houston, Tex. March 23–28, 1980.

[a] For symbols see nomenclature list.

TABLE 8

Sources of (equilibrium) adsorption data for testing the solvophobic model [a]

Compounds	Equilibrium	Adsorption duration (hours)	Adsorbent	Adsorption capacity [b] $\bar{p}_i$ (molar basis)	Source
Aliphatics (alcohols, ketones, aldehydes, acids, acetates)	Single solute	2	Westvaco Nuclear GAC (grade WV-G); ground	Q_m'	D. M. Giusti; R. A. Conway; and C. T. Lawson, *J. WPCF*, Vol. 46, No. 5, 1974, pp. 947–65
Aliphatics (alcohol, ketones, aldehydes, acetates)	Single solute	2	Calgon GAC Filtrasorb 400; ground	(K_f,n) and (Q^ob)	W. B. Arbuckle; R. J. Romagnoli, "Prediction of Preferentially Adsorbed Compounds in Bisolute Column Studies," presented at 87th AIChE Natl. Mtg., Boston, Mass. Aug. 19–22, 1979
Aromatics (substituted benzenes)	Single and multisolute	48	Calgon GAC Filtrasorb 400; GAC as is	(K_f,n) single and mixed	M. A. El-Dib; M. I. Badawy, *Water Research*, Vol. 13, 1979, pp. 255–58
Aromatics (alkyl phenols)	Single	4	Amoco's PX-21 sorbent	(Q^o,b)	P. C. Singer; C. Yen, "Adsorption of Alkyl Phenols by Activated Carbon," presented before Div. Env. Chem., ACS 176th Natl. Mtg., Miami Beach, Fla., Sept. 10–15, 1978

[a] Summarized from Georges Belfort, "Selective Adsorption of Organic Homologues onto Activated Carbon from Dilute Aqueous Solutions. Solvophobic Interaction Approach–II" Presented before the Env. Chem. Symp., ACS 179th National Meeting, Houston, Tex., March 23–28, 1980.

[b] Adsorption capacities: Q_m'—arbitrary experimental value; (K_f,n)—Freundlich model; (Q^o,b)—Langmuir model.

total or hydrocarbonaceous surface area of a solute molecule (A_{S_i} = TSA, HSA), and phenomenological parameters—such as partition coefficients, solubility, Taft and Hammet parameters, and steric parameters—are all currently being pursued.

In order to calculate the cavity terms in Equations 24-26, the total surface area of each solute molecule (or hydrocarbonaceous moiety) is needed. Dr. Belfort continued, "We first used A_{S_i}'s from the literature (S. C. Valvani, S. H. Yalkowsky, and G. L. Amidon, *J. Phys. Chem.*, Vol. 80, No. 8, 1976, pp. 829-35) and later obtained the original computer programs for calculating A_{S_i} directly from Hermann at Eli Lilly and Co. The input data for Hermann's program is very bulky and time-consuming to prepare. We therefore developed the Molecular Build program to provide this data automatically. In fact, we have recently developed a simplified version of Hermann's program which provides A_{S_i}'s on a hand calculator within the first decimal point and at a fraction of the cost."

Correlations. The adsorption data

FIGURE 3

Flowsheet for calculating correlation equations for homologous organic series

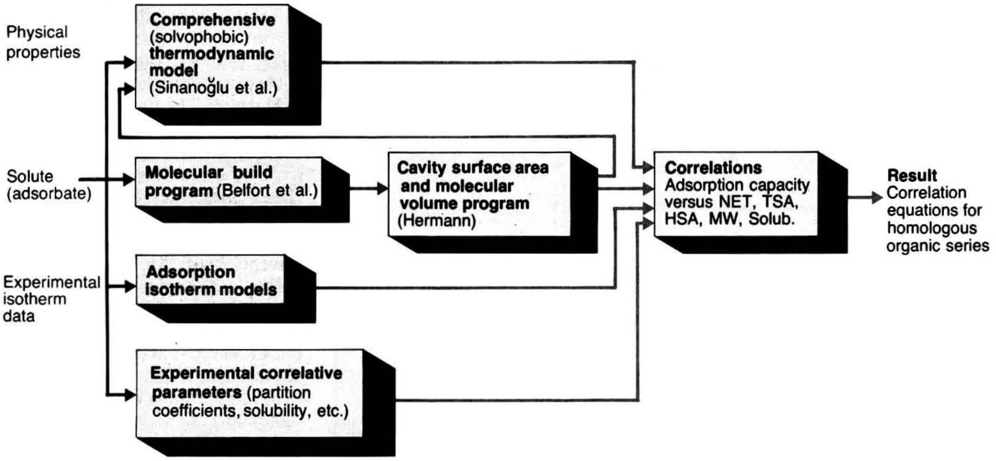

Source: Belfort, G., "Relating Organic Solute–Aqueous Solution Interactions with Removal Processes: Solvophobic Interaction Approach," in preparation. *Gordon Altshuler, Adriano Baglioni, James Mullens, Bob Tonti, and James Nicoletti have worked on the computer aspects of the solvophobic model, experimental adsorption isotherm model, correlative parameters and the molecular build program, respectively. Dr. Kusuma Thallum and Chuck Feerick are currently involved in measuring adsorption isotherms for various homologous series of organic compounds. Funding for these studies at RPI have come from Jesse M. Cohen's Physical Chemical Treatment Section, Municipal Environmental Research Laboratory. U.S. EPA, 26 W. St. Clair St., Cincinnati, Ohio. Jim Westrick was originally and Richard A. Dobbs is, at present, project monitor for EPA on this study.

FIGURE 4

Normalized free energy change[a]

a) Alcohols R-OH **b) Organic acids R-COOH**

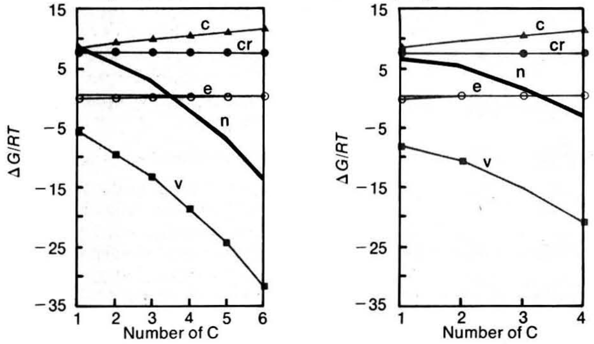

c) Aldehydes R-CHO **d) Methyl ketones C-(R)C=O**

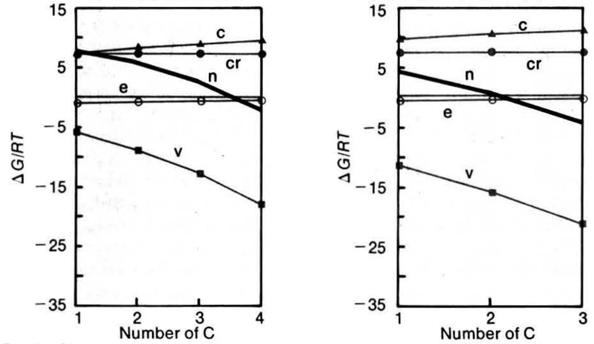

[a] See Equation 21

FIGURE 5

Solvophobic model test[a]

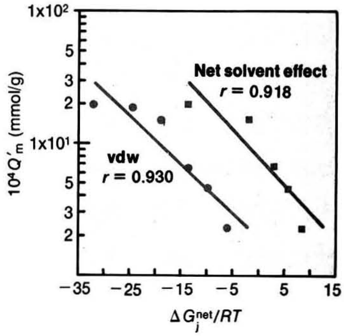

[a] See Equation 24, Table 7

for testing the solvophobic model were taken from four sources and are summarized in Table 8. In this review, a few representative correlations will only be given to show how the theory is used to determine the dominant solute/solvent interactions and to predict adsorption capacity for several homologous groups under single- and multisolute conditions.

In Figure 4, the normalized free energy change for each term in Equation 21 (excluding ΔG_{mix}^{net} and ΔG_{red}^{mix}) is plotted as a function of carbon number for different aliphatic homologous groups. Notice that in all cases the van der Waals dispersion

FIGURE 6

Plot of the logarithm of the extent of adsorption versus hydrocarbonaceous surface area for aliphatic alcohols, ketones, aldehydes, and acids as per the simplified solvophobic model[a]

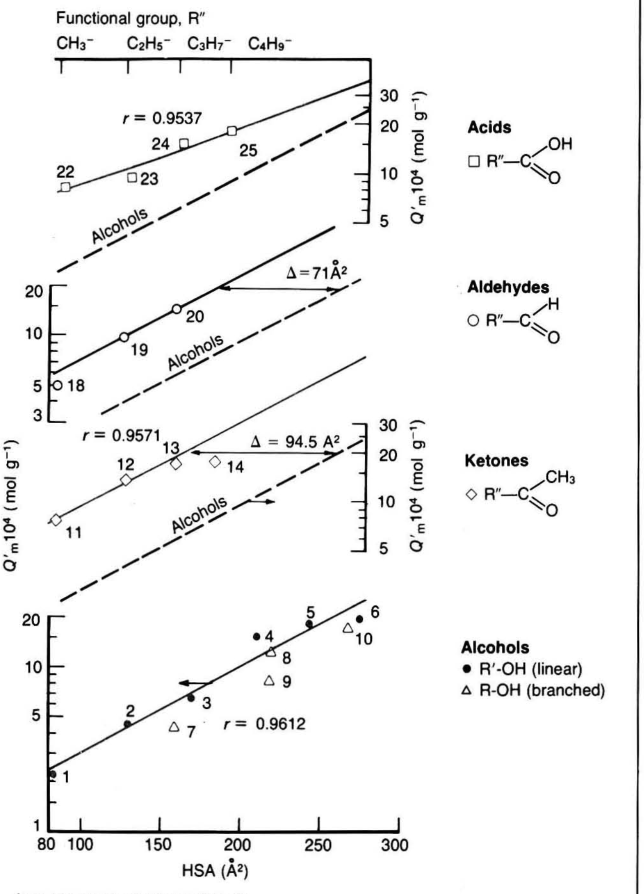

[a] Adsorption data for Giusti et al. (Table 8)

term is dominating and always opposite in sign to the cavity term. Both of these results are consistent in that (a) *dispersion forces* dominate during activated carbon adsorption of relatively nonpolar solutes, and (b) that the *surface* and *inverse volume forces* counteract each other.

Using the results in Figure 4a, the comprehensive solvophobic model is tested in Figure 4 by correlating the $\Delta G^{net}_{(solvent\ effect)}$(and ΔG^{net}_{vdw}) with the adsorption capacity ($\ln \bar{p}_i = \ln Q'_m$) of normal alcohols according to Equation 24 in Table 7. Similar correlations for all the different aliphatic homologues shown in Figure 5 give correlation coefficients $r > 0.918$ and for most of the cases the cavity term gives the best correlation (usually $r > 0.956$). "This led us immediately to suggest that perhaps the theory could be simplified by correlating adsorption capacity with the surface area of a solute molecule only, instead of with the comprehensive model," said Belfort.

The simplified model as described by Equation 25 in Table 7 is tested by plotting the logarithm of the extent of adsorption versus hydrocarbonaceous area (total minus functional group surface area, i.e., TSA − PSA = HSA) for the same single aliphatic organics plotted in Figure 4. The results are shown in Figure 6 and confirm with excellent correlations the simplified model.

Two different sets of aromatic organics were analyzed by Belfort. In both cases $\ln \bar{p}_i$ is correlated with total surface area as shown in Figures 7 and 8. The correlation for $\ln K_f$ versus A_{S_i} shown in Figure 7 is better for the mixed-solute isotherms than for the single-solute isotherms. The difference in slope and magnitude for the two correlations illustrates the dependence of solute adsorption on the *reduced surface tension* due to the presence of mixed solutes in the solvent during the adsorption process (see Traube's quotation). The drop in extent of adsorption under mixed-solute conditions is more severe for the smaller solutes, since under single-solute conditions the larger molecules have ipso facto a larger adsorption capacity and therefore are less affected by changes in the solvent properties. For HPLC, Horvath et al. found a four-order drop in benzoic acid retention due to the addition of either acetonitrile or methanol to water. This reduction was explained by a drop of the surface tension of the *mixed solvent* from about 72 dynes cm^{-1} to 28 dynes cm^{-1}. It thus appears from Figure 7 that even under competition the extent of adsorption for an aromatic homologous series can be predicted very well with the simplified solvophobic model.

An excellent correlation coefficient is obtained for five different single-solute alkyl phenols for log $Q°b$ versus A_{S_i} as shown in Figure 8. A similar correlation of ln $Q°b$ versus molecular weight gives a lower coefficient of correlation (0.9548). Quoting Belfort, "Clearly, the use of molecular weight as a parameter does not take the branching or the position of isomer into account, whereas cavity surface area does."

Future research

The tip of the iceberg has only been touched. The development of the comprehensive solution theory should continue and the theory should be refined and applied to other important solvent-mediated reactions. Quoting from Halicioğlu's thesis, Belfort pointed to at least one weakness in the theory, "In spite of various uncertainties in polar forces in dense media (as determined by existing methods), the theory gives a somewhat reasonable estimate of the effect." Although the solvophobic theory as outlined here is restricted to un-ionized solutes, it could in principle be extended to polar and/or ionized solutes (private communication, O. Sinanoğlu). Although it has been assumed that the adsorption of organic molecules is dominated by dispersion forces, the solvophobic theory could be used to describe effects on adsorption of a wide range of phenomena, including pH and ionic strength. A comprehensive model requires microscopic details, not yet available, of the extent of surface heterogeneity and electrostatic forces. Also, the solvophobic theory, as with the net adsorption energy approach, does not provide information on the shape or type of adsorption isotherm for a particular solute.

"Two refinements are now being incorporated into our application of the theory" said Belfort. "The first has to do with including the reduction term. It appears to be relatively constant for a homogeneous series and would not affect conclusions in our second paper. The second refinement has to do with the microscopic interfacial tension. The development presented here incorporates microscopic surface tension through an empirical equation for nonpolar liquids and used for polar liquids as well. The correction due to curvature appears to fall away for relatively small symmetrical molecules. Because this is somewhat unsettling, we have developed a phenomenological correction term for the curvature correction which does not fall away for such molecules."

With respect to the application and testing of the theory, Belfort's group at Rensselaer Polytechnic Institute are involved in developing a comprehensive experimental data base for specific homologous groups. Competition, branching aliphatic-aromatic mix of a solute, and position of organic group relative to the functional group on an aromatic ring are some variables being tested. Cross correlations between homologous groups are also being evaluated.

FIGURE 7

Plot of the logarithm of the extent of adsorption versus total surface area for aromatic organics with different alkyl functional groups as per the simplified solvophobic model[a]

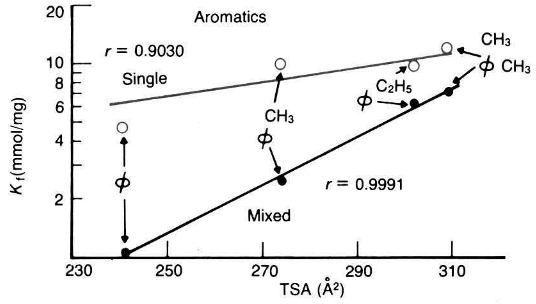

[a] Adsorption data from El-Dib and Badawy (Table 8)

FIGURE 8

Plot of the logarithm of the extent of adsorption versus total surface area for alkyl phenols as per the simplified solvophobic model[a]

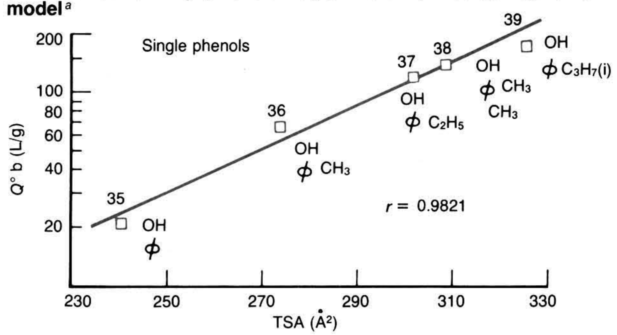

[a] Adsorption data from Singer and Yen (Table 8)

Concluding remarks

The results obtained by Belfort and co-workers from adapting the solvophobic theory to the association adsorption process have been impressive. Quoting from the conclusion of Belfort's second paper, "A detailed analysis of the effect of the solvent on this process yields an expression for the extent of adsorption with essentially no adjustable constants. The comprehensive solvophobic model is tested for the extent of adsorption of a series of normal aliphatic alcohols. Excellent linear correlations ($r > 0.918$) are obtained. The theory incorporates a wide span of experimental conditions including a comparison of the adsorption of similar organic compounds on different adsorbents (not tested yet), and a comparison of the adsorption of different organic solutes on the same adsorbent.

"Under special conditions and assumptions, simplified analytical expressions result, allowing the prediction of the extent of adsorption as a function of the simple geometric characteristics of the solute or its nonpolar moieties.

"The simplified model is tested for the aqueous adsorption of aliphatic homologous series, such as alcohols, ketones, aldehydes, acid, and acetates, and aromatic homologous series, such as alkyl benzenes and alkyl phenols. In an overwhelming number of cases, the model successfully correlates the adsorption data within homologous groups. As a comparison, similar correlations with molecular weight are poorer for 6 out of 8 cases tested. Branching and position isomerism are well accounted for by the theory. Multicomponent adsorption of a homologous aromatic series exhibit an excellent correlation.

"The ability to predict the effects of even simple structural modifications in the adsorption of organic molecules from dilute aqueous solutions onto activated carbon (or other adsorbents) could be of great value in the design and operation of large-scale commercial water or wastewater treatment plants."

In addition to the adsorption process, Belfort believes that the solvophobic theory has much wider implications, "We are obviously aware of the wide significance of our results. Clearly, relating the single- and multicomponent adsorption capacities from a solution onto a solid surface and obtaining such excellent correlations from the fundamental interactions involved should be of interest not only in chemical engineering but in physical and biological chemistry, and surface science in general. We are at present trying to generalize the application of this theory for correlating the removal of homologous organic compounds by widely different unit processes, such as adsorption, hyperfiltration, and biological metabolism. Solvent interactions cannot be overlooked in these and many other processes."

—Stanton Miller

PRINCIPLES OF DESALINATION

Second Edition/Parts A and B

Edited by K. S. SPIEGLER and A. D. K. LAIRD

Since publication of the first edition of *Principles of Desalination* in 1966, many advances in the field of water desalination have occurred. The worldwide installed capacity of desalination plants has increased more than tenfold and is still rapidly increasing. This second edition provides an up-to-date account of these advances and discusses current methods of water desalination, as well as those presently under development.

In addition to the chapters on specific desalting methods for sea and brackish water, the book considers the general energetics and economics of desalination and the preparation of ultrapure water (e.g., for nuclear reactors). It also tabulates many important properties of sea water and other saline solutions.

Principles of Desalination, Second Edition will provide readers with overviews of current desalting methods before they approach the journal and patent literature. It will be of interest to environmental scientists, mechanical, chemical, and civil engineers, chemists, earth scientists, and biologists.

Part A/1980, 384 pp., $41.00 ISBN: 0-12-656701-8
Part B/1980, 480 pp., $52.00 ISBN: 0-12-656702-6
Set price for Parts A & B: $85.00 ($93.00 if purchased separately).

Set prices are not valid in Australia or New Zealand. Valid only on purchase of both volumes.

ENVIRONMENTAL AND CLIMATIC IMPACT OF COAL UTILIZATION

Edited by JAG J. SINGH and ADARSH DEEPAK

With world oil becoming increasingly scarce and costly, coal is again a key fuel in fulfilling our energy demands. However, the utilization of coal and its liquid and gaseous derivative fuels creates unique environmental and climatic problems. Responding to the need for up-to-date, in-depth research in this field, nearly seventy scientists from university, industry, and government laboratories gathered at the Symposium on Environmental and Climatic Impact of Coal Utilization, in Williamsburg, Virginia, on April 17-20, 1979. This book presents the proceedings of that symposium where recognized experts reviewed our present knowledge and active researchers offered their latest findings. The entire spectrum of coal-related problems is dealt with here—atmospheric pollution (ground, tropospheric, and stratospheric), the environmental climatic impact of pollutants, and techniques for measuring pollutants and their impact.

1980, 646 pp., $39.50 ISBN: 0-12-646360-3

LIQUID SCINTILLATION COUNTING

Recent Applications and Development

Edited by CHIN-TZU PENG, DONALD L. HORROCKS and EDWARD L. ALPEN

This book contains the proceedings of the International Conference on Liquid Scintillation Counting, Recent Applications and Development, held on August 21-24, 1979 at the University of California, San Francisco.

Volume 1: PHYSICAL ASPECTS

SECTION HEADINGS: General—History. Scintillation Physics and Scintillators. Quenching. Radioactivity Standards. Advances in Instrumentation. Alpha Counting. Čerenkov Counting. Special Discussion.

1980, 414 pp., $27.50 ISBN: 0-12-549901-9

Volume 2: SAMPLE PREPARATION AND APPLICATIONS

SECTION HEADINGS: Sample Preparation. Sample Preparation and Flow Counting. Emulsion (Solgel) Counting. Application-Chemiluminescence and Bioluminescence. Application—Environmental Monitoring. Application—Biomedical and Radioimmunoassays. Index.

1980, 538 pp., $32.00 ISBN: 0-12-549902-7

Send payment with order and save postage and handling charge.

Prices are subject to change without notice.

Academic Press, Inc.

A Subsidiary of Harcourt Brace Jovanovich, Publishers
111 FIFTH AVENUE, NEW YORK, N.Y. 10003
24-28 OVAL ROAD, LONDON NW1 7DX

CIRCLE 1 ON READER SERVICE CARD

Risk assessment: the Supreme Court rules

Michael R. Deland
ERT, Concord, MA

In a case decided just prior to its summer recess, the U.S. Supreme Court held that the benzene standards written by the Labor Department's Occupational Safety and Health Administration (OSHA) were invalid on the grounds that OSHA had not made a "threshold" finding that benzene poses a significant health risk and that a new lower standard is therefore "reasonably necessary or appropriate" (Industrial Union Department *v.* American Petroleum Institute, 48 *Law Week* 5022). The plurality opinion, from which four justices dissented, directly impacts other ongoing standard setting within OSHA, EPA, and other agencies and will shape the environmental rule-making process.

Burden of proof

OSHA argued that there is ample evidence to support the conclusion that there is no absolutely safe level for a carcinogen and therefore the burden belongs to industry to prove that a safe level for exposure can be determined. The Court, rejecting this argument, stated that "the burden was on the agency to show, on the basis of substantial evidence, that it is at least more likely than not that long-term exposure . . . presents a significant risk of material health impairment."

This was qualified by the finding that "significant risk" is not a "mathematical straitjacket," but rather that the agency has the responsibility to define significant risk on the basis of the "best available evidence." Thus, while regulatory agencies retain considerable flexibility, are free to use "conservative assumptions" and to risk "error on the side of overprotection," they can no longer impose the entire burden on industry. At the very least, the regulators now have a threshold responsibility to establish the need for more stringent standards.

Cost–benefit analysis

One important related question, which was directly addressed only in a separate opinion by Justice Powell, is the relationship between the expected benefits of regulation and the cost to industry. Powell found that "the statute requires the agency to determine that the economic effects of its standard bear a reasonable relationship to the expected benefits." A standard is neither "reasonably necessary" nor "feasible" if it requires "expenditures wholly disproportionate to the expected health and safety benefits."

The full Court is expected to confront this issue during its fall term in a case brought by the steel industry challenging OSHA's standards for coke oven emissions (American Iron & Steel Institute *v.* OSHA, No. 78-919). Further highlighting this debate, the U.S. Court of Appeals for the District of Columbia recently rejected arguments by the lead industry that EPA did not properly weigh economic considerations in holding that the agency had not exceeded its authority by "promulgating a primary air quality standard for lead which is more stringent than necessary to protect public health."

EPA and OSHA cancer policies

At stake are the cancer policies of both agencies. OSHA's is in the early stages of litigation while EPA's "airborne carcinogen policy," originally proposed in October 1979, has been further delayed to provide additional opportunity for public comment when EPA's Science Advisory Board Subcommittee meets in November.

Reacting initially to the benzene decision, EPA's assistant administrator for pesticides and toxic substances was quoted as saying, "The Court may have set an impossible standard. By the time the proof arrives in the form of dead bodies, it will be too late." Since then the agency has closed ranks behind the position that it is complying with the degree of analysis required by the Court to determine a "significant risk" and that its carcinogen policy and other standard setting therefore will not be affected.

Continuing debate

While the Supreme Court did reject out-of-hand OSHA's benzene standard and did shift the agency's traditional concept of burden of proof, it by no means resolved the critical question of risk assessment upon which so much of environmental regulation now hinges. Still very much at issue is how a significant risk can be quantified. By its plurality 5–4 decision, the Court served notice that to achieve agreement within the legal community is every bit as difficult as reaching concensus among scientists. The minority viewed the key issue in such cases to be one of "scientific uncertainty" and felt that "the existing evidence may frequently be inadequate to make the threshold finding of 'significance' . . ." It further hinted that in cases where human lives are at stake, a cost–benefit analysis may not be appropriate—a position long espoused by environmental groups.

The debate over how to approach the regulation of carcinogens has just been joined and is certain to be one of the more pervasive and persistent environmental problems of this decade.

0013-936X/80/0914-1051$01.00/0

ES&T
FEATURES

Aquasols: the behavior of small particles in aquatic systems

An introduction to the processes involved in the transport and removal of particles that have major effects on water quality

Charles R. O'Melia
The Johns Hopkins University
Baltimore, Md. 21218

Solid particles exert substantial effects on the chemical composition of fresh, estuarian, and marine waters. For example, Turekian (1977) stated that such particles control the concentrations of trace metals in water from initial weathering reactions on land to final deposition in marine sediments. Lal (1977) indicated that solid particles play a vital role in ocean chemistry, scavenging several elements and providing a source for others.

Most pollutants of concern to human health and environmental quality are associated with solid particles. The treatment of wastewaters and water supplies primarily involves the removal of particles. Consequently, the physical processes involved in the transport and removal of particles in natural aquatic systems and in water and wastewater treatment plants can be expected to have major effects on water quality.

The purposes of this feature article are twofold: (1) to describe certain physical processes that affect the transport and fate of solid particles in aquatic systems, and (2) to illustrate, using case studies, our understanding of these processes and the extent of their effects.

Processes and effects

Three physical processes are considered throughout this article. The first is Brownian or molecular diffusion, in which random motion of small particles is brought about by thermal effects. The driving force for this transport is a function of kT, the product of Boltzmann's constant and absolute temperature. The kinetic energy of water molecules is transferred to small particles during the continuous bombardment of these particles by the surrounding water molecules. Transport by Brownian diffusion depends on these thermal effects only and is independent of such factors as fluid flow and gravity forces.

The second process affecting particle transport in aquatic systems is fluid shear, either turbulent or laminar. Velocity differences or gradients occur in all real flowing fluids. Hence, particles that follow the motion of the suspending fluid will travel at different velocities. These fluid and particle velocity differences or gradients can produce interparticle contacts among particles suspended in the fluid. Particle transport in this case depends upon the mean velocity gradient, G.

The third force considered here is gravity, which produces vertical transport of particles and depends upon the buoyant weight of these particles, represented here by $d_p^3(\rho_p - \rho)g$ in which d_p is particle size, ρ_p and ρ are the densities of the particles and the fluid respectively, and g is the gravity acceleration.

These physical processes are few in number and are simple in concept. They are also numerous in occurrence and complex in effects. Four case studies will be summarized. Two are examinations of particle deposition at water–solid interfaces: filtration by packed beds in laminar flow, and deposition on pipe walls in turbulent flow. Two examples will consider particle transport within aquatic systems: a water treatment plant and a lake.

Deposition at water–solid interfaces

Packed-bed filtration. We examine here the performance of packed-bed filters as used extensively in water and wastewater treatment for the removal of particles. The approach is adapted from the early work of Friedlander (1958) which deals with the filtration of aerosols. Consider a single spherical grain of filter media as illustrated in Figure 1. The flow of fluid around the collector is laminar, depicted by the streamlines. Particles in the flowing fluid may be transported to the spherical collector by three mechanisms: Brownian diffusion (molecular effects), interception (a form of velocity gradient), and sedimentation (gravity effects).

Feature articles in ES&T *have by-lines, represent the views of the authors, and are edited by the Washington staff. If you are interested in contributing an article, contact the managing editor.*

The problem, expressed in mathematical form, is:

$$\frac{\partial C}{\partial t} + \mathbf{v}\nabla C = D\nabla^2 C + (\rho_p - \rho)\frac{gm}{3\pi\mu d_p}\nabla C \quad (1)$$

Here C is the concentration of particles at some location and time; t is time; $\mathbf{v}$ is the velocity of the fluid at some location and time, assumed to follow Stokes' equations for laminar flow around a sphere; D is the Brownian or molecular diffusion coefficient of the particle; μ is the viscosity of the fluid; and m the mass of particles in suspension. A steady state is assumed so that the first term on the left side of Equation 1 equals zero.

The second term on the left side of Equation 1 describes the advective flow of fluid towards the collector. Suspended particles that follow the flow of suspending fluid exactly may, depending upon their size and the size of the collector, be intercepted by the media grain. This interception can be visualized as a form of velocity gradient coagulation where one particle with a velocity equal to that of the fluid collides with a second stationary particle with a velocity of zero. The effects of molecular diffusion are described by the first term on the right side of Equation 1, and the effects of the gravity force are described by the second term on that side.

Integration of Equation 1 has been accomplished by several investigators. Depending upon boundary conditions and simplifying assumptions used, analytical and numerical solutions with different complexities are achieved. The results describe the concentration distribution of particles in the flowing fluid in the region around the sphere. By differentiating

FIGURE 1
Particle transport to a single collector in a packed-bed filter.

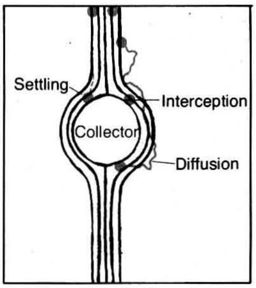

FIGURE 2
Effects of suspended particle size on the efficiency of a single collector in a typical packed-bed filter.

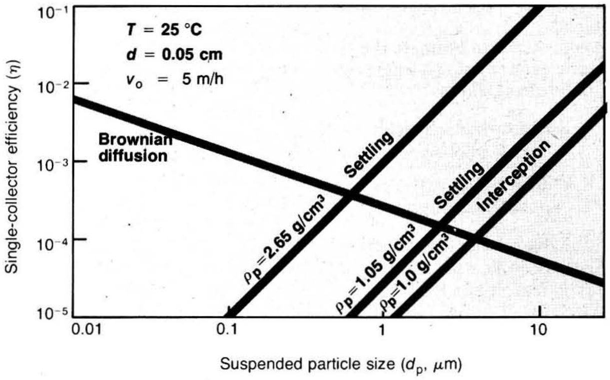

FIGURE 3
Effects of suspended particle size and filtration time on the performance of a typical packed-bed filter.

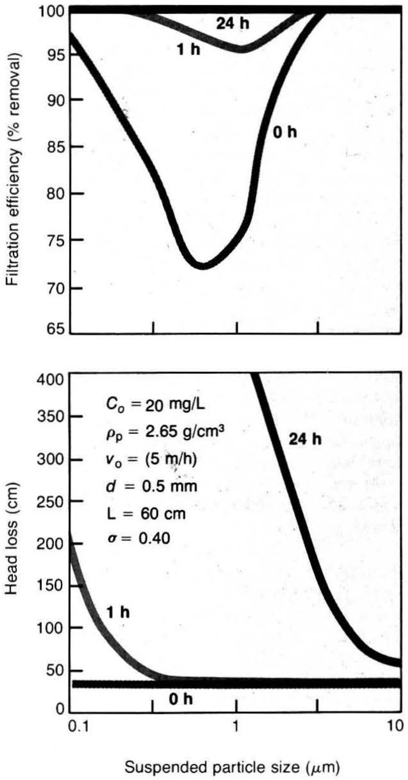

this result and solving for the concentration distribution at the surface of the collector, the local or microscopic flux of particles to the collector can be determined.

The next step is to estimate the removal efficiency (η) of this single collector, defined as follows:

$$\eta = \frac{\text{Rate at which particles strike a collector}}{\text{Rate at which particles approach a collector}}$$

Some available solutions are illustrated by Equations 2 a, b, and c, taken from the work of Yao et al. (1971):

$$\eta_D = 4Pe^{-2/3} = 0.9\left[\frac{\bar{k}T}{\mu d_p d v_0}\right]^{2/3} \quad (2a)$$

$$\eta_I = \frac{3}{2}\left(\frac{d_p}{d}\right)^2 \quad (2b)$$

$$\eta_G = \frac{(\rho_p - \rho)g}{18\mu v_0} d_p{}^2 \quad (2c)$$

Here η_D, η_I, and η_G are the single-collector removal efficiencies for diffusion, interception, and gravity considered separately as transport processes; Pe is the Peclet number; d is the diameter of the collector; and v_0 is the approach velocity of the fluid.

The significance of these particle transport processes is depicted graphically in Figure 2, in which the single-collector efficiency is plotted as a function of the size of the particles in suspension for conditions representative of water and wastewater filtration. An important conclusion here is that small particles, in this case smaller than about 1 μm in diameter, are transported and removed predominantly by Brownian diffusion. Larger particles are transported by interception and gravity. Analogies between these effects of suspended particle size on removal from suspension in packed-bed filters and phenomena that occur in certain other aquatic systems are to be expected. The efficiency of zooplankton feeding in natural waters is one such case.

We continue our scale-up from the microscopic flux at a point on a single media grain through the total efficiency of such a single grain to consider the total removal efficiency and head loss of a complete filter bed of length L. The removal efficiency of a clean bed has been described by:

$$\frac{C_e}{C_o} = e^{-(3/2)\alpha(1-\sigma)\eta(L/d)} \quad (3)$$

Here C_o and C_e are the influent and effluent concentrations of suspended particles, respectively; σ is the porosity of the clean filter bed; and α is the collision or sticking efficiency of the water–solid system. This latter factor reflects the aqueous and surface chemistry of the system and is defined as the number of contacts between suspended particles and filter media that successfully result in attachment and removal divided by total number of contacts that occur.

The effects of suspended particle size and filtration time are illustrated in Figure 3. These results are based on the work of O'Melia and Ali (1978) and Tobiason (1979). The filtration efficiency and the head loss development of a typical packed-bed filter are presented as functions of suspended particle size and filtration time. The influence of the three transport mechanisms on removal efficiency is illustrated in Figure 3a. A window or region of minimum removal efficiency exists for particles in the size range of 1 μm. Effective removal of submicron particles can be accomplished, including viruses.

Removal efficiency increases appreciably as time proceeds. This increased efficiency is accompanied by an increased head loss (Figure 3b). An important conclusion is that small particles exert much more substantial head losses than larger ones when comparisons are based on similar masses of material removed from suspension. In this filtration analysis, the improvement in filtration efficiency with time is based on a consideration that particles removed from suspension early during a filter run can act as filter media and accomplish the removal of additional particles later in the run.

Deposition in pipes. Particle deposition from the suspending fluid to pipe walls has important effects in many systems of engineering interest. Examples include a reduction in the carrying capacity of transmission mains due to increased pipe friction, and reduction in the heat-transfer capabilities of condenser tubes in power plant cooling systems. The approach here is similar in structure to that used in considering packed-bed filtration.

We begin by considering a small section of the pipe and evaluating a local mass-transfer coefficient which is analogous to the single-collector efficiency developed for filters. Following this, we scale up the results to a pipe of some total length L. Important particle transport mechanisms are Brownian diffusion and sedimentation. The approach is again patterned after earlier work by Friedlander (1957) in aerosol systems.

Brownian diffusion is considered first. Schematic representations of the velocity and the concentration distributions during turbulent flow in a circular pipe are presented in Figure 4. The velocity distribution is the result of processes affecting the transport of momentum within the fluid. This momentum may be transported by turbulent eddies and by molecular or viscous effects, represented by the coefficients of turbulent diffusivity (ϵ) and kinematic viscosity (ν) with typical dimensions being cm^2/s.

Within the turbulent core, ϵ is much greater than ν, and the fluid velocity, u, is almost constant. In the region near the pipe wall, ν is much greater than ϵ and a laminar sublayer or velocity boundary layer exists in which u increases linearly with the distance from the wall. Between these two regions, a buffer zone exists in which momentum can be transported by both turbulent and viscous effects.

Similarities exist when considering the concentration distribution within the pipe. In the turbulent pipe core, transport of mass by turbulent eddies is considerably greater than the transport of mass by molecular diffusion. These processes are characterized by ϵ_m, the turbulent mass diffusivity, and D, the Brownian or molecular diffusion coefficient. Within the turbulent core, ϵ_m is considerably greater than D, and a uniform concentration is observed. In the region near the wall, turbulent eddies become weaker and transport by Brownian diffusion becomes significant.

Here it is important to consider differences in water between the molecular coefficients for the transport of momentum, ν, and of mass, D. The kinematic viscosity of water, ν, is in the order of 10^{-2} cm^2/s, while molecular diffusion coefficients, D, are in the order of 10^{-5} cm^2/s or smaller. The ratio (ν/D) is termed the Schmidt number (Sc) and is in the order of 1000 or greater in water. In contrast, coefficients of turbulent momentum and mass diffusivity (ϵ and ϵ_m) are similar.

The result is that turbulent eddies too weak to affect momentum transport in the laminar sublayer (i.e., $\epsilon < 10^{-2}$ cm^2/s) can significantly affect mass transport up to a very small distance from the wall. There exists at water–solid interfaces a concentration boundary layer which is significantly thinner than the corresponding velocity boundary layer and within which both turbulent and molecular transport can be significant.

Using Friedlander's analysis for Brownian diffusion (1977) and formulating a separate analysis for the effects of gravity, Bliss and O'Melia (1979) presented and tested the following equations for the local mass-transport coefficients describing deposition on pipe walls in turbulent flow due to diffusion (k_D) and sedimentation (k_S).

$$k_D = 0.042 \left(\frac{D}{d}\right) Re f^{1/2} Sc^{1/3} \tag{4a}$$

$$k_S = \frac{(\rho_p - \rho)g}{18\pi\mu} d_p^2 \cos\phi \tag{4b}$$

Here *Re* is the Reynolds number of the pipe; *f* is the Fanning friction factor; $\bar{d}$ is the pipe diameter; and ϕ is the angle that the pipe axis makes with the horizontal direction. Integrating the local flux along a pipe of length *L*, the following equation is obtained:

$$\frac{C_e}{C_o} = e^{-4\alpha k L/U\bar{d}} \tag{5}$$

Here C_o and C_e are the influent and effluent particle concentrations for the pipe system; *U* is average fluid velocity; and *k* is the appropriate mass-transport coefficient.

FIGURE 4

Schematic velocity and concentration distributions within a circular pipe in turbulent flow.

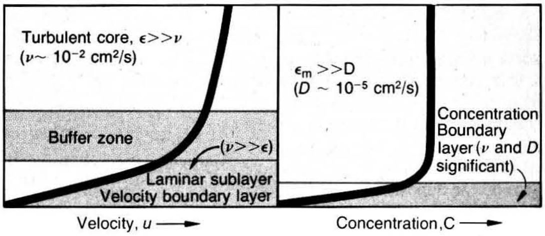

FIGURE 5

Effects of suspended particle size on mass-transport coefficients for deposition on horizontal pipe walls.

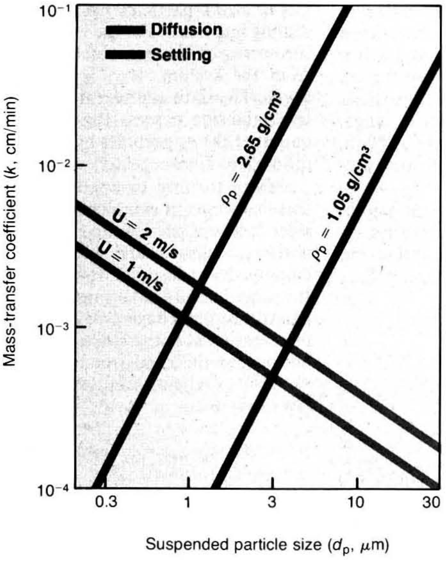

FIGURE 6

Effects of particle size on collision rate coefficients for coagulation processes.

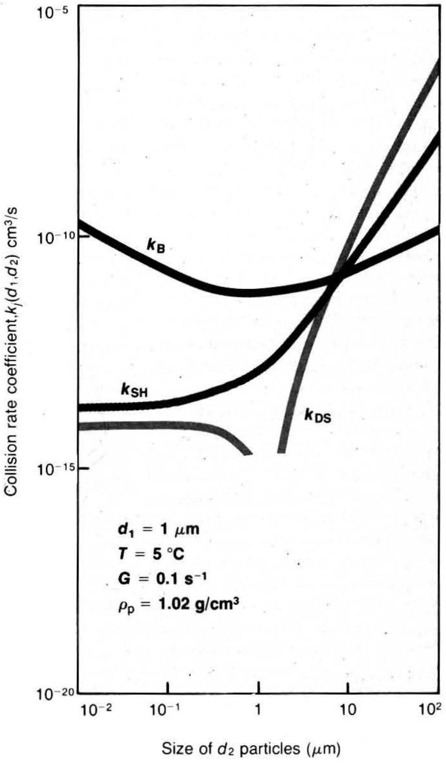

It is instructive to examine the effects of the size of the particles suspended in the water on the local mass-transport coefficient for deposition. These are illustrated in Figure 5. The results are remarkably similar in form to the results obtained for the transport of particles to spherical collectors within packed beds in laminar flow. A region about 1 μm in size exists for which particle transport to the pipe walls is a minimum. For smaller particles, transport by Brownian diffusion is effective; for larger particles, transport by gravity is effective when the pipes are horizontal. Very extensive effects of the density of the suspended particles on the deposition of the larger particles are predicted and observed.

It is expected that analyses of this type have considerable application in evaluating the head loss in transmission mains, the fouling of condensers in power plants, and the design of fixed-film biological reactors in wastewater treatment plants.

Transport within aquatic systems

We proceed now to some concepts about coagulation within aquatic systems; then we will examine the effects of coagulation in water and wastewater treatment plants and in lakes. The basic developments describing coagulation rates in aquatic systems were presented by Smoluchowski in 1917. Since that time these have been applied primarily to homodisperse colloids, i.e., those in which the particles have only one size at the onset of coagulation. Note here that particles in natural waters span a size range of several orders of magnitude. Again following the lead of Smoluchowski, let us examine how coagulation rates become more rapid when suspensions are heterodisperse.

Collisions between suspended particles in water can occur by three different processes, viz., Brownian diffusion (thermal effects), fluid shear (flow effects), and by differential settling (gravity effects). The particle size distribution of the suspension being coagulated has important effects on the significance of these three processes. Equations for the coagulation of heterodisperse suspensions are cumbersome; for didactic purposes the collisions between particles of two different sizes are considered first.

The rate at which particles of sizes d_1 and d_2 come into contact by the jth transport mechanism is given by:

$$R_j(d_1,d_2) = k_j(d_1,d_2) \cdot n(d_1) \cdot n(d_2) \qquad (6)$$

Here $R_j(d_1,d_2)$ is the collision rate (collisions/volume·time); $k_j(d_1,d_2)$ is the "bimolecular" rate coefficient for the jth mechanism (volume/time); and $n(d_1)$ and $n(d_2)$ are the number concentrations of particles of sizes d_1 and d_2, respectively (volume^{-1}).

The rate coefficients for the three transport processes are given by Equations 7 a, b, and c.

$$k_{\mathrm{B}} = \frac{2\bar{k}T(d_1 + d_2)^2}{3\mu\,(d_1 \cdot d_2)} \qquad (7a)$$

$$k_{\mathrm{SH}} = \frac{(d_1 + d_2)^3}{6} G \qquad (7b)$$

$$k_{\mathrm{DS}} = \frac{\pi}{72\nu}(\rho_{\mathrm{p}} - \rho)g(d_1 + d_2)^3 \cdot |d_1 - d_2| \qquad (7c)$$

Here k_{B}, k_{SH}, and k_{DS} are the bimolecular collision rate coefficients for transport by Brownian diffusion, fluid shear, and differential settling, respectively.

These rate coefficients are compared in Figure 6 for a case that is illustrative of a sedimentation tank in a water treatment plant during the winter season and the hypolimnion of a lake during the summer season. Results are presented for the collisions of particles with a size d_2 ranging from 0.01 μm to 100 μm with particles of size d_1 = 1 μm. Values of T = 5 °C, ρ_{p} = 1.02 g/cm^3, and G = 0.1 s^{-1} have been assumed. The collision rate by Brownian motion is a minimum for $d_1 = d_2$ = 1 μm; i.e., it is a minimum for a homodisperse suspension. Collisions by differential settling do not occur in homodisperse suspensions, since when $d_1 = d_2$, $k_{\mathrm{DS}} = 0$ (Equation 7c). Coagulation by Brownian diffusion dominates in this example for particles in the micron and submicron range. For particles larger than about 7 μm, coagulation by gravity forces predominates.

A general model for the transport of particles in aquatic systems that includes the effects of coagulation and gravity is described by Equation 8.

$$\frac{dn_{\mathrm{k,I}}}{dt} = \frac{1}{2}\sum_{\mathrm{i+j=k}} \alpha k(\mathrm{i,j})_{\mathrm{I}} \cdot n_{\mathrm{i,I}} \cdot n_{\mathrm{j,I}} - n_{\mathrm{k,I}} \sum_{\mathrm{i=1}}^{\infty} \alpha k(\mathrm{i,k})_{\mathrm{I}} \cdot n_{\mathrm{i,I}} + \frac{w_{\mathrm{k,H}}}{z_{\mathrm{I}}} n_{\mathrm{k,H}} - \frac{W_{\mathrm{k,I}}}{z_{\mathrm{I}}} n_{\mathrm{k,I}} \pm W_{\mathrm{k,I}} + q_{\mathrm{o}} \cdot n_{\mathrm{k,o}} - q_{\mathrm{o}} \cdot n_{\mathrm{k,I}} \qquad (8)$$

The aquatic system is segmented into a number of vertical boxes, denoted here as H, I, J, K, L . . . etc. These could correspond to the epilimnion, thermocline, and hypolimnion (3 boxes) in a lake, or various depths in a settling tank in a treatment plant. The particles in the water are subdivided into a number of size compartments, denoted as h, i, j, k, l . . . etc. Equation 8 is a general equation for the particles of size k in, for example, box I. Here $n_{\mathrm{k,I}}$ denotes the concentration of particles of size k in box I; $k(\mathrm{i,j})_{\mathrm{I}}$ denotes a collision frequency function that depends on the mode of interparticle contact; $w_{\mathrm{k,H}}$ is the settling velocity of particles of size k in box H located directly above box I; z_{I} is the depth of box I; $W_{\mathrm{k,I}}$ is the rate of production or destruction of particles by biological and chemical processes in box I; and q_{o} is the areal hydraulic loading or overflow rate into and out of box I.

The left side of Equation 8 describes the rate at which the number concentration of particles with size k and location I changes with time (particle/m^3·s). The first term on the right side expresses the rate of formation of particles of size k (or volume v_{k}) from particles having the total volume v_{k}. The condition i + j = k under the summation denotes the condition that $v_{\mathrm{i}} + v_{\mathrm{j}} = v_{\mathrm{k}}$. The factor ½ is needed since collisions are counted twice in this summation.

The second term on the right side of Equation 8 describes the loss of particles of size k by growth to form large aggregates; this occurs when a size k particle collides with and attaches to a particle of any size i. The third term describes the addition of particles of size k to box I by settling from above (box H). The fourth term expresses the loss of size k particles from box I by settling into box J. For the bottom box, this corresponds to removal of particles from the system. $W_{\mathrm{k,I}}$ is described above. The sixth and seventh terms on the right side express the input and output of the n_{k} particles by hydraulic inflow and discharge.

Before turning to applications of these concepts, it is important to consider inputs of particles to the systems under evaluation and the methods employed to describe these inputs. Investigations of both atmospheric and aquatic systems have provided useful information about particle size distributions in these environments. Observations frequency follows a power law of the form:

$$\frac{dN}{d(d_{\mathrm{p}})} = n(d_{\mathrm{p}}) = \mathrm{A} \cdot d_{\mathrm{p}}^{-\beta} \qquad (9)$$

where dN is the concentration of particles in the size range d_{p} to $d_{\mathrm{p}} + d(d_{\mathrm{p}})$ and $n(d_{\mathrm{p}})$ is defined as a particle size distribution function. A is a coefficient related to the total concentration of particulate matter in this system.

Measurements indicate that for aquatic particles larger than about 1

FIGURE 7

Performance of flocculation, sedimentation, and filtration processes.

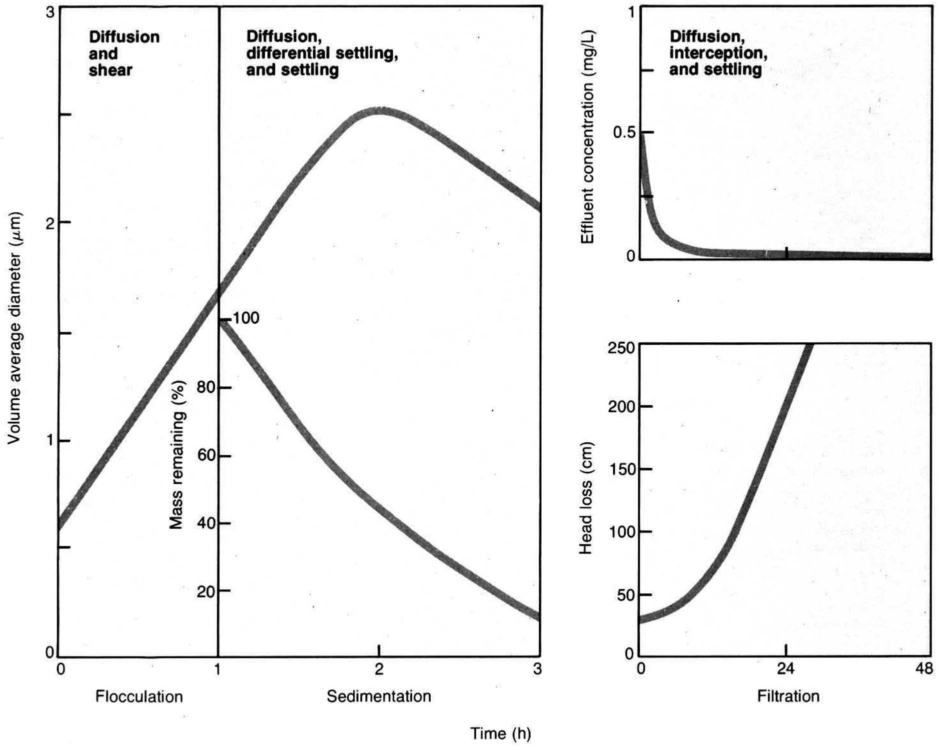

μm in size (i.e., those detectable by present electronic or optical measurements), values of the exponent β range from 2 to 5. Often, a value of β of 4 is observed. For example, Lerman et al. (1977) reported measurements of size distributions at four locations in the north Atlantic. Fifty-three size distributions derived from samples taken at depths ranging 30–5100 m yielded a mean value of $\beta = 4.01 \pm 0.28$. In part because of observations such as these, a value of $\beta = 4$ is used in much of the analysis presented subsequently.

Model for water treatment plants. A model for the performance of coagulation, sedimentation, and filtration processes in water treatment plants has been developed by Lawler et al. (1980). The model for the coagulation basin is a simplification of Equation 8: One well-mixed box is assumed; collisions are restricted to Brownian diffusion and fluid shear processes only; and the removal of mass from the system by sedimentation is not permitted. The model for the settling basin divides

TABLE 1

The water source and the treatment system

System component	Parameter	Assigned value
Raw water	Volume concentration	50 ppm
	Mass concentration	132 mg/L
	Particle density	2.65 g/cm^3
	Particle size range	0.3–30 μm
	β	4.0
	Temperature	25 °C
Flocculation tank	Collision efficiency factor	1.0
	Flow type	Plug flow
	Detection time	1 h
	Velocity gradient	10 s^{-1}
Settling tank	Flow type	Plug flow
	Detention time	2 h
	Tank depth	4 m
	Overflow rate	2 m/h
Filter	Filtration rate	5 m/h
	Media size	0.5 mm
	Media depth	60 cm
	Clean bed porosity	0.4

FIGURE 8

Particle size distribution functions in a model lake without coagulation (α = 0).

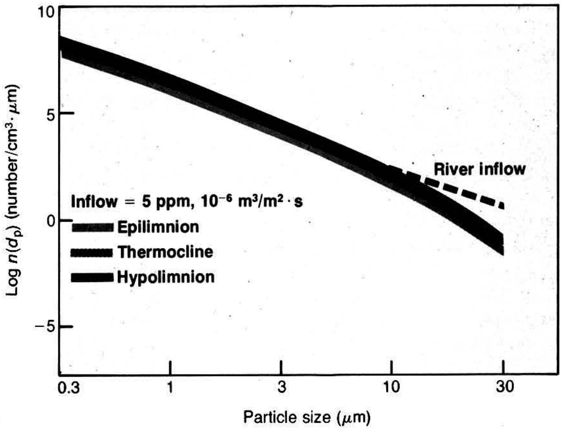

FIGURE 9

Particle volume distributions in a model lake without coagulation (α = 0).

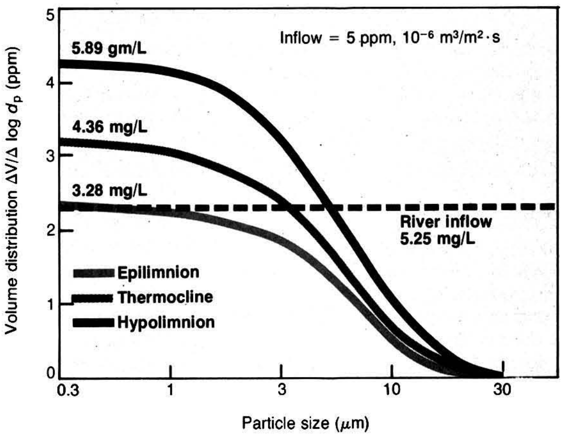

TABLE 2

Parameters in lake example[a]

Parameter	Epilimnion	Thermocline	Hypolimnion
z (m)	10	5	50
T (°C)	25	15	5
μ (g/cm · s)	0.8915×10^{-2}	1.146×10^{-2}	1.515×10^{-2}
ρ (g/cm^3)	0.997	0.999	1.000
ρ_p (g/cm^3)	1.05	1.05	1.05
G (s^{-1})	10	0.1	1.0
q_0 (m/s)	10^{-6} [b]	0	0
α	0, 10^{-3}	0, 10^{-3}	0, 10^{-3}

[a] The river input is assumed to contain 5.0 ppm by volume of particles or 5.25 mg/L of particles with a density of 1.05 g/cm^3. The particles are distributed over a size range of 0.3–30 μm, and β = 4.

[b] This corresponds to the Stokes' settling velocity of a 5.6-μm particle having a density of 1.05 g/cm^3 in water at 25 °C.

that tank into four vertical boxes, considers collisions by Brownian diffusion and differential settling only, and permits removal of mass by sedimentation at the bottom of the tank. The filtration model is based on the work of O'Melia and Ali (1978). Because modeling of filtration is still restricted to considerations of monodisperse suspensions, the heterodisperse effluent from the settling tank is converted to a monodisperse suspension with an equivalent volume average diameter for assessing filtration performance.

A representative set of results is presented in Figure 7. These are based on selected water source and treatment system characteristics summarized in Table 1. On the left side of Figure 7, the increase in volume average diameter of the suspended particles is plotted as a function of time in the flocculation basin. Particle growth occurs as expected, brought about in this case by contact opportunities provided by Brownian diffusion and fluid shear.

In the middle of Figure 7, the volume average diameter and the mass concentration of solids remaining in suspension are plotted as functions of time in the sedimentation tank. The volume average diameter continues to increase substantially during the first portion of the settling tank. Average particle size then decreases during the last portion of the tank as larger particles are removed from the system by gravity settling. Overall settling performance results in the removal of about 85% of the particles on a mass basis. The effects of Brownian diffusion, differential settling, and simple gravity sedimentation are responsible for extensive coagulation and removal of particles in such settling tanks.

The performance of a packed-bed filter is illustrated on the right side of Figure 7. Brownian diffusion, interception, and gravity settling within the filter enable effluent concentrations from the plant to be reduced to less than 0.1 mg/L. Particle removal within the filter is accomplished at the expense of an increase in head loss, but a filter run of more than a day in length is expected.

These and other results permitted Lawler et al. to reach the following conclusions. First, particle concentration and size distribution have extensive, complex, predictable, and dominant effects on the performance of individual treatment units and on overall performance in water treatment plants. Second, flocculation basins which are designed to cause coagulation by fluid shear also induce extensive coagulation by Brownian diffusion. Third, settling basins actually act as flocculation basins with differential settling and Brownian diffusion producing extensive aggregation. Fourth, Brownian diffusion, interception, and settling produce effective removal in filtration processes. Finally, present knowledge about these processes is not utilized effectively and can have significant conceptual and practical advantages.

Particles in lakes. The results described here are preliminary. They are taken from a study to evaluate the extent and significance of coagulation and settling processes in lakes. The general approach is to take the model for particles in aquatic systems as presented in Equation 8 and apply it to limnetic systems. To facilitate the analysis, a model lake was chosen. Appropriate descriptive information is presented in Table 2. The lake is divided into three vertical compartments during the stratification period: the epilimnion or well-mixed zone, the thermocline or region of rapid temperature and density changes with depth, and the hypolimnion representing the bottom waters of the lake. The analysis was conducted by Bowman and Clark (1979).

The particle concentrations that would result in such a lake in the absence of coagulation are represented in Figures 8 and 9. The coagulation process is eliminated by setting $\alpha = 0$ in Equation 8. Under these conditions, particles enter the lake in the river inflow, are discharged downstream in the river outflow, and also settle by gravity from the epilimnion through the thermocline and hypolimnion into the lake sediments.

The results are expressed in terms of the particle size distribution function as related to particle size (Figure 8) and as the particle volume concentration as a function of particle size (Figure 9). Effects are seen most easily in the volume distribution, Figure 9. The river inflow contains 5 ppm of particles; for $\beta = 4$ this corresponds to an equal distribution of particle volume with every logarithmic size interval. Hence, 2.5 ppm in volume is contained in the particle size range 0.3–3 μm and the remaining 2.5 ppm is contained in the size range 3–30 μm (note the horizontal line for the river inflow in Figure 9).

One expected result is observed; particles larger than about 5 μm in size, i.e., those with settling velocities greater than the hydraulic loading or the overflow rate of the lake, are removed to a considerable extent from all of the lake compartments. Similarly, submicron particles which have

FIGURE 10

Particle size distribution functions in a model lake with slow coagulation (α = 0.001).

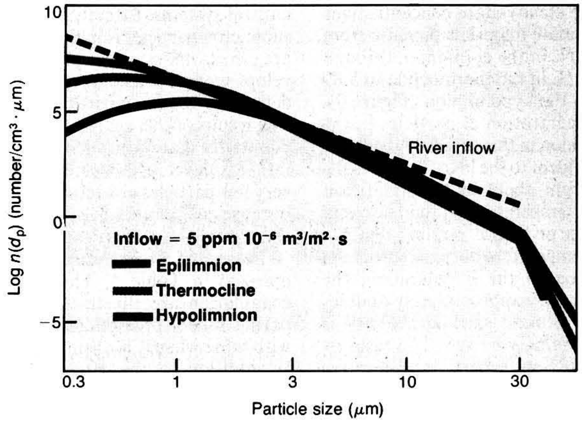

FIGURE 11

Particle volume distributions in a model lake with slow coagulation (α = 0.001).

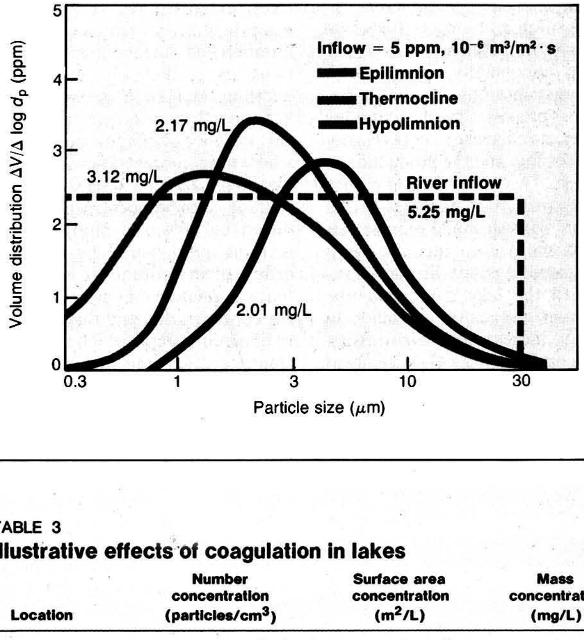

TABLE 3

Illustrative effects of coagulation in lakes

Location	Number concentration (particles/cm^3)	Surface area concentration (m^2/L)	Mass concentration (mg/L)
River inflow	3.41×10^7	2.29×10^{-2}	5.25
	α = (No coagulation)		
Epilimnion	3.39×10^7	2.14×10^{-2}	3.25
Thermocline	4.51×10^7	2.85×10^{-2}	4.36
Hypolimnion	6.08×10^7	3.85×10^{-2}	5.89
	α = 0.001 (Slow coagulation)		
Epilimnion	1.53×10^7	1.52×10^{-2}	3.12
Thermocline	1.81×10^6	0.76×10^{-2}	2.17
Hypolimnion	2.6×10^5	0.30×10^{-2}	2.01

settling velocities significantly smaller than the hydraulic loading are not removed from any lake compartment.

This second observation is instructive. The steady-state concentrations of particulate materials increase from 3.28 mg/L in the epilimnion through 4.36 mg/L in the thermocline to 5.89 mg/L in the hypolimnion (Figure 9). The concentration of particles in the hypolimnion in this case is higher than in the influent to the lake. These results are brought about by the significant effect of temperature on fluid viscosity and hence on Stokes' settling velocity. As the temperature decreases from the epilimnion to the hypolimnion, the fluid viscosity approximately doubles and the Stokes' settling velocity is correspondingly halved. The result is that steady-state particle concentrations must increase with depth, so that mass concentrations at the bottom of the lake are approximately twice those that result in the epilimnion. This vertical distribution is a direct consequence of the balance between hydraulic loading and gravity forces on the particles in the lake.

We do not usually observe such particle distributions in the lakes. Some other processes must occur. One possibility, not discussed here, is zooplankton feeding and the production of fecal pellets. This would further reduce the concentration of particles in the epilimnion, but still would require that mass concentrations increase with depth. A second possibility is coagulation with the lake compartments. Coagulation can cause particles to aggregate, increasing their settling velocities and speeding their removal from the lake.

This possibility is examined in Figures 10 and 11. These results are for a system identical to the one previously examined, save that $\alpha = 0.001$. Stated another way, one out of every 1000 contacts predicted by Smoluchowski's equations are considered to result in successful attachment and the formation of an aggregate. Coagulation is seen to have extensive effects on the particle size distribution function (Figure 10) and on the volume distribution (Figure 11).

The results indicate that coagulation occurs in all three lake compartments: epilimnion, thermocline, and hypolimnion. Removal of submicron particles is accomplished in all compartments; coagulation occurs by Brownian diffusion, fluid shear, and differential settling and permits removal of aggregates by gravity settling. Particle concentrations no longer increase with depth; in this case the steady-state particle concentrations decrease from the epilimnion to the thermocline and the hypolimnion.

These predicted results are more consistent with observations in the natural systems. Effective removal of submicron particles is indicated. There are efforts underway at present to develop measurement techniques for detecting submicron particles in water. The results of this analysis indicate the possibility that when such instrumentation is developed, we may find that very few particles are actually present, because coagulation has incorporated them into larger aggregates.

These and other results are summarized in Table 3. The effects of coagulation are illustrated by comparing model predictions for $\alpha = 0$ with those when α is assumed $= 0.001$. In addition to the effects on mass concentration as described in Figures 9 and 11 and summarized in the last column of Table 3, it can be seen that the influence of coagulation on number and surface concentrations are even more extensive. In the absence of coagulation, steady-state particle number and surface area concentrations are predicted to increase with depth in the lake in the same manner as for particle mass concentrations. In the presence of coagulation, however, where mass concentrations are reduced by about 50% from 3 mg/L to 2 mg/L, surface area concentrations are reduced by 80% and number concentrations are lowered by almost two orders of magnitude. It is concluded that coagulation can profoundly affect the concentration and flux of particles in limnetic systems which in turn exert significant controls on the transport and fate of pollutants associated with these particles.

Concluding remarks

First, available evidence indicates that most pollutants in water are particles or are associated with particles. Second, the transport and fate of particles (and the pollutants associated with them) are controlled in aquatic systems by physical processes, i.e., Brownian diffusion, fluid motion, and gravity. Third, present knowledge permits description and control of these processes in treatment and transport systems for water supply and wastewater disposal. Fourth, extension of these concepts to natural aquatic systems can be expected to provide significant new insights into the functioning of these natural systems and the flow of materials (including nutrients and pollutants) through them, and to permit improved management and control of man's impacts on these systems.

Acknowledgments

The author is pleased to acknowledge the ideas and assistance of Waris Ali, Margaret Bliss, Kathleen Bowman, Sheldon Friedlander, Desmond Lawler, James Morgan, Werner Stumm, John Tobiason, and Kuan-Mu Yao, among the many teachers, co-workers, and students who have contributed to this work.

Additional reading

Bliss, M. J.; O'Melia, C. R. "Physical Aspects of Biofouling," Presented at 34th Annual Purdue Industrial Waste Conference, West Lafayette, Ind., 1979.

Bowman, K.; Clark, M. Unpublished results, Department of Environmental Sciences and Engineering, University of North Carolina, Chapel Hill, 1979.

Friedlander, S. K. "Theory of Aerosol Filtration," *Ind. Eng. Chem.* **1958,** *50,* 1161–64.

Friedlander, S. K. "*Smoke, Dust, and Haze*"; John Wiley and Sons: New York, 1977.

Friedlander, S. K.; Johnston, H. F. "Deposition of Suspended Particles from Turbulent Gas Streams," *Ind. Eng. Chem.* **1957,** *49,* 1151–56.

Lal, D. "The Oceanic Microcosm of Particles," *Science* **1977,** *198,* 997–1009.

Lawler, D. F.; O'Melia, C. R.; Tobiason, J. E. "Integral Water Treatment Plant Design: From Particle Size to Plant Performance," In "Particulates in Water: Characterization, Fate, Effects, and Removal"; Kavanaugh M.; Leckie J. O., Eds.; ACS Advances in Chemistry Series, 1980.

Lerman, A.; Carder, K. L.; Betzer, P. R. "Elimination of Fine Suspensions in the Oceanic Water Column," *Earth and Planetary Science Letters* **1977,** *37,* 61–70.

O'Melia, C. R.; Ali, W. "The Role of Retained Particles in Packed Bed Filtration," *Prog. Water Technol.* **1978,** *10* (5/6), 123–37.

Smoluchowski, M. "Versuch einer Mathematischen Theorie der Koagulations-Kinetiks Kolloider Lösungen," *Z. Physik. Chem.* **1917,** *92,* 129–68.

Tobiason, J. "Packed Bed Filtration: Experimental Investigation and Conceptual Analysis of a Filter Ripening Model," Unpublished master's report, Department of Environmental Sciences and Engineering, University of North Carolina, Chapel Hill, 1979, 136 pp.

Turekian, K. *Geochim. Cosmochim. Acta* **1977,** *41,* 1139–44.

Yao, K. M.; Habibian, M. T.; O'Melia, C. R. "Water and Wastewater Filtration: Concepts and Applications," *Environ. Sci. Technol.* **1971,** *5,* 1105–12.

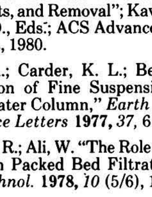

Dr. Charles R. O'Melia *is professor of environmental engineering at The Johns Hopkins University. Dr. O'Melia's research interests are in aquatic chemistry, water and wastewater treatment, and predictive modeling of natural waters.*

Trace metal catalysis in aquatic environments

Once an inexplicable nuisance to chemical kineticists, it may now play a role in pollution control

Michael R. Hoffmann
W. M. Keck Laboratories
California Institute of Technology
Pasadena, Calif. 91125

Current research in the fate of pollutants in aquatic environments has been focused on pathways for pollutant transformation. Important pathways that have been identified for major organic and inorganic pollutants include redox reactions, autoxidations, and hydrolysis reactions. Many reactions in these general categories can be catalyzed by specific homogeneous or heterogeneous transition metal complexes (*1*). Today, large-scale synthetic processes such as the autoxidation of acetaldehyde to acetic acid depend on the catalytic influence of soluble transition metals and specific organometallic complexes (*2*).

Historically, trace metal catalysis was an inexplicable nuisance phenomenon for the kineticist. Impurities in solvents, reagents, and reactants frequently resulted in nonreproducible rates of chemical reactions and unusual empirical rate laws. Trace metal concentrations as low as 0.1–10 nM influence the rates of some peroxide reactions (*3*). For example, the decomposition of peroxymonosulfuric acid, a suggested intermediate (*4*) in the autoxidation of SO_2 dissolved in aqueous aerosols, is accelerated significantly by nanomolar amounts of some divalent first-row transition metals (*5*). Similarly, ferrous ions promote the oxidation of a wide variety of aromatic substrates by hydrogen peroxide (*6*). Other chemical reactions involving oxidation/reduction, hydrolysis, decarboxylation, transamination, and bromination have been shown to be sensitive to trace metal catalysis (*7*).

The principal objectives of the article are to explore the possible roles that trace metals may play in the catalysis of aquatic reactions; to focus specifically on the kinetic and mechanistic aspects of hydrolysis, redox, and autoxidation reactions; and, finally, to explore the applicability of certain catalytic reactions for pollution control.

The word "catalyst" has been defined in many ways. Ostwald (*8*) originally defined a catalyst as a substance that changes the speed of a chemical reaction without undergoing a chemical change itself. Bredig (*9*) expanded the definition to include substances that may be chemically altered but are not involved in a whole number stoichiometric relationship among reactants and products. Bell (*10*) subsequently defined a catalyst for a homogeneous reaction to be a substance that appears in the rate expression with a reaction order greater than its stoichiometric coefficient.

Regardless of its current colloquial definition, the common notion is that the function of a catalyst is to lower the activation energy of a given reaction. As illustrated in Figure 1, the catalyst in a homogeneous system will alter the reaction mechanism to one having a lower activation energy without changing the point of equilibrium for a reaction as predicted by the law of microscopic reversibility (*3*). Since the catalyst is involved in the rate-determining step, and consequently the molecular composition of the activated complex (*11*), a discussion of catalytic activity requires consideration of detailed reaction mechanisms. Therefore, the role of trace metal catalysis in aquatic reactions will be discussed in terms of postulated reaction mechanisms which are consistent with kinetic observations.

Hydrolysis reactions

An important pathway for the transformation of organic esters in aquatic environments is the reaction known as hydrolysis or solvolysis. Most often hydrolysis reactions in natural systems are sensitive to specific acid or base catalysis (*12*). In acid-catalyzed ester hydrolysis, the role of the proton, according to Bender and Brubacher (*13*), is to provide a reaction pathway of lower energy by withdrawing electrons and therefore weakening the bond to be broken. A mechanism for acid catalysis has been suggested by Bender (*14*):

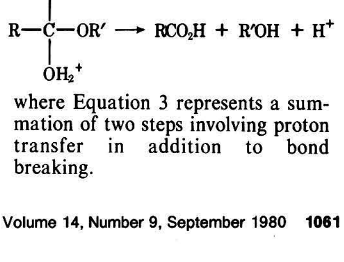

$$\mathrm{R{-}\overset{\overset{\displaystyle O}{\|}}{C}{-}OR'} + \mathrm{H^+} \rightleftharpoons \mathrm{R{-}\overset{\overset{\displaystyle OH}{|}}{C}{-}OR'} \qquad (1)$$

$$\mathrm{R{-}\overset{\overset{\displaystyle OH}{|}}{C}{-}OR'} + \mathrm{H_2O} \rightleftharpoons \mathrm{R{-}\underset{\underset{\displaystyle OH_2^+}{|}}{\overset{\overset{\displaystyle OH}{|}}{C}}{-}OR'} \qquad (2)$$

$$\mathrm{R{-}\underset{\underset{\displaystyle OH_2^+}{|}}{\overset{\overset{\displaystyle OH}{|}}{C}}{-}OR'} \longrightarrow \mathrm{RCO_2H} + \mathrm{R'OH} + \mathrm{H^+} \qquad (3)$$

where Equation 3 represents a summation of two steps involving proton transfer in addition to bond breaking.

0013-936X/80/0914-1061$01.00/0 © 1980 American Chemical Society

FIGURE 1

Effect of a catalyst

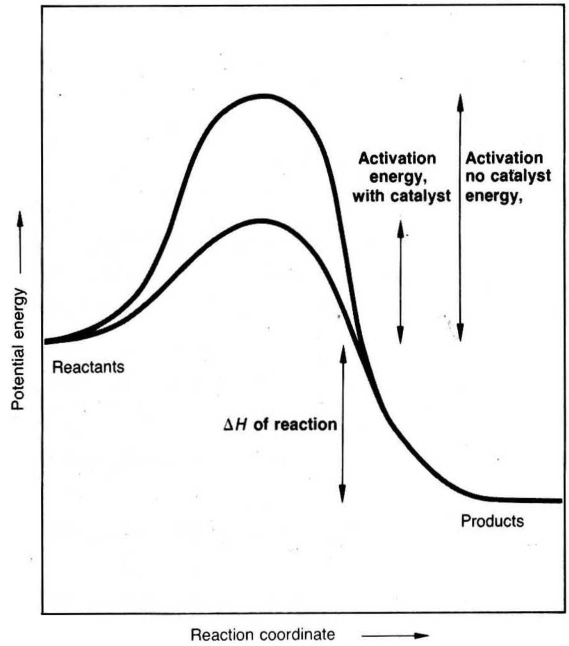

FIGURE 2

Hydrolysis reactions

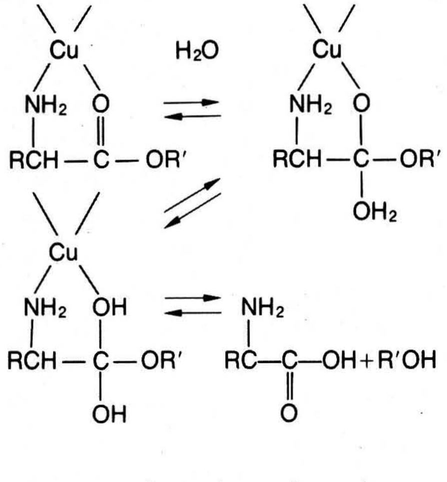

Proposed mechanism for the Cu^{2+} – catalyzed hydrolysis of phenylalanine ethyl ester is shown along with the catalytic order over the pH range of 7–8.

Positively charged metal ions can function effectively as Lewis acids in these reactions and can be expected to catalyze reactions which are similarly catalyzed by Brönsted acids. For simple esters the proton is a more efficient catalyst due to its higher charge density. However, metals appear to be more catalytically active with substrates containing additional functional groups such as amino acid esters. An important factor in metal catalysis appears to be the ability of the metal ion to coordinate with the substrate and remove electron density from a site subject to bond breaking or nucleophilic attack (*7*). For example, Co(II) and Cu(II) have been shown to be effective catalysts for the hydrolysis of glycine methyl ester in the pH range of 7–8 (*15*); likewise Cu(II) proved to be more effective than either H^+ or OH^- for the catalytic hydrolysis of phenylalanine ethyl ester (*16*). A mechanism consistent with the observed rate law:

$$\frac{-d[S]}{dt} = \nu = k_h\,[S][Cu^{2+}] \quad (4)$$

for the rapid hydrolysis of α-amino acids, S, is shown in Figure 2 where there is a direct complexation of Cu^{2+} by the ester group. In general, the effectiveness of metal ion catalysts parallels their formation constants for complexation with the same substrate (i.e., $k_h \alpha \beta$).

Decarboxylation reactions are also catalyzed by a variety of metal ions. Prue (*17*) investigated the metal-ion-catalyzed decarboxylation of acetone-dicarboxylic acid:

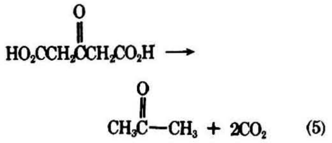

$$HO_2CCH_2\overset{O}{\overset{\|}{C}}CH_2CO_2H \longrightarrow CH_3\overset{O}{\overset{\|}{C}}{-}CH_3 + 2CO_2 \quad (5)$$

over a wide pH range and found that the deprotonated acid, A^{2-}, was most strongly catalyzed by metal ions. He found a linear free energy relationship between the rate constant for the catalytic pathway and the dissociation constant for the corresponding metal-malonate complex. In this case the activated complex was postulated to be similar to the bidentate chelate, malonate. The order of catalytic activity was reported as: $Cu^{2+} > Ni^{2+} > Zn^{2+} > Co^{2+} > Mn^{2+} > Cd^{2+}$. Similar catalytic effects were reported by Gelles and Salama (*18*) for the decarboxylation of oxaloacetic acid for which the following order of catalytic activity was observed: $Cu^{2+} > Zn^{2+} > Co^{2+} > Ni^{2+} > Mn^{2+} > Ca^{2+}$.

Metal ions catalyze other hydrolysis reactions (*7*) which may be of importance environmentally, such as the hydrolysis of tripolyphosphate:

$$P_3O_{10}^{5-} + H_2O \rightarrow HP_2O_7^{3-} + HPO_4^{2-} \quad (6)$$

Catalytic activity is again correlated to the ability of a particular metal to form a complex with the substrate. In aqueous solution at pH 7-9 the tripolyphosphate anion is extremely stable; however, with the addition of Cu^{2+}, Zn^{2+}, or Pb^{2+}, the hydrolysis reaction is accelerated greatly (*19*).

Redox reactions

Transition metals that have several stable oxidation states are frequently active as catalysts involving electron transfer. Catalysis in many redox reactions results from a special combination of relative rates when an active metal exists in more than one oxidation state (*11*). The catalytically active metal can be oxidized and reduced cyclically at a rapid rate with a concomitant catalytic influence on a slower reaction.

Redox reactions such as the oxidation of Cr(III) to Cr(VI) by $S_2O_8^{2-}$ are often thermodynamically favorable but kinetically slow (*20*). The oxidation of Cr(III) proceeds according to the following stoichiometric equation:

$$2Cr^{3+} + 3S_2O_8^{2-} + 7H_2O \rightarrow Cr_2O_7 + 6SO_4^{2-} + 14H^+ \quad (7)$$

with a $\Delta G° = -530$ kJ/mol. In the absence of catalytic influences the reaction rate is imperceptible. Upon the addition of Ag^+ the reaction proceeds at a measurable rate according to the following rate law (*21*):

$$-\frac{3}{2}\frac{d[Cr(III)]}{dt} = k_1[S_2O_8^{2-}][Ag^+] \quad (8)$$

For redox reactions, the rate law is often first order in oxidant and zero order in reductant when catalyzed by trace metals. The best evidence that trace metals are involved in a reaction mechanism is an unusual empirical rate law (*3*).

For the oxidation of Cr(III), Yost (*21*) proposed the following alternative rate-determining steps:

$$S_2O_8^{2-} + Ag^+ \underset{k_{-1}}{\overset{k_1}{\rightleftarrows}} 2SO_4^{2-} + Ag^{3+} \quad (9)$$

or

$$S_2O_8^{2-} + Ag^+ \underset{k_{-1}}{\overset{k_1}{\rightleftarrows}} SO_4^{2-} + \cdot SO_4^- + Ag^{2+} \quad (10)$$

TABLE 1

Kinetic data for autoxidation of sulfide—comparison of results

Reference	Reaction	Water	pH	$t_{1/2(min)}$[a]
1	$HS^- + O_2$	Seawater	8.0	280
2	$HS^- + O_2$	Distilled[b]	7.9	3000
3	$HS^- + O_2$	Seawater	8.2	24
4	$HS^- + O_2$	Seawater	7.8	175
5	$HS^- + O_2$	Fresh[c]	7.6	880
6	$HS^- + O_2$	Distilled	11.0	570
7	$HS^- + O_2$	Fresh	8.6	2200
8	$HS^- + O_2$	Fresh	8.0	114
9	$HS^- + O_2$	Seawater	7.7	600
10	$HS^- + O_2$	Distilled[b]	8.7	2220
11	$HS^- + O_2 +$ CoTSP[d]	Distilled	8.3	7

[a] Calculated from reported data

[b] EDTA added

[c] Simulated

[d] CoTSP = Co(II)-4,4′,4″,4‴-tetrasulfophthalocyanine = 2×10^{-9}M

(1) Almgren, T.; Hagstrom, I. *Water Res.* **1974,** *8*, 395.
(2) Chen, K. Y.; Morris, J. C. *Environ. Sci. Technol.* **1972,** *6*, 529.
(3) Ostlund, H. G.; Alexander, J. *J. Geophys. Res.* **1963,** *68*, 3395.
(4) Cline, J. D.; Richards, F. A. *Environ. Sci. Technol.* **1969,** *3*, 838.
(5) O'Brien, D. J., Birkner, F. B. *Environ. Sci. Technol.* **1977,** *12*, 1114.
(6) Avrahami, M., Golding, R. M. *J. Chem. Soc.* **1968, (***A***)**, 647.
(7) Demirjian, Y. A. "The Electrochemical Characterization of the Rates of Oxidation of Soluble Sulfides by Molecular Oxygen"; Ph.D. Thesis, University of Michigan, Ann Arbor, 1971.
(8) Moussavi, M. "Autoxidation of Aqueous Sulfide in the Presence of Phenols—Kinetics and Products"; Ph.D. Thesis, University of Southern California, Los Angeles, 1974.
(9) Sorokin, Y. I. *Okeanologiya* **1971,** *11*, 423.
(10) Lim, B. C. H. "Kinetics and Mechanism of the Oxidation of Sulfide by Oxygen Catalyzed by Homogenous Organometallic Complexes"; M.S. Thesis, University of Minnesota, 1979.
(11) Hoffmann, M. R.; Lim, B. C. *Environ. Sci. Technol.* **1979,** *13*, 1406.

The independence of the reaction rate on the concentration of Cr(III) suggests that the product of the decomposition of the activated complex, $AgS_2O_8^-$, is the active oxidant.

From an environmental standpoint, the oxidation of Cr(III) by O_2 is a reaction that is thermodynamically favored under certain pH conditions but kinetically hindered. Conceivably, this reaction is also sensitive to trace metal catalysis. If so, the notion of safe disposal of Cr(III) in aquatic systems must be examined in light of its potential catalytic conversion to toxic Cr(VI) under suitable oxidizing conditions.

Other redox reactions, such as the oxidation of oxalic acid by chlorine, are sensitive to catalysis by metals with multiple oxidation states. Mn(III) catalyzes the oxidation as follows:

$$Mn^{3+} + C_2O_4^{2-} \overset{\beta_1}{\rightleftarrows} MnC_2O_4^+ \quad (11)$$

$$MnC_2O_4^+ \xrightarrow[\text{Slow}]{k} Mn^{2+} + CO_2 + CO_2^{-}\cdot \quad (12)$$

$$CO_2^{-}\cdot + Cl_2 \rightarrow CO_2 + Cl\cdot + Cl^- \quad (13)$$

$$Cl\cdot + Mn^{2+} \rightarrow Mn^{3+} + Cl^- \quad (14)$$

$$C_2O_4^{2-} + Cl_2 \rightarrow 2CO_2 + 2Cl^- \quad (15)$$

where Equation 15 represents the overall stoichiometry or the summation of Equations 11-14. This reaction sequence is an example of catalysis by a metal that has two stable oxidation states differing by two electrons (i.e., Mn(II) and Mn(IV)). The intermediate oxidation state, Mn(III), is unstable with respect to disproportionation (*22*) with K ~ 10^9:

$$2Mn^{3+} + 2H_2O \rightleftarrows Mn^{2+} + MnO_2 + 4H^+ \quad (16)$$

Although Mn^{3+} is highly unstable, it may be sufficiently persistent under suitable conditions to expect a significant catalytic influence.

Another mode of metal catalysis for redox reactions is the phenomenon of induced catalysis. This occurs when a relatively fast reaction between an oxidant and reductant forces a slow reaction between one of the former reactants and another substance (*3, 11*). Again, the reaction of oxalic acid and chlorine will be used to illustrate this catalytic phenomenon.

The oxidation of $C_2O_4^{2-}$ by Cl_2 is accelerated by the reaction of Fe(II) and Cl_2. A mechanism proposed by Taube (*23*) is as follows:

$$\mathrm{Fe(II)} + Cl_2 \rightarrow \mathrm{Fe(III)} + Cl_2^- \quad (17)$$

$$Cl_2^- + HC_2O_4^- \rightarrow H^+ + 2Cl^- + C_2O_4^{-}\cdot \quad (18)$$

$$C_2O_4^{-}\cdot + Cl_2 \rightarrow Cl_2^- + 2CO_2 \quad (19)$$

$$Cl_2 + C_2O_4^- \rightarrow Cl_2^- + 2CO_2 \quad (20)$$

$$Cl_2^- + C_2O_4^- \rightarrow 2Cl^- + 2CO_2 \quad (21)$$

$$Cl_2^- + Cl_2^- \rightarrow 2Cl^- + Cl_2 \quad (22)$$

This catalytic scheme differs fundamentally from the $\mathrm{Cr(III)}/S_2O_8^{2-}/Ag^+$ reaction in that the apparent catalytic metal, Fe(II), is not regenerated. Metals such as Cu(II), Ni(II), and Co(II) also exert a positive catalytic effect on the above reaction.

Autoxidation reactions

The term autoxidation refers to general reactions of oxidizable materials with molecular oxygen although earlier definitions were more restrictive. In general, reactions of triplet ground-state oxygen with singlet spin-state reductants are slow in the absence of catalytic influences because they involve a change in spin multiplicity and because a significant amount of bond deformation or alteration of a permanent nature may occur. Most often autoxidations are undesirable for commercial materials because of resulting damage and reduced lifetimes. Autoxidations are greatly accelerated by trace metals such as Cu(II), Co(II), Fe(II), Mn(II), Ni(II), and many of their coordination complexes.

The autoxidation of H_2S and HS^- in both fresh and seawater systems has been shown to be sensitive to trace metal catalysis by Mn(II), Cu(II), Fe(II), Ni(II), and Co(II) (*24, 25*). A general characteristic of trace metal catalysis, as mentioned above, is the occurrence of nonreproducible reaction rates and unusual empirical rate laws. The kinetics of the autoxidation of sulfide have been studied by a number of investigators under slightly different experimental conditions. These results are summarized in Table 1. From comparison of the reported half-lives in Table 1 as measured by different investigators, it is obvious that the reaction may be sensitive to a variety of catalytic influences in addition to trace metals. These include general base, microbial, and surface catalysis. The reported half-lives vary from days to minutes under similar concentration conditions and the observed kinetic orders vary from one investigator to another.

FIGURE 3

Radical mechanism for SO_2 autoxidation

Initiation	SO_3^{2-}	+	M^+	$\xrightarrow{k^1}$	$SO_3^{\cdot-}$	+	$M\cdot$
	$h\nu$	+	SO_3^{2-}	$\xrightarrow{k_0}$	$SO_3^{\cdot-}$	+	$\bar{e}$ (aq)
Propagation	$SO_3^{\cdot-}$	+	O_2	$\xrightarrow{k_2}$	$SO_5^{\cdot-}$		
	$SO_5^{\cdot-}$	+	SO_3^{2-}	$\xrightarrow{k_3}$	SO_5^{2-}	+	$SO_3^{\cdot-}$
	$SO_5^{\cdot-}$	+	HSO_3^-	$\xrightarrow{k_{3'}}$	HSO_5^-	+	$SO_3^{\cdot-}$
Oxidation	SO_3^{2-}	+	SO_5^{2-}	$\xrightarrow{k_4}$	$2SO_4^{2-}$		
Termination	$SO_3^{\cdot-}$	+	$SO_5^{\cdot-}$	$\xrightarrow{k_5}$	$S_2O_6^{2-}$	+	O_2
	$SO_5^{\cdot-}$	+	$SO_5^{\cdot-}$	$\xrightarrow{k_6}$	$S_2O_6^{2-}$	+	$2O_2$

Radical mechanism rate laws

Thermal reaction

k_2 Slow; k_5 Termination

$$(1)\ \nu = \frac{d\,[SO_4^{2-}]}{dt} = \left(\frac{k_2 k_1 k_3}{k_5}\right)^{1/2} [M^+]^{1/2} [SO_3^{2-}] [O_2]^{1/2}$$

k_3 Slow; k_6 Termination

$$(2)\ \nu = k_3 \left(\frac{k_1}{k_6}\right)^{1/2} [M^+]^{1/2} [SO_3^{2-}]^{3/2}$$

Photochemical reaction

$$(3)\ \nu = \left(\frac{k_0 k_2}{k_5}\right)^{1/2} [SO_3^{2-}] [O_2]^{1/2}$$

Hoffmann and Lim (*1*) have studied the catalytic autoxidation of sulfide over the pH range 5–12. The catalytic effects of Co(II), Ni(II), and Cu(II)-4,4′,4″,4‴-tetrasulfophthalocyanine as shown in Figure 3 were determined. The reaction kinetics were characterized in terms of a rate law of the general form:

$$\frac{-d[HS^-]}{dt} = \frac{k[\mathrm{Catalyst}][O_2][HS^-]}{K_C + K_B[O_2] + K_A[HS^-] + [O_2][HS^-]} \quad (23)$$

which reduces to a rate law with an apparent zero-order dependence on $[O_2]$ when $[O_2] \gg [HS^-] > K_C$ and $K_B > [HS^-]$:

$$\nu = k[\mathrm{Catalyst}][HS^-] \quad (24)$$

Mechanistically, the rate law of Equation 23 combined with spectroscopic information indicates that the reaction proceeds via the formation of a tertiary activated complex in which O_2 and HS^- are reversibly bound to the metal complex as shown below:

$$\mathrm{Co(II)TSP} + O_2 \overset{\beta_1}{\rightleftarrows} \mathrm{Co(III)TSP\text{-}}O_2\cdot \quad (25)$$

$$\mathrm{Co(III)TSP\text{-}}O_2\cdot + HS^- \overset{\beta_2}{\rightleftarrows} \mathrm{Co(II)TSP} + HSO_2^- \quad (26)$$

$$\mathrm{Co(III)TSP\text{-}}O_2\cdot + HS^- \underset{\text{Slow}}{\overset{k}{\rightleftarrows}} \mathrm{Co(II)TSP} + HSO_2^- \quad (27)$$

$$HSO_2^- + O_2 \underset{\text{Rapid}}{\xrightarrow{k'}} HSO_4^- \quad (28)$$

The rate constant, k, over a wide range of pH was found to be $1.0 \pm 0.2 \times 10^5$ $M^{-2}\ min^{-1}$ with a catalytic turnover number > 100 000. For example, the half-life for the uncatalyzed reaction is approximately 50 h, whereas the half-life when [CoTSP] = 0.1 nM was reduced to 5 min (*1*). The mechanism shown above is a nonradical enzyme-like mechanism. Frequently, autoxidation reactions proceed via free radical reactions initiated by a suitable metal catalyst, and their rate laws are characterized often by nonintegral reaction orders in catalyst concentration. Catalytic autoxidation of SO_2 by transition metals dissolved in submicron water aerosols has been suggested (*4, 24–28*) as a viable nonphotolytic pathway for the rapid formation of sulfuric acid in relatively humid atmospheres. However, present experimental evidence in the laboratory and field shows considerable disagreement on the relative rates of SO_2 transformation to H_2SO_4 in microdroplets.

Inconsistent reaction rates, rate laws, and pH dependencies have been observed for aqueous solution kinetic studies of the reaction of $SO_2 \cdot H_2O$ and oxygen as pointed out by Hegg and Hobbs (*27*), Larson et al. (*4*), and

Beilke and Gravenhorst (*28*). Redox reactions sensitive to homogeneous trace metal catalysis exhibit reaction rate laws that are often first order in one reactant and zero order in the other. The autoxidations of SO_2 and H_2S in aqueous solution fall into this general category of redox reactions. For example, oxygen concentrations in water are reduced to near zero levels in mass-transfer studies of aeration equipment by the addition of SO_3^{2-} and an appropriately soluble Co(II) salt. The reduction of oxygen proceeds according to the stoichiometry:

$$H_2O \cdot SO_2 + \tfrac{1}{2}\, O_2 \rightarrow H_2SO_4 \qquad (29)$$

In one experimental study (*29*), a nonintegral rate law, with a zero-order dependence on oxygen

$$-d[H_2O \cdot SO_2]/dt = \nu_M$$
$$= k_M[\mathrm{Co(II)}]_T^{0.5}[SO_3^{2-}]^{1.5} \qquad (30)$$

was observed for the catalytic effect of hexaquo Co(II). A suitable mechanism for the thermal initiation of a free radical reaction is shown in Figure 3 based on the original mechanism proposed by Bäckström (*30*). Using the steady-state and long-chain length approximations for a free radical, closed-sequence catalytic process (*31*), two different rate laws are predicted. When the k_3 step is assumed to be the rate-determining step and k_6 the termination step, the rate law given in Equation 2 of the figure is obtained mathematically. However, when the reaction is initiated by UV radiation or the thermal reaction is limited by the k_2 step, different rate laws are predicted. Laboratory studies of the liquid-phase oxidation of SO_2 by O_2 have suggested many different rate laws, reaction rates, and pH dependencies under similar conditions.

In general, the majority of experimental results show that the homogeneous aqueous-phase reaction rate has an overall reaction order of 3 with first-order dependencies on $[M^+]$, $[SO_3^{2-}]$, and $[H^+]$. Some free radical mechanisms postulated by various investigators are inconsistent with experimentally determined reaction orders.

Bassett and Parker (*33*) reported evidence for formation of a discrete complex of manganese, oxygen, and two sulfite ions in their study of the autoxidation of SO_3^{2-}. Matteson et al. (*32*) also postulated an intermediate complex of O_2–Mn(II)–SO_2 for SO_2 oxidation in aqueous aerosol droplets. In both these studies, the anticipated radical termination product, dithionic acid, was not observed. These results suggest an enzymelike pathway given in Equations 25–28. A hypothetical mechanism involving the nominal activation of molecular O_2 by a suitable metal catalyst followed by complexation and oxidation of sulfite would be as follows:

$$\mathrm{Co(II)} + O_2 \overset{\beta_1}{\rightleftarrows} \mathrm{Co(III)}O_2\cdot \qquad (31)$$

$$\mathrm{Co(III)}O_2\cdot + SO_3^{2-} \overset{\beta_1}{\rightleftarrows}$$
$$\mathrm{Co(III)}O_2 \cdot SO_3^{2-} \qquad (32)$$

$$\mathrm{Co(III)}O_2 \cdot SO_3^{2-} \xrightarrow[\text{Slow}]{k_3}$$
$$\mathrm{Co(III)}O \cdot SO_4^{2-} \qquad (33)$$

$$\mathrm{Co(III)}O \cdot SO_4^{2-} + SO_3^{2-} \overset{\beta_4}{\rightleftarrows}$$
$$^{2-}SO_3\mathrm{Co(III)}O \cdot SO_4^{2-} \qquad (34)$$

$$^{2-}SO_3\mathrm{Co(III)}O \cdot SO_4^{2-} \xrightarrow[\text{Fast}]{k_5}$$
$$\mathrm{Co(II)} + 2SO_4^{2-} \qquad (35)$$

where Equation 33 would be the rate-determining step. Using a determinant procedure for a system of nonhomogeneous linear equations obtained from steady-state considerations (*35*), a rate law similar in form to Equation 23 is obtained. This equation can be reduced under certain conditions to give a rate expression which is zero order in oxygen and first order in both catalyst and sulfite concentration.

Sheldon and Kochi (*35*) have summarized a sequence of reactions that may be involved in the catalytic autoxidation of various hydrocarbons. For a generalized hydrocarbon, RH, a probable sequence of simultaneous reactions would be as follows:

$$M^{2+} + O_2 \rightleftarrows M^{3+}\text{-}O_2\cdot \qquad (36)$$

$$M^{3+}\text{-}O_2\cdot + RH \rightarrow$$
$$M^{2+} + R\cdot + HO_2\cdot \qquad (37)$$

$$M^{3+}\text{-}O_2\cdot + RH \rightarrow$$
$$M^{3+}\text{-}O_2H + R\cdot \qquad (38)$$

$$M^{3+}\text{-}O_2\cdot + RH \rightarrow$$
$$M^{3+} + R^- + HO_2\cdot \qquad (39)$$

or

$$M^{3+}\text{-}O_2\cdot + RH \rightarrow$$
$$M^{3+} + R\cdot + HO_2^- \qquad (40)$$

where M^{2+} is a catalytically active metal. A characteristic of most autoxidations is the formation of reactive peroxide intermediates as shown in Equations 37–40.

In commercial autoxidations, M^{2+} is frequently Co(II) or an associated organometallic complex. For example, Uri (*36*) proposed a mechanism for Co(II) stearate catalysis of the autoxidation of methyl linoleate that is consistent with the generalized sequence above:

$$\mathrm{Co(II)} + O_2 \overset{\beta_1}{\rightleftarrows} \mathrm{Co(II)}\text{-}O_2 \qquad (41)$$

$$\mathrm{Co(II)} + RH \overset{\beta_2}{\rightleftarrows} \mathrm{Co(II)}RH \qquad (42)$$

$$\mathrm{Co(II)}O_2 + \mathrm{Co(II)}RH \xrightarrow{k}$$
$$\mathrm{Co(II)} + \mathrm{Co(III)}R + HO_2 \qquad (43)$$

$$\mathrm{Co(II)}O_2 \cdot RH \xrightarrow{k}$$
$$\mathrm{Co(III)}R + HO_2\cdot \qquad (44)$$

Similar Co(II)-catalyzed mechanisms for the autoxidation of benzylthiol (*37*), cumene (*38*), acrolein (*38*), and 2-mercaptoethanol (*39*) have been proposed. Certain transition metal complexes are capable of reversibly binding and activating molecular oxygen (*41–43*). The commonly accepted mode of O_2 attachment to Co(II) complexes involves dioxygen apically bound in a bent configuration in which a *d*-electron from Co(II) is transferred to O_2, producing $O_2\cdot$ bound to Co(III). It is this attached superoxide that is thought to be the active catalytic site.

Catalytic activity of metal phthalocyanines in aqueous solution has been reported by Cook (*13, 44*) for the autoxidation of HI and benzaldehyde and Wavnerova and co-workers (*45, 46*) for the autoxidation of hydroxylamine and hydrazine.

Pollution control applications

Transition metals and associated complexes may prove to be useful from a commercial standpoint for improved pollution control systems. The catalyzed autoxidation of H_2S and SO_2 and other reduced sulfur compounds in the presence of homogeneous (*47, 48*) or heterogeneous (*39*) organometallic complexes may provide convenient and economical methods for sulfur pollution control. The principal products of the metal phthalocyanine-catalyzed autoxidation of H_2S and mercaptans in sour refinery distillates were reported to be colloidal sulfur, polythionates, and sulfate (*49*). Conceivably, similar catalytic systems could be used for the autoxidation of selected organic pollutants for industrial wastewater treatment.

Improved catalytic ability, elimination of recovery problems, and longer catalyst lifetimes may be achieved with supported organometallic catalysts (*50–52*). Mass et al. (*39*) have reported on enhanced catalytic autoxidation of mercaptoethanol by Co(II) tetraminophthalocyanine attached to cross-linked polyacrylamide. Autoxidation of Klaus plant

FIGURE 4.

A possible application

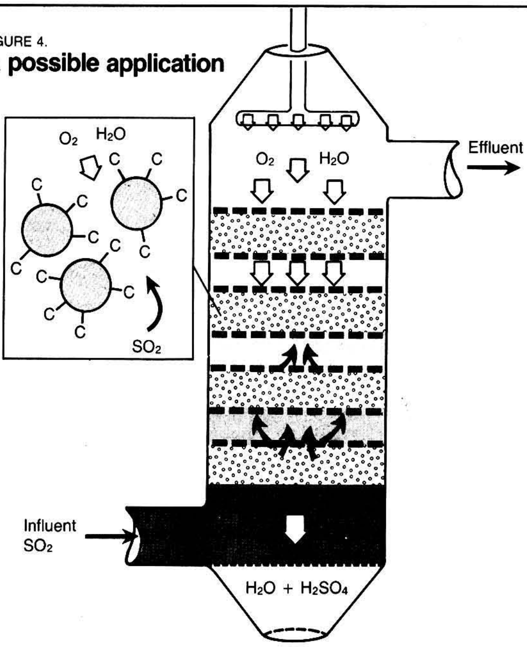

A potential application of polymer-supported organometallic catalysts for SO_2 stack-gas scrubbing is illustrated above. The active catalyst, C, is supported on appropriate solid supports and placed in fixed beds in a countercurrent flow reactor.

effluents or SO_2 in flue gases by supported organometallic complexes such as the phthalocyanines may provide an economical method for emission reduction. Figure 4 illustrates a hypothetical countercurrent reactor with fixed beds of solid supported catalyst that could be used for SO_2 scrubbing with the production of H_2SO_4 as an alternative to limestone slurry scrubbers which produce an unusable solid reaction product. Research along these lines is currently underway in this laboratory.

References

(1) Hoffmann, M. R.; Lim, B. C. *Environ. Sci. Technol.* **1979,** *13,* 1406.
(2) Parshall, G. W. *Science* **1980,** *208,* 1221.
(3) Edwards, J. O. "Inorganic Reaction Mechanism"; Benjamin: New York, 1965.
(4) Larson, T. V.; Horike, N. R.; Halstead, H. *Atmos. Environ.* **1978,** *12,* 1597.
(5) Ball, D. L.; Edwards, J. O. *J. Phys. Chem.* **1958,** *62,* 343.
(6) Walling, C. *Acct. Chem. Res.* **1975,** *8,* 125.
(7) Basolo, F.; Pearson, R. G. "Mechanisms of Inorganic Reactions," 2nd ed.; Wiley: New York, 1967.
(8) Ostwald, W. *Physik. Z.* **1902,** *3,* 313.
(9) Bredig, G. *Ulmann's Enzyke Technol. Chem.* **1909,** *6,* 670.
(10) Bell, R. P. "Acid and Base Catalysis," 2nd ed.; Cornell University Press: Ithaca, 1971.
(11) King, E. L. "Catalysis in Homogeneous Reactions in a Liquid Phase," In "Catalysis: Fundamental Principles"; Emmett, P. H., Ed.; Reinhold: New York, 1955; Vol. II, Part 2.
(12) Wolfe, N. L.; Zepp, R. G.; Paris, D. F. *Water Res.* **1978,** *12,* 561.
(13) Bender, M. L.; Brubacher, L. J. "Catalysis and Enzyme Action"; McGraw-Hill: New York, 1973.
(14) Bender, M. L. *Chem. Revs.* **1960,** *60,* 53.
(15) Kroll, H. *J. Am. Chem. Soc.* **1952,** *74,* 2036.
(16) Bender, M. L.; Turnquest, B. W. *J. Am. Chem. Soc.* **1957,** *79,* 1889.
(17) Prue, J. E. *J. Chem. Soc.* **1952,** 2331.
(18) Gelles, E.; Salama, A. *J. Chem. Soc.* **1958,** 3689.
(19) Thilo, E. *Advan. Inorg. Chem. Radiochemistry* **1962,** *4,* 31.
(20) Fronaeus, S.; Ostman, C. O. *Acta. Chem. Scand.* **1956,** *10,* 320.
(21) Yost, D. M. *J. Am. Chem. Soc.* **1926,** *48,* 152.
(22) Cotton, F. A.; Wilkinson, G. "Advanced Inorganic Chemistry"; Wiley-Interscience: New York, 1972; p. 849.
(23) Taube, H. *J. Am. Chem. Soc.* **1946,** *68,* 611.
(24) Krebs, H. A. *Biochem Z.* **1929,** *204,* 343.
(25) Chen, K. Y.; Morris, J. C, *J. Sanit. Eng. Div., ASCE, 98,* 215.
(26) Cheng, R. T.; Corn, M.; Frohliger, J. O. *Atmospheric Environ.* **1971,** *5,* 987.
(27) Hegg, D. A.; Hobbs, P. V. *Atmospheric Environ.* **1978,** *12,* 241.
(28) Beilke, S.; Gravenhorst, G. *Atmospheric Environ.* **1978,** *12,* 231.
(29) Chen, T.; Barron, C. H. *Ind. Eng. Chem. Fund.* **1972,** *11,* 466.
(30) Bäckström, H. *Z. Physik. Chem.* **1934,** *258,* 122.
(31) Boudart, M., "The Kinetics of Chemical Processes"; Prentice-Hall, Inc.: Englewood Cliffs, N.J., 1968.
(32) Matteson, M. J.; Stober, W.; Luther, H. *Ind. Eng. Chem. Fund.* **1969,** *8,* 677.
(33) Bassett, H.; Parker, W. G. *J. Chem. Soc.* **1951,** 1540.
(34) Laidler, K. J.; Bunting, S. J. "The Chemical Kinetics of Enzyme Action"; Clarendon Press: Oxford, England, 1973.
(35) Sheldon, R. A.; Kochi, J. K. *Oxidation Combustion Revs.* **1973,** *5,* 135.
(36) Uri, N. *Nature* **1956,** *177,* 1177.
(37) Dance, I. G.; Conrad, R. C.; Cline, J. E. *Chem. Comm.* **1974,** 13.
(38) Hara, T.; Ohkatusu, Y.; Osa, T. *Bull. Chem. Soc. Japan* **1975,** *48,* 85.
(39) Mass, T. A.; Kuijer, M.; Zwart, J. *Chem. Comm.* **1976,** 87.
(40) Collman, J. P. *Accts. Chem. Res.* **1977,** *10,* 265.
(41) Basolo, F.; Hoffmann, B. M.; Ibers, J. A. *Accts. Chem. Res.* **1975,** *8,* 384.
(42) Jones, R. D.; Summerville, D. A.; Basolo, F. *Chem. Revs.* **1979,** *79,* 139.
(43) Cook, A. H. *J. Chem. Soc.* **1938,** 1761.
(44) Cook, A. H. *J. Chem. Soc.* **1938,** 1768.
(45) Wagnerova, D. M.; Schertnerova, E.; Veprek-Siska, J. *Collect. Czech. Chem. Commun.* **1974,** *38,* 3096.
(46) Wagnerova, D. M.; Schertnerova, E.; Veprek-Siska, J. *Collect. Czech. Chem. Commun.* **1973,** *38,* 756.
(47) Urban, P.; Rosenwald, R. H., U.S. Patent 3 530 063, Sept. 23, 1970.
(48) Pikl, J., U.S. Patent 2 860 116, Nov. 11, 1958.
(49) Urban, P. *Chem. Abstr.* **1962,** *56,* P6251f.
(50) Pittman, C. U.; Smith, L. R.; Hanes, R. M. *J. Am. Chem. Soc.* **1975,** *97,* 1742.
(51) Robinson, A. L. *Science* **1976,** *194,* 1261.
(52) Hartley, F. R.; Vezey, P. N. *Adv. Organomet. Chem.* **1977,** *15,* 189.

Michael R. Hoffmann *received his B.A. degree in chemistry from Northwestern University in 1968 and his Ph.D. from Brown University in 1973 with a degree program in chemical kinetics. After receiving his Ph.D., Dr. Hoffmann was appointed a Research Fellow at the California Institute of Technology under the NIEHS postdoctoral training program. His research has been focused on applied environmental kinetics in the areas of chemical catalysis, oxidation of reduced sulfur compounds, microbial catalysis, and ligand substitution. From 1975 to 1979, Dr. Hoffmann was an assistant professor of environmental engineering in the Department of Civil and Mineral Engineering at the University of Minnesota. In the summer of 1980, he moved to the California Institute of Technology where he was appointed an associate professor of environmental engineering science.*

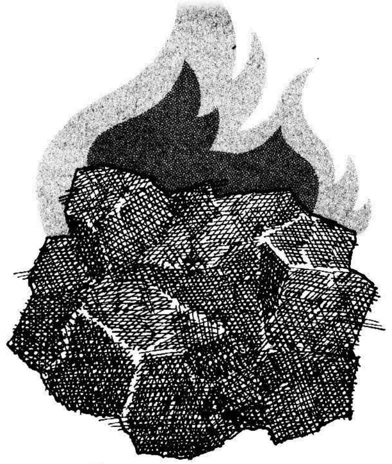

Natural gas can help coal burn cleaner

A relatively small "investment" of gas might sharply increase the amount of coal power plants could use, without the accompanying penalties of increased SO_x emissions and need for expensive air-cleaning equipment

Benjamin Schlesinger
American Gas Association
Arlington, Va. 22209

Oil backout legislation currently before the Congress—the proposed Powerplant Fuels Conservation Act of 1980, which passed the Senate in June—contains a special "select gas use" provision designed to make it easier for converting facilities to meet Clean Air Act standards. A new Section 301 (a) (3) of the Powerplant and Industrial Fuel Use Act of *1978* (PL 95-620) would be added, which would empower the secretary of energy to "allow the use of natural gas in conjunction with coal in such quantities as may be necessary to assist [existing electric power plants converting from oil to coal] in meeting applicable environmental requirements."

Whatever the fate of the proposed oil backout legislation this year, the concept of select gas use in dual coal- and gas-capable boilers has received its first legislation recognition. What does this approach toward air quality control entail? How would it work? Would it be economical?

Background

The idea of blending different fuels, such as coal-oil slurries, gas-liquids, for economic or environmental protection reasons, is not a new concept. The advantages of coal conversion based on blended fuels were recognized by the Congress when it created special "fuel mixtures" exemption categories for both new and existing boilers as part of the Fuel Use Act.

Because natural gas emits virtually no sulfur oxides or particulate matter when combusted (Table 1), state public utility regulators, the public, and environmental interest groups alike encouraged industries and electric power companies to burn gas until the early 1970s, when supplies of gas appeared to become inadequate. Now, with the more favorable outlook for natural gas supplies, which resulted from enactment of the Natural Gas Policy Act of 1978 (PL 95-621), as well as a brightened outlook for gas from unconventional and supplemental sources, it makes sense to suggest that natural gas can play a key, although more selective role in helping to mitigate air emissions, thereby facilitating coal conversion.

Facility conversion

In order to determine how select gas use might reduce emissions, as existing boilers convert from oil to coal, it was assumed that some mixture of coal and natural gas could be combusted in the

Basis for the emission reduction analysis

The following was assumed for this analysis of existing power plant conversions:

- Natural gas is available to, and can be used in all of the power plants listed by the administration in its legislative proposal to Congress without reducing gas supplies for other users.
- The prohibitions contained in the Fuel Use Act (PL 95-620) on gas use in power plants after 1990 would not hinder existing oil-fired power plants from converting to coal as a primary fuel supplemented by select use of gas.
- The EPA "bubble" concept would be applicable to power plants converting from oil to coal and select use of gas; this means that retrofitting these plants to burn coal with gas is not considered a "major modification" for Clean Air Act regulation purposes.
- The average heating value of coal used in U.S. power plants is 22 million Btu/t.
- Electric power plants converting to coal will operate at a 70% load factor, regardless of their previous load factor with oil.

0013-936X/80/0914-1067$01.00/0 © 1980 American Chemical Society

51 electric power plants named in Phase I of the administration's proposed oil backout legislation.

Preliminary analyses by the Economic Regulatory Administration, part of the U.S. Department of Energy (DOE), and by the Environmental Protection Agency (EPA) indicate that the administration's proposed coal conversion program could increase national SO_x emissions by 227 000-345 000 tpy, the DOE and EPA estimates, respectively (Table 2). This increase would raise total SO_x emissions by about 1% over the present level of 35.3 million tpy, and would thereby negate about one-third of the environmental progress in SO_x control achieved by industry between 1970 and 1975. Since some scientists believe sulfur oxide emissions return to earth in various forms, with attendant undesirable environmental effects, absolute SO_x limitation at sources continues to be a national objective.

Currently, the electric power plants which the administration proposes to convert to coal emit an estimated 513 000 tpy of SO_x, excluding two oil-fired units which presently emit higher levels of SO_x than allowed for coal use under their state implementation plans (SIPs). Thus, if 48 of the Phase I-named facilities were converted to coal (excepting the two present coal SIP violators and the one currently burning natural gas), they would collectively emit between 666 000 tpy (DOE estimate), and 833 000 tpy (EPA estimate) of SO_x. This would be an increase of 153 000-320 000 tpy, respectively.

However, when a limited amount of gas is burned—either in the same boiler or in a separate boiler in the same facility—SO_x emissions from the facility could be prevented from increasing beyond current levels. Thus, according to the DOE estimate, combustion of a 77% coal to 23% gas mixture would maintain SO_x emissions at the level previously emitted by oil combustion. According to the EPA estimate, the coal to gas ratio would have to be 62%/38% (Table 3). In overall terms, 280-460 billion ft^3/y more gas use (a 1-3% increase nationally) would permit up to 42 million tpy more coal use (a 7% increase) *without increasing SO_x emissions.*

The "bubble" concept

The EPA could establish a mechanism under existing law, in conjunction with its announced "bubble" concept, that would permit facilities to control emissions on a site or even regional basis, rather than force each emission source within a particular site to

TABLE 1

Comparison of air pollutant emissions (pounds per billion Btu)

Air pollutants	Gas	Oil	Coal
Sulfur oxides	0.6	830-920	660-4390
Particles	5-15	140-720	60-9440
Carbon monoxide	17-20	40	44-88
Hydrocarbons	1-8	7	13-44
Nitrogen oxides	80-700	130-760	670-2440

Sources: U.S. EPA, U.S. DOE, and Hittman Associates, Inc. (Columbia, Md.)

TABLE 2

Sulfur dioxide emissions of power plants [a]

State	Number of plants	Capacity (MW)	Emissions (1000 tpy) Current actual	Emissions (1000 tpy) Maximum allowable coal SIP
Arkansas	2	938	24.35	100.7
Connecticut	5	1 458	15.54	27.3
Delaware	1	389	8.86	14.7
Florida	1	490	10.83	26.6
Georgia	2	294	20.27	20.7
Illinois	1	1 010	13.89	27.3
Maine	1	105	6.00	9.9
Maryland	4	2 018	40.38	62.9
Massachusetts	7	2 849	126.92	142.1
Michigan	2	557	9.01	20.9
New Hampshire	1	150	6.70	13.5
New Jersey	6	1 688	13.97	62.8
New York	8	4 856	147.50	176.7
Pennsylvania	2	303	3.43	3.9
Rhode Island	1	50	1.02	1.2
Virginia	4	2 042	53.32	110.5
Total	48	19 197	501.99	821.7

[a] Originally named in Phase I of S. 2470—DOE estimates.

Note: Total excludes three plants listed in administration proposal. One of those plants burns gas; the other two are presently emitting more SO_x than their coal SIP allows.

Source: Draft Energy Regulatory Administration, U.S. Department of Energy analysis of "Sulfur Dioxide Emission Estimates" (Washington, D.C., March 31, 1980).

TABLE 3

Estimated volume of gas required to maintain current sulfur oxide emissions in Phase I power plants (1000 tpy)

	EPA expected SO_x emissions [a]	DOE expected SO_x emissions [b]	Actual oil emissions	EPA emissions increase	DOE emissions increase
100% Coal 0% Gas	833	666	513	320	153
77% Coal 23% Gas	666	513	513	153	0
62% Coal 38% Gas	513	413	513	0	(100)[c]

[a] Assumes coal emissions equals maximum allowed in SIP.

[b] 80% of EPA emissions—assumes coal quality 80% allowed by SIP to allow for variability in coal.

[c] Absolute reduction in SO_x emissions.

comply with every source standard. For example, a power plant that burns natural gas in one boiler and coal in its remaining boilers would be evaluated only on the basis of total emissions from the entire facility. Applying this concept to oil-fired power plants would allow their conversion to coal, and the select use of gas, without any cumulative SO_x impact.

While any detailed cost estimate would require site-specific data, one example of the cost-effective potential of applying this select gas use concept to EPA's bubble concept is the Norwalk, Conn., power plant (Connecticut Light and Power Co.). A mixture of 73% coal and 27% gas would enable this oil-fired facility to convert from oil to coal *without flue gas desulfurization (FGD) scrubbers,* and still meet Connecticut's coal use SIP at the 80% level.

Nonattainment areas

Two key national policy objectives—increased coal use to offset imported oil, and public health maintenance through air quality control—come into severe conflict when attempts are made to site new coal-fired industrial and utility boilers in or near the nation's "nonattainment" areas. These areas are so named because they fail to achieve National Ambient Air Quality Standards (NAAQS) for one or more pollutants. Any industrial growth and consequent emission increases in these regions must be accompanied by reduced emissions from existing sources, as required by SIPs.

Nonattainment in many locations, however, often exhibits peaking characteristics, as illustrated in Figure 1, which plots all 24-h average particulate levels recorded at one nonattainment station in 1976. These were portrayed in sequence, from the year's best day to its worst day. Typically, only a few days or weeks out of the year are actually in violation of the NAAQS for short averaging times. For example, Figure 1 suggests that in East Liverpool, Ohio, 24-h standards for total suspended particulate matter (TSP) actually were violated only 18 days in 1976 (the three violating days times six, since particles are recorded every sixth day). Inspection of 1976 data shows this city was one of the nation's worst nonattainment stations that year.

Superimposing the particulate emissions associated with a hypothetical new 1000-MW coal-fired power plant 10 miles upwind of the East Liverpool monitoring station would cause an upward shift in the curve in Figure 1. This is shown as the upper curve.

From the East Liverpool example, a strategy of select use of gas capability as part of the new coal-fired power plant could be applied in a combination of three ways to prevent the worsening of NAAQS violation:

- environmental "peak shaving," whereby operation with gas is required during all violating days
- planned seasonal operation with gas if violations have a history of occurring only during certain times of year, such as summertime inversions
- combustion of gas in part of the new facility, such as in a single-boiler unit, all year round to reduce the incremental pollution of the entire project, while reducing any remaining NAAQS violations by other means.

National estimates

Expansion of the new facilities analysis to a national level by the procedure described below roughly quantifies the fuel use impact of the environmental "peak shaving" approach. Note that even a rough quantification of the other two approaches would require substantial additional site- and project-specific information.

On the basis of EPA National Aerometric Data Bank Standards Reports for 1976, seven sample nonattainment stations were selected from among the most severe TSP and SO_2 nonattainment areas throughout the U.S. They were East Liverpool, Ohio;

FIGURE 1

1976 daily particulate emissions recorded at East Liverpool, Ohio[a]

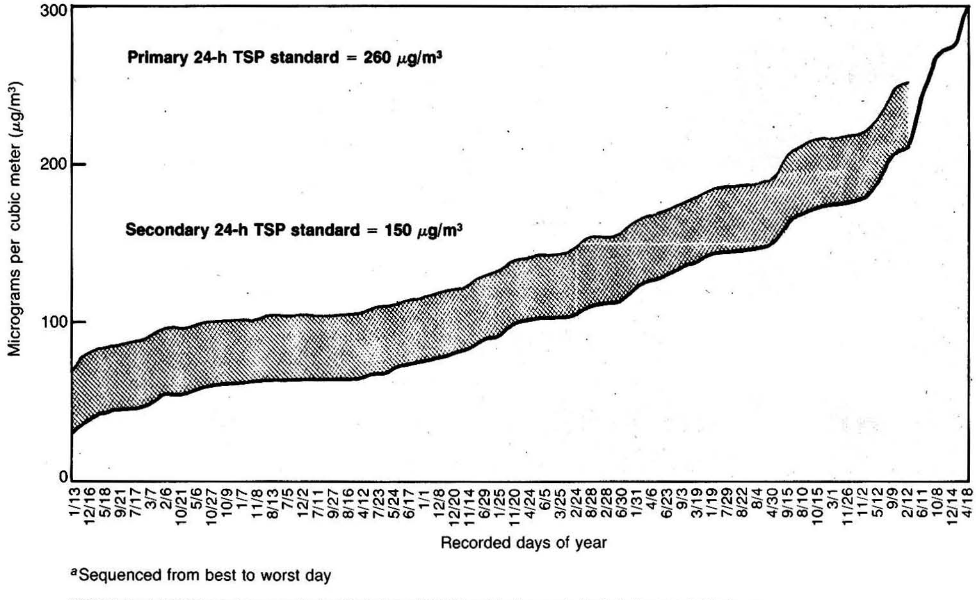

[a] Sequenced from best to worst day

NOTE: Estimated added emissions caused by hypothetical new 1000-MW coal-fired power plant indicated by cross-hatched area

Jefferson County, Ohio; Baltimore, Md.; Greenlee County, Ariz.; Rubidoux, Calif.; St. Louis, Mo.; and Steubenville, Ohio. These stations' daily maximum 24-h TSP and SO_2 readings for 1976 were plotted in ascending order, as shown in Figure 1, and were measured against the primary TSP/SO_2 NAAQS. Under the Clean Air Act, delay in attainment of NAAQS for other contaminants, such as NO_x or carbon monoxide, is permitted until 1987.

The estimated emissions of the new 1000-MW coal-fired power plant with best available control technology (for instance, FGD with 90% removal, and electrostatic precipitators) were added to the existing loadings. The new curves were compared to the respective primary standards to determine the number of days the region would be above the 24-h primary standards for either TSP or SO_2. Gas would then be burned to avoid further NAAQS violations on the resulting above-standard days. Incremental emissions of the 1000-MW power plant were estimated as follows:

- The 2000-MW Ohio Edison Stratton plant is located 10 miles upwind of the East Liverpool monitoring station.
- North Ohio Valley Air Authority personnel estimate that the Ohio Edison plant accounted for 65–75% of both TSP and SO_2 values at the East Liverpool station in 1976. Thus, 70% of the arithmetic mean 1976 TSP and SO_2 values at East Liverpool were assumed to represent impacts of a 2000-MW plant. These values were then halved to approximate the impacts of a 1000-MW coal-fired power plant.
- Because the Ohio Edison Stratton plant was equipped only with electrostatic precipitators in 1976, the calculated SO_2 impacts were adjusted to reflect the impact of flue gas desulfurization equipment, assuming that scrubbers would remove 88% of the SO_2.
- The estimated increment to 24-h maximum ambient SO_2 and TSP levels caused by a 1000-MW coal-fired power plant were calculated for each of the other six regions to account for differences in local coal sulfur content. This was done by multiplying the value obtained by the ratio of local coal sulfur content to that of East Liverpool's.

Quantifying gas demand

The arithmetic average of the number of coal days and gas days was determined for the seven regions as explained above. The resulting breakdown of the 82% coal days and 18% gas days required in order to meet 24-h primary TSP and SO_2 standards was then assumed to be nationally representative, accounting for all site-specific and seasonal variations as follows:

- Table 4 lists the seven nonattainment areas, analyzed together with the number of days of compliance with short averaging time NAAQS, assuming the impact of the new 1000-MW coal-fired power plant 10 miles upwind.

TABLE 4

Estimated days of coal and gas required under select use strategy [a]

Location	Primary standards Coal	 Gas
Baltimore, Md.	256 Days	110 Days
East Liverpool, Ohio	342	24
Greenlee County, Ariz.	261	105
Jefferson County, Ohio	325	41
Rubidoux, Calif.	331	35
St. Louis, Mo.	284	82
Steubenville, Ohio	310	56
Total, 7 areas	2109 (82%)	453 (18%)

[a] For one new 1000-MW coal-fired boiler to meet 24-h NAAQS in seven sample nonattainment areas in 1976.

Source: Charts for each pollutant for each station were drawn from EPA's NA271 yearly summary computer printout pages for each station.

- State-by-state compilations of all U.S. air quality monitoring stations reported nonattainment in 1976 for TSP and SO_2 were assembled from EPA data. The compilations also list the number of stations failing to attain NAAQS for short averaging times only, with ambient NAAQS met.
- The 1976 nationwide average ratio of stations with *only* short averaging time NAAQS violations to *total* nonattainment stations was 32% and 38%, respectively, for TSP and SO_2.

The proportion of partial use of natural gas to reduce emission levels of particles and SO_x was then developed under two separate air quality enforcement cases:

- *Control of both annual and short averaging time NAAQS.* From arithmetic mean determinations, as described above, air quality monitoring data for 1975 and 1976 indicate that 38% of the nation's nonattainment areas for SO_2 were in compliance with the annual, but not the short averaging time NAAQS. (The comparable figure for ambient particles was 32%.) Planned increases in U.S. coal use suggest that in 1985 the characteristics of nonattainment will show similar geographic patterns; thus it is assumed that about one-third will continue to violate short-term NAAQS. On this basis, one third of the 5.5 quad shortfall in U.S. coal use by 1985, or 1.8, is expected in these areas. This level of coal use shortfall, relative to the April 1977 National Energy Plan (NEP-I) forecast, was derived from an American Gas Association analysis. The 1.8 quads were then allocated into 82% coal and 18% gas, to arrive at the estimated fuel use increases shown in Table 5. The utility/industrial split for new coal use was assumed to be 60/40.
- *Control of short averaging time NAAQS only.* At the remaining two-thirds of nonattainment areas, those violating both short and long averaging time NAAQS, it was assumed that alternative means are either available now, or could be made available to offset violations of annual NAAQS. Extending the added fuel use to the remaining two-thirds of nonattainment areas on a straight-line basis yields the estimates shown in Table 5. For these stations, however, it was assumed that the resulting coal use increases will fall 50/50 into utility/industrial applications, along lines of NEP-I.

Conclusions for new facilities

The foregoing estimate of the impact of allowing gas to be burned in new coal-fired boilers on a partial basis reveal the following (Table 5):

- By 1985, approximately 190 million more tons of coal (4.5 quads, or a national increase of some 30%) can be burned annually in new power plants and new large industrial boilers

TABLE 5

Estimated increase in 1985 use of coal and gas[a]

Analysis cases	New coal-fired boilers included	Increased fuel use (quadrillion Btu)		
		Coal	Gas	Total
(A) Select gas used to maintain short averaging time NAAQS in areas with short averaging time violations only.	Industrial	0.5	0.1	0.6
	Electric utility	1.0	0.2	1.2
	Total	1.5[b]	0.3	1.8
(B) Select gas used to maintain short averaging time NAAQS where both short and annual NAAQS are in violation.	Industrial	2.2	0.5	2.7
	Electric utility	2.3	0.5	2.8
	Total	4.5[c]	1.0	5.5

[a] Facilitated by select gas use strategy.
[b] Approximately 60 million tpy of subbituminous coal.
[c] Approximately 190 million tpy, as above.

Notes: Select gas use strategy assumed to apply only in SO_2 and particulate nonattainment areas as of 1976. Alternate means to offset violations of annual NAAQS assumed to be available where needed in case (B). One quad assumed to equal 1 trillion ft^3.

located in nonattainment areas with a select gas use strategy (analysis case "B" in Table 5, extending to all U.S. areas of nonattainment).

- In conjunction with this strategy, an estimated 1.0 trillion ft^3/y of gas nationally (about a 5% increase in U.S. gas use) would be required by 1985 to prevent new coal-fired facilities from violating NAAQS.
- Under a more limited select gas use strategy, extending to nonattainment areas with short averaging time NAAQS violations only, the use of 0.3 trillion ft^3/y of gas would enable combustion of an additional 60 million tons (1.5 quads) per year of coal (analysis case "A" in Table 5).
- Finally, along with contribution to increased U.S. coal use, enhanced emergency capability benefits would be realized by new coal-fired facilities which are sited in nonattainment areas. Their gas capability, both physical and legal, would enable continued operations during restrictions or stoppage of coal supplies for any reason and malfunction or maintenance of plant equipment related to coal use, such as flue gas scrubber outages or breakdowns.

Undoubtedly, enough serious air quality situations will remain at some locations to preclude coal use altogether in new facilities, even with select use of gas. In addition, increasing use of coal gasification will often resolve the coal use vs. environmental effects dilemma in nonattainment areas and elsewhere. Thus, further site-specific studies of facility location decisions and Clean Air Act licensing problems would be required to pin down the precise quantities of coal which may be used in new facilities, and accompanying requirements for gas, under the select gas use strategy.

Nevertheless, application of this strategy appears to promise considerably more coal use—and in an earlier time frame—than anticipated by the DOE in its November 1978 draft Environmental Impact Statement on the Fuel Use Act. That law states categorically that "a boiler was assumed to be exempt [from FUA coal conversion requirements] if located in a county that is designated as an air quality 'nonattainment' area . . ."

Select gas policy

Natural gas would be sold on a premium basis, whether the gas is used throughout the year in part of the facility, or part of the year in the whole facility. Moreover, if natural gas is made available on this premium, assured basis to a coal-burning facility, the gas could be stored by the utility for use in emergencies.

Under the current Clean Air Act, select gas use seems unlikely to replace flue gas scrubbers in *new* facilities; rather, it can enhance siting of new coal-fired boilers which otherwise comply fully with all applicable emission control standards, such as BACT or NSPS. While no revision to the Fuel Use Act is evidently required to implement this strategy, clarification and, in some cases, changes in existing regulations pursuant to both of these laws may be needed, particularly in regulations pursuant to Section 123 of the Clean Air Act. In some *existing* facilities which convert from oil to coal, however, even the scrubber requirement may be waived with select gas use under the "bubble" concept.

Finally, it must again be reiterated that this analysis is preliminary in nature. Analysis of specific facilities and locations would be required to assess accurately the benefit of the select gas use strategy in order to develop a more precise national estimate.

Acknowledgments

This article summarizes two energy analyses prepared by the American Gas Association—Analysis of Select Use of Gas to Enhance Coal Conversion (June 1979) and Analysis of Select Gas Use in Utility Coal Conversion for Limiting Sulfur Emissions (April 1980). The author gratefully acknowledges the assistance of AGA President George H. Lawrence, Michael I. German, Nelson E. Hay, and William Parham in the preparation of these analyses.

Additional reading

U. S. DOE and U.S. EPA, "Energy/Environment Fact Book"; Washington, D.C., March 1978, p. 4.

Office of Technology Assessment, U.S. Congress, "The Direct Use of Coal"; Washington, D.C., April 1979, pp. 222–25.

U.S. EPA, "Air Pollution Control; Recommendation for Alternative Emission Reduction Options Within State Implementation Plans; Policy Statements," *Federal Register,* Dec. 11, 1979, p. 71780.

American Gas Association, "An Analysis of the Constraints on Converting Large Industrial and Utility Boilers from Natural Gas to Coal"; Arlington, Va., Nov. 23, 1977.

American Gas Association, "Evaluation of the President's Proposed Supply-Side Energy Strategy"; Arlington, Va., Sept. 6, 1977.

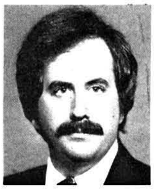

Benjamin Schlesinger *is vice-president, policy evaluation and analysis, of the American Gas Association. He supervises policy and energy studies on key economic, financial, and environmental issues facing the gas industry, and is also responsible for managing the AGA's gas supply and demand forecasting and statistical activities. Schlesinger has been with the AGA since 1977.*

ES&T PRODUCTS

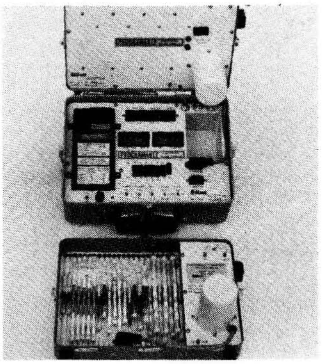

Programmable air sampler
Sampler can be programmed to turn on and off within a 24-h period over 7 days. Sampling tubes for heat desorption, solvent extraction, and color detection can be accommodated. Sensitivity ranges from sub-parts per million to parts per 10^{-17} in some cases. A constant-volume pump draws air through any of 23 sample tubes; sample time, day, number, and flow are automatically recorded on a built-in printer. The unit can operate for a month on rechargeable batteries. Gilian Instruments **104**

Dissolved oxygen meter
This hand-held unit features a 3½ digit LCD display, automatic 0–50 °C temperature compensation, a 90% response time of 10 s, and an accuracy of 0.1 mg/L. The electrode has a teflon membrane and 40″ of cable. The range is 0–19.9 ppm. Great Lakes Instruments **105**

Hi-vol calibration kit
Portable device attaches to the intake orifice of the high-volume air sampler for in-house or field calibration. The calibration manometer readings are then compared with sampler flowmeter readings to generate a calibration curve. Staplex **106**

Need more information about any items? If so, just circle the appropriate numbers on one of the reader service cards bound into this issue and mail in the card. No stamp is necessary.

Tracer gas monitor
Unattended measurement of tracer gases is possible with this automated monitor. The microprocessor-controlled electron-capture gas chromatograph is optimized for measurement of gases such as sulfur hexafluoride and selected fluorocarbons. Applications include meteorology, halocarbon surveillance, infiltration studies, and leak detection. Systems, Science, and Software **108**

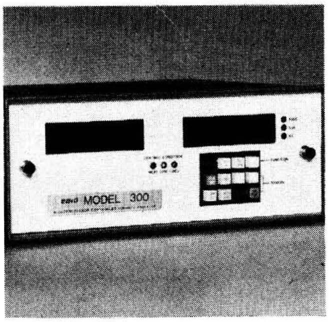

Optical hygrometer
This chilled-mirror optical instrument offers a nominal accuracy of ±0.2 °C with a dew point range of −100 °F to 212 °F. A microprocessor performs continuous optical balancing to compensate for the effects of sample contaminants. Sample pressures from vacuum to 300 psia can be used. EG&G Environmental Equipment **109**

Salinity drop tester
Samples are dropped on a flat electrode plate to provide electric conductivity readings in the range 0.02–255 milliohms/cm. Readout is either absolute or temperature-corrected. The unit is powered by a rechargeable battery. GLA-Agricultural Electronics **110**

***Companies interested in a listing** in this department should send their releases directly to Environmental Science & Technology, Attn: Products, 1155 16th St., N.W., Washington, D.C. 20036*

Air monitoring badge
Two 300-mg strips of activated charcoal are contained in the badge, used to determine time-weighted averages of exposure to organic vapors in the air. Sampling time can range from 15 min to 16 h. The manufacturer claims that its capacity is 3 times that of other passive monitors and its sensitivity 1½ times that. A backup section in the badge contains the second strip which indicates if "breakthrough," or saturation, has occurred during sampling. DuPont. **111**

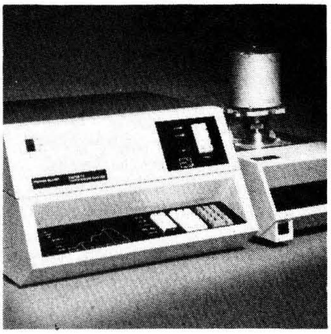

Differential thermal analysis
Furnace has a standard operating range of up to 1500 °C and can be heated at program rates of up to 100 °C per min. The system features automatic correction of baseline slope and zero offset. The microprocessor controller provides a basis for specifying and storing complete analytical methods. Perkin-Elmer **112**

Organic spill detection
Two models that eliminate corrosion-prone gold-lined cells and optical balancing are available. Both use a nondispersive infrared detection method; one is designed specifically to monitor compounds that other systems normally miss, including insoluble and volatile organics. Astro **113**

Aqueous ClO_2 analyzer
A polarographic sensor is used to detect concentration of ClO_2 in aqueous solution. As ClO_2 passes through the sensor, which consists of a gas-permeable membrane, gold cathode, silver anode, and buffered electrolyte, the compound is reduced at the cathode, causing a current to flow. The current, proportional to the ClO_2 concentration, is then amplified and displayed on a taut bandmeter. According to the manufacturer, the system is free from interference by chlorine in the sample. No reagents or sample pumps are required. Delta Scientific **118**

Ozone analyzer
Chemiluminescent analyzer has a full scale range of 0.0–1.0 ppm with a minimum detection limit of 2 ppb. An internal battery and gas source provide up to 10 h of operation. Gas supply connections and an external power supply/charger are provided for longer operating periods. Ethylene supply, battery level, air flow, and other operating parameters are continuously monitored; problems are indicated by an LED display and an audible alarm. Alarm and recorder outputs are provided. Columbia Scientific **117**

Flowmeter
Stainless steel, ½″ meter is designed for use with corrosive or caustic fluids. Four range scales are available: 0.5–4 gpm, 0.5–6 gpm, 1.0–12 gpm, and 0.0–16 gpm. The meters are rated at pressures up to 3000 psi and temperatures up to 240 °F. Racine Federated **114**

Stack sampler
High-capacity sampler can be used for in-stack particle sizing of heavy grain loadings. The sampler fits a standard 3″ port, can withstand temperatures of up to 1500 °F, and has a capacity of several grams per stage. Two impaction chambers followed by a cyclone and a backup filter thimble provide automatic fractionation into 4 size ranges. Flow rate range is 0.2–0.5 cfm. Andersen Samplers **115**

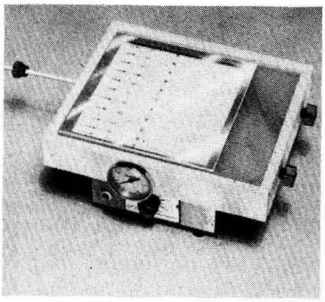

TLC visualization chamber
Thin-layer chromatography plates are heated in the presence of ammonium bicarbonate vapors to induce fluorescent derivatives of most organics compounds separated on the plates. The unit includes a device for removal of fumes and a stainless steel tray so reagents do not come into direct contact with the TLC plates. The chamber can also be used to char TLC plates after treating with sulfuric acid, for intrinsic charring, and for charring after spraying or dipping with most common reagents. Analtech **116**

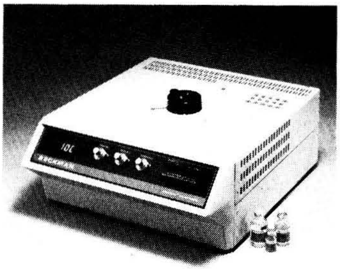

ES&T

LITERATURE

Oil/brine spill cleanup. Brochure tells how to save at least $25 000/acre by cleaning up oil or brine without having to remove and replace topsoil. Trick is special chemical treatment. Lawton Specialty Co., Inc. of Texas **167**

Conductivity meter. Bulletin No. 509 describes Portable Conductivity Meter with 3-in-1 probe, range 0–100 000 μmhos/cm, temperatures 0–40 °C, salinity 0–70 parts per thousand. Can be standardized. Fisher Scientific Co. **168**

Solar electricity. Brochure describes systems for the direct conversion of solar energy into electricity. Modules, arrays, and storage are also discussed. Solar Power Corp. **169**

pH transmitter. Bulletin 4174A explains pH field transmitter. Can be used in situations calling for watertight and explosionproof conditions. Can also do redox measurements. Beckman Instruments, Inc. **170**

Multicomponent analysis. Technical Paper UV-1 (Pub. 23-5953-4751) tells how up to 12 components can be analyzed by a UV/vis spectrophotometer. Large time savings. Hewlett-Packard **171**

HPLC detector. Brochure tells about CMX 20-Amperometric high-performance liquid chromatography (HPLC) detector. Another brochure announces Light Scattering Symposium to be held in San Francisco on Aug. 23. Chromatix **172**

Air velocity. Bulletin describes Model 810LV air velocity monitor and transducer which can range 0–5 m/s and 0–50 m/s. Datametrics **173**

Laboratory supplies. May 1980 catalog lists a whole array of lab supplies, including samplers, environmental products, safety equipment, and others. Interex Corp. **174**

Mobile laboratories. Brochure describes custom-built mobile laboratories based on standard "Chevy" van; for environmental sampling and other uses. Comfortable working conditions. Van Tech Corp. **175**

Sulfur analyzer. Bulletin No. 475A describes totally automated sulfur analyzer system with recyclable reagents. Direct digital display in %-S or ppmS. Fisher Scientific Co. **176**

Calibration standards. Binder contains all information necessary to help the environmental scientist develop dynamic primary standards, gravimetrically calibrated. Justifying data and math are included. Analytical Instrument Development, Inc. **177**

Ammonia measurement. Brochure, "Procedure 502," tells how to measure ammonia in water/wastewater by ion-selective electrode by use of ASTM/EPA-approved methods. Range 0.03–100 ppm. Orion Research **178**

Water clarification. Bulletin, "The BETZ Approach to Successful Water Clarification," describes new treatment approach to meet influent water clarification needs. BETZ Laboratories, Inc. **179**

ppb Analysis. Application Note 3 explains how ions can be measured to parts per billion (ppb) concentrations. Applications include rainwater, ambient SO_2 (as SO_4^{2-}). Dionex Corp. **180**

Safety supplies. June 1980 catalog lists safety supplies for compliance with OSHA regulations. Interex Corp. **181**

Synfuels. News release lists seminar proceedings on synfuels, as well as the Environmental Glossary and Environmental Statutes 1980 and the 6th edition of the Environmental Law Handbook. Government Institutes, Inc. **182**

Air sampling. Catalog lists many items of air-sampling equipment and accessories—more than 1000 test instruments. SKC Inc. **183**

pH electrode. Bulletin 400 describes low-cost pH electrode/flow cell usable to 65 °C and 100 psig. Sensorex **184**

Odor control. Pollution Control Release 115 explains how odors at waste-treatment plants can be eliminated with hydrogen peroxide and gives case histories. FMC Corp. **185**

Water-treatment chemicals. "Fort Pierce Adjusts to Meet Requirements" documents activated-sludge treatment with chemicals to avoid a sewer moratorium. Allied Chemical **186**

SO_2 removal. Bulletin describes line of packed-tower absorbers for SO_2, hydrogen chloride, chlorine, and other gaseous pollutants. Capacities 390–62 000 cfm. Swemco Inc. **187**

Chromatography. Ultrogel® Reference List 1975–1979 has over 500 entries concerning use of Ultrogel products for gel filtration and certain types of chromatography. LKB Instruments, Inc. **188**

Coal analysis. Technical report explains how energy dispersive x-ray fluorescence is used to analyze all elements (including trace elements) found in coal and why this is important. EG&G ORTEC **189**

Lab apparatus. Instrument catalog lists Precision® lab equipment, including analytical, autoclaves, stills. GCA/Precision Scientific Group **190**

Radiation safety. Release announces radiation monitoring equipment now available, even for public use. Dosimeter Corporation of America **191**

Aerosol analysis. Autoion™ Application Note 1 tells how ion chromatography can be used to determine ions in aerosols and to analyze about 90 samples in 24 h, for each ion of interest. Dionex Corp. **192**

Monitoring. Bulletin F616 describes recording charts that are very versatile for environmental monitoring applications. Esterline Angus Instrument Corp. **193**

Wastewater bacteria. Reference chart illustrates types of microorganisms most often found in wastewater-treatment plants. Polybac Corp. **194**

Well-level monitor. Brochure describes deep-well-level monitor for tight control and monitoring of water supplies. Drexelbrook Engineering Co. **195**

Sludge sensors. Brochure describes sensors that can be used in sludge-treatment systems in order to upgrade system performance and optimize control. Arthur Technology **196**

Need more information about any items? If so, just circle the appropriate numbers on one of the reader service cards bound into this issue and mail in the card. No stamp is necessary.

***Companies interested in a listing** in this department should send their releases directly to Environmental Science & Technology, Attn: Literature, 1155 16th St., N.W., Washington, D.C. 20036*

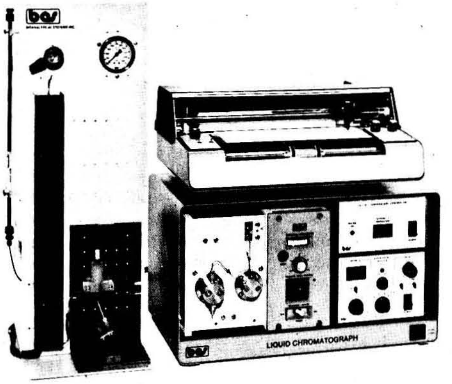

ES&T BOOKS

Stack Monitor Markets. 80 pages and 40 tables. William T. Lorenz & Co., 311 Commonwealth Ave., Boston, MA 02115. 1980. $150, first copy; $25, each additional copy; $15 discount for enclosing payment.

For air pollution compliance, stacks will have to be monitored, and "regs" are growing ever tighter. Thus, this year's stack-analyzer market will grow 90% to $170 million by 1985. Noncompliance monitors, now enjoying a $50-million market, will see a $105-million market by 1985. This report provides complete documentation as to why.

Commonsense in Nuclear Energy. Fred Hoyle, Geoffrey Hoyle. 88 pages. W. H. Freeman & Co., 660 Market St., San Francisco, CA 94104. 1980. $7, hard cover; $3.95, paper.

The authors discuss the danger, or rather the relative lack of it, from nuclear fission energy, and foresee energy shortages of serious proportions if nuclear power is banned. They discuss real dangers from chemicals and coal, and the state of the art of "soft" technologies. They examine the problem of nuclear waste, "if not exactly trivial, not a cause for serious concern," and other related matters.

Atmospheric Dispersion Modeling. 87 pages. Publications Department, Air Pollution Control Association, PO Box 2861, Pittsburgh, PA 15230. 1980. $10 ($8 for APCA members).

This work contains 13 articles on the subject. They include short-term models, validation of the EPA Gaussian model, urban dispersion models, river-valley plume dispersion, and other modeling concepts, including critical reviews and SO_2 concentrations.

Introduction to Environmental Science. Joseph M. Moran, et al. xi + 658 pages. W. H. Freeman & Company, 660 Market St., San Francisco, CA 94104. 1980. $16.95, hard cover.

This text covers many aspects of the field. It considers population, ecosystems, environmental change, the energy crisis, earth resources, water pollution, and the many other subjects germane to the environment.

Lignite Technology. Perry Nowacki, Ed. x + 228 pages. Noyes Data Corp., Mill Road at Grand Ave., Park Ridge, NJ 07656. 1980. $42, hard cover.

Lignite and "low-rank coal" are a large U.S. resource, but they also can present problems in their recovery and use. This book, aimed at presenting the latest state of the art in the field, discusses the resource amount, preparation, direct combustion with air pollution control needs, and gasification/liquefaction.

Atmospheric Pollution 1980. Michael M. Benarie, Ed. xi + 440 pages. Elsevier North-Holland, Inc., 52 Vanderbilt Ave., New York, NY 10017. 1980. $73.25, hard cover.

This book (Studies in Environmental Science 8) contains 61 papers presented at the 14th International Colloquium on Atmospheric Pollution, held in Paris, France, in May. It covers modeling, computer programs, pollutant formation and fate/transport, particulate chemistry, monitoring networks, and many other relevant topics. Effects on humans and vegetation are also discussed.

Solar Energy Technology Handbook. Part A: Engineering Fundamentals. William C. Dickerson, Paul N. Cheremisinoff, Eds. xi + 882 pages. Marcel Dekker Inc., 270 Madison Ave., New York, NY 10016. 1980. $85, hard cover.

Articles by 57 contributors are presented. They provide up-to-date material on thermal collectors, photovoltaics, bioconversion, wind, energy storage, and the solar resource itself. These technologies are discussed in detail; engineering fundamentals, together with working formulas, are presented. Look for Part B: Applications, Systems Design, and Economics to come out later this month.

Cadmium in the Environment. Part 1. Jerome O. Nriagu, Ed. xii + 682 pages. John Wiley & Sons, Inc., 605 Third Ave., New York, NY 10016. 1980. $70, hard cover.

This part describes sources, distribution, transformations, and flow of

(continued on page 1079)

ES&T READER SERVICE REPLY CARD. . . . .

It's computer processed

for fast

response

to your inquiries.

AND, IT'S

FREE

ES&T SEPTEMBER 1980

VALID THROUGH
JANUARY 1981

ADVERTISED PRODUCTS: 1 2 3 4 5 6
7 8 9 10 11 12 13 14 15 16 17
18 19 20 21 22 23 24 25 26 27 28
29 30 31 32 33 34 35 36 37 38 39
40 41 42 43 44 45 46 47 48 49 50
51 52 53 54 55 56 57 58 59 60 61
62 63 64 65 66 67 68 69 70 71 72
73 74 75 76 77 78 79 80 81 82 83
84 85 86 87 88 89 90 91 92 93 94

NEW PRODUCTS: 101 102 103 104 105 106 107
108 109 110 111 112 113 114 115 116 117 118
119 120 121 122 123 124 125 126 127 128 129
130 131 132 133 134 135 136 137 138 139 140
141 142 143 144 145 146 147 148 149 150 151
152 153 154 155 156 157 158 159 160 161 162
163 164 165 166 167 168 169 170 171 172 173
174 175 176 177 178 179 180 181 182 183 184
185 186 187 188 189 190 191 192 193 194 195

NAME:
TITLE:
FIRM:
STREET:
CITY:
STATE: ZIP:
PHONE: ( )

TO VALIDATE THIS CARD, PLEASE CHECK ONE ENTRY FOR EACH CATEGORY BELOW:

Intensity of product need:
- ☐ 1. Have salesman call
- ☐ 2. Need within 6 months
- ☐ 3. Future project

Employees at this location:
- ☐ 1. Under 25
- ☐ 2. 25 - 99
- ☐ 3. 100 - 299
- ☐ 4. 300 - 499
- ☐ 5. 500 - 999
- ☐ 6. 1000 - 2999
- ☐ 7. Over 3000

Areas of your responsibility:
- ☐ A. Air pollution only
- ☐ B. Water pollution only
- ☐ C. Waste treatment only
- ☐ D. Air & Water pollution
- ☐ E. Air & Waste treatment
- ☐ F. Water & Waste treat.
- ☐ G. Air/Water/Waste
- ☐ H. Other Environmental

This copy of ES&T is . . .
- ☐ 1. Personally addressed to me in my name
- ☐ 2. Addressed to other person or to my firm.

Principal product to which my work relates:
- ☐ A. Oil/Gas/Petroleum
- ☐ B. Plastics/Resins
- ☐ C. Rubber
- ☐ D. Drugs/Cosmetics
- ☐ E. Food/Beverages
- ☐ F. Textile/Fiber
- ☐ G. Pulp/Paper/Wood
- ☐ H. Soaps/Cleaners
- ☐ I. Paint/Coating/Ink
- ☐ J. Agrichemicals
- ☐ K. Stone/Glass/Cement
- ☐ L. Metals/Mining
- ☐ M. Machinery
- ☐ N. Auto/Aircraft
- ☐ O. Instrument/Controls
- ☐ P. Inorganic Chemicals
- ☐ Q. Organic Chemicals
- ☐ R. Other Manufacturing
- ☐ S. Design/Construction
- ☐ T. Utilities
- ☐ U. Consulting Services
- ☐ V. Federal Government
- ☐ W. State Government
- ☐ X. Municipal Government
- ☐ Y. Education

Membership status:
- ☐ 1. I am an ACS member
- ☐ 2. Not an ACS member

Circle 94 for subscription form to ES&T

NEED MORE INFORMATION?

CIRCLE a key number. . .

SEND IN the postage paid reply card. . .

AND GET free data on any product advertised in this issue. . .

NO POSTAGE
NECESSARY
IF MAILED
IN THE
UNITED STATES

BUSINESS REPLY CARD
FIRST CLASS Permit #27346 Philadelphia, Pa.

POSTAGE WILL BE PAID BY ADDRESSEE

Environmental
Science & Technology

P.O. BOX #7826
PHILADELPHIA, PA 19101

NO POSTAGE
NECESSARY
IF MAILED
IN THE
UNITED STATES

BUSINESS REPLY CARD

FIRST CLASS Permit #27346 Philadelphia, Pa.

POSTAGE WILL BE PAID BY ADDRESSEE

Environmental
Science & Technology

P.O. BOX #7826
PHILADELPHIA, PA 19101

NEED MORE INFORMATION?

CIRCLE a key number. . .

SEND IN the postage paid reply card. . .

AND GET free data on any product advertised in this issue. . .

ES&T SEPTEMBER 1980

VALID THROUGH
JANUARY 1981

ADVERTISED PRODUCTS: 1 2 3 4 5 6
7 8 9 10 11 12 13 14 15 16 17
18 19 20 21 22 23 24 25 26 27 28
29 30 31 32 33 34 35 36 37 38 39
40 41 42 43 44 45 46 47 48 49 50
51 52 53 54 55 56 57 58 59 60 61
62 63 64 65 66 67 68 69 70 71 72
73 74 75 76 77 78 79 80 81 82 83
84 85 86 87 88 89 90 91 92 93 94

NEW PRODUCTS: 101 102 103 104 105 106 107
108 109 110 111 112 113 114 115 116 117 118
119 120 121 122 123 124 125 126 127 128 129
130 131 132 133 134 135 136 137 138 139 140
141 142 143 144 145 146 147 148 149 150 151
152 153 154 155 156 157 158 159 160 161 162
163 164 165 166 167 168 169 170 171 172 173
174 175 176 177 178 179 180 181 182 183 184
185 186 187 188 189 190 191 192 193 194 195

NAME: ______________________
TITLE: ______________________
FIRM: ______________________
STREET: ______________________
CITY: ______________________
STATE: ______________ ZIP: ________

TO VALIDATE THIS CARD, PLEASE CHECK ONE ENTRY FOR EACH CATEGORY BELOW:

Intensity of product need:
- ☐ 1. Have salesman call
- ☐ 2. Need within 6 months
- ☐ 3. Future project

Employees at this location:
- ☐ 1. Under 25
- ☐ 2. 25 - 99
- ☐ 3. 100 - 299
- ☐ 4. 300 - 499
- ☐ 5. 500 - 999
- ☐ 6. 1000 - 2999
- ☐ 7. Over 3000

Areas of your responsibility:
- ☐ A. Air pollution only
- ☐ B. Water pollution only
- ☐ C. Waste treatment only
- ☐ D. Air & Water pollution
- ☐ E. Air & Waste treatment
- ☐ F. Water & Waste treat.
- ☐ G. Air/Water/Waste
- ☐ H. Other Environmental

This copy of ES&T is . . .
- ☐ 1. Personally addressed to me in my name
- ☐ 2. Addressed to other person or to my firm.

Principal product to which my work relates:
- ☐ A. Oil/Gas/Petroleum
- ☐ B. Plastics/Resins
- ☐ C. Rubber
- ☐ D. Drugs/Cosmetics
- ☐ E. Food/Beverages
- ☐ F. Textile/Fiber
- ☐ G. Pulp/Paper/Wood
- ☐ H. Soaps/Cleaners
- ☐ I. Paint/Coating/Ink
- ☐ J. Agrichemicals
- ☐ K. Stone/Glass/Cement
- ☐ L. Metals/Mining
- ☐ M. Machinery
- ☐ N. Auto/Aircraft
- ☐ O. Instrument/Controls
- ☐ P. Inorganic Chemicals
- ☐ Q. Organic Chemicals
- ☐ R. Other Manufacturing
- ☐ S. Design/Construction
- ☐ T. Utilities
- ☐ U. Consulting Services
- ☐ V. Federal Government
- ☐ W. State Government
- ☐ X. Municipal Government
- ☐ Y. Education

Membership status:
- ☐ 1. I am an ACS member
- ☐ 2. Not an ACS member

Circle 94 for subscription form to ES&T

ES&T READER SERVICE REPLY CARD. . . . .

It's computer processed

for fast

response

to your inquiries.

AND, IT'S

FREE

cadmium in the environment. It looks at metal in humans, the nature of cadmium and its uses, cadmium in the atmosphere and natural waters, chemical reactions in nature, plant uptake, and toxicity. Cadmium in forest and marsh ecosystems is also discussed.

Biological Monitoring for Environmental Effects. Douglas L. Worf, Ed. xii + 227 pages. Lexington Books, D. C. Heath and Co., 125 Spring St., Lexington, MA 02173. 1980. $22.95, hard cover.

Among topics covered are scenarios on alternative futures for biological monitoring, federal/state programs, coastal waters, use of vegetation, benthic organisms, and plants as mutagen monitors. Other scientific subjects are treated, as well as regulatory and policy issues.

Chemical Mutagens. Vol. 6. Frederick J. de Serres, Alexander Hollaender, Eds. xix + 485 pages. Plenum Press, 227 W. 17th St., New York, NY 10011. 1980. $49.50, hard cover.

This book explains principles and methods for the detection of chemical mutagens. Among subjects discussed are mechanisms of cell transformation, commercial screening of environmental chemicals, genelocus mutation, in vitro and in vivo screening needs, and many other topics related to this discipline.

Priority Toxic Pollutants. Marshall Sittig, Ed. x + 370 pages. Noyes Data Corp., Mill Rd. at Grand Ave., Park Ridge, NJ 07656. 1980. $54, hard cover.

This work covers priority pollutants from acenaphthene to zinc. It looks at occurrence, physical/chemical properties, groups at risk, existing guidelines/standards, uses of the substances in question, current levels of exposure, and proposed criteria (summarized).

Renewable Energy Prospects. Wilfrid Back et al., Eds. xv + 310 pages (numbered 711–1021). Pergamon Press, Inc., Maxwell House, Fairview Park, Elmsford, NY 10523. 1980. $50, hard cover.

Papers contributed were presented at a nonfossil, nonnuclear fuel conference held in Honolulu, HI. They go into numerous aspects of alternative energy, including resources, availability, economics, climatic effects, demand/supply, and developing countries' possibilities.

Petroleum in the Marine Environment. x + 371 pages. American Chemical Society, 1155 16th St., NW, Washington, DC 20036. 1980. $42, hard cover.

These papers were presented at ACS' 176th National Meeting. They offer an overview, analytical methods, discussions of distribution, hydrocarbon extraction, analysis in sediments, and other related matters.

Environmental Impact of Nonpoint Source Pollution. Michael R. Overcash, James M. Davidson, Eds. xii + 449 pages. Ann Arbor Science Publishers Inc., Box 1425, Ann Arbor, MI 48106. 1980. $29.95, hard cover.

Control of point sources of water pollution is only part of the battle. Nonpoint source control remains a problem and is probably a much "tougher nut to crack." Papers given in this book discuss nonpoint sources of pesticides, pathogens, nitrogen, phosphorus, and sediment. Land use as a nonpoint source and predictive methods for such sources are also covered.

(continued on page 1080)

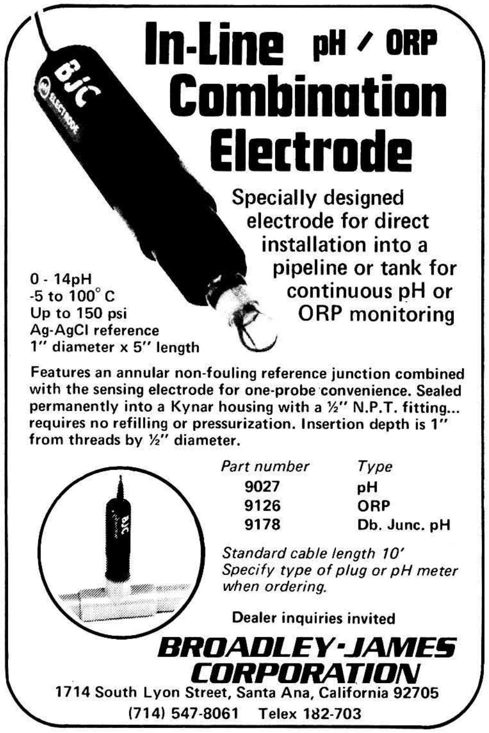

BOOKS (*continued*)

Three Mile Island: Prologue or Epilogue? Daniel Martin. ix + 253 pages. Ballinger Publishing Co., 17 Dunster St., Cambridge, MA 02138. 1980. $14.50, hard cover.

This book explains the structure of Three Miles Island's nuclear plant, gives a minute-by-minute description of what took place, and goes over testimony at various levels of government. Particular emphasis is given to communications problems, as well as those perceived for safety procedures and inspection processes. The author argues that reactors cannot really be fail-safe.

Microbiology for Environmental Scientists and Engineers. Anthony F. Gaudy, Jr., Elizabeth T. Gaudy. xvi + 736 pages. McGraw-Hill, 1221 Avenue of the Americas, New York, NY 10020. 1980. $25.95, hard cover.

Microorganisms offer a most important means to evaluate environmental effects. This textbook looks into microorganisms by discussing water quality control, chemical nature of cells, life-support systems, aerobic and anaerobic metabolism, responses to changes in the environment, and pathogens. Growth and energy generation/utilization are also covered.

Analyzing and Interpreting Air Monitoring Data. UNEP and WHO. WHO Publications Centre USA, 49 Sheridan Ave., Albany, NY 12210. 1980. $4.25, paper.

This guide is a contribution to the Global Environment Monitoring System (GEMS). It offers valid statistical approaches to the analysis of air monitoring data, and their refinement from reams of raw data to understandable finished products of reduced data.

Inside EPA Weekly Report. Periodical. Inside Washington Publishers, Box 7167, Ben Franklin Station, Washington, DC 20044. 1980. $395/y (charter subscriptions, $345/y), inside US; add $45/y for Canada and foreign.

This periodical is aimed at giving the reader a feeling for what is going on and what is probably to come at EPA, almost from a within-EPA viewpoint. For example, "hit lists" under noncompliance penalties, rule waiver possibilities, research plans, and other topics are covered. Related federal activity is included.

Moving California Toward A Renewable Energy Future. Laura B. King et al. 100 + pages. Natural Resources Defense Council, Inc., 25 Kearny St., San Francisco, CA 94108. 1980. $8, paper.

This report proposes that California can meet its energy needs through 1995 without any new nuclear or coal-fired power plants. It also says that cost-effective conservation measures can cut out all growth in electricity and natural gas demand after 1985. Resources considered include geothermal, cogeneration, hydro, wind, solar, and biomass. NRDC also believes that the alternative sources would cost less and provide more jobs.

Journal of the Cooling Tower Institute. Jack V. Matson, Ed. Periodical. Journal of the Cooling Tower Institute, Box 56184, Houston, TX 77027. 1980. $20/y to libraries; $10/y to nonmembers; $6/y to members.

This periodical considers cooling towers and what goes on inside them, as well as how to optimize their performance. Chemistry of cooling tower water, treatment methods, and many other pertinent topics are covered.

MEETINGS

September 21–26 Pacific Grove, CA
Risk/Benefit Analysis in Water Resources Planning and Management. Engineering Foundation and U.S. Dept. of the Interior, Office of Water Research and Technology

Write: Engineering Foundation, 345 E. 47th St., New York, NY 10017

September 25–26 Baton Rouge, LA
5th Annual Analytical Chemistry Symposium. Baton Rouge Analytical Instrument Discussion Group

Write: Garry Lash, Symposium Chairman, Hewlett-Packard Co., 3239 Williams Blvd., Kenner, LA 70063

September 27 Las Vegas, NV
I. Hazardous Waste Management. II. Pretreatment of Industrial Wastewaters for Discharge into Municipal Sewers. The AWARE Corporation

Write: The AWARE Corporation, Box 40284, Nashville, TN 37204

September 28–29 St. Paul, MN
Water, Human Values and the 80s. Freshwater Society

Write: Gloria McDonald, Freshwater Society, 2500 Shadywood Rd., Box 90, Navarre, MN 55392

September 28–October 3
Philadelphia, PA
7th Annual Meeting of the Federation of Analytical Chemistry and Spectroscopy Societies. FACSS

Write: Sydney Fleming, Engineering Physics Laboratory, Experimental Station, E-357, E.I. du Pont de Nemours & Co., Wilmington, DE 19898

September 28–October 3
Las Vegas, NV
Water Pollution Control Federation Conference. Water Pollution Control Federation

Write: Robert A. Canham, WPCF, 2626 Pennsylvania Ave., NW, Washington, DC 20037

September 30–October 3
Atlantic City, NJ
8th North American Motor Vehicle Emissions Control Conference. U.S. EPA and the New Jersey State Department of Environmental Protection

Write: Joseph Soporowski, Jr., Conference Coordinator, c/o Dept. of Environmental Science, Rutgers University, Box 231, New Brunswick, NJ 08903

September 30–October 3
Chicago, IL
Strategic Planning for Disposal of Solid Wastes. The Center for Energy and Environmental Management

Write: Center for Energy and Environmental Management, Box 536, Fairfax, VA 22030

October 1–3 University Park, PA
4th Symposium on Electron Microscopy and X-Ray Applications to Environmental and Occupational Health Analysis. Pennsylvania State University and the University of Denver (Denver Research Institute)

Write: Clayton O. Ruud, Conference Chairman, 159 Materials Research Laboratory, Pennsylvania State University, University Park, PA 16802

October 2 Chicago, IL
EPA's Regulation of New Chemical Substances. Center for Energy and Environmental Management

Write: Center for Energy and Environmental Management, Box 536, Fairfax, VA 22030

October 3 Chicago, IL
EPA Testing Requirements Under ISCA. Center for Energy and Environmental Management

Write: Center for Energy and Environmental Management, Box 536, Fairfax, VA 22030

October 6–9 Houston, TX
EXPOCHEM '80. University of Texas

Write: Dr. Albert Zlatkis, Chemistry Dept., University of Houston, Houston, TX 77004

October 6–9 Denver, CO
Joint Symposium on Stationary Combustion NO_x Control. U.S. EPA and the Electric Power Research Institute

Write: Keith Bentz, Symposium Coordinator, Acurex Corporation, 485 Clyde Ave., Mountain View, CA 94042

October 7–8 Philadelphia, PA
5th Symposium on Aquatic Toxicology. American Society for Testing and Materials, Committees E-35 and D-19

Write: J. Gareth Pearson, U.S. Army Medical Bioengineering R&D Laboratory, Ft. Detrick, Frederick, MD 21701

October 7–8 Los Angeles, CA
3rd Annual Conference on Environmental Regulation—Solutions to the Regulatory Maze. California Business Law Institute and the Association of Energy Engineers

Write: California Business Law Institute Seminars, Box 3727, Santa Monica, CA 90403

October 7–9 Gatlinburg, TN
Analytical Chemistry in Environmental Regulation and Control. Oak Ridge National Laboratory and its Analytical Chemistry Division

Write: W. S. Lyon, Oak Ridge National Laboratory, Box X, Oak Ridge, TN 37830

October 9–10 Niagara Falls, NY
Major International Technical Conference on Toxic Air Contaminants, Health Effects, Monitoring and Control. Air Pollution Control Association (Middle Atlantic States Section, Niagara Frontier Section and Ontario Section)

Write: J. D. Scalise, Ashland Petroleum Company, 4545 River Rd., Tonawanda, NY 14150

October 9–10 Houston, TX
Destruction Methods for Toxic Organic Chemicals. McGraw-Hill Seminar Center

Write: Priscilla Robertson, McGraw-Hill Seminar Center, 305 Madison Ave., Rm. 3112, New York, NY 10017

(continued on page 1082)

October 10–12 Denver, CO
2nd Annual Symposium of the International Association for the Advancement of Appropriate Technology for Developing Countries. IAAATDC, the Solar Energy Research Institute, and the University of Denver
Write: Suzanne Faulhaber, University of Denver, Dept. of Economics, University Park, Denver, CO 80208

October 11–12 San Diego, CA
Urban Lakes—Design and Management Workshop. Academy of Arts & Sciences of Aquatic Ecosystems
Write: Dr. William A. Hanson, Westlake Lake Management, 32353 Trunfo Canyon Blvd., Westlake Village, CA 91361

October 12–15 Washington, DC
3rd Annual Conference on Environmental Issues. The Edison Electric Institute and Envirosphere Company
Write: Stuart Patterson, Envirosphere Company, Two World Trade Center, New York, NY 10048

October 14–16 Atlanta, GA
3rd World Energy Engineering Congress. Association of Energy Engineers and the Alliance to Save Energy
Write: 3rd World Energy Engineering Congress, Association of Energy Engineers, 4025 Pleasantdale Rd., Ste. 340, Atlanta, GA 30340

October 15–16 Chicago, IL
Cost Benefit Analysis in Environmental Regulation: Will It Clear the Air or Muddy the Water? The Conservation Foundation and the Illinois Institute of Natural Resources
Write: Conference Coordinator, The Conservation Foundation, 1717 Massachusetts Ave., NW, Washington, DC 20036

October 15–17 Washington, DC
Management of Uncontrolled Hazardous Waste Sites. U.S. EPA in affiliation with U.S. Coast Guard, Chemical Manufacturers Association, National Solid Waste Management Association, and Hazardous Materials Control Research Institute
Write: Beverly Walcoff, Hazardous Materials Control Research Institute, 9300 Columbia Blvd., Silver Spring, MD 20910

October 16–17 Washington, DC
Synfuels and the Environment: Progress or Paralysis? Inside EPA, the Weekly Report, and The Energy Bureau
Write: Robert W. Nash, The Energy Bureau Inc., 41 E. 42nd St., New York, NY 10017

October 16–17 Houston, TX
Engineering '80. American Association of Engineering Societies, Inc.
Write: American Association of Engineering Societies, Inc., 345 E. 47th St., New York, NY 10017

October 19–23 Richland, WA
Coal Conversion and the Environment. U.S. DOE and Battelle Memorial Institute, Pacific Northwest Laboratories
Write: Patricia M. Bresina, Symposium Secretary, Biology Dept., Battelle, Pacific Northwest Laboratories, Richland, WA 99352

October 20–23 Washington, DC
AOAC's 94th Annual Meeting. Association of Official Analytical Chemists
Write: Kathleen Fominaya, AOAC, 1111 N. 19th St., Ste. 210, Arlington, VA 22209

October 28–30 Columbus, OH
5th International Symposium on Polynuclear Aromatic Hydrocarbons. Battelle Columbus Laboratories
Write: Dr. Alf Bjorseth, Battelle Columbus Laboratories, 505 King Ave., Columbus, OH 43201

Courses

September 22–24 Washington, DC
Preparation of Environmental Impact Statements. George Washington University, Continuing Engineering Education
Fee: $510. *Write:* Registrar, Continuing Engineering Education, George Washington University, Washington, DC 20052

September 22–24
East Brunswick, NJ
Stack Sampling and Ambient Air Monitoring. Center for Professional Advancement
Fee: $520. *Write:* The Center for Professional Advancement, General Information, Box H, East Brunswick, NJ 08816

September 22–24 Minneapolis, MN
Aerosol Measurement. Institute of Technology, Dept. of Mechanical Engineering, University of Minnesota
Fee: $450. *Write:* Joe Kroll, Dept. of Conferences, 335 Nolte Center, 315 Pillsbury Dr., SE, University of Minnesota, Minneapolis, MN 55455

September 22–26 Appleton, WI
Water and Wastewater Control. The Institute of Paper Chemistry
Fee: $500. *Write:* Kathy Stanek, Office of Continuing Education, Institute of Paper Chemistry, Box 1039, Appleton, WI 54912

September 22–26 Detroit, MI
I. Hazardous Materials Training. II. Hazardous Waste Management. Vanderbilt University and several other government and private organizations
Fee: $595. *Write:* Dr. Thomas H. F. Smith, Director, Environmental Resources Group, IMS America, Ltd., Ambler, PA 19002

September 23–25 Akron, OH
Industrial Hygiene Sampling Methods. American Industrial Hygiene Association
Fee: $400. *Write:* J. R. Conti, American Industrial Hygiene Association, 475 Wolf Ledges Pkwy., Akron, OH 44311

September 23–26 Phoenix, AZ
Quality Assurance for Air Pollution Measurement Systems. Air Pollution Training Institute
Fee: Lecture course-$22 per student day, laboratory course-$35 per student day. *Write:* Registrar, Air Pollution Training Institute, MD-20, Research Triangle Park, NC 27711

September 29–October 1
Washington, DC
Energy Forecasting. George Washington University, Continuing Engineering Education
Fee: $495. *Write:* Registrar, Continuing Engineering Education, George Washington University, Washington, DC 20052

September 29, 30–October 1, 2
San Francisco, CA
Hazardous Chemical Safety Management. Eastek Corporation
Fee: $480. *Write:* Short Course Registrar, Eastek Corporation, 3543 Baldwin Dr., Easton, PA 18042

October 5–24 Boston, MA
Program in Environmental Policy and Management. Harvard University, School of Public Health
Fee: $2500. *Write:* Emily Maughan, Program in Environmental Policy and Management, Executive Programs in Health Policy and Management, Harvard School of Public Health, 677 Huntington Ave., Boston, MA 02115

October 6–8 Washington, DC
Methodologies for Environmental Impact Studies. George Washington University, Continuing Engineering Education
Fee: $510. *Write:* Registrar, George Washington University, Continuing Engineering Education, Washington DC 20052

(continued on page 1083)

October 6–10 Nashville, TN
Industrial Toxicology. Vanderbilt University and various other government and private organizations

Fee: $595. *Write:* Dr. Thomas H. F. Smith, Director, Environmental Resources Group, IMS America, Ltd., Ambler, PA 19002

October 14–17 Detroit, MI
Hazardous Chemical Safety Management. Eastek Corporation

Fee: $480. *Write.* Short Course Registrar, Eastek Corporation, 3542 Baldwin Dr., Easton, PA 18042

October 15–17 East Brunswick, NJ
High Purity Gas Technology. The Center for Professional Advancement

Fee: $535. *Write:* Rosanne Razzano, Dept. NR, The Center for Professional Advancement, Box H, East Brunswick, NJ 08816

October 15–17 Washington, DC
Stack Sampling of Air Pollutants. George Washington University, Continuing Engineering Education

Fee: $525. *Write:* Registrar, Continuing Engineering Education, George Washington University, Washington DC 20052

October 16–17 Dallas, TX
Environmental Laws and Regulations, Introductory Course. Government Institutes, Inc.

Fee: $425. *Write:* Margureite Leishman, Government Institutes, Box 5918, Washington, DC 20014

International

September 21–26 Athens, GA
International Symposium on Nutrient Cycling in Agricultural Ecosystems. University of Georgia, USDA Science and Education Administration, and the National Science Foundation

Write: Dr. Robert L. Todd, Dept. of Agronomy and Institute of Ecology, University of Georgia, Athens, GA 30602

October 9–15
Dusseldorf, West Germany
INTERKAMA '80. Alliance International, Inc.

Write: Alliance International, Inc., 1301 W. 22nd St., Ste, 813, Oakbrook, IL 60521

October 16–17 Atlanta, GA
International Symposium on Environmental Pollution. Alena Enterprises of Canada

Write: Vijay Mohan Bhatnagar, Alena Enterprises of Canada, Box 1779, Cornwall, Ontario K6H 5V7, Canada

(continued on page 1085)

Principles of Genetic Toxicology
by **David Brusick**
Litton Bionetics, Kensington, Maryland

This book provides nongeneticists with an introduction to the fundamentals of genetic toxicology. Suitable for use as a textbook, **Principles of Genetic Toxicology** also serves as a reference for toxicologists, chemists, and administrative personnel seeking information on biological and chemical safety evaluation. approx. 275 pp., illus., 1980, $25.00

Polluted Rain
edited by **Taft Y. Toribara, Morton W. Miller,**
and **Paul E. Morrow**
University of Rochester Medical Center

Polluted Rain begins with an analysis of the sources of pollution and a description of some of the mechanisms for the formation of these offensive materials. Present systems for monitoring the pollutants are outlined and, because pollution problems transcend state and national boundaries, the current status of the legal implications of this hazard is explained. **Environmental Science Research, Volume 17.** 514 pp., 1980, $49.50

Environmental Education
Principles, Methods, and Applications
edited by **Trilochan S. Bakshi**
Athabasca University, Canada
and **Zev Naveh**
Technion–Israel Institute of Technology, Israel

Environmental Education brings together internationally known ecologists and educators who are involved in science education. Emphasizing transdisciplinary concepts, the volume integrates theoretical, methodological, and practical aspects of the field. **Environmental Science Research, Volume 18.** 300 pp., 1980, $32.50

How to Obtain Abundant Clean Energy
by **Linda Baine McGown**
California State University, Long Beach
and **John O'M. Bockris**
Texas A&M University

Explaining why industrialized society's dependence on nonrenewable energy sources can only lead to disaster, the authors of this crucial volume discuss in a clear and objective fashion what energy actually is, where we get it now, why present sources won't work for the future, and what alternatives are available. A unique aspect of this work is the emphasis on the use of hydrogen as an energy medium—a viable alternative to nuclear sources. 276 pp., illus., 1980, $14.95

THE LANGUAGE OF SCIENCE
Plenum
PUBLISHING CORPORATION

227 West 17th Street, New York, N.Y. 10011

CIRCLE 10 ON READER SERVICE CARD

ENVIRONMENTAL IMPACT SPECIALIST

Sverdrup & Parcel and Associates, Inc., the engineering, architectural and planning firm of Sverdrup Corporation, is seeking a project leader with demonstrated experience in conducting EIS and NEPA related studies for environmental projects, as well as transportation facilities and electric utilities. Advanced engineering degree preferred. The position is in our St. Louis office.

We offer a challenge and responsibility in a group dedicated to professional growth. Send resume in confidence to Personnel Office, Sverdrup & Parcel and Associates, Inc., 801 North Eleventh, St. Louis, MO 63101.

Sverdrup

An Equal Opportunity Employer M/F/H

SENIOR ENVIRONMENTAL ENGINEERS

WAPORA, Inc., a leading environmental contract research company, is looking for senior environmental engineers for its offices in New York City; suburban Philadelphia; Chevy Chase, Maryland; Atlanta; Cincinnati; Dallas and Chicago. Environmental impact experience highly desirable. Project management positions, as well as administrative openings exist for personnel who can manage programs, write well, and help in marketing.

Send resume, including salary history, in confidence to:

WAPORA, Inc.
6900 Wisconsin Avenue
Chevy Chase, MD 20015
Attn: Dr. J. I. Bregman, President

EOE M/F Principals Only

RESEARCH ASSOCIATE

Energy/Environment

The East-West Center is a national educational institution founded by the U.S. Congress in 1960 to promote better relations and understanding among nations through cooperative programs of study, research, and training. These programs focus on crucial problems of mutual concern to countries of Asia and the Pacific and the United States. Staff, visiting scholars, senior professionals, and graduate degree students form teams which work on these problems. All Center programs are multinational and multidisciplinary. In its staff, the Center seeks excellence in team research; commitment to the development of policy aids, educational products, and practical applications of such research; and ability to work cooperatively with those from other cultures and disciplines.

Applications and nominations are being accepted for a full-time academic staff position in the Center's Environment and Policy Institute. In addition, Fellowships and Research Internships are available from time to time.

Candidates for the staff position must have a Ph.D. or its acadmeic equivalent plus at least three years of experience in research on the *environmental* aspects of one or more of the following areas:

1. Coal production, conversion, or combustion, including the implications for air quality standards;
2. Off-shore oil exploration and production and the effects of oil on aquatic systems;
3. Growing and processing fuelwood or agricultural crops for energy.

Cover letter should give examples of demonstrated ability to: (a) discover knowledge about natural resource and environmental issues, especially at the international level; (b) develop applications of this knowledge, for example, curricula, educational materials, policy aids; and (c) design and implement research and education projects and activities in a team context, preferably mutinational. Experience in Asia/Pacific region as well as in the United States preferred. Working proficiency in the English language required.

Salary commensurate with extent of experience and qualifications. Additional current cost-of-living allowance of 12.5% (subject to change). All nominees will be contacted to determine interest. Applications with cover letter, complete curriculum vitae, and names and addresses of three professional references must be postmarked no later than October 31, 1980. Starting date flexible. Send to Rebecca Dixon, Personnel Division, Dept. 11, East-West Center, 1777 East-West Road, Honolulu, Hawaii 96848.

An Equal Opportunity Employer M/F

Post-doctoral position available immediately to study the movement of pollutants in the environment. Applicants must have a strong background in aquatic chemistry, hydrology or environmental biogeochemistry. Field experience is necessary. Apply giving resumé and names of 3 referees to: **Dr. F. H. Rigler, Chairman, Department of Biology, McGill University, 1205 Avenue Docteur Penfield, Montréal, P. Q. H3A 1B1.** Deadline for applications is September 15, 1980.

ENVIRONMENTAL ENGINEER

Project Leader/Faculty Member Ph.D. in Environmental or Chemical Engineering, with good knowledge of kinetics of biological waste treatment systems, to direct research in new ways of handling pulp and paper mill effluents and sludges, teach graduate level courses and supervise student research in Environmental Engineering. Some knowledge of pulp and paper processes and industrial experience desirable.

Write: Director of Personnel
The Institute of Paper Chemistry
P. O. Box 1039, Appleton, WI 54912
An Affirmative Action/Equal Opportunity Employer

The South Florida Water Management District is seeking candidates for an experienced, professional position involving chemical work in limnological research on Lake Okeechobee. Duties include the design and conducting of limnological studies on Lake Okeechobee, Florida with strong emphasis on eutrophication models, water quality relationships, and chemical limnology. Graduation from college with a bachelor's degree in limnology and two years' responsible experience in chemical limnology or eutrophication modeling; or a master's degree in limnology with a specialization in chemical limnology or eutrophication modeling. Salary range $17,326.40. Please send resume to the **South Florida Water Management District, Employee Relations Office, P.O. Box "V", West Palm Beach, FL 33402.** Equal Opportunity Employer.

ENGINEERING DEAN, CLEMSON UNIVERSITY

The college has 131 faculty, 2,530 students, 9 undergraduate programs, 12 Masters/9 Ph.D. programs, $5.5 million contracts/grants in force, and a $6.2 million state budget. Qualifications: earned Ph.D.; academic administration experience; evidence of scholarly achievements. Nominations by October 6; applications by October 17, 1980. Contact: Chairperson, Dean Search; College of Engineering; Clemson University; Clemson, S. C. 29631. An equal opportunity, affirmative action employer.

CLASSIFIED ADVERTISING RATES

Rate based on number of insertions used within 12 months from date of first insertion and not on the number of inches used. Space in classified advertising cannot be combined for frequency with ROP advertising. Classified advertising accepted in inch multiples only.

Unit	1-T	3-T	6-T	12-T	24-T
1 inch	$70	$67	$64	$62	$60

(Check Classified Advertising Department for rates if advertisement is larger than 10″.)
SHIPPING INSTRUCTIONS:
Send all material to

Environmental Science & Technology
Classified Advertising Department
25 Sylvan Rd. South
Westport, CT. 06880
(203) 226-7131

October 20–22 Pittsburgh, PA
41st International Water Conference. Engineers' Society of Western Pennsylvania

Write: Engineers' Society of Western Pennsylvania, William Penn Hotel, 530 Wm. Penn Pl., Pittsburgh, PA 15219

October 20–25
Buenos Aires, Argentina
5th International Congress on Clean Air. International Union of Air Pollution Prevention Association

Write: North/South Travel, 200 W. 58th St., New York, NY 10019

Call for Papers

September 15, 1980 deadline
Energy in the Man-Built Environment—The Next Decade. American Society of Civil Engineers, Urban Planning and Development Division

Conference will be held in Vail, CO, August 3–5, 1981. *Write:* William F. Ayer, American Society of Civil Engineers, 345 E. 47th St., New York, NY 10017

September 30 deadline
Symposium–Workshop on Solid Wastes from Urban and Industrial Sources. U.S. EPA and a host of other U.S. and Italian scientific and government organizations

Symposium will be held June 10–12, 1981 in Rome, Italy. *Write:* William J. Lacy, U.S. Program Committee RD-680, U.S. EPA, Washington, DC 20460

October 1 deadline
Emerging Environmental Solutions for the Eighties. Institute of Environmental Sciences

Meeting will be held May 4–7, 1981 in Los Angeles, CA. *Write:* Dr. Halsey B. Chenoweth, Westinghouse Electric Corporation, Box 746, Mail Stop 454, Baltimore, MD 21203

November 1 deadline
1st Asian and Pacific Chemistry Congress. Singapore National Institute of Chemistry and the Singapore National Academy of Science

Congress will take place in Singapore, April 26–May 1, 1981. *Write:* The Congress Secretary, 1st ASPAC Congress, Singapore Professional Centre, 129B, Block 23, Outram Park, Singapore 0316

November 30 deadline
1981 International Symposium on Environmental Pollution. Alena Enterprises of Canada

Symposium will be held Nov. 16–17, 1981 in Miami Beach, FL. *Write:* V. M. Bhatnagar, Alena Enterprises of Canada, Box 1779, Cornwall, Ontario K6H 5V7 Canada

CLASSIFIED SECTION ■ POSITIONS OPEN

ENVIRONMENTAL ENGINEER

Ecology and Environment, Inc., with offices in 16 U.S. cities and 9 countries, offers outstanding growth opportunities for experienced environmental scientists and engineers. Our consulting projects range from environmental monitoring of the Trans-Alaska Pipeline to studies for the new industrial complex at Yanbu on the Red Sea. Founded in 1970, E & E is expanding rapidly in all areas of environmental consulting.

Currently, we are seeking a well qualified environmental or sanitary engineer with a Master's degree and 3–5 years experience in water quality analysis and/or industrial wastewater treatment to join our headquarters technical staff in Buffalo. Project assignments will include environmental impact assessments, industrial pollution control and hazardous waste management.

Interested candidates should send a current resume and salary requirements to Joan Collins at:

ecology and environment, inc.
International Specialists
in the
Environmental Sciences

P.O. Box D,
Buffalo, New York 14225
AN EQUAL OPPORTUNITY EMPLOYER

SENIOR EPIDEMIOLOGIST ENVIRONMENTAL HEALTH

GEOMET Technologies, Inc., a leading contract research organization in environmental and occupational health, is seeking a qualified individual for a challenging career opportunity as SENIOR EPIDEMIOLOGIST. Candidates must possess a doctoral degree in epidemiology and *recognized* professional experience, preferably in environmental health. The responsibilities of the position include design, development, conduct and marketing of epidemiological studies; statistical design and analyses for other research studies and technical assistance in a variety of on-going projects. Work experience in interdisciplinary research is required. Outstanding verbal and written communication skills are essential.

GTI offers competitive salaries, commensurate with education and experience and a comprehensive employee benefits package. Please forward resume to:

Dr. Niren L. Nagda, Director
Environmental Exposure and Effects Assessment
GEOMET Technologies, Inc.
15 Firstfield Road
Gaithersburg, Maryland 20760
(301) 948-0755
EOE m/f

ENVIRONMENTAL SERVICES MANAGER

Colorado Springs

Colorado Interstate Gas Company has an immediate need for a manager to administer company environmental regulatory compliance activities (primarily EPA), provide environmental engineering & planning services, and permit new facilities.

The successful candidate will train, develop, and guide expanding staff; initiate company policies & procedures; and audit facilities, records, and procedures for regulatory compliance. Must have sound managerial skills and suitable Federal regulatory experience. Engineering or other acceptable undergraduate degree required. MBA preferred. Oil & gas experience highly desirable.

Salary ($30's) commensurate with experience and job requirements. Complete company-paid benefit package. Exceptional opportunity for career growth. Please rush resume complete with salary requirements in confidence to Employment Section, COLORADO INTERSTATE GAS COMPANY, P.O. Box 1087, Colorado Springs, Colorado 80944. We are an equal opportunity employer m/f.

COLORADO INTERSTATE GAS COMPANY
A Subsidiary of The Coastal Corporation

Sanitary Engineer needed for two years in Niger, West Africa to assist in training sanitation aides and design a country-wide environmental sanitation program. Masters degree in Sanitary Engineering with at least three years of experience. Working knowledge in French required. Salary negotiable, generous fringe benefits. Send resume to: **Africare, Inc. 1601 Connecticut Avenue, N.W., Washington, D.C. 20009.**

INDUSTRIAL POSITIONS AVAILABLE

Various U.S. locations. Minimum requirements are a BS degree and two years U.S. experience in design and use of equipment and systems for environmental control and assessment. Client companies pay agency fee plus interview and relocation. Send resume and current salary or call collect (215) 735-4908 for confidential application.

ATOMIC PERSONNEL, INC., Box J-1
1518 Walnut St., Phila., Pa. 19102

professional consulting services directory

COMPLETE ENVIRONMENTAL SERVICES

- PERMIT PLANNING
- AMBIENT MONITORING
- METEOROLOGY & DIFFUSION MODELING
- ENVIRONMENTAL IMPACT STATEMENTS
- ORGANIC/INORGANIC ANALYSES
- HAZARDOUS WASTE CHARACTERIZATION & CONTROL
- PROCESS/CONTROL ENGINEERING
- ENERGY SYSTEMS STUDIES
- STACK TESTING

GCA offers 20 years experience serving Industry & Government.

For Information Contact
V.P. Marketing

GCA
GCA CORPORATION
Technology Division
213 Burlington Rd., Bedford, Mass 01730
(617) 275-5444

MESOMET INC

Computerized Meteorological and Environmental Services
Dr. Walter A. Lyons, President
Certified Consulting Meteorologists

- Power plant fumigation studies
- Shoreline and coastal zone meteorological measurement and analyses
- Long Range Pollution Transport Assessment
- Cost effective use of remote sensing technology including acoustic sounders
- Mesoscale air pollution and meteorological models
- 24-Hour Operational Forecasting Center for ICS. Field Program Support

35 East Wacker Drive, Chicago, Ill. 60601
(312) 263-5921
Washington Area Office (301) 292-5303

ENVIRONMENTAL CONSULTANTS INC

ANALYTICAL TESTING AND SAMPLING SERVICES:

- EPA—Drinking water
- Certified bacteriological testing
- N.P.D.E.S. Permit
- Priority pollutant analysis
- Workplace environments
- EPA Hazardous wastes evaluation
- Particle identification and sizing
- Process Quality Control
- Research and Development

USING:

Gas chromatography/Mass spectrometry; Atomic Absorption Spectroscopy; Infrared spectroscopy; Microscopy; TOC; E.P.A. and OSHA certified methods.

CONSULTATION—PLANNING

391 NEWMAN AVE
CLARKSVILLE, INDIANA 47130
812-282-8481

Since 1885
Service to Industry
Stearns-Roger

COMPLETE ENVIRONMENTAL SERVICES:

Environmental impact assessments . . . Pollutant emission, air quality & water quality monitoring . . . Dispersion estimates . . . Ecological consulting . . . Meteorological field studies & consulting services. Contact

ENVIRONMENTAL SCIENCES DIVISION
(303) 758-1122

P. O. Box 5888
Denver, Colorado 80217

ENVIRONMENTAL PLANNING and PROBLEM SOLVING for INDUSTRY and GOVERNMENT

• AIR • WATER • SOLIDS • NOISE • ODOR

- **Measurement**
- **Impact Assessment**
- **Control**
- **Permit Planning**
- **Information Systems**
- **Modeling**

TRC Environmental Consultants, Inc.

125 Silas Deane Highway
Wethersfield, Ct. 06109
(203) 563-1431

8775 East Orchard Rd.
Suite 816
Englewood, CO 80111
(303) 779-4940

Woodward-Clyde Consultants

- Site Selection Studies
- Impact Assessment Evaluation
- Decision and Risk Analyses
- Environmental Field and Laboratory Studies

Environmental Systems Division
Headquarters San Francisco, CA

Other offices in Clifton, NJ • Washington, D C Anchorage, AK • San Diego, CA

RMT LABORATORIES

RESIDUALS MANAGEMENT TECHNOLOGY, INC.
CONSULTANTS IN INDUSTRIAL SOLID AND HAZARDOUS WASTE MANAGEMENT

Specializing in Waste Analyses:

- Hazardous Waste
- Leaching tests
- RCRA Regulations
- Ground & surface water monitoring
- NPDES Permits
- Waste water
- Drinking water

1406 E. WASHINGTON AVE. BOX C SUITE 124 MADISON, WI 53703 (608) 255-2134

SMALL PARTICLE ANALYSIS

BY ELECTRON MICROSCOPY

ERNEST F. FULLAM, INC.
P O BOX 444 • SCHENECTADY, N Y 12301
TELEPHONE 518-785-5533

SUPPLIER OF
ACCESSORIES FOR MICROSCOPY

WRITE OR PHONE FOR INFORMATION

Laboratory and Process Development
Industrial Waste Water Control
Liquid and Solid Incineration
Air Pollution Control
In-Plant Control and Process Modifications
Environment Impact and Permits

CATALYTIC, INC.

Consultants • Engineers • Constructors
Environmental Systems Division
Centre Square West
1500 Market St.,
Philadelphia, PA 19102 • 215-864-8000
Charlotte, NC 704-524-4220
Baton Rouge, LA 504-293-6200

WILSON LABORATORIES

ANALYTICAL & RESEARCH CHEMISTS & BIOLOGISTS
A DIVISION OF WILSON & COMPANY, ENGINEERS & ARCHITECTS
AAA Certification in Kansas, Missouri, Oklahoma and New Mexico

*** AIR, WATER & NOISE POLLUTION**
*** PROCESS STUDIES — SYSTEMS DESIGN**
*** WATER, SEWAGE & WASTE SYSTEMS**

Complete Laboratory Services

SALINA, KS 67401
528 N. 9TH ST.
(913) 825-7186

WATER
WASTEWATER
SOLID WASTES

- Chicago
- New York
- Philadelphia
- Richmond
- Tampa
- Atlanta
- Phoenix

222 S Riverside Plaza Chicago 60606

GREELEY AND HANSEN

ENGINEERS
Since 1914

Complete Analytical Services

SINCE 1919

- Screening of Industrial Waste for EPA Priority Pollutants using Finnigan OWA-30 GC/MS.
- NPDES & SPDES Organic & Inorganic Testing.
- Drinking Water Analysis to EPA Standards.
- Bioassay, Bioaccumulation & Toxicity Studies of Industrial Waste, Municipal Sludge & Dredge Spoils.
- Leachate Potential Studies & Analysis.
- Total Instrumental Analysis: A.A., GC/MS, G.C., I.R., TOC & TOD.

NEW YORK TESTING LABORATORIES
81 Urban Avenue, Westbury, N.Y. 11590
(516) 334-7770

ENTROPY ENVIRONMENTALISTS, INC.

AIR POLLUTION MEASUREMENT IS OUR BUSINESS

P.O. Box 12291
Research Triangle Park, N.C. 27709
919-781-3550

MASS SPECTROMETRY

- Priority Pollutants
- *State of the Art* Equipment & Service
- International Record
- 10 yrs.-(313) 894-4440

SHRADER Analytical and Consulting Lab
Call • Will Visit

3450 Lovett Ave. • Detroit, MI 48210

professional consulting services directory

Scott Environmental Technology, Inc.

The Air Pollution Specialists
- Research and Consulting
- Source Emissions Testing
- Control Device Efficiency
- Continuous Source Monitoring
- Ambient Monitoring
- Fuel Additive & Automotive Testing

Route 611, Plumsteadville, PA 18949
215 – 766-8861
2600 Cajon Blvd., San Bernardino, CA 92411
714 – 887-2571
1290 Combermere St., Troy, MI 48084
313 – 589-2950

TAMS
ENGINEERS AND ARCHITECTS

Environmental Planning Department
655 Third Avenue, New York, N.Y. 10017
(212) 867-1777

- Environmental Impact Studies
- Aquatic and Terrestrial Ecology
- Natural Resources Planning
- Land Use Planning
- Socioeconomic Studies
- Air, Noise and Water Quality
- Field and Laboratory Services

Washington, D.C. Boston Seattle
Anchorage

Environmental Testing Services

- EPA Priority Pollutants—GC/MS
- Hazardous Waste Characterization
- Work Environment Analyses
- Organic/Inorganic Analyses
- TOC and TOCL

Water • Effluents • Soils • Sludges

Plug in **The Research Connection**
FOREMOST RESEARCH
6363 Clark Avenue
Dublin, California 94566
(415) 828-1440

RAYTHEON

OCEAN SYSTEMS CO.
Environmental & Oceanographic Services
P.O. Box 360, Portsmouth, RI.
USA, 02871, (401)847-8000

DAMES & MOORE
Engineering and Environmental Consultants

Geotechnical and Environmental Engineering
Environmental Impact Assessment
Meteorology and Air Quality Monitoring
Water Pollution Control Engineering
Modelling and Numerical Analyses
Permitting and Licensing Consultation

San Francisco • Denver
Chicago • New York • Atlanta
Offices in Principal Cities Throughout the World

Enviro-Med Laboratories, Inc.
414 W. CALIFORNIA - RUSTON, LA. 71270 - 318-255-0060
1012 S. ACADIAN THRUWAY - BATON ROUGE, LA. 70806 - 504-343-4314

Sampling, Testing, and Consulting
HAZARDOUS WASTE—AIR—SOLID WASTE—GC/MS PRIORITY POLLUTANTS—WASTEWATER

CAPABILITY PERFORMANCE

Precision Meteorological Instruments

Environmental Services For:

- Air Quality
- Energy Development and Use
- Meteorological Engineering
- Field Data Collection

Meteorology Research, Inc.
464 West Woodbury Road
Altadena, California 91001
(213) 791-1901
Telex-675421
A Subsidiary of Cohu, Inc.

KEMRON®

Ambient & Emission Air Monitoring

Also Industrial Hygiene, Liquid & Solid Waste, Effluent, and Water Quality Analysis.

Call 614/374-2222.

Kemron 235 Second Street Marietta Ohio 45750
Borg-Warner Corporation

POLLUTION ABATEMENT

Custom engineering and construction of pollution abatement facilities.

POLLUTION ABATEMENT GROUP
BAKER BROS.
DIVISION OF SYSTEMS ENGINEERING AND MANUFACTURING CORP

International Headquarters Telex 924 328
(617) 344 1700 CAMPANELLI PARKWAY STOUGHTON, MASS 02072

CAMP DRESSER & McKEE INC.
Offices Throughout the U S

One Center Plaza
Boston Massachusetts 02108

CDM
environmental engineers, scientists, planners, & management consultants

WESTON
DESIGNERS CONSULTANTS

HEADQUARTERS West Chester, PA 19380 • 215-692-3030
OFFICES Atlanta, GA • Boston, MA • Camden, NJ
Chicago, IL • Cleveland, OH • Concord, NH
Houston, TX • Nashville, TN • New Orleans, LA
New York, NY • Richmond, VA • St. Paul, MN
Washington, DC • Amman, Jordan • Cairo, Egypt

HAVENS AND EMERSON, INC.
Environmental Engineers
Cleveland, OH Saddle Brook, NJ
Atlanta, GA St. Louis, MO

professional consulting services directory

INDEX TO THE ADVERTISERS IN THIS ISSUE

CIRCLE INQUIRY NO.		PAGE NO.
1	**Academic Press, Div. of H.B.J.** Flamm Advertising	1050
2	**Alpkem Company** Alpkem Advertising	1080
3	**Anderson Laboratories** Jim Rappport Advertising	1074
22	**Beckman Instruments** Ayer, Jorgensen, MacDonald	1073
4	**Bioanalytical Systems, Inc.**	1075
19	**Broadley James Corporation** Wescon Advertising	1079
5	**Dasibi Environmental Corporation**	1033
6	**ERT** Impact Advertising Inc.	1013
20	**Finnigan Institute**	1079
14	**Foxboro Analytical** Shepherd, Tibball & Galog	1076
23	**ISCO** Farneaux Associates Advertising	1041
7	**Martek Instruments, Inc.** Tekmar Marketing Services	1043
8	**Matheson** Kenyon Hoag Associates	1019
31-34	**Mine Safety Appliance** Ketchum, MacLeod & Grove, Inc.	1036
17	**Monsanto Company** Advanswers Media/Programming, Inc.	1021
18	**Parker-Hannifin Corporation** Amundsen/Clark, Inc.	IFC
10	**Plenum Publishing Corporation** Plenum/DaCapo Advertising	1083
16	**Radian Corporation** RAdian Advertising Agency	OBC
11	**Rockwell International** Campbell-Ewald Company	1016
21	**Rohm & Haas** Al Paul Lefton Company, Inc.	1044
12	**Ventron Division of Thiokol Corp.** Impact Advertising Inc.	1035
13	**Whatman, Inc.** J. S. Lanza & Associates	1072
15	**Carl Zeiss, Inc.** Shaw & Todd, Inc.	1022

	PAGE NO.
CLASSIFIED SECTION	1084-1085
SERVICES DIRECTORY	1086-1088

Advertising Management for the
American Chemical Society Publications
CENTCOM, LTD.

Thomas N. J. Koerwer, President; James A. Byrne, Vice President; Alfred L. Gregory, Vice President; Clay S. Holden, Vice President; Benjamin W. Jones, Vice President; Robert L. Voepel, Vice President; 25 Sylvan Rd. South, Westport, Connecticut 06881 (Area Code 203) 226-7131

ADVERTISING SALES MANAGER
Alfred L. Gregory

SALES REPRESENTATIVES

Atlanta, Ga. . . . Donald B. Davis, CENTCOM, LTD., Phone (Area Code 203) 226-7131
Boston, Ma. . . . Thomas Carey, CENTCOM, LTD., (Area Code 212) 972-9660
Chicago, Ill. . . . Bruce Poorman, CENTCOM, LTD., 540 Frontage Rd., Northfield, Ill 60093 (Area Code 312) 441-6383
Cleveland, Oh. . . . Bruce Poorman, CENTCOM, LTD., 17 Church St., Berea, OH 44017 (Area Code 216) 234-1333
Denver, Co. . . . Clay S. Holden, CENTCOM, LTD., (Area Code 213) 325-1903
Houston, Tx. . . . Robert E. LaPointe, CENTCOM, LTD., (Area Code 415) 781-3430
Los Angeles, Ca. . . . Clay S. Holden, Robert E. LaPointe, CENTCOM, 3142 Pacific Coast Highway, Suite 200, Torrance, CA 90505, (Area Code 213) 325-1903
New York, N.Y. . . . Thomas Carey, CENTCOM, LTD., 60 E. 42nd Street, New York 10165 (Area Code 212) 972-9660
Philadelphia, Pa. . . . Thomas Carey, CENTCOM, LTD., GSB Building, Suite 510, 1 Belmont Ave., Bala Cynwyd, Pa 19004 (Area Code 215) 667-9666
San Francisco, Ca. . . . Robert E. LaPointe, CENTCOM, LTD., Suite 303, 211 Sutter Street, San Francisco, CA 94108. Telephone: 415-781-3430
Westport, Ct. . . . Thomas Carey, CENTCOM, LTD., 25 Sylvan Rd. South, Westport, Ct. 06881, (Area Code 203) 226-7131
United Kingdom
Reading, England . . . Malcolm Thiele, Technomedia Ltd., Wood Cottage, Shurlock Row, Reading RG10 OQE. Telephone: 073-581-302
Manchester, England . . . Jill E. Loney, Technomedia Ltd., 216 Longhurst Lane, Mellor, Stockport SK6 5PW. Telephone: 061-427-5660
Continental Europe . . . Andre Jamar, Rue Mallar 1, 4800 Verviers, Belgium. Telephone: (087) 22-53-85. Telex No. 49263
Tokyo, Japan . . . Shigeo Aoki, International Media Representatives Ltd., 2-29 Toranomon 1-chrome, Minato-Ku, Tokyo 105 Japan. Telephone: 502-0656

PRODUCTION DEPARTMENT
PRODUCTION DIRECTOR
Joseph P. Stenza
PRODUCTION MANAGER
Donna C. Bifano

ES&T
RESEARCH

Removal and Recovery of Organic Pollutants from the Aquatic Environment. 2. Removal and Recovery of Dodecylbenzenesulfonate from Aqueous Solution by Cross-Linked Poly(*N*-benzyl-4-vinylpyridinium Halide)

Nariyoshi Kawabata* and Toshio Morigaki

Department of Chemistry, Faculty of Polytechnic Science, Kyoto Institute of Technology,
Matsugasaki, Sakyo-ku, Kyoto 606, Japan

■ Cross-linked poly(*N*-benzyl-4-vinylpyridinium bromide) (BVP resin in the bromide form) was found to have an excellent capacity for removing sodium dodecylbenzenesulfonate (DBS) from aqueous solution. The breakthrough capacity of the resin with <1-ppm leakage in the effluent was surprisingly greater than those observed with commercial anion exchange resins and porous styrene–divinylbenzene resin with no ion exchange functional group. The breakthrough capacity of the BVP resin for DBS adsorption was scarcely affected by the presence of sodium chloride, sodium sulfate, sodium hydroxide, and hydrochloric acid. Elution of the adsorbed DBS from the BVP resin was easily accomplished by a simple treatment with methanolic hydrochloric acid, and the BVP resin was efficiently regenerated as the chloride form. DBS was concentrated into 20–25 wt % solution. The BVP resin in the chloride form showed much the same ability for the adsorption of DBS as the resin in the bromide form.

Removal of organic pollutants from the aquatic environment by synthetic resins is important not only because it protects the environment from pollution, but also because it economically uses raw materials, since the resins can be regenerated and the organic pollutants can be recovered without chemical change. An attractive feature of synthetic resins is that they can be manufactured with surfaces of predetermined charactistics. It is possible to design a resin for specific adsorption application. In the preceding paper of this series (*1*), we proposed using the vinylpyridine–divinylbenzene copolymer for removal and recovery of phenol from wastewater. In the present work, we have attempted to find a new polymeric adsorbent for removal and recovery of sodium dodecylbenzenesulfonate (DBS) from aqueous solution, which is more useful than those available at the present.

Sodium alkylbenzenesulfonate has frequently been used as the surface-active component of detergents and is a common component of laundry, municipal, and other types of wastewaters. Previous studies have shown that strong base (*2, 3*) and weak base (*4*) anion exchange resins are effective in the removal of alkylbenzenesulfonate from aqueous solution. Alkylbenzenesulfonate may also be adsorbed by the styrene–divinylbenzene resin with no ion exchange functional group (*5*), but the capacity was much less than that observed for anion exchange resins. However, a serious defect of anion exchange resins for the adsorption of alkylbenzenesulfonate is that the capacity of the resins is conspicuously reduced by the presence of sodium chloride and other inorganic salts (*4*). On the other hand, as we have reported in the preceding paper of this series (*1*), the vinylpyridine–divinylbenzene copolymer did not adsorb sodium chloride and other inorganic salts. The capacity of the copolymer for phenol adsorption was scarcely affected by the presence of these inorganic salts. Therefore, we attempted to use vinylpyridine–divinylbenzene copolymer as a polymeric adsorbent for the removal and recovery of DBS from aqueous solution.

Experimental

Reagents. 4-Vinylpyridine provided by Koei Chemical Co. Ltd., Osaka, Japan, and commercial products of divinylbenzene, styrene, ethanol, and toluene were purified by distillation before polymerization. The distilled divinylbenzene was a mixture of *m*-divinylbenzene (41.5%), *p*-divinylbenzene (14.4%), ethylstyrene (40.1%), and diethylbenzenes (3.9%). Commercial products of 2,2′-azobis(isobutyronitrile), methanol, benzene, petroleum ether, benzyl bromide, sodium dodecylbenzenesulfonate (DBS), hydrochloric acid, sodium hydroxide, and other chemicals were used without further purification. Deionized water was used throughout the experiments. Nitrogen was purified by passing through a tube containing copper turnings in a furnace at 170 °C.

Polymeric Adsorbents. Pulverized copolymers of 4-vinylpyridine with divinylbenzene were prepared as described (*1*). The mean particle diameter was 0.15 mm in the dry state and 0.20 mm in the wet state. Cross-linked poly(*N*-benzyl-4-vinylpyridinium bromide), i.e., BVP resin in the bromide form, was prepared from benzyl bromide and 4-vinylpyridine–divinylbenzene copolymer as follows. The pulverized copolymer of 4-vinylpyridine with divinylbenzene containing 72 mol % 4-vinylpyridine (80 g) was added to methanol (1.2 L). The mixture was kept at room temperature for about 20 h, and the methanol was separated by filtration. The copolymer was mixed with benzene (1 L) at room temperature. After 1 h, benzene was separated by filtration. The swollen co-

0013-936X/80/0914-1089$01.00/0 © 1980 American Chemical Society

polymer was added to benzene to form a 1-L suspension in a 1-L three-necked flask connected with a mechanical stirrer and a reflux condenser. The mixture was stirred and 100 g of benzyl bromide was added; the solution was allowed to react at 60–65 °C for 3 h under stirring. After the reaction, the polymer was separated by filtration, and was washed by benzene, methanol, and water followed by drying in vacuo to constant weight. The mean particle diameter was 0.30 mm in the dry state and 0.40 mm in the wet state. The density was 1.40 g/cm^3 at 16 °C. In order to determine the content of the pyridinium group, the BVP resin in the bromide form was transferred into the nitrate form by treatment with 100× excess 1 N potassium nitrate in a batch method. Titration of the eluted solution with standard 0.1 N silver nitrate using eosin as the indicator showed that 42% of the pyridyl group contained in the copolymer was transferred into the pyridinium group.

For comparison with the BVP resin, four commercial resins provided by Rohm & Haas Co., Philadelphia, Pa., were used. Amberlite IRA-400 was used as a strong base anion exchange resin, because it has a styrene–divinylbenzene matrix with a quarternary ammonium group. This resin was used both in the chloride form and in the hydroxide form. The particle size was 0.38–0.45 mm. Amberlite IR-45, which has a styrene–divinylbenzene matrix with primary, secondary, and tertiary amino groups, was used as a weak base anion exchange resin. This resin was used in the free base form. The particle diameter was 0.36–0.46 mm. Amberlite XAD-2 and XAD-4 were used as porous styrene–divinylbenzene resins with no ion exchange functional group. The surface areas of XAD-2 and XAD-4 were claimed to be 300 and 784 m^2/g, respectively. These commericial resins were preconditioned as was described in the preceding paper of this series (*1*).

Adsorption Tests. A series of batch studies was conducted in order to obtain preliminary information on the adsorption characteristics of 4-vinylpyridine–divinylbenzene copolymer. In this case, 1.2 g of the copolymer was added to 150 mL of a 4000-ppm aqueous DBS solution in a 300-mL Erlenmeyer flask, and the mixture was kept at 30 ± 1 °C under stirring. After the mixture reached equilibrium, the concentration of DBS was determined.

Column studies were conducted using a 1.0-cm diameter glass column with a fritted glass filter connected to a 200-mL dropping funnel in a down-flow fashion at room temperature. The preconditioned resin was placed in the column. In a typical experiment, 8.0 g (wet) of the BVP resin in bromide form was loaded; the height of the resin bed was 17 cm. The bed was carefully backwashed to eliminate entrained air and then tapped to ensure packing of the bed. The dropping funnel was used to contain influent solution. Samples were taken manually and were checked for DBS concentration. The flow rate was 3 bed volumes/h throughout this work. The influent concentration of DBS was controlled at 1800 ppm. The capacity of the resins for DBS adsorption was determined by the continuous flow column method based on the breakthrough capacity, i.e., the total amount of DBS adsorbed by the resins until the effluent concentration of DBS reached 1 ppm.

Equilibrium adsorption tests were conducted by placing weighed quantities of resins and samples of aqueous DBS solution in a 300-mL beaker (sealed with polyethylene film) in a water bath, which was maintained at 30 ± 1 °C and magnetically stirred. After the mixture reached equilibrium, the concentration of DBS was determined.

Recovery of Adsorbed DBS from Polymeric Adsorbents. Polymeric adsorbents were treated with 1800 ppm of aqueous DBS solution by a continuous flow column method until the effluent concentration of DBS reached 1 ppm. Elution of the adsorbed DBS from the above resins was conducted by the continuous flow column method using methanol or methanolic 2 N hydrochloric acid as the eluant, with a flow rate of 3 bed volumes/h in a down-flow fashion. The recovered DBS solution was neutralized using saturated aqueous sodium carbonate solution, and methanol and water were removed by distillation. DBS was left in the residue contaminated with some sodium chloride.

Concentration Determination. Quantitative analyses of DBS in aqueous and/or methanolic solution were performed with Shimadzu UV-200S, UV-100-01, and UV-100-02 spectrophotometers. The concentration was determined based upon the absorptivities at 222 nm, or with the aid of methylene blue. Concentrations of sodium carbonate and bicarbonate were determined by titration with standard hydrochloric acid. Concentrations of chloride and bromide anions were determined by titrations with standard silver nitrate solution. The concentration of sulfate anion was determined by titration with standard EDTA solution.

The solution pH values were determined with a Toa Electronics Model HM-5B pH meter.

Results and Discussion

Adsorption of DBS on Vinylpyridine–Divinylbenzene Copolymer as Studied by a Series of Preliminary Batch Experiments. In order to obtain preliminary information concerning the characteristics of the vinylpyridine–divinylbenzene copolymer needed for the adsorption of DBS in aqueous solution, we carried out a series of adsorption experiments by a batch method using 1.2 g of various 4-vinylpyridine–divinylbenzene copolymers and 150 mL of 4000-ppm aqueous DBS solution. After the mixtures reached equilibrium, the amount of adsorbed DBS was determined. The adsorption capacity is shown in Figure 1 as a function of the mole fraction of 4-vinylpyridine in the copolymer. Figure 1 shows a maximum adsorption capacity for 4-vinylpyridine of about 70 mol %.

Adsorption of DBS on Various Polymeric Adsorbents Studied by the Continuous Flow Column Method. The capacities of various polymeric adsorbents for DBS adsorption were determined by the continuous flow column method. Pulverized 4-vinylpyridine–divinylbenzene copolymer containing 72 mol % 4-vinylpyridine was used as a representative of the vinylpyridine–divinylbenzene copolymers. The breakthrough curves are shown in Figure 2. The breakthrough capacities of each polymeric adsorbent for DBS adsorption are summarized in Table I.

The strong base anion exchange resin in the hydroxide form showed a much higher capacity for DBS adsorption than the

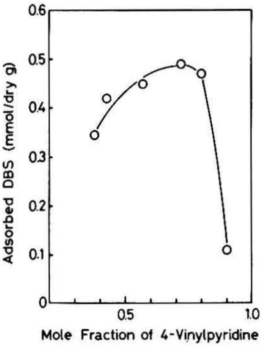

Figure 1. Amount of DBS adsorbed by 4-vinylpyridine–divinylbenzene copolymer as a function of the mole fraction of 4-vinylpyridine in the copolymer studied by a series of batch experiments: copolymer, 1.2 g; DBS solution, 150 mL; DBS concentration, 4000 ppm; temperature, 30 ± 1 °C

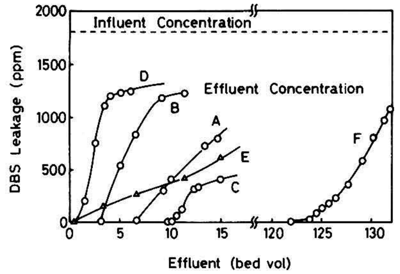

Figure 2. Breakthrough curves for the removal of DBS from aqueous solution by various polymeric adsorbents studied by the continuous flow column method: flow rate, 3 bed volumes/h; influent concentration of DBS, 1800 ppm; (A) 4-vinylpyridine–divinylbenzene copolymer containing 72 mol % 4-vinylpyridine; (B) Amberlite IRA-400 in the chloride form; (C) Amberlite IRA-400 in the hydroxide form; (D) Amberlite IR-45 in the free base form; (E) Amberlite XAD-4; (F) the BVP resin in the bromide form prepared from 4-vinylpyridine–divinylbenzene copolymer and benzyl bromide

Table I. Breakthrough Capacities of Polymeric Adsorbents for DBS Adsorption[a]

polymeric adsorbent	adsorption capacity mg/ dry g	mequiv/ dry g
pulverized copolymer of 4-vinylpyridine with divinylbenzene containing 72 mol % 4-vinylpyridine	59	0.17
strong-base anion exchange resin in the hydroxide form (Amberlite IRA-400)	49	0.14
strong-base anion exchange resin in the chloride form (Amberlite IRA-400)	14	0.04
weak-base anion exchange resin in the free base form (Amberlite IR-45)	0	0.00
porous styrene–divinylbenzene resin with no ion-exchange functional group (Amberlite XAD-4)[b]	0	0.00
the BVP resin in the bromide form prepared from 4-vinylpyridine–divinylbenzene copolymer and benzyl bromide	903	2.59
the BVP resin in the chloride form obtained by regeneration of the above resin spent for DBS adsorption using methanolic 2 N hydrochloric acid	854	2.45

[a] Determined by the continuous flow column method using 1800 ppm of aqueous DBS solution. The flow rate was 3 bed volumes/h. [b] Claimed to have a surface area of 784 m^2/g.

resin in the chloride form. The weak base anion exchange resin and the porous styrene–divinylbenzene resin with no ion exchange functional group showed negligibly small breakthrough capacities for DBS adsorption. On the other hand, the 4-vinylpyridine–divinylbenzene copolymer containing 72 mol % 4-vinylpyridine showed a higher adsorption capacity than the commercial strong base anion exchange resin in the hydroxide form.

However, the capacity of the 4-vinylpyridine–divinylbenzene copolymer for DBS adsorption was considerably lower when compared with the capacity of the copolymer observed for the adsorption of phenol (*1*). Previous work indicated that 1 g of the copolymer containing 72 mol % 4-vinylpyridine adsorbed 275 mg (2.92 mequiv) of phenol until the effluent concentration of phenol reached 1 ppm (*1*), but the copolymer adsorbed only 0.17 mequiv/dry g of DBS, as shown in Table I. In order to improve the adsorption capacity of the vinylpyridine–divinylbenzene copolymer for DBS adsorption, we attempted to transfer the copolymer into a polymeric adsorbent containing a quarternary ammonium group. We attempted to transfer the pyridyl group of the copolymer into the pyridinium group by reaction with benzyl bromide.

Reaction of the copolymer with benzyl bromide in benzene transferred 42% of the pyridyl group of the copolymer into the pyridinium group (details are described under Experimental). This quarternary ammonium type resin, i.e., poly(*N*-benzyl-4-vinylpyridinium bromide) (designated as the BVP resin in the bromide form) was found to be an excellent polymeric adsorbent for the adsorption of DBS from aqueous solution. The continuous-flow column study revealed that the BVP resin in the bromide form had a surprisingly higher breakthrough capacity for DBS adsorption from aqueous solution than the commercial strong base anion exchange resin, as can be seen in Figure 2 and Table I.

The adsorption capacity depends upon the size and shape of the resins. The surface area, the size of the pore, the cross-linkage, and the hydrophilicity are also important factors that exert influences upon the adsorption capacity. Clearly, exact numerical comparison of the adsorption capacities of resins must be made using ion exchange and adsorbent particles of similar factors. Further research is required for the exact numerical comparison of adsorption capacity. However, it would be very interesting if the BVP resin in bromide form showed a surprisingly greater breakthrough capacity for DBS adsorption than Amberlite IRA-400 in hydroxide form, in spite of the fact that their particle sizes are similar, although their shapes are different.

Titrations of the effluent solutions with standard 0.1 N silver nitrate solution using eosin as indicator showed that the bromine of the BVP resin in the bromide form was quantitatively removed during DBS adsorption. The amount of adsorbed DBS corresponded to that of the pyridinium group of BVP resin in the bromide form. This result clearly indicates that adsorption of DBS by BVP resin in the bromide form undergoes an ion exchange mechanism. That is:

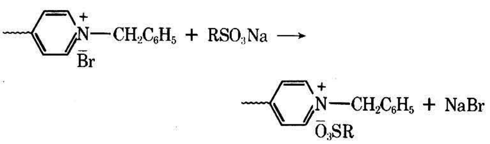

In the adsorption of DBS from aqueous solution, a strong base anion exchange resin (Amberlite IRA-400) in the hydroxide form showed a breakthrough capacity of 49 mg/dry g (0.14 mequiv/dry g), which was only about 4% of the ion exchange capacity (3.75 mequiv/dry g) of the resin. The strong base anion exchange resin in chloride form showed a breakthrough capacity of 14 mg/dry g (0.04 mequiv/dry g), which was only 1% of the ion exchange capacity of the resin. The quarternary ammonium group on the inside of the pore of the resin did not appear to be useful for the adsorption of DBS. On the contrary, the pyridinium group of the BVP resin was demonstrated to be used quantitatively for the adsorption of DBS as was mentioned above. An important factor seemed to be the fact that the BVP resin in the bromide form swelled considerably in water. That is, 1 g of the resin adsorbed about 2 g of water. Thus, the effective surface area of the BVP resin for the adsorption of DBS in water appeared to be much higher than that of the anion exchange resins.

Effect of Some Inorganic Salts in Aqueous DBS Solution on the Breakthrough Capacity of Polymeric Adsorbents for DBS Adsorption. In the practical use of polymeric adsorbents for the removal of DBS from wastewater, it is difficult to avoid the presence of some inorganic salts. Inorganic anions in wastewater reduce the capacity of the

Table II. Breakthrough Capacities of Polymeric Adsorbents for DBS Adsorption in the Presence of Inorganic Salts[a]

	adsorption capacity, mequiv/dry g		
polymeric adsorbent	I[b]	II[c]	III[d]
strong-base anion exchange resin in the hydroxide form (Amberlite IRA-400)	0.14	0.05	0.06
the BVP resin in the bromide form prepared from 4-vinylpyridine–divinylbenzene copolymer and benzyl bromide	2.59	2.56	2.29
the BVP resin in the chloride form obtained by regeneration of the above resin spent for DBS adsorption using methanolic 2 N hydrochloric acid	2.45	2.56	2.54

[a] Determined by the continuous flow column method using 1800 ppm of aqueous DBS solution. The flow rate was 3 bed volumes/h. [b] In the absence of inorganic salt. [c] In the presence of 0.05 mol/L sodium chloride. [d] In the presence of 0.025 mol/L sodium sulfate.

anion exchange resin for DBS adsorption (*4*). As we have pointed out in the preceding paper of this series (*1*), however, the vinylpyridine–divinylbenzene copolymer did not adsorb inorganic anions, and the capacity of the copolymer for phenol adsorption was scarcely affected by the presence of inorganic salts. Nevertheless, we were afraid that the BVP resin could adsorb inorganic anions and the presence of inorganic salts could reduce the capacity of the resin for DBS adsorption, because the BVP resin was a sort of strong base anion exchange resin and adsorbed DBS through an ion exchange mechanism. Contrary to this anxiety, the BVP resin in the bromide form did not adsorb sodium sulfate, sodium carbonate, and sodium bicarbonate. The breakthrough capacity of the BVP resin in bromide form for DBS adsorption was scarcely affected by the presence of sodium chloride and sodium sulfate, as shown in Table II. On the contrary, the breakthrough capacity of the strong base anion exchange resin in hydroxide form for the adsorption of DBS was conspicuously reduced in the presence of these inorganic salts, as shown in Table II. This selectivity of adsorption is very important in the practical use of the BVP resin for wastewater treatment.

Effect of Acid and Alkaline Materials in Aqueous DBS Solution on the Capacity of the BVP Resin for DBS Adsorption. In the practical use of polymeric adsorbents for removal and recovery of DBS from wastewater, it is also difficult to avoid the presence of acid and alkaline materials. In order to obtain some information on this subject, we have investigated the effects of the presence of hydrochloric acid and sodium hydroxide in aqueous DBS solution on the capacity of the BVP resin in the bromide form for DBS adsorption. Results are summarized in Table III.

The capacity of the BVP resin in bromide form for DBS adsorption was scarcely affected by the presence of hydrochloric acid and sodium hydroxide. The pH of the effluent solution before the breakthrough point indicated that the BVP resin adsorbed neither acid nor alkaline materials. It should be noted that it was extremely difficult to transfer the BVP resin in the bromide form into the resin in the hydroxide form. When the resin in the bromide form was treated with a large amount of 1 N aqueous sodium hydroxide solution by the column method, none of the bromine was removed from the resin. This result shows the striking effect of the pyridinium group on the adsorption of DBS in wastewater when compared with the usual quarternary ammonium group of the strong base anion exchange resins. Thus, the BVP resin was concluded to be a polymeric adsorbent with an unusual quarternary ammonium group.

Adsorption Equilibrium for DBS and Polymeric Adsorbents. The experimental isotherms for DBS adsorption on various polymeric adsorbents are shown in Figure 3. Here, the pH of the system was not controlled. After the mixture of aqueous DBS solution and polymeric adsorbent reached equilibrium, the pH of the system was observed in the range 7.6–8.6 (4-vinylpyridine–divinylbenzene copolymer containing 72 mol % 4-vinylpyridine), 5.9–6.5 (the BVP resin in the bromide form), 8.9–10.9 (Amberlite IRA-400 in the hydroxide form), 5.6–6.0 (IRA-400 in the chloride form), 7.5–10.0 (IR-45 in the free base form), 6.3–6.8 (XAD-2), 6.2–6.7 (XAD-4), and 6.2–6.6 (copolymer of styrene with divinylbenzene containing 57 mol % styrene). Figure 3 indicates that the BVP resin has adsorption capacities for DBS similar to those of the strong base anion exchange resins in the experimental isotherms. The results show that the estimation of adsorption characteristics in the continuous flow column method is not strictly evaluated by the equilibrium adsorption experiments.

Recovery of DBS from Polymeric Adsorbents. In addition to the DBS adsorption, the other major objective of this

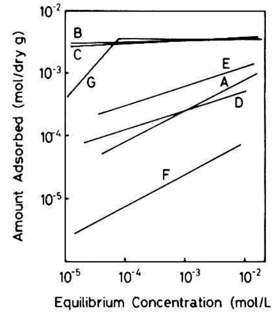

Figure 3. DBS adsorption isotherms on various polymeric adsorbents at 30 °C: (A) 4-vinylpyridine–divinylbenzene copolymer containing 72 mol % 4-vinylpyridine; (B) Amberlite IRA-400 in the hydroxide form; (C) Amberlite IR-45 in the free base form; (D) Amberlite XAD-2; (E) Amberlite XAD-4; (F) styrene–divinylbenzene copolymer containing 57 mol % styrene; (G) the BVP resin in the bromide form prepared from 4-vinylpyridine–divinylbenzene copolymer and benzyl bromide

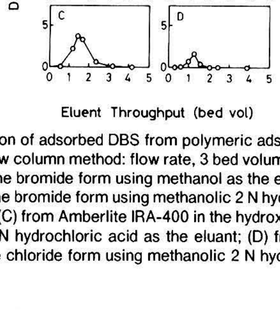

Figure 4. Elution of adsorbed DBS from polymeric adsorbents by the continuous flow column method: flow rate, 3 bed volumes/h; (A) from BVP resin in the bromide form using methanol as the eluant; (B) from BVP resin in the bromide form using methanolic 2 N hydrochloric acid as the eluant; (C) from Amberlite IRA-400 in the hydroxide form using methanolic 2 N hydrochloric acid as the eluant; (D) from Amberlite IRA-400 in the chloride form using methanolic 2 N hydrochloric acid as the eluant

Table III. Effect of Acid and Alkaline Materials in Aqueous DBS Solution on the Breakthrough Capacity of the BVP Resin in the Bromide Form for DBS Adsorption[a]

	run no.			
	1	2	3	4
DBS, ppm	1800	1800	1800	1800
hydrogen chloride, mmol/L	6.0			
sodium hydroxide, mmol/L			2.0	6.0
pH of the influent solution	2.1	6.0	10.9	11.7
pH of the effluent solution before the breakthrough point	2.3–2.5	6.5–6.8	9.6–10.9	10.9–11.8
breakthrough capacity for DBS adsorption, mg/dry g	870	900	895	930

[a] Determined by the continuous flow column method using 1800 ppm of aqueous DBS solution. The flow rate was 3 bed volumes/h.

work is to recover as much DBS as possible from the polymeric adsorbents. We first examined the elution of DBS from the BVP resin by the continuous flow column method using methanol as the eluant. The results are shown in Figure 4A. The elution was difficult, and only 13% of the adsorbed DBS was recovered from the resin by 3 bed volumes of methanol. On the other hand, elution using methanolic 2 N hydrochloric acid was found to be very effective for the recovery of DBS from the BVP resin as is shown in Figure 4B. The adsorbed DBS was quantitatively eluted by 4 bed volumes of the methanolic 2 N hydrochloric acid, and the resin was completely regenerated as the resin in the chloride form. DBS was concentrated to 20–25 wt % solution. When 4 bed volumes of aqueous 2 N hydrochloric acid was used, only 1% of the adsorbed DBS was eluted from the resin.

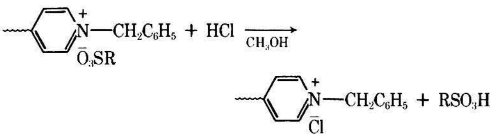

For comparison, the elution of DBS from commercial strong-base anion exchange resins both in hydroxide and chloride forms was conducted using methanolic 2 N hydrochloric acid as the eluant by the continuous flow column method. Results are shown in Figures 4C and 4D, respectively. The anion exchange resin in the hydroxide form was completely regenerated by about 4 bed volumes of the eluant, and DBS was quantitatively removed from the resins. However, the concentration of DBS in the eluted solution was only 3–4 wt %, because the capacity of the anion exchange resin for DBS adsorption was low.

Thus, both the commercial strong-base anion exchange resin and the BVP resin were easily and efficiently regenerated to the corresponding chloride form when about 3 bed volumes of the methanolic 2 N hydrochloric acid was used as the eluant. However, there is an advantage in the use of the BVP resin. The BVP resin in the bromide form was completely transferred into the chloride form during the elution. The regenerated BVP resin, i.e., the BVP resin in the chloride form, showed many of the same characteristics for adsorption of DBS from aqueous solution as the resin in the bromide form, as can be seen in Table I. This result indicates that the BVP resin has a definite advantage for adsorption of DBS from aqueous solution over the commercial strong base anion exchange resin. As shown in Table I, the strong base anion exchange resin in the chloride form exhibited a much lower capacity for DBS adsorption than the resin in hydroxide form. Therefore, the regenerated strong-base anion exchange resin should be transferred into the hydroxide form before adsorption of DBS from aqueous solution. On the other hand, the regenerated BVP resin in chloride form showed much the same order of adsorption capacity for DBS as the original resin in the bromide form; thus, the transfer of the regenerated resin into the original form is not necessary in this case.

Literature Cited

(1) Kawabata, N.; Ohira, K. *Environ. Sci. Technol.* **1979,** *13,* 1396–1402.
(2) Abrams, I. M.; Lewon, S. M. *J. Am. Water Works Assoc.* **1962,** *54,* 537–543.
(3) Gustafson, R. L.; Lirio, J. A. *Ind. Eng. Chem. Prod. Res. Dev.* **1968,** *7,* 116–120.
(4) Hinrichs, R. L.; Snoeyink, V. L. *Water Res.* **1976,** *10,* 79–87, and references cited therein.
(5) Gustafson, R. L.; Paleos, J. "Organic Compounds in the Aquatic Environment"; Faust, S. D., Hunter, J. V., Eds.; Marcel Dekker: New York, 1971; Chapter 10.

Received for review October 19, 1979. Accepted April 21, 1980. Work supported in part by a Grant-in-Aid for Scientific Research from the Ministry of Education of Japan (No. 403049).

Resistance to Photochemical Decomposition of Polycyclic Aromatic Hydrocarbons Vapor-Adsorbed on Coal Fly Ash

W. A. Korfmacher[1]
School of Chemical Sciences, University of Illinois, Urbana, Ill. 61801
E. L. Wehry and G. Mamantov
Department of Chemistry, University of Tennessee, Knoxville, Tenn. 37916
D. F. S. Natusch*
Department of Chemistry, Colorado State University, Fort Collins, Colo. 80523

■ Five polycyclic aromatic hydrocarbons (benzo[*a*]pyrene, pyrene, anthracene, fluoranthene, and phenanthrene) have been adsorbed, from the vapor phase, onto coal fly ash, and the susceptibility of each of the adsorbed compounds to photodecomposition has been studied. Benzo[*a*]pyrene, pyrene, and anthracene all photolyze efficiently in liquid solution but are highly resistant to photodegradation when adsorbed on fly ash. However, benzo[*a*]pyrene and anthracene photolyze with high efficiency when adsorbed on activated alumina. Thus, the photosensitivity of an adsorbed polynuclear hydrocarbon is strongly dependent upon the nature of the surface upon which the compound is adsorbed. Phenanthrene and fluoranthene are resistant to photodecomposition both in liquid solution and as adsorbates on fly ash. The environmental consequences of the resistance of polycyclic aromatic hydrocarbons adsorbed on fly ash to photochemical transformation are discussed.

It has recently been reported that both airborne particulate matter (*1*) and stack-collected fly ash from a coal-fired power plant (*2, 3*) contain substances that are directly mutagenic (as indicated by the Ames test) without metabolic activation. In the latter studies, while the majority of mutagenic activity was assigned to polar compounds, strong evidence indicating that a portion of the observed mutagenicity was attributable to nonpolar organic compounds was acquired. While definitive identification of these mutagenic substances has not yet been reported, it is suspected that many are polycyclic aromatic hydrocarbons (PAHs) or derivatives, heteroatom analogues, or oxidative degradation products, of PAHs (*1–4*). Indeed, PAH vapors present in the stack system of a coal-fired power plant can be adsorbed rapidly onto the surfaces of co-entrained fly ash particles at, or close to, the stack exit (*5–8*); several PAHs have been demonstrated to be both mutagenic (after activation by hepatic microsomal oxidation) and carcinogenic (*4, 9, 10*).

The carcinogenic potential of atmospheric particulate polycyclic organic matter may conceivably be modified as a result of photochemical decomposition or reactions with atmospheric oxidants. While the view occasionally has been advanced that PAHs are chemically inert and thus are removed from the atmosphere only by rainfall or slow sedimentation of particulate matter (*11*), the more common presumption has been that atmospheric PAHs can undergo relatively facile photodecomposition (*4*). The high photosensitivity of many aromatic hydrocarbons in liquid solution is well known (*12*). More recently, several studies have indicated that solid PAHs, or PAHs adsorbed on solid surfaces, are photoreactive. For example, it is often noted that, upon exposure to ultraviolet, PAH spots on alumina or silica thin-layer chromatography plates fade or change in color, indicating the occurrence of photolysis (*13–17*).

Thomas et al. (*18*) formed a soot by incomplete combustion of propane, and subjected the particulate matter so formed to photolysis (the nature of the light source was not specified). The soot was analyzed for its benzo[*a*]pyrene (BaP) content before and after illumination; more than 50% of the BaP initially present was destroyed by 40 min of illumination. Barofsky and Baum (*19*) exposed several PAHs, adsorbed on carbon needle field desorption emitters, to ultraviolet (high-pressure mercury lamp); BaP, anthracene, benz[*a*]anthracene, and pyrene all underwent photooxidation to carbonyl compounds. Indeed, polycyclic quinones can be isolated from sampled airborne particles (*20*), and their presence in such samples is often postulated to result from photolysis of adsorbed PAHs (*4*) in the atmosphere or on high-volume sampler filter media.

Lane and Katz (*21*) examined the photodegradation of BaP, benzo[*b*]fluoranthene, and benzo[*k*]fluoranthene in the form of thin dispersions of the solid compounds in glass dishes. Solid BaP was observed to be extremely photosensitive, exhibiting a half-life of only 5.3 h when illuminated with a General Electric Quartzline lamp. The other two compounds appeared much more resistant to photolysis. The rates of photodegradation of all three compounds increased substantially when they were illuminated in the presence of O_3. It should, however, be noted that the physical form of the PAHs in these experiments was not actually representative of atmospheric conditions.

Very recently, Fox and Olive (*22*) have noted that anthracene, added by sublimation to filter-collected atmospheric particulate matter, underwent efficient photodecomposition upon exposure to sunlight. Several oxygen-containing photoproducts were identified; some indications of the occurrence of photopolymerization reactions of anthracene also were noted. Evidence for participation of singlet molecular oxygen in the photooxidation of anthracene on particulate matter was obtained. Peters and Seifert (*23*) recently have reported that BaP deposited from liquid solution onto dust-coated glass fiber filters underwent rapid photodegradation when exposed to the output of an unfiltered 400-W halogen lamp, and concluded that oxidative degradation phenomena (including photochemical oxidation) may be a significant BaP loss mechanism in high-volume sampling.

The extent to which PAHs adsorbed on fly ash or other environmental particulate matter are susceptible to photodecomposition is of considerable importance, for several reasons. First, if rapid photolysis of adsorbed PAHs occurs, diurnal variations in the concentrations of PAHs in plumes emitted from power plants may occur. Second, if certain PAHs have half-lives in the atmosphere of "only hours or days", as has been commonly assumed (*4*), such compounds cannot serve as reliable "air pollution" or "polycyclic organic matter" indicators, a use for which analytical results for BaP in sampled airborne particles often have been suggested (*4, 23*). Finally, the ultimate photolysis products of most PAHs are carbonyl compounds; these substances, or intermediates in

---

[1] Present address, Chemistry Division, HFT-154, National Center for Toxicological Research, Jefferson, Ark. 72079.

0013-936X/80/0914-1094$01.00/0

their formation, may be more hazardous than the parent PAHs. Indeed, it has recently been reported (*24*) that samples of BaP adsorbed on silica gel which were then illuminated with 254-nm ultraviolet yielded preparations that were mutagenic toward *Salmonella typhimurium* strains; BaP itself was not mutagenic toward *S. typhimurium*. Though the identities of the mutagenic substances were not ascertained, they evidently were more polar than BaP; it seems reasonable to suppose that one or more photooxidation products of BaP was responsible for the observed mutagenicity.

Very few studies of the photochemistry of PAHs adsorbed on fly ash have been performed, and the influence of the nature of the substrate upon the photochemical behavior of adsorbed PAHs has received virtually no scrutiny. Jäger and Rakovic (*25*) noted that sulfonation reactions of adsorbed pyrene and BaP with SO_2 were accelerated by illumination with an unfiltered 125-W mercury lamp. Fisher, Chrisp, and Raabe (*3*) have very recently reported that mutagenic stack-collected fly ash samples could be subjected to prolonged illumination by ultraviolet (mercury lamp) or sunlight without appreciable loss of mutagenicity, despite their previous inference (*2*) that the bulk of the mutagenic activity of these samples was associated with organic compounds. These results imply either that the principal compounds responsible for the mutagenicity of the fly ash are not PAHs, or else that PAHs (which are known to be photosensitive under most experimental conditions) are stabilized with respect to photochemical transformation by adsorption onto fly ash surfaces. We previously reported preliminary results (*26–28*) which strongly suggest that, contrary to expectation (*25*), PAHs are indeed much less susceptible to photolysis when adsorbed onto fly ash than when exposed to light as dry powders, in liquid solution, or adsorbed onto alumina, silica gel, or glass surfaces. In the present paper, we describe studies, under controlled laboratory conditions, of photolysis of a number of PAHs vapor-adsorbed on fly ash surfaces; vapor adsorption was employed to simulate, as closely as possible under laboratory conditions, the actual mode of deposition of PAHs onto environmental fly ash.

Experimental

Materials: Polycyclic Aromatic Hydrocarbons. The following PAHs were obtained from the indicated sources and, unless otherwise noted, were used as received: benzo[*a*]pyrene, Aldrich Chemical Company; pyrene, Aldrich; phenanthrene, Eastman Organic Chemicals (purified by vacuum sublimation); anthracene, Matheson, Coleman and Bell (purified by vacuum sublimation); and fluoranthene, Duke Standards Corporation.

Fly Ash. The fly ash used in this study was collected from the electrostatic precipitators of the State Line, Illinois, power plant. The plant burned a 40:60 wt % mixture of high- and low-sulfur coals. The fly ash was size-fractioned using U.S. standard size series sieves, which were shaken for 1 h using a portable sieve shaker (Model RX-24, W. S. Tyler, Inc.). The 45–74-μm particle diameter size range, which constituted 46.5% by weight of the fly ash, was used. Samples of this fly ash were subjected to exhaustive Soxhlet extraction with benzene and methanol, and were shown not to contain detectable quantities of PAHs both by gas chromatography and ultraviolet absorption spectrophotometry (*29*). The specific surface area of this fly ash was determined to be 7.12 m^2/g, as determined by the BET method using three different partial pressures of nitrogen. In using fly ash in the 45–74-μm size range, it was assumed that the surface chemistry of these particles would be similar to that of smaller (<5 μm) fly ash particles; this assumption is supported by the results of surface analyses of various fly ashes (*27*).

Solvents. All solvents used for extractions, liquid chromatography, and ultraviolet spectrophotometry were of Distilled in Glass (Burdick and Jackson) or equivalent quality.

Thin-Layer Chromatography Plates. Several studies were performed of photodegradation of PAHs adsorbed on commercial alumina plates (Uniplate 250-GF, Analtech, Inc.).

Methods: Preparation of Fly Ash Samples. PAHs were adsorbed onto the fly ash from the vapor phase using a vapor diffusion cell (*30*) and expanded-bed adsorption apparatus (*31*) described in detail elsewhere. After their removal from the adsorption train, samples were usually split, with a portion of each fly ash sample being stored in the dark as a "blank" to determine the stability of the adsorbed PAH in the absence of light.

Light Sources. In an effort to minimize the dependence of experimental results upon the characteristics of a single illumination source, a number of different sources were employed. These included: (a) General Electric 275-W incandescent Sunlamp; (b) two 40-W fluorescent Vitalite sunlamps (Duro-Lite Lamps, Inc.); (c) 150-W xenon compact arc lamp (Model 901C-11, Canrad-Hanovia); (d) 500-W Quartzline lamp (Model 500T3/C1. General Electric); and (e) high-pressure mercury arc lamp (Model BH-6, General Electric). The 150-W xenon and Quartzline lamps were the two sources used most frequently, owing to similarities in their spectral output distributions in the 290–440-nm wavelength region to that of natural sunlight (*21, 32, 33*). Unless otherwise indicated, the output of the source was not filtered prior to impinging upon the sample. Sunlight was also employed for illumination in several experiments.

Illumination Geometries. Figure 1 shows the sample container used for most exposures to light of PAHs vapor-adsorbed on fly ash. The cell, fabricated of quartz or Pyrex, was 7 cm in length, had a diameter of 4.5 cm, and typically was loaded with 0.3 g of fly ash. The cell was rotated at 0.5 rpm and was illuminated transversely. The indentations in the cell walls served to produce additional agitation of the fly ash as the cell was rotated (to decrease the probability that an appreciable fraction of the adsorbed PAH was physically screened from the incident light). The cell contained air at ambient pressure in all experiments.

Occasionally, "thin-layer chromatography" style plates of fly ash were fabricated by the conventional TLC slurry technique; a solution of PAH was then spotted onto the plate with a Pasteur micropipet, and the solvent was then evaporated. The plates were then illuminated in either upright or flat position (usually the former), depending upon the light source.

Analytical Procedures. After illumination was terminated, a weighed quantity of the fly ash sample was extracted with benzene or cyclohexane for 24 h in a micro-Soxhlet apparatus (Fisher Scientific 20-650); the thimbles (Whatman cellulose, 10 × 50 mm) had been preextracted for 24 h with the same solvent used in the analytical extraction.

The resulting extract was analyzed for the parent PAH and/or decomposition products by UV–visible absorptiometry

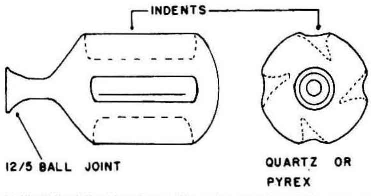

Figure 1. Cell for illumination of fly ash samples: left, side view; right, end-on view; length = 7 cm; diameter = 4.5 cm

(Cary Model 17), fluorescence spectrometry (Aminco-Bowman spectrophotofluorometer), or liquid chromatography (chromatograph constructed from Laboratory Data Control components, using a Whatman Partisil PXS 10-ODS 25-cm column and methanol–water mixtures as mobile phase). Gas chromatography (Varian Aerograph 2700 chromatograph, using a temperature-programmed 1.5% Dexsil 300 on acid-washed Gas-Chrom Q column and a flame ionization detector) was used for analysis in some liquid-solution illumination experiments.

Results

The experimental observations are described individually for each PAH.

a. Benzo[*a*]pyrene. A dilute cyclohexane solution of BaP (8×10^{-6} M) underwent extensive photodegradation upon illumination; in a typical experiment, 10-h exposure of such a solution to light from an unfiltered 150-W xenon lamp effected consumption of 44 ± 6% of the quantity of BaP initially present. In contrast, only modest photodecomposition of BaP adsorbed on fly wash was observed. A listing of typical experimental results, using a wide variety of illumination conditions, is compiled in Table I. In no case was a major portion of the initial quantity of BaP destroyed, even when prolonged exposure (e.g., sample LBAP10, for which 100 h of exposure to an unfiltered 150-W xenon lamp was used) or a lamp extremely rich in ultraviolet radiation (BH6 mercury lamp, 6-h exposure, sample LBAP9) was employed. These observations indicate that BaP which has been vapor-adsorbed on fly ash is surprisingly resistant to photodecomposition.

Moreover, it is probable that the results overestimate the extent to which adsorbed BaP underwent photodecomposition. As noted in Table I, "blank" samples of BaP adsorbed on fly ash but then stored in the dark underwent appreciable decomposition. No attempt was made to correct the analytical results in the illumination experiments for occurrence of this "dark reaction"; particularly for prolonged exposure experiments, however, the extent of "nonphotochemical" decomposition of adsorbed BaP is likely to have been appreciable. Consequently, much of the apparent "photodegradation" of adsorbed BaP may actually have resulted from a nonphotochemical process, and it therefore is conceivable that light plays a minor role in the chemical transformation of BaP vapor-deposited on fly ash. The proclivity of certain PAHs to undergo "dark" decomposition reactions when adsorbed on fly ash will be treated elsewhere (*34*).

That the decreases in adsorbed BaP concentration were due to chemical reactions (rather than vaporization or mechanical transport phenomena) was demonstrated by means of a search for degradation products of BaP by liquid chromatography. Example chromatograms are shown in Figure 2. Because of the small concentrations of decomposition products (due to the relatively small extent of decomposition of BaP under all conditions) and the need to employ gradient elution to achieve satisfactory separations (resulting in a noisy, sloping base line), no attempts were made to identify the products or to determine the yields with which they were formed. What is important, however, is that degradation products indeed were observed, and that virtually identical product species appear to be formed whether the fly ash samples were illuminated or stored in the dark.

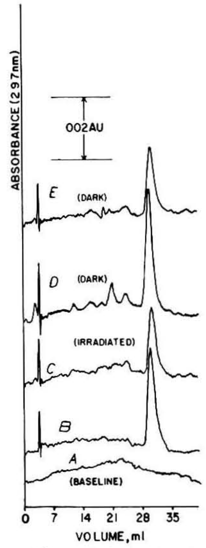

Figure 2. High-pressure LC results from extracts of one batch of BaP adsorbed on fly ash. Curve A is the solvent base line (UV absorption detector, λ 297 nm; solvent, methanol–water mixtures; gradient eluant composition varying from 50% methanol (original) to 70% methanol (final)). The remaining curves are chromatograms of methanol extracts from portions of the fly ash sample: (B) immediately after vapor adsorption of BaP onto fly ash; (C) after illumination of fly ash with xenon lamp for 24 h; (D) after storage of fly ash in the dark for 276 h; (E) after storage of fly ash in the dark for 300 h. The BaP elution peak occurs at ca. 30 mL; note the appearance of minor degradation product peaks at $v < 27$ mL

It is important to know whether the photoreactivity of adsorbed BaP depends upon the nature of the adsorbent. For this purpose, thin-layer chromatography (TLC) plates were

Table I. Representative Data for Photolysis of Benzo[*a*]pyrene Vapor-Adsorbed on Illinois State Line Fly Ash

sample code	illumination source	illumination duration, h	original [BaP], μg/g	final [BaP] μg/g	% change [a]	distance of source from sample, cm
LBAP2	Quartzline	2.5	110	99	−10	35
LBAP4	Quartzline	11.3	110	93	−16	35
8IR1	xenon	5	76	65	−14	48
LBAP10	xenon	100	44	37	−16	39
LBAP11	sunlamp	23	10	9	−10	19
LBAP9	BH6 mercury	6	44	40	−9	52
8IR4	sunlight	3.8	76	63	−17	
8IR0	none	190[b,c]	76	68	−11	
BAP2	none	1335[b]	44	36	−18	

[a] Determined by UV and fluorescence or high-pressure liquid chromatographic analysis of BaP following extraction. The "original" concentration was found by extraction and analysis immediately following completion of vapor deposition of BaP on the fly ash. [b] Elapsed time between preparation of fly ash sample and extraction (dark storage). [c] During the last 23 h, this sample was rotated (in the dark) in the sample cell used for photochemical illumination experiments.

fabricated from fly ash for comparison with conventional alumina TLC plates. Solutions of BaP (4×10^{-4} M) in methanol were spotted (100 μL total volume) onto each set of plates. The plates were illuminated with an unfiltered 150-W xenon lamp and were then extracted with methanol. The extracts were analyzed for their BaP content by liquid chromatography. For an alumina TLC plate, illumination for 80 min effected loss of 40–50% of the quantity of BaP initially present. When fly ash TLC plates were illuminated with the same lamp for the same duration, however, the quantity of BaP was virtually unchanged (less than 10% decomposition). Consequently, it seems clear that not all solid surfaces stabilize BaP with respect to photodecomposition to the same extent, and that fly ash is remarkably effective in that regard.

b. Pyrene. Solutions of pyrene in cyclohexanone (7.7×10^{-4} M) underwent significant photodecomposition when irradiated with a 275-W sunlamp; in a typical experiment, when 50 mL of such a solution was illuminated for 7.5 h, only 10 ± 2% of the initial quantity of pyrene remained at the conclusion of the experiment (as determined by gas chromatographic analysis of the illuminated solution compared with that of an aliquot portion of the original solution). In contrast, pyrene adsorbed on fly ash was extremely resistant to photochemical transformation even when prolonged exposures were used, as indicated in Table II. The most direct comparison with the solution data is afforded by sample 9B, in which only 13% loss of pyrene was effected by illumination with a 275-W sunlamp for 24 h (as compared with 90% decomposition in liquid solution upon illumination with the same lamp for only 7.5 h). Therefore, as for BaP, adsorption of pyrene onto fly ash appears to stabilize it toward photodegradation. In the absence of light, pyrene adsorbed on fly ash underwent negligible decomposition over periods of storage as long as 20 days. Thus, unlike the situation for BaP, the entire decrease in quantity of pyrene upon illumination presumably can be attributed to photochemical action.

c. Anthracene. Cyclohexanone solutions of anthracene (2.6×10^{-3} M) underwent facile photolysis; in a typical experiment, 60 ± 9% of the anthracene initially present in 50 mL of such a solution was destroyed by 2.5-h illumination with a 275-W sunlamp. However, anthracene vapor-adsorbed on fly ash was resistant to photodecomposition; representative data are compiled in Table III.

Liquid chromatographic analysis of photolyzed solutions indicated the principal photoproduct (both in liquid solution and adsorbed on fly ash) to be 9,10-anthraquinone. When adsorbed on fly ash, anthracene was also observed to undergo slow decomposition in the dark; the principal product of the "dark reaction" also was anthraquinone. As in the case of BaP, the principal degradation route for adsorbed anthracene appears to be nonphotochemical, and illumination does not effect a major increase in the extent of decomposition (Table III).

As in the case of BaP, TLC plate experiments (using alumina and fly ash substrates) were performed. Methanolic solutions (0.01 M) of anthracene were spotted on TLC plates, which were then illuminated (unfiltered 150-W xenon lamp) for 3 h. Greater than 95% of the anthracene initially present on the alumina TLC plates was destroyed by such illuminations, as indicated by liquid chromatography of a methanol extract of the irradiated plates, which indicated virtually complete conversion of anthracene to anthraquinone (Figure 3). In contrast, no detectable photolysis was observed for anthracene adsorbed on a fly ash TLC plate (i.e., no detectable quantity of anthraquinone was found in a methanol extract of the illuminated fly ash TLC plates). As for BaP, the photochemical behavior of adsorbed anthracene is seen to be strikingly dependent upon the identity of the substrate, with fly ash acting to stabilize the adsorbed PAH.

d. Other Compounds. Both phenanthrene and fluoranthene were observed to be resistant to photodecomposition in liquid solution. For example, 9.5-h illumination of cyclohexanone solutions of fluoranthene (2.5×10^{-3} M) typically produced decomposition of 10% or less of the initial quantity of fluoranthene. Similar results were noted for phenanthrene. No significant decomposition (either photochemical or nonphotochemical) was observed for either fluoranthene or phenanthrene vapor-adsorbed on fly ash (illumination periods as great as 3.3 h using a 150-W xenon lamp were employed).

Discussion

Three common PAHs (BaP, anthracene, and pyrene) are greatly reduced in susceptibility to photodecomposition when adsorbed on fly ash, as compared with their photoreactivity

Table II. Representative Data for Photolysis of Pyrene Vapor-Adsorbed on Illinois State Line Fly Ash

sample code	illumination source	illumination duration, h	original [P], μg/g	final [P], μg/g	% change [a]	distance of source from sample, cm
9B	sunlamp	24	291	253	−13.1	13.5
1B	sunlight	5	271	254	−6.2	
4A	vitalites	87	272	254	−6.6	76
7A	vitalites	90	291	275	−5.4	17
6F	none	430 [b]	231	228	−1.3	
5E	none	354 [b]	495	496	+0.2	

[a] Determined by UV or GC analysis for pyrene (P) following extraction. The "original" concentration was found by extraction and analysis immediately following completion of vapor deposition of P on the fly ash. [b] Elapsed time between solvent extractions performed to determine the "original" and "final" pyrene concentrations.

Table III. Representative Data for Photolysis of Anthracene Vapor-Adsorbed on Illinois State Line Fly Ash

sample code	illumination source	illumination duration, h	original [A], μg/g	final [A], μg/g	% change [a]	distance of source from sample, cm
IRAN1	xenon	3	300	249	−17	48
IRAN3	xenon	12	300	222	−26	48
IRAN2	xenon	24	300	222	−26	48
AN2-4	none	554 [b]	300	264	−12	

[a] Determined by high-pressure LC or UV analysis for anthracene (A) following extraction. The "original" concentration was found by extraction and analysis immediately following completion of vapor deposition of A on the fly ash. [b] Elapsed time between preparation of fly ash sample and extraction (dark storage).

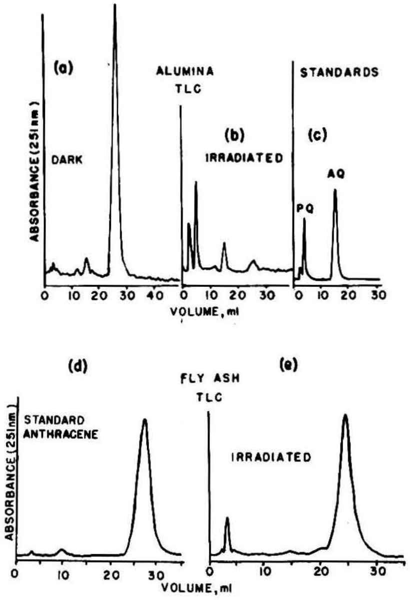

Figure 3. High-pressure LC analyses of methanol extracts of anthracene adsorbed on alumina and fly ash TLC plates: (a) alumina plate stored in the dark; (b) alumina plate illuminated for 3 h with xenon lamp; (c) *p*-benzoquinone (PQ) and 9,10-anthraquinone (AQ) standards; (d) anthracene standard; (e) fly ash plate illuminated for 3 h with xenon lamp; distance from source to plate = 48 cm. In all cases, the high-pressure LC solvent was 50% aqueous methanol

in liquid solution. For two of the compounds (BaP and anthracene), the extent of photolysis for a given period of illumination is strongly dependent upon the nature of the adsorbent, with photodegradation proceeding to a much greater extent on an alumina substrate than on a fly ash surface. These results are strikingly concordant with a recent report (*3*) that the mutagenicity of stack-collected fly ash samples is virtually unchanged by ultraviolet illumination. Observation of nonphotochemical degradation of several PAHs (*26, 27, 34*), together with the present results, implies that chemical transformation of adsorbed PAHs in the atmosphere may be determined largely by the rates of thermal reactions, with photochemistry playing a rather minor role. This conclusion is markedly at variance with most accepted estimates (*4*) of the importance of photochemical processes in the degradation of adsorbed atmospheric PAHs.

The mechanism(s) by which fly ash surfaces stabilize PAHs to photolysis is presently unclear. The effect may be partially physical in nature. For example, when adsorbed on fly ash particles, many PAH molecules may deposit inside the fly ash pore structure and thus be physically shielded from the incident light. Moreover, fly ash is colored, and may therefore act as an "inner filter" (*35*) by absorbing a significant fraction of the incident light. If the PAH adsorbed on fly ash is present in greater than "monolayer" quantities, only the top one or two molecular layers of adsorbate would likely be able to photodecompose; the lower layers would be screened from the exciting light by the outermost layers (*21*). While each of these "physical" factors may be important, it seems improbable that they can account for the observed diminution of photochemical activity of PAHs adsorbed on fly ash, for two reasons. First, care was exercised to ensure that the quantity of PAH vapor-adsorbed onto the fly ash was substantially less than that required to form a monolayer. Second, with the exception of the "inner-filter effect", each of the aforementioned arguments applies both to fly ash and alumina, yet the susceptibility to photolysis of PAHs adsorbed on these two surfaces is radically different.

Hence, it is likely that "chemical" factors play an important role in the suppression of photochemistry of PAHs adsorbed on fly ash. Relatively strong binding of PAHs to a surface (such as fly ash) could effectively stabilize adsorbate molecules with respect to photolysis by decreasing the mean lifetimes of their electronically excited states, especially if the surface in question contains species that can quench excited singlet or triplet states of organic molecules. Indeed, fly ash surfaces typically contain appreciable concentrations of transition-metal ions (*36–39*); metal ions are known to be efficient quenchers of excited states of many organic molecules (*40*). Such photodecomposition as does take place of PAHs adsorbed on fly ash tends to occur relatively rapidly, with prolongation of illumination producing little additional photodecomposition. This observation suggests that, in the case of partial monolayer coverage of a fly ash surface by an adsorbate, there may be two principal types of adsorption sites. At one "type" of site, photodecomposition would be relatively efficient; at the other (presumably more active) class of site, excited-state quenching may be very efficient, with the result that virtually no PAH molecules adsorbed at such sites undergo photolysis.

Substantial additional study (including examination of a variety of different fly ashes and measurement of excited-state lifetimes of PAHs absorbed on fly ash) obviously will be required before the resistance to photodegradation of PAHs adsorbed on fly ash can be understood. Irrespective of their origin in fundamental chemical or physical phenomena, the findings reported here are of considerable environmental significance. Based on these results, significant diurnal variations in the concentration of PAHs present in plumes emitted from coal-fired power plants are not anticipated. One would, however, expect to observe significant differences between PAH transformation rates in plumes of different power plants, due to the differing surface characteristics of the various emitted fly ashes. Moreover, the present results have important implications for the possible long-range transport of atmospheric PAHs (*41*). The present results do not address possible chemical interactions of adsorbed PAHs with other possible constituents of the atmosphere, such as O_3, SO_2, NO_x (*42*). It is evident that common presumptions (*4*) regarding the nature and extent of chemical transformation of atmospheric particulate polycyclic organic matter may be seriously in error, and additional investigations of these phenomena are urgently needed.

Acknowledgment

We thank J. Q. Chambers (University of Tennessee) for use of the liquid chromatograph and M. Schure (Colorado State University) for measurement of the fly ash surface area.

Literature Cited

(1) Pitts, J. N., Van Cauwenberghe, K. A., Grosjean, D., Schmid, J. P., Fitz, D. R., Belser, W. L., Jr., Knudson, G. B., Hynds, P. M., *Science*, **202**, 515 (1978).
(2) Chrisp, C. E., Fisher, G. L., Lammert, J. E., *Science*, **199**, 73 (1978).
(3) Fisher, G. L., Chrisp, C. E., Raabe, O. G., *Science*, **204**, 879 (1979).
(4) Committee on Biologic Effects of Atmospheric Pollutants, "Particulate Polycyclic Organic Matter", National Academy of Sciences, Washington, D.C., 1972.
(5) Natusch, D. F. S., *Environ. Health Perspect.*, **22**, 78 (1978).
(6) Natusch, D. F. S., Tomkins, B. A., in "Carcinogenesis—A Comprehensive Survey", Vol. 3, Jones, P. W., Freudenthal, R. I., Ed., Raven Press, New York, 1978, p 145.

(7) Miguel, A. H., Ph.D. Thesis, University of Illinois, Urbana, Ill., 1976.
(8) Löfroth, G., *Chemosphere*, **7**, 791 (1978).
(9) Searle, C. E., "Chemical Carcinogens", American Chemical Society, Washington, D.C., 1976.
(10) Jones, P. W., Freudenthal, R. I., "Carcinogenesis—A Comprehensive Survey", Vol. 3, Raven Press, New York, 1978.
(11) Fishbein, L., in "Chemical Mutagens", Vol. 4, Hollaender, A., Ed., Plenum Press, New York, 1976, p 219.
(12) Bowen, E. J., *Advan. Photochem.*, **1**, 23 (1963).
(13) Inscoe, M. N., *Anal. Chem.*, **36**, 2505 (1964).
(14) Van Duuren, B. L., *Int. J. Environ. Anal. Chem.*, **1**, 233 (1972).
(15) Seifert, B., *J. Chromatogr.*, **131**, 417 (1977).
(16) Hellman, H., *Fresenius Z. Anal. Chem.*, **295**, 24 (1979).
(17) Issaq, H., Andrews, A. W., Janini, G. M., Barr, E. W., *J. Liq. Chromatogr.*, **2**, 319 (1979).
(18) Thomas, J. F., Mukai, M., Tebbens, B. D., *Environ. Sci. Technol.*, **2**, 33 (1968).
(19) Barofsky, D. F., Baum, E. J., *J. Am. Chem. Soc.*, **98**, 8286 (1976).
(20) Pierce, R. C., Katz, M., *Environ. Sci. Technol.*, **10**, 45 (1976).
(21) Lane, D. A., Katz, M., in "Fate of Pollutants in the Air and Water Environments", Suffet, I. H., Ed., Wiley-Interscience, New York, 1977, p 137.
(22) Fox, M. A., Olive, S., *Science*, **205**, 582 (1979).
(23) Peters, J., Seifert, B., *Atmos. Environ.*, **14**, 117 (1980).
(24) Gibson, T. L., Smart, V. B., Smith, L. L., *Mutat. Res.*, **49**, 153 (1978).
(25) Jäger, J., Rakovic, M., *J. Hyg. Epidemiol. Microbiol. Immunol.*, **18**, 137 (1974).
(26) Korfmacher, W. A., Natusch, D. F. S., Taylor, D. R., Wehry, E. L., Mamantov, G., in "Polynuclear Aromatic Hydrocarbons", Jones, P. W., Lever, P., Eds., Ann Arbor Science Publishers, Ann Arbor, Mich., 1979, p 165.
(27) Korfmacher, W. A., Natusch, D. F. S., Taylor, D. R., Mamantov, G., Wehry, E. L., *Science*, **207**, 763 (1980).
(28) Natusch, D. F. S., Korfmacher, W. A., Miguel, A. H., Schure, M. R., paper presented in the Proceedings of the Symposium on Process Measurements for Environmental Assessment, Atlanta, Ga., Feb 1978.
(29) Korfmacher, W. A., Ph.D. Thesis, University of Illinois, Urbana, Ill., 1978.
(30) Miguel, A. H., Natusch, D. F. S., *Anal. Chem.*, **47**, 1705 (1975).
(31) Miguel, A. H., Korfmacher, W. A., Wehry, E. L., Mamantov, G., Natusch, D. F. S., *Environ. Sci. Technol.*, **13**, 1229 (1979).
(32) Sisson, W. B., Caldwell, M. M., *Photochem. Photobiol.*, **21**, 453 (1975).
(33) Peterson, J. T., "Calculated Actinic Fluxes (290–700 nm) for Air Pollution Photochemistry Applications", EPA-600/4-76-025, U.S. Environmental Protection Agency, Washington, D.C., 1976.
(34) Korfmacher, W. A., Mamantov, G., Wehry, E. L., Natusch, D. F. S., manuscript in preparation.
(35) Wehry, E. L., in "Analytical Photochemistry and Photochemical Analysis", Fitzgerald, J. M., Ed., Marcel Dekker, New York, 1971, p 173.
(36) Linton, R. W., Williams, P., Evans, C. A., Jr., Natusch, D. F. S., *Anal. Chem.*, **49**, 1514 (1977).
(37) Keyser, T. R., Natusch, D. F. S., Evans, C. A., Jr., Linton, R. W., *Environ. Sci. Technol.*, **12**, 768 (1978).
(38) Hulett, L. D., Dunn, H. W., Dale, J. M., Emery, J. F., Lyon, W. S., Murty, P. S., in "Measurement, Detection, and Control of Environmental Pollutants", Beck, E. R. A., Ed., International Atomic Energy Agency, Vienna, Austria, 1976, p 29.
(39) Coles, D. G., Ragaini, R. C., Ondov, J. M., Fisher, G. L., Silberman, D., Prentice, B. A., *Environ. Sci. Technol.*, **13**, 455 (1979).
(40) Wehry, E. L., in "Practical Fluorescence", Guilbault, G. G., Ed., Marcel Dekker, New York, 1973, p 120.
(41) Björseth, A., Lunde, G., Lindskog, A., *Atmos. Environ.*, **13**, 45 (1979).
(42) Pitts, J. N., *Phil. Trans. R. Soc. London, Ser. A*, **290**, 551 (1979).

Received for review September 12, 1979. Accepted April 25, 1980. The research described herein was supported in part by Grants R803950030 from the U.S. Environmental Protection Agency, Duluth, Minn., EE-77-S-02-4347 from the U.S. Department of Energy, and NSF ENV 74-24276 from the National Science Foundation, and by Contract RP-332-1 with the Electric Power Research Institute.

Covalent Binding of Aromatic Amines to Humates. 1. Reactions with Carbonyls and Quinones

George E. Parris

Division of Chemical Technology, Food and Drug Administration, Washington, D.C. 20204

■ The reaction of several ring-substituted anilines with humate has been studied in aqueous solution. The primary amines bind to humate in two phases. Initially, a rapid, reversible equilibrium is established, which may represent formation of imine linkages with the humate carbonyls. Subsequently, there is a slow reaction that is not readily reversed. The slow reaction is thought to represent 1,4 addition to quinone rings followed by tautomerization and oxidation to give an amino-substituted quinone. The slow reaction is not likely to be imine formation or other processes that require primary amines because *N*-methylaniline, a secondary amine, also reacts with humate. These processes represent ways in which aromatic amines may be converted to latent forms with undetermined effects on the biosphere.

A number of important pesticides, dyes, explosives, and other industrial chemicals contain moieties that are converted to aromatic amines in the environment. Several lines of evidence indicate that aromatic amines become bound to soil organic matter (e.g., humates) by covalent bonds. Important questions have been raised concerning the lability of the amine–humate adduct. In particular, more information is needed about the bioavailability of the aromatic amine moiety, and methods for systematically monitoring these residues are lacking. In this paper, some variables affecting the rate and extent of the reactions between aromatic amines and humates are investigated and discussed in terms of possible modes of adduct formation.

Hsu and Bartha (1, 2) proposed formation of imines (anils, Schiff's bases) to account for the reversible binding of aromatic amines to soil organic matter. Imine formation, Reaction 1, is a well-known reaction (*3–5*). The reaction is very fast and fully reversible. Water is one of the products of the reaction, and an excess of water tends to drive the equilibrium back to the amine and carbonyl compound. It is likely that amines react with carbonyl groups in humate, but it is not clear where the equilibrium (Reaction 1) lies in aqueous media.

$$\mathrm{ArNH_2 + O{=}CR_2 \rightleftarrows ArN{=}CR_2 + H_2O} \qquad (1)$$

Cranwell and Haworth (*6*) and later Hsu and Bartha (*1, 7*) proposed reactions that could lead to the incorporation of primary amines (e.g., aromatic amines and amino acids) into soil organic matter in modes that would be relatively resistant to hydrolysis and not readily exchangeable. The first step in this process involves a reversible Michael addition to quinonelike structures (present in humic matter due to oxidation of phenols). The addition is followed by tautomerization and oxidation yielding aminoquinones (Reactions 2 and 3). The amino group may react further by essentially the same addition–tautomerization–oxidation sequence to form a variety of nitrogen heterocycles (Reaction 4). The nature of the resulting heterocycle will depend upon the reactive sites (R) in the humate juxtaposed to the aminoquinone.

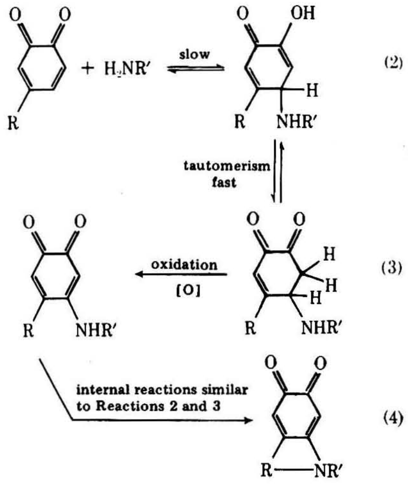

R = quinone moiety in humate

As a rule of thumb, progression along this sequence of reactions is expected to make the amine moiety more resistant to removal from the humate. After the addition reaction (Reaction 2), the amine residue should not be removed from the humate by simple extraction, but prior to oxidation (and perhaps even after oxidation in some cases) it might be displaced from the humate by a suitable competing reagent. After oxidation (Reaction 3) and particularly after reaction with quinone moieties near the site of the initial addition (Reaction 4), the amine moiety probably resists vigorous acid (*6*) or base (*7*) hydrolysis.

It is currently impossible to prove or disprove the existence of these or other linkages of amines to humates by direct spectroscopic means. Indirect support for certain mechanisms can be obtained by selectively blocking humate functional groups before attempting binding experiments. Experiments with compounds that serve as models of humate functional groups demonstrate reactions that might occur with humic matter, but extrapolation of these results to soil organic matter is speculative. With these facts in mind, we report the results of our experiments on the reaction of aromatic amines with humates and compounds that are models of carbonyl and quinone functional groups in humates. The working hypothesis that guided the experiments reported here is that the results pertain to the position and dynamics of Reaction 1 and the rate of Reaction 2.

Experimental

Materials. All chemicals not specifically cited were reagent grade products obtained from commercial dealers. The amines are listed in Table I and abbreviations used in the text are given.

Table I. Gas Chromatographic Retention Times[a]

compound	abbreviation	rel retention time[b]
aniline	A	0.34
N-methylaniline	NMA	0.51
2-toluidine	2MA	0.55
3-toluidine	3MA	0.55
4-toluidine	4MA	0.59
2-chloroaniline	2CA	0.63
4-chloroaniline	4CA	0.84
2-chloronitrobenzene	2CNB	1.00
2,5-dichloroaniline	25DCA	1.49
3,4-dichloroaniline	34DCA	2.22

[a] Perkin-Elmer Model 3920, injector 250 °C, column 150 °C isothermal, detector interface 220 °C; column 6 ft × 4 mm i.d. glass, 10% OV-101 on 80/100 mesh Chromosorb W-HP; helium carrier gas, 33 mL/min. [b] Solvent peak 0.66 min; retention time of 2CNB was 4.74 min.

Humate H-1. Commercially prepared sodium humate (Aldrich Chemical Co., Milwaukee, Wis.) was extracted sequentially with acetone and methanol in a Soxhlet apparatus. Upon evaporation, the acetone extract yielded a light yellow solid (0.01 g/g of humate). The solid obtained from the methanol (0.03 g/g of humate) was brown. The black solid remaining after these extractions was designated H-1. About 30% of H-1 was found to be insoluble in distilled water. The insoluble material appears to be humin.

Humate H-2. Commercial sodium humate was suspended in distilled water (10 g/L) in a shallow bowl. After 5 days the dark liquid was decanted from a gray solid that had settled. The solid obtained by evaporating the dark liquid was extracted with methanol to remove any organic contaminants and designated H-2.

Humate H-3. The commercial product was suspended in 0.5 M sodium hydroxide and centrifuged. The liquid was decanted and a solid was precipitated by adjusting the pH to 2 with HCl. This cycle was repeated three times; the base-soluble solid was then washed with distilled water and freeze-dried. This product, H-3, is an acid rather than a sodium salt, and it does not dissolve readily in water until the pH is raised to about 9. Once dissolved, H-3 will stay in solution at pH 4.

Humate H-RB. Humate H-2 (1.54 g) was treated with 0.21 g of sodium borohydride in 20 mL of pH 9 sodium borate buffer. Foaming was dispersed with 6 mL of 2-propanol. After 1 h, gas evolution was very slow and an additional 0.1 g of $NaBH_4$ was added. The reaction mixture was allowed to stand for 3 days; it was then taken to dryness and methanol was added to destroy any remaining borohydride. A control sample of H-2 was carried through the same procedure excluding addition of $NaBH_4$.

Humate H-RS. Humate H-2 (0.62 g) was treated with 5.0 mL of a dilute HCl solution containing 0.437 g of $SnCl_2$. The solution was mixed by shaking and allowed to stand for 18 h before use in binding experiments. A control sample of H-2 was similarly treated with dilute HCl not containing $SnCl_2$.

Model Compounds. In the course of these studies 3,4-dimethoxybenzaldehyde (veratraldehyde) and 1,4-benzoquinone were used to model simple aldehyde and quinone functional groups that are found in humic matter. Each of these compounds was reacted with 4-chloroaniline on a preparative scale to obtain products that may simulate aniline–humate interactions.

N-(4-Chlorophenyl)-3,4-dimethoxybenzaldehydeimine was prepared by dissolving 1.3 g of 4-chloroaniline and 1.7 g of veratraldehyde in 10 mL of methanol. Within 15 min, the imine precipitated as white needles. The product was recrystallized 5 times from methanol, and three crops of white needles were collected (0.2, 1.0, and 0.5 g, respectively). The product's infrared spectrum showed no N—H and no C═O absorptions. The starting aldehyde absorbs at 1660 cm^{-1}. In the product, the 1689–1471-cm^{-1} region where the C═N absorption is expected is obscured by other bands. This product melted at 83–84 °C. The compound did not decompose to 4CA when injected onto the GC-N/P in anhydrous methanol.

The reaction of *p*-benzoquinone with ring-substituted and *N*-methylanilines in methanol produced deep red solutions. When the quinone was in large excess, the solution was stable for long periods, but when the molar ratio of amine to quinone was 1:1 the red solution rapidly produced a brown precipitate. The amines used in this study did not react with 1,4-hydroquinone in methanol on the time scale at which reaction occurred with 1,4-benzoquinone. However, as 1,4-hydroquinone was oxidized by air to 1,4-benzoquinone the solution did slowly turn red.

The infrared spectra of the red and brown products isolated by column chromatography (benzene/silica gel) from the reaction of 4-chloroaniline with 1,4-benzoquinone in methanol showed only one band for N–H stretching. It is known that primary amines have two N–H bands in their infrared spectra, secondary amines have only one (*8*), and imines ($RN{=}CR_2$) have none; therefore, the products appear to be *N*-(4-chlorophenyl)aminobenzoquinones. In the spectrum of the brown products, the peaks attributable to the 4-chlorophenyl group (1550, 1460, 1380, 1270, 1080, 1000, 810, and 520 cm^{-1}) were more predominant than in the red products.

Buffers. In one set of experiments, commercial aqueous buffers were used as solvents. Unexpected peaks soon appeared in the chromatograms. The commercial buffers contain formalin (aqueous formaldehyde, 0.05%), which reacts with amines to form imines. These imines were identified by mass spectrometry. All the experiments reported here used buffers prepared from reagent chemicals in the laboratory: pH 4 potassium phthalate, pH 7 phosphate, and pH 9 borate. The buffers were rather weak (e.g., 0.05 *m*) and the actual pH of the humate solutions when pH 7 buffer was used was between 7 and 8. For this reason, results refer to the "buffer used" unless it is stated that the pH was measured.

Gas Chromatography. A Perkin-Elmer Model 3920 gas chromatograph with nitrogen–phosphorus detector was used routinely to determine aromatic amines. Good chromatographic separations (Table I) were achieved using a 6 ft × 4 mm i.d. glass column packed with 10% OV-101 on 80/100 mesh Chromosorb W-HP. Helium carrier gas was used at 33 mL/min. The injector temperature was 250 °C and the detector interface was 220 °C. The column was usually run isothermally at 150 °C. However, in a few experiments, 2,4-dichlorotoluene was used as an internal standard with a flame ionization detector, and a lower column temperature, i.e., 115 °C, was required to separate early eluting compounds from the methanol solvent front.

Binding and Release Experiments. Typical binding/release experiments were run in test tubes (10–20 mL) closed with aluminum foil lined screw caps. Humate (0.5–1.0 g) was placed into the tared tube and solvent or buffer was added. The test compounds (usually in mixtures of three–five compounds) were added in methanol solution (1.00–5.00 mL of 1 or 0.1 mg/mL) by pipet. The tubes were shaken as necessary to ensure mixing and stored at ambient temperature (21–23 °C) or kept in a 30 °C bath as noted. When methanol was the solvent, extraction was achieved by repetitive centrifugation and decantation of the liquid. When water was the solvent, the liquid was extracted several times with ethyl acetate. In kinetic experiments with humate, aliquots of the reaction mixture were periodically drawn by pipet, extracted, concentrated, and analyzed.

In the first two preliminary experiments, absolute recoveries were determined using external standards. It soon became apparent that the precision of this method was limited to a standard deviation of ±20% due principally to compounding of errors in volumetric transfers. A systematic error due to incomplete extraction and losses in the drying and concentration steps was also introduced. The latter losses were particularly significant when the extracts were concentrated to 1 mL and they tended to be greater for lower boiling aromatic amines. Thus, for the remaining experiments where higher precision and optimum recoveries were desired, an internal standard, 2-chloronitrobenzene, was added to the amine before it was mixed with the humate or model compounds, and results are reported as recovery relative to the internal standard. By concentrating the extracts with the internal standard only to 5 mL the precision of analysis was limited only by the random variations in detector response and retention times inherent to the GC-N/P system and the measurement of peak heights. The precision was typically ±5% except when peaks less than 10 mm (usually late eluting peaks, i.e., 25DCA and 34DCA) had to be compared with the internal standard. In these cases precision fell to ±10%. The recovery efficiency of all aromatic amines was acceptable, and over a long series of measurements the absolute recovery of the internal standard was found to be 104 ± 21% standard deviation.

Kinetic Experiments with Model Compounds. In kinetic experiments with model compounds, samples of the aqueous methanol reaction mixtures (e.g., 5 μL) were directly injected into the gas chromatograph. Unreacted anilines were determined relative to an internal standard. Linear first-order rate plots, $\ln [A] = -kt + \ln [A]_0$, were obtained for each substituted aniline in the reaction with benzoquinone over more than 90% of the reaction, except for 25DCA and NMA, which were not followed beyond about 30% completion.

Results and Discussion

Characterization of Humates. To ensure that the humate materials used in this study were similar to materials employed in other studies, they were examined by infrared spectroscopy. The spectra were similar to those published by other authors (*9–11*). The humate fractions that had been removed by extraction with organic solvents contained less –OH and more aliphatic C–H than the bulk of the material. The reduced humate H-RB had less absorption in the 1700–1800-cm^{-1} region than H-2, and H-RB had more intense absorption in the 1400–1300- and 1100–1000-cm^{-1} regions. These changes are indicative of reduction of carbonyl functional groups ($\nu_{C=O}$ 1700–1750 cm^{-1}) to alcohols (ν_{C-OH} 1300–1000 cm^{-1}).

Preliminary Experiments. Several preliminary experiments were carried out to determine the effects of certain variables (e.g., nature of the aromatic amine, solvent/pH, ratio of amine to humate, time of reaction, etc.) upon the binding and release of amines by humate. These experiments allowed the development of methodology for more precise kinetic experiments which followed. Since the preliminary experiments were run for arbitrary reaction periods, they do not distinguish between processes that have reached equilibrium and processes that are still approaching equilibrium at some undetermined rate.

Abbreviations for amines (e.g., A = aniline, 4CA = 4-chloroaniline, 25DCA = 2,5-dichloroaniline) are found in Table I.

Competitive Displacement. Fuchsbichler and Suss (*12*) reported that radiolabeled 4CA were extracted from soil more efficiently with solutions of unlabeled 4CA or 34DCA than with pure water or salt solutions. This experiment demonstrates that there must be a limited number of specific binding sites for which various amines compete. We decided to confirm this observation for our humate systems and use it to estimate the number of exchangeable sites per gram of humate.

A sample of humate H-1 was pretreated with a great excess of 4CA (4.7 mequiv/g of humate) in methanol for 3 days, after which the humate was repeatedly extracted with methanol, washed with CH_2Cl_2, and dried. We anticipated that aniline would be a more reactive amine than 4CA. We added a large amount of aniline (18 μequiv/g of humate) in 1% acetic acid/methanol to the humate and let the mixture equilibrate for 1 day. From the methanol extracts, 5.4 μequiv of 4CA/g of humate was recovered, compared to 1.4 μequiv of 4CA/g of humate recovered in a control without aniline. Since the small amount of aniline could not have significantly affected the gross properties of the solvent, the enhanced recovery with aniline indicates a specific effect. The result also suggests that the humate has at least 4 μequiv of sites for exchangeable binding of primary amine per gram. (There may be more exchangeable and unexchangeable sites.)

Binding and Release of 2CA, 4CA, and 34DCA in Two Solvent Systems. In Table II, a binding and release experiment involving competition of 2CA, 4CA, and 34DCA is summarized. The effects of the amine/humate ratio and solvent are examined. In the binding phase, methanol with either 3% acetic acid or 3% aqueous ammonia (the aqueous ammonia contained 30% NH_3 in water) was used as solvent, and the amines were left in contact with the humate for 3 days. Upon extraction (two 10-mL portions of methanol) and analysis, it was found that the absolute recoveries of all three amines were high in the presence of ammonia (considering that the extracts were concentrated to 1 mL before analysis; see Experimental). In the experiments in which acetic acid was used in the solvent, 4CA was not recovered as efficiently from humate H-1 as 2CA and 34DCA. Also, lower recoveries are experienced when the ratio of amine to humate is lower.

A third 10-mL methanol extract of each sample was taken and analyzed separately to confirm that all free amines had been removed.

In the release phase of the experiment, the humate samples were treated with 3% acetic acid/methanol containing aniline (e.g., 30 μequiv/g of humate). After 3 days the samples were extracted and analyzed. No additional amine was recovered from the humate originally treated with ammonia, but appreciable amounts were recovered from the humate samples originally treated with acetic acid. In particular, 4CA and 34DCA appear to have been selectively sequestered in the binding phase of the experiment.

These experiments demonstrate that there is a reversible (e.g., exchangeable) mode of binding of aniline to humates. The binding sites appear to be saturating at high amine concentrations. Ammonia may be blocking sites by forming imines with available carbonyls or other reactions.

The Ortho Substituent Effect. To determine whether the lack of binding displayed by 2CA relative to 4CA in the preceding experiment was due to steric or electronic effects, parallel binding experiments were run between 2MA and 4CA and between 4MA and 4CA. (This experimental design was chosen because 2MA and 4MA were not resolved in the chromatograms and could not be analyzed simultaneously.) After 5 days in 50% aqueous methanol solution at 30 °C (treatment levels were 8.3 to 11 μequiv of each amine/g of humate H-2), the recoveries of the amines were determined relative to 2CNB internal standards. In both experiments 52% of the 4CA was recovered, but only 34% of the 4MA was recovered while 85% of the 2MA was recovered. These results indicate that ortho substituents inhibit binding of aromatic amines regardless of whether the substituent is electron withdrawing (Cl–) or electron donating (CH_3–).

Blocking Humate Carbonyls. In principle it is possible to deduce which functional groups of humate are responsible for amine binding by selectively blocking them prior to attempting binding experiments (*1*). In practice, this approach is less than ideal because (a) it is impossible to modify one functional group without having effects on the overall properties of the humate, and (b) it is not easy to demonstrate spectroscopically that all the chosen sites were blocked.

Treatment of humate with $SnCl_2$ (*13*) yielded a product that was difficult to manipulate. Tin salts were entrained and the product was not soluble in water. In binding experiments, it behaved much like normal humate.

Reduction of simple carbonyl compounds (*14, 15*) by sodium borohydride has been well established, and this experience

Table II. Binding and Release of Aromatic Amines by Sodium Humate[a]

	solvent system								
	3% AcOH/CH_3OH			3% AcOH/CH_3OH			3% $NH_3(H_2O)/CH_3OH$		
treatment level, μequiv/g of H-1	2-CA 13	4-CA 14	3,4-DCA 11	2-CA 0.85	4-CA 0.87	3,4-DCA 0.70	2-CA 1.0	4-CA 1.1	3,4-DCA 0.85
(I) Binding Phase[b]									
absolute % recovery[c] after 3 days									
(a) first two methanol extracts	51	24	50	37	7.0	21	63	68	65
(b) third methanol extract	0.5	0.2	0.2	0.02	<0.1	<0.1	0.4	0.8	<1
(c) total	51	24	50	37	7.0	21	63	69	65
Treatment with aniline, μequiv g of H-1, 3% AcOH/CH_3OH	32			26			31		
	2-CA	4-CA	3,4-DCA	2-CA	4-CA	3,4-DCA	2-CA	4-CA	3,4-DCA
(II) Release Phase[b]									
absolute % recovery[c] after 3 days (two CH_3OH extractions)	1.8	17	12	3.2	4.9	3.7	<0.5	<0.5	<0.5
total recovered[c]	53	41	62	40	13	25	63	69	65

[a] The humate is H-1. [b] Ambient temperature 21–23 °C. [c] Extract concentrated to 1.0 mL.

has been applied to reduction of aldehyde and ketone functional groups in lignin. There are few references to reduction of quinones (*16–18*), but it appears that some quinones can be reduced by this reagent. There do not appear to be any references to reduction of humates with sodium borohydride, but it seems likely that all readily accessible, simple carbonyl functional groups and some "core" functional groups (*19*) can be reduced by an excess of sodium borohydride. Infrared spectra of H-2 and H-RB show some changes indicative of carbonyl reduction by borohydride.

When H-RB and a control of H-2 were treated with A, 2CA, 4CA, 25DCA, and 34DCA in methanol for 3 days, it was observed that recovery of the amines relative to 2CNB was not much better from H-RB than from the unreduced control. However, the recoveries of the amines from the control were so high (e.g., aniline 76% relative to 2CNB) that any difference between H-RB and H-2 would necessarily be small. Previous experiments (Table II) had shown that under basic conditions recoveries of all amines are high. Thus, the humate samples were washed twice with portions of 3% acetic acid/methanol solution and the binding experiment was repeated. This time, enough binding was achieved in the control to make the experiment a valid test. There were significant differences in the recoveries of unbound aniline (54% H-RB, 32% H-2) and 4CA (65% H-RB, 54% H-2) relative to 2CNB. Although more 34DCA was recovered from H-2 (86%) than H-RB (77%), these results are probably within experimental error. Generally, 2CA and 25DCA were recovered nearly quantitatively from both humates (i.e., they do not show significant binding). These results suggest that reduction with sodium borohydride did affect the ability of humate to bind amines, but the effect is not as clear-cut as might be expected if simple carbonyl functional groups were responsible for the bulk of the binding.

Kinetic Experiments with Humate. In spite of the difficulties of interpreting reactions involving complex and ill-defined materials like sodium humate, several kinetic experiments were conducted. The first kinetic runs were set up as competitive reactions in which a mixture of aniline, 2CA, 4CA, 25DCA, and 34DCA (with 2CNB as internal standard) in methanol was added to an aqueous buffer solution of sodium humate (H-2). Aliquots of the liquid were periodically taken for determination of extractable amines. Figure 1 shows a typical set of data in which percent recovery of the amines relative to 2CNB is plotted as a function of time. Binding apparently occurs in two temporal phases.

Phase I Binding. The very first set of data, taken minutes after mixing the reagents, shows small differences in the recoverability of the amines (see, e.g., Figure 1). While the data are not precise enough to reveal sharp distinctions, the trends observed for the initial extraction suggested that (a) all amines were recovered more efficiently when humate was in alkaline buffer than when neutral or acid buffer was used, and (b) even with acid buffers, 25DCA and 2CA were efficiently recovered. All the amines were quantitatively (92–101%) recovered from pH 4 buffer without humate.

Phase II Binding. After the initial binding equilibrium was established (i.e., phase I), the recoveries of aniline, 4CA, and 34DCA continue to decrease slowly (Figure 1). This binding appears to be only partially reversible. For example, in Figure 1, the dashed lines and circles indicate the recoveries of the amines from a sample of the reaction mixture treated at 287 h with excess aniline and extracted at 420 h for comparison to the untreated reaction mixture. Note that the aniline appears to have significantly enhanced the recovery of 4CA, 34DCA, and even 2CA.

In a similar experiment, aniline, 4CA, and 34DCA (30 μequiv each/g of humate) in pH 7 buffer were allowed to react for 195 h at which time recoveries of aniline, 4CA, and 34DCA were 48, 43, and 71%, respectively. A large amount of 3MA (3500 μequiv/g of humate) was added as a neat liquid to avoid changing the concentration of the other reactants. After 68 h, recoveries of aniline, 4CA, and 34DCA were 52, 71, and 83%, respectively. However, even after 476 h the recoveries of aniline, 4CA, and 34DCA were still incomplete: 72, 75, and 94%, respectively.

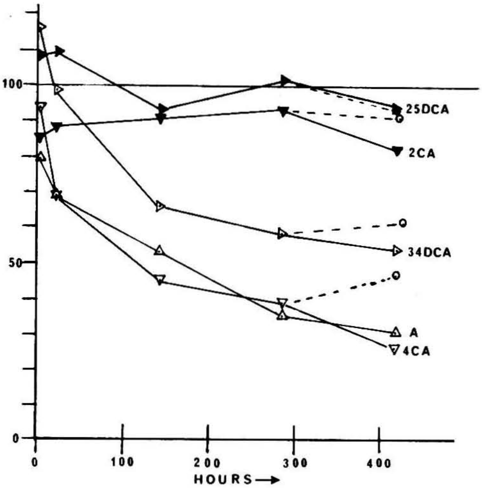

Figure 1. Recovery of substituted anilines from humate in aqueous pH 7 buffer at 30 °C. The initial concentration of humate was 16 g/L (1.64 g of H-2 in 100 mL of pH 7 phosphate buffer to which 3.00 mL of methanol containing the substituted anilines was added). The initial concentrations of the substituted anilines were as follows: A, 4.4 × 10^{-4} M; 2CA, 2.7 × 10^{-4} M; 4CA, 3.3 × 10^{-4} M; 25DCA, 2.1 × 10^{-4} M; 34DCA, 1.8 × 10^{-4} M. The data are plotted as percent recovery relative to 100% 2-chloronitrobenzene. The circles indicate recovery of the corresponding amines from an aliquot of the reaction mixture treated with 16 × 10^{-4} M of aniline at 287 h and extracted at 420 h.

The Kinetic Order of Phase II Binding. Data for the rate of binding of aniline to humate were taken from two of the competitive runs (employing five amines in each) and two other runs in which only aniline and 2CNB were added to the humate in pH 7 buffer. The initial "phase II" rate of binding of aniline, $-\mathrm{d}[\mathrm{A}]/\mathrm{d}t$ at $t = 0$, was determined from plots of concentration vs. time. The results are summarized in Table III and indicate that the rate of binding of aniline varies as the product of the concentrations of aniline and humate.

The reaction thus appears to be first order in aniline and first order in humate. However, this is probably not a simple second-order reaction. If the observed rate were a composite rate, it would still have a second-order relationship as shown by this derivation:

$$-\mathrm{d}[\mathrm{A}]/\mathrm{d}t = k_1[\mathrm{A}][\mathrm{S}_1] + k_2[\mathrm{A}][\mathrm{S}_2]\ldots k_n[\mathrm{A}][\mathrm{S}_n] = \sum_i k_i[\mathrm{A}][\mathrm{S}_i]$$

where S_i are different reactive sites in the humate each with a unique rate constant k_i. When the reaction begins ($t = 0$), $[\mathrm{S}_i]_0 = C_i[\text{humate}]_0$, where C_i is a constant characteristic of the humate, so that at $t = 0$;

$$-\mathrm{d}[\mathrm{A}]/\mathrm{d}t = \sum_i (k_iC_i[\mathrm{A}]_0[\text{humate}]_0) = (\sum_i k_iC_i)[\mathrm{A}]_0[\text{humate}]_0$$

and $\Sigma_i k_iC_i$ is an apparent second-order rate constant deter-

Table III. Initial Rate of Phase II Binding of Aniline with Humate in pH 7 Buffer at 30 °C

initial concentrations		product	initial phase II rate	calcd
aniline, $\times 10^{-4}$ M	humate, g/L	$[A][H]$, $\times 10^{-4}$ M·g/L	$-d[A]/dt$, $\times 10^{-4}$ M/h	2nd-order rate constant, L/(g·h)
14[a]	30	420	0.031	7.38×10^{-5}
5.7	41	234	0.022	9.40×10^{-5}
5.7	26	148	0.019	12.8×10^{-5}
4.4[a]	16	70	0.0058	8.29×10^{-5}
				av $(9.47 \pm 2.05) \times 10^{-5}$

[a] Competitive runs.

mined by dividing the initial rate by the initial concentrations of humate and aromatic amine.

Reactions of Primary Amines with Model Compounds. As reported by Hsu and Bartha (*1*), amines appear to react with humate by two distinct mechanisms. In the absence of methods to directly determine the nature of the chemical bonds between the amines and humate, reactions with model compounds allow the proposed mechanisms to be tested. The results of experiments with model compounds can never prove what is happening, but they can sometimes show what is not happening.

Formation and Decomposition of Imines. Veratraldehyde (3,4-dimethoxybenzaldehyde) was chosen as a humate–model carbonyl. When a mixture of aniline, 2CA, 4CA, 25DCA, 34DCA (e.g., 10^{-3} M), and 2CNB internal standard was mixed with veratraldehyde (10^{-1} M) in 77% CH_3OH/23% H_2O (v/v, pH 5 was due to traces of acid), an equilibrium was established immediately. Direct injection of the reaction mixture into the chromatograph showed loss of free aniline and 4CA within seconds of mixing the aldehyde and amines, and the established concentrations did not change over a period of 5 days. To prove that the imine/aniline equilibrium is rapidly established under these conditions, a sample of the imine formed from 4CA and veratraldehyde was dissolved in methanol and found to be stable indefinitely even when traces of acetic acid were added because a stoichiometric amount of water is required for hydrolysis (Reaction 1). However, when water was added to the solution of the imine (solution diluted to 16% CH_3OH/84% H_2O), free 4CA was immediately liberated. Formation constants (K_f) for imines are usually cited as the equilibrium constant (K_{eq}) for Reaction 1 divided by the concentration of water:

$$K_f = \frac{K_{eq}}{[H_2O]} = \frac{[\text{imine}]}{[\text{amine}][\text{carbonyl}]}$$

Formation constants were calculated for the imines of anilines ($K_f = 9.0\ M^{-1}$) and 4CA ($K_f = 3.6\ M^{-1}$) with veratraldehyde at 22 °C in 77% CH_3OH/23% H_2O, but the formation constants for the other imines were too small to measure at the concentrations used here (e.g., they are less than 1 M^{-1}). The thermodynamic equilibrium constants are, of course, much larger since the concentration of water in this solution is about 15 M (e.g., K_{eq} for aniline–imines $9\ M^{-1} \times 15\ M = 135$). These results are similar to those reported by other workers (*3*).

Experiments in which 4CA was displaced from the 4CA imine of veratraldehyde were also conducted. These reactions were run in anhydrous methanol, which made the rates very slow because no more than a catalytic amount of water was present. It was observed that the extent (and rate) of displacement of 4CA by other amines was aniline > 34DCA ≫ 2CA.

These results are similar to the rapid, reversible (phase I) binding of aromatic amines observed with humate. It is reasonable to propose, as Hsu and Bartha (*1*) did, that imine formation occurs to a significant extent in nonaqueous systems (e.g., anhydrous methanol or dry soil). However, in aqueous systems (e.g., flooded soil) imine formation will tend to be limited by the large excess of water (i.e., $[H_2O]/[ArNH_2] \gg 100$) in spite of favorable equilibrium constants (i.e., $K_{eq} \approx 100$). In other words, we can write:

$$[\text{imine}]/[\text{amine}] = K[\text{humate carbonyl}]_{\text{free}}/[H_2O]$$

$$\frac{[\text{bound amine}]}{[\text{free amine}]} = \frac{K([\text{humate carbonyl}]_0 - [\text{imine}])}{[H_2O]}$$

for the rapidly exchangeable, imine-bound anilines where $K = 10$ to 1000 (*3*) and $[\text{humate carbonyl}]_0 = [\text{humate}] \times 10^{-3}$ equiv of carbonyl/g (*20*).

Reactions of Primary Amines with Quinones. Primary amines may reversibly form imines with quinones, but the isolatable products are the less labile quinone substitution products (Reactions 2 and 3).

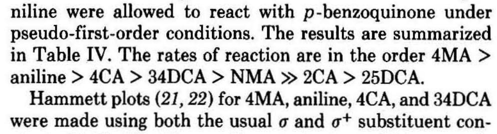

(5)

For comparison of reactivities of various amines with humate (Figure 1) and quinones, quantitative rate experiments were conducted. Ring-substituted anilines and *N*-methylaniline were allowed to react with *p*-benzoquinone under pseudo-first-order conditions. The results are summarized in Table IV. The rates of reaction are in the order 4MA > aniline > 4CA > 34DCA > NMA ≫ 2CA > 25DCA.

Hammett plots (*21, 22*) for 4MA, aniline, 4CA, and 34DCA were made using both the usual σ and σ^+ substituent constants (Table IV). The reaction constants ρ, which were calculated from the σ and σ^+ plots, were −1.5 and −1.8, respectively. However, the data are better correlated with the σ^+ constants, which were developed for application to systems in which substituents directly conjugate with an electron-demanding reaction center in the transition state. These results may be compared with $\rho = -0.99$ obtained for the nucleophilic reaction of substituted phenoxides with ethyl iodide in ethanol at 43 °C, and the equilibrium constants for protonation of substituted anilines by formic acid in 67% aqueous pyridine where $\rho = -1.43$ (*22*).

Preparative scale reaction between *p*-benzoquinone and 4CA produced several colored products. The use of high concentrations and quinone/amine ratios approaching 1:1 leads to multiple substitution on the quinoid ring and other side reactions (23–25), which were minimized under the conditions of the rate study.

Table IV. Reaction of Substituted Aniline with *p*-Benzoquinone under Competitive Pseudo-First-Order Conditions

compound	initial[a] concn, M	k_1, s^{-1}	$k_1/[Q]$,[a] $M^{-1}\ s^{-1}$	log (k/k_0)[b]	σ[b]	σ^+[c]
4-methylaniline	0.86×10^{-3}	2.8×10^{-3}	2.9×10^{-2}	0.42	−0.17	−0.26
aniline	1.37×10^{-3}	1.1×10^{-3}	1.1×10^{-2}	0	0	0
4-chloroaniline	1.02×10^{-3}	0.87×10^{-3}	0.90×10^{-2}	−0.087	+0.23	+0.04
3,4-dichloroaniline	0.67×10^{-3}	0.16×10^{-3}	0.17×10^{-2}	−0.81	+0.60	+0.43
2-chloroaniline	0.83×10^{-3}	0.055×10^{-3}	0.057×10^{-2}			
2,5-dichloroaniline	0.57×10^{-3}	0.0062×10^{-3}	0.0064×10^{-2}			
N-methylaniline[d]	0.76×10^{-3}	0.10×10^{-3}	0.12×10^{-2}			

[a] Temperature 22–23 °C, solvent 71% CH_3OH/29% H_2O, initial quinone concentration $[Q] = 97 \times 10^{-3}$ M, except for *N*-methylaniline, where $[Q] = 84 \times 10^{-3}$ M. [b] $\text{Log}(k/k_0) = \rho\sigma$, $\rho = -1.50$, $r^2 = 0.954$. [c] $\text{Log}(k/k_0) = \rho^+\sigma^+$, $\rho^+ = -1.79$, $r^2 = 0.998$. [d] Reaction carried out similarly to other runs except that flame ionization detection was used with a column temperature of 115 °C, and 2,4-dichlorotoluene (24DCT) was used as an internal standard. Under these conditions the retention time of NMA is 7.6 min and the retention time of 24DCT is 10.8 min. Reaction was followed to 67% completion.

Reaction of a Secondary Amine with Humate and Model Compounds. Inspection of Reactions 1, 2, and 3 suggests that it may be possible to distinguish between some of the possible mechanisms of covalent bond formation by comparing the reactivity of primary $ArNH_2$ and secondary ArNHR amines toward humates and model compounds. Secondary amines, such as NMA, cannot form imines (*3–5*), but as shown in Table IV, NMA reacts with *p*-benzoquinone to form the same sort of red product as the ring-substituted anilines. Note that the rate of reaction of NMA with *p*-benzoquinone is about the same as 34DCA, and the reaction goes to completion given enough time.

In a competitive experiment NMA (5.0×10^{-4} M) and 4CA (6.7×10^{-4} M) were reacted with humate H-2 (19 g/L, measured pH 4 after adjustment with acetic acid and 94% H_2O/6% CH_3OH, v/v). Recoveries of NMA and 4CA after 0.5 h were found to be 97 and 63%, respectively, relative to 2CNB. When the reaction was allowed to proceed for 8 days before extraction and analysis, recoveries of NMA and 4CA were only 60 and 22%, respectively, relative to 2CNB. Recoveries of NMA and 4CA from a sample of humate H-3 prepared by base extraction and reprecipitation of commercial humate (16 g/L, measured pH 4 after adjustment with acetic acid and 94% H_2O/6% CH_3OH, v/v) run in parallel with the H-2 humate experiment for 8 days were 46 and 15% relative to 2CNB.

These results are compatible with Reaction 2 being the rate-limiting step for introduction of the amine moiety into the humate. The use of a secondary amine is a useful tool because it is blocked from forming imines and heterocyclic compounds. If phase II addition does represent addition to quinones by Reaction 2, the partial reversibility observed for phase II is readily explained. Either a simple reversal of Reaction 2 (i.e., retro-Michael reaction (*26*)) or direct substitution as in Reaction 6 can occur (*23, 25*).

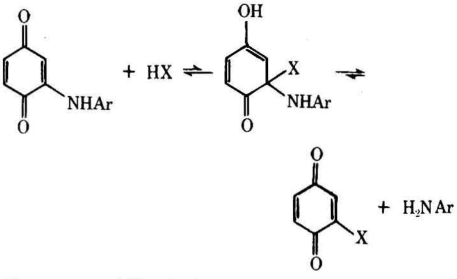

(6)

Summary and Conclusions

Experiments indicate that covalent binding (as inferrred from lack of recoverability by simple extraction) of ring-substituted anilines to humates involves two different chemical reactions. When an aniline is mixed with humate, a reversible equilibrium is very rapidly established. This equilibrium is thought to represent reaction of the amino group with aldehyde and ketone groups in the humate to form imine linkages. The second reaction is very slow and not readily reversible. This slow reaction is thought to represent addition of the amines to quinoidal structures followed by oxidation of the product to a nitrogen-substituted quinoid ring. Subsequent to this initial addition, further reactions may occur in loco to lock the amine moiety into the humate as part of a heterocycle. The effects of chloro and methyl substituents on the aniline ring are compatible with these interpretations. In addition, the conclusions are supported by the observation that *N*-methylaniline (which cannot form imines, but which adds to quinoid rings) reacted slowly with humate.

Acknowledgment

The author thanks Pasquale Lombardo and Gregory Diachenko for helpful discussions and criticism of the manuscript. Gregory Diachenko prepared the humate H-3 used in this study.

Literature Cited

(1) Hsu, T. S., Bartha, R., *Soil Sci.*, **116**, 444–52 (1974).
(2) Hsu, T. S., Bartha, R., *Soil Sci.*, **118**, 213–20 (1974).
(3) Ogata, Y. Kawaski, A., in "The Chemistry of the Carbonyl Group", Vol. 2, Zabicky, J., Ed., Wiley-Interscience, New York, 1970, pp 1–70.
(4) Layer, R. W., *Chem. Rev.*, **63**, 489–508 (1963).
(5) Sprung, M. M., *Chem. Rev.*, **26**, 297–335 (1940).
(6) Cranwell, P. A., Haworth, R. D., *Tetrahedron*, **27**, 1831–7 (1971).
(7) Hsu, T. S., Bartha, R., *J. Agric. Food Chem.*, **24**, 119–22 (1976).
(8) Dyer, J. R., "Applications of Absorption Spectroscopy of Organic Compounds", Prentice-Hall, Englewood Cliffs, N.J., 1965, p 36.
(9) Hergert, H. L., in "Lignins: Occurrence, Formation, Structure and Reactions", Sarkanen, K. V., Ludwig, C. H., Eds., Wiley-Interscience, New York, 1971, pp 267–97.
(10) Biederbeck, V. O., Paul, E. A., *Soil Sci.*, **115**, 357–66 (1973).
(11) Stevenson, F. J., Goh, K. M., *Geochim. Cosmochim. Acta*, **35**, 471–83 (1971).
(12) Fuchsbichler, G., Suss, A., *Chemosphere*, 345–50 (1978).
(13) Mathur, S. P., *Soil Sci. Soc. Am. Proc.*, **36**, 611–6 (1972).
(14) Brown, H. C., *J. Chem. Educ.*, **38**, 173–9 (1961).
(15) Smith, D. C., *Nature (London)*, **176**, 927–8 (1955).
(16) Thomson, R. H., "Naturally Occurring Quinones", 2nd ed., Academic Press, New York, 1971.
(17) Linn, B. O., Page, A. C., Wong, E. L., Gale, P. H., Shunk, C. H., Folkers, K., *J. Am. Chem. Soc.*, **81**, 4007–10 (1959).
(18) Langemann, A., Isler, O., in "Biochemistry of Quinones", Morton, R. A., Ed., Academic Press, New York, 1965, pp 121–8.
(19) Cheshire, M. V., Cranwell, P. A., Falshaw, C. P., Floyd, A. J., Haworth, R. D., *Tetrahedron*, **23**, 1667–82 (1967).
(20) Riffaldi, R., Schnitzer, M., *Soil Sci.*, **115**, 349–56 (1973).

(21) Roberts, J. D., Caserio, M. C., "Basic Principles of Organic Chemistry", W. A. Benjamin, New York, 1965, pp 960–2.
(22) Gordon, A. J., Ford, R. A., "The Chemist's Companion", Wiley, New York, 1972, pp 144–9.
(23) Hickinbottom, W. J., "Reactions of Organic Compounds", 3rd ed., Wiley, New York, 1957, pp 284–7.
(24) Hashimoto, S., Takashima, H., *Chem. Abstr.*, **85**, 62765p (1976).
(25) Cajipe Baisas, G. J., Ph.D. Thesis, University of Michigan, 1974, Order No. 74-19, 241, Xerox University Microfilms, Ann Arbor, Mich. 48106.
(26) Bergmann, E. E., Ginsburg, D., Pappo, R., *Org. React.*, **10**, 179–558 (1959).

Received for review September 10, 1979. Accepted May 2, 1980.

Sorption of Iodide on Copper

Zia Haq, G. Michael Bancroft*, and William S. Fyfe

Departments of Chemistry and Geology, The University of Western Ontario, London, Ontario N6A 5B7, Canada

Gordon Bird and Vincent J. Lopata

Whiteshell Nuclear Research Establishment, Atomic Energy of Canada Limited, Pinawa, Manitoba R0E 1L0, Canada

■ The kinetics and thermodynamics of the sorption of iodide on Cu metal, Cu_2O, and CuO have been studied using an ion-selective electrode and a radioactive ^{125}I tracer to measure I^- in solution. ESCA, SEM, and XRD techniques have been used to measure and characterize I^- directly on the copper metal surface. The copper surface consists of hydrated or hydroxylated Cu_2O, but both copper metal and Cu_2O sorb I^- rapidly from solutions having $[I^-] \geq 10^{-6}$ M. Sorption on copper progresses in two steps: formation of a $Cu^+(I^-)(OH^-)$ complex on the surface, followed by crystallization of CuI and release of OH^- into solution. The concentration of I^- in solution (and thus the amount of iodide sorbed at low concentrations) is controlled by the solubility product of CuI ($K_{sp} = 1.1 \times 10^{-12}$). Desorption of iodide from copper metal also is consistent with $[I^-]$ in solution being controlled by the solubility product of CuI. Oxidation of the copper surface to CuO results in much poorer sorption of I^-.

^{129}I is potentially one of the more mobile nuclear fission products because of its long half-life ($t_{1/2} = 1.7 \times 10^7$ years) and tendency to go into solution as an anion that is not retarded by interaction with silicate minerals. As noted very recently by Strachan (*1*), research for removing ^{129}I from nuclear waste has been directed mainly toward the scrubbing processes in reprocessing streams (*2–4*), rather than immobilizing the ^{129}I for long-term storage. Precipitation of ^{129}I as $Ba(IO_3)_2$ (*3*) or PbI_2 (*5*) and incorporation of ^{129}I into sodalite (*1*) have been proposed for long-term storage.

Many countries are now considering multiple containment measures for nuclear waste, which would include sorbent buffers and backfill, as well as stable containers or hosts such as glasses, ceramics, or crystalline solids (*6, 7*). The overall system could include sorbents for isotopes such as ^{129}I, which may be leached from the initial immobilizing medium. Copper metal appeared to us to be an attractive sorber for I for several reasons. First, iodine is known to concentrate around copper deposits (*8*) in nature. Second, a preliminary study of I^- sorption on copper showed that considerable I^- is taken out of solution (*9*). Third, copper has been proposed as an excellent stable container for nuclear waste (*7*). We felt that Cu metal as a container, or a copper salt in the buffer/backfill material, could serve to sorb leached ^{129}I from the waste.

In this work we present detailed results of I^- sorption and desorption on copper metal, Cu_2O, and CuO, using surface-sensitive probes such as electron spectroscopy for chemical analysis (ESCA) (*10, 11*), radiometric tracers, and scanning electron microscopy (SEM) to follow the sorption reaction directly and to elucidate the kinetics, mechanism, and thermodynamics of I^- uptake. The ESCA technique is ideally suited for studying surface reactions on smooth substrates (*12, 13*) like that of sheet copper.

Experimental

The copper metal used was Fisher electrolytic dust, having a grain size of about 30 μm. Fisher reagent grade Cu_2O and CuO and powdered natural cuprous oxide (cuprite) from Ontario were also used. Five grams of the above was added to 50 mL of dilute (10^{-2} to 10^{-6} M) NaI solutions at 22 °C for varying times. Sorbed I^- was determined by measuring the residual I^- in the solution with a pH meter and an Orion specific-ion electrode, having a linear sensitivity down to I^- concentrations of 2×10^{-8} M. The radiometric tracer experiments were carried out at room temperature using 25 mL of NaI solution containing ^{125}I tracer, and 0.25 g of Cu, Cu_2O, or CuO. The analyses were made by β-counting the ^{125}I tracer and comparing the counts in the copper solutions with counts in a similar solution without the copper. Deionized water in Teflon or polyethylene bottles was used throughout.

For the ESCA and SEM observations, polycrystalline copper sheet (purity of at least 99.9%) was cut to 2.1 cm × 1.0 cm plates, degreased in acetone, and then dipped into 5% HNO_3 for 1 min. After the samples were rinsed in water and subsequently dried with acetone, they were suspended in 100 mL of NaI solutions of strengths 8×10^{-8}, 8×10^{-7}, 8×10^{-6}, 8×10^{-5}, and 8×10^{-4} M. At the end of the elapsed periods they were removed from the solution, washed thoroughly in water, and dried by sluicing with acetone before being used for ESCA, SEM, and X-ray diffraction measurements.

Black CuO was grown on the sheet copper plates by enclosing them in a sealed glass tube partially filled with water and heating at 100 °C for 1 week. For sorption experiments, these plates were then suspended in NaI solutions as for copper metal above. A CuI standard for ESCA measurements was prepared by a long-established method (*14*). The sorption capacity of powdered CuO was treated with the I^- sensitive electrode and by radiometric counting.

For desorption studies, Fisher electrolytic granular copper (grain size 100–150 μm) was used instead of the finer dust, since it was easier to filter and transfer. Iodide was first sorbed onto this copper by adding 20 g of Cu to 200 mL of 10^{-4} M NaI and leaving the solution for 72 h. The I^- sorption was followed with the specific-ion electrode. The solution was then decanted, and the copper was washed with water to remove residual I^-. The copper was then added to 100 mL of water at 22 or 82 °C in a stoppered Nalgene bottle, and the desorbed I^- was measured with the specific-ion electrode.

The ESCA spectra were obtained using a McPherson ESCA 36 spectrometer and an aluminum anode. The angle between the incident photons and analyzed electrons was ~90°. Eight

0013-936X/80/0914-1106$01.00/0

copper plates could be mounted on the sample wheel. After an initial broad scan from 1000- to 0-eV binding energies showed no impurity peaks, narrow scans (10–20 eV) were made of the Cu 2p, O 1s, I 3d, and C 1s lines of interest to obtain good counting statistics. The Cu $2p_{1/2}$ line (rather than the larger Cu $2p_{3/2}$ line) was used to monitor copper on the surface because the I $3p_{3/2}$ level overlaps with the Cu $2p_{3/2}$ line. The C 1s contaminant peak was small (less than 30% of the O 1s peak intensity) in all cases.

The spectra were computed using a program written by Coatsworth et al. (*15*). Each spectrum was fitted with an analytical function consisting of Gauss–Lorentz functions and a linear base-line correction. The computed areas were of prime importance in determining the I coverage on the copper plates.

Results and Discussion

(a) The Powder Sorption. Summary plots of the I^- sorption on 5-g Cu powder samples as measured with the specific-ion electrode are shown in Figure 1. Well over 90% of the I^- in the 10^{-4} and 10^{-5} M solutions is sorbed, while, in the higher (10^{-2} and 10^{-3} M) and lower (10^{-6} M) concentrations, a smaller percentage of iodide is sorbed. However, the amount of I^- sorbed does increase as the solution concentration increases: 2×10^{-8} mol from 10^{-6} M, 4.5×10^{-7} mol from 10^{-5} M, 4.8×10^{-6} mol from 10^{-4} M, 1.5×10^{-5} mol from 10^{-3} M, and 2.5×10^{-5} mol from 10^{-2} M, with resulting iodide solution concentrations being 6×10^{-7}, 1×10^{-6}, 4×10^{-6}, 7×10^{-4}, and 1×10^{-2} M, respectively. The pH of all solutions began at about 5.3 and rose at the same rate as the decrease in solution I^- concentration. Both pH and I^- level out after a few hours for the 10^{-6} and 10^{-5} M solutions, and within 24 h for the larger I^- concentrations. Thus, for the 10^{-4} M NaI solution, the pH rise begins at 5.2 and levels out at 7.2 after 24 h. The equilibrium pH values increase uniformly from 6.5 for the 10^{-6} M solution to 9.9 for the 10^{-2} M solution. This increase in pH shows a release of OH^- and/or uptake of H^+ from solution. The evidence below strongly indicates that the former predominates. Most importantly, the final I^- concentrations and pH are controlled largely by the solubility products of Cu_2O and CuI (vide supra).

In similar studies using radioactive ^{125}I tracer solution to follow the sorption kinetics, the sorption curves were found to have exactly the same shape. The copper continued to sorb over a longer time period with maximum sorption being reached within 14 days and little change occurring thereafter. In the 10^{-3} M experiment, approximately 96% of the I^- was sorbed, and the solution concentration fell to approximately 4×10^{-5} M.

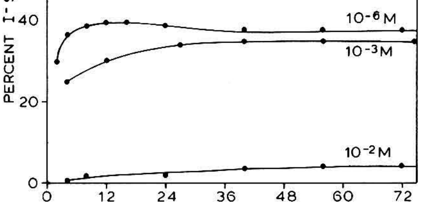

Figure 1. Sorption-time plot of total I^- (as percent of initial concentration) in 50 mL of NaI solution of 10^{-6}–10^{-2} on 5 g of copper powder at 22 °C as measured with the specific-ion electrode.

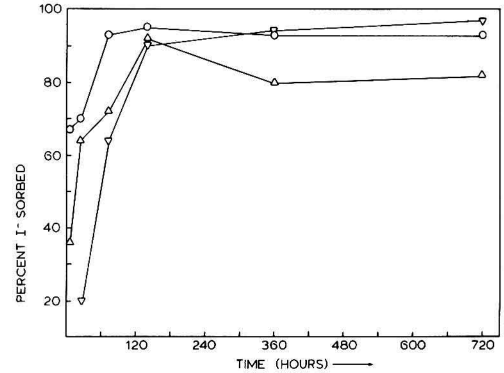

Figure 2. Effect of temperature on I^- sorption on copper: (▽) 5 °C; (○) 22 °C; and (△) 82 °C. Five grams of copper powder in 50 mL of 10^{-4} M NaI solution has been used.

Approximately 75% of the I^- was removed from the 10^{-5} M solution, which dropped in concentration to approximately 3×10^{-6} M. Both these results support the conclusions of the specific-ion electrode study; i.e., solubility of CuI is the major control on maximum sorption. The differences between the specific-ion electrode study and the radiometric tracer study are probably due to the different starting materials. No attempt was made to correlate surface areas and oxide layer thickness between the starting materials, and for this reason the results of the specific-ion electrode studies and the tracer experiments cannot be quantitatively compared.

Figure 2 shows the effect of temperature on the I^- sorption from 10^{-4} M NaI. Although less I^- is sorbed at 82 °C relative to the lower temperatures, it is still 80% of total I^- at 82 °C. The decrease could be due to the formation of CuO, which does not sorb I^- (vide infra).

We have also measured the sorption of I^- on powdered CuO and Cu_2O and natural minerals. The sorption of I^- (10^{-4} M NaI) on CuO and powdered cuprite (Cu_2O) is shown in Figure 3. Although there is a rapid, initial uptake of I^- by CuO, the

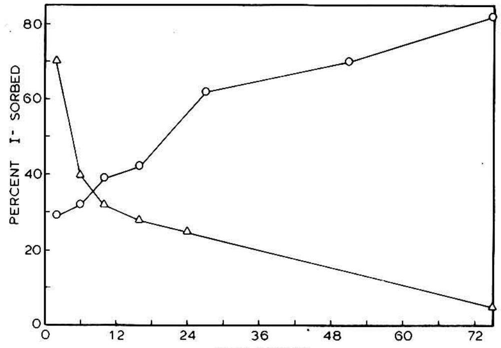

Figure 3. I^- sorption on Cu_2O (natural cuprite) and CuO at 22 °C. Five grams of oxide in 50 mL of 10^{-4} M NaI solution; (○) cuprite; (△) CuO.

sorbed I$^-$ is quickly released to the solution. In contrast, Cu_2O sorbs I$^-$ with a similar, albeit slower, rate to the Cu powder. After 72 h, the Cu_2O has removed over 80% of the I$^-$ from the solution. ESCA measurements on the CuO-coated copper plates showed no I$^-$ on the surface. Studies of I$^-$ sorption by CuO and Cu_2O using radiometric tracer methods gave similar results. Little or no I$^-$ was sorbed on CuO.

Sorption of I$^-$ on both Cu_2O and copper metal occurs essentially on Cu_2O surfaces. We have not attempted to compare the nature of the oxide layer on the metal with that of Cu_2O. It is expected that the differences in the sorptive capacity and sorption kinetics of the two systems relate to differences in the nature of this oxide layer. In some preliminary experiments with copper metal under redox conditions that suppress the formation of Cu_2O, we found the sorption of I$^-$ is greatly decreased.

Finally, we have observed that, at 22 °C, continuous aeration of the iodide solution does not affect the terminal value of sorption. When the solution at 82 °C is aerated even intermittently, the sorption fell to two-thirds of the nonaerated value. At higher temperatures, the passage of air through the solution promotes the formation of CuO and the sorption is lowered.

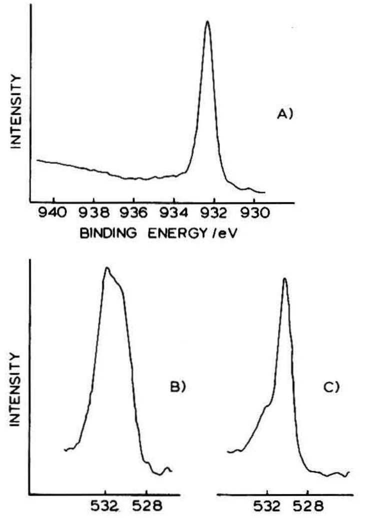

Figure 4. ESCA spectra of: (A) the Cu $2p_{3/2}$ line on a blank Cu plate (note that there is no noticeable shakeup peak at 940 eV); (B) the O 1s region on the same blank Cu plate; (C) the O 1s region after being in 8×10^{-4} M NaI solution for 72 h. Note the decrease in the peak at ~532 eV in C relative to B.

(b) ESCA and SEM Studies. The ESCA spectra (Figure 4) show that the surface of the Cu plates in this study consists of a fairly thick (at least several hundred nanometers) layer of hydrated or hydroxylated Cu_2O surface. Although our Cu $2p_{3/2}$ binding energy (Table I) is in good agreement with that for Cu_2O, the Cu $2p_{3/2}$ binding energies cannot be used to distinguish between Cu and Cu_2O because the Cu $2p_{3/2}$ binding energies are virtually identical for the two substances (*16*). However, there are three strong pieces of evidence that rule out appreciable Cu metal near the surface. First, the $L_3M_{4,5}M_{4,5}$ Auger kinetic energy of ~917.5 eV is in good agreement with that for Cu_2O, and ~1 eV lower than that for Cu (*16*). The Auger parameter α' of 1849.6 is in excellent agreement with the value given previously for Cu_2O (*16*). Second, the plates showed large oxide O 1s peaks at ~530 eV, which did not decrease in intensity even after 10 min of Ar ion etching. Third, the calculated Cu:O ratio from the O 1s and Cu $2p_{1/2}$ peak areas is very close to 2:1. We use the intensity formula (*17, 18*) to calculate this ratio:

$$\frac{I_{\mathrm{Cu}2p_{1/2}}}{I_{\mathrm{O}1s}} = \frac{n_{\mathrm{Cu}}}{n_{\mathrm{O}}} \frac{\sigma_{\mathrm{Cu}}}{\sigma_{\mathrm{O}}} \frac{(\mathrm{K.E.})^{1.7}_{\mathrm{Cu}\,2p_{1/2}}}{(\mathrm{K.E.})^{1.7}_{\mathrm{O}\,1s}}$$

where n is the number of atoms, σ is the cross-section for photoelectron production (*19*), and K.E. is the kinetic energy of the outgoing photoelectron. Substituting in the calculated cross-sections from Scofield (*19*) (2.93 b for O 1s and 8.66 b for Cu $2p_{1/2}$), the measured kinetic energies, and the computed peak areas, we obtain a Cu:O ratio of 1.8:1, in reasonable agreement with the stoichiometric ratio of 2:1. We have found this treatment to give quantitative atomic ratios in previous work (*18*).

The existence of appreciable CuO on the surface can be ruled out on the basis of binding energy (the Cu $2p_{3/2}$ binding energy is about 1 eV higher than that in Cu_2O (*16*)), the narrow symmetric Cu 2p lines (Figure 4A), the absence of strong shake-up satellites at ~8 eV from the primary 2p peaks (*20*), and the Cu:O ratio of 1.8:1. For example, the Cu:O ratio calculated for our CuO sample using the intensity formula is ≤1:1. All this evidence indicates strongly that the surface contains less than 10% CuO.

There are several lines of evidence that show that these Cu_2O surfaces are heavily hydroxylated and/or hydrated, with the OH or H_2O loosely held. The major O 1s peak on the blank after short times of reaction is near 532 eV, characteristic of an OH oxygen rather than an oxide oxygen (*21, 22*). For example, the oxide oxygen peak of Cu_2O is at about 530 eV (*23*), with a 532-eV shoulder, which is most likely an OH oxygen (Figure 4B) (*22*). After sorption of I$^-$, the O 1s peak consistently shifts toward 530 eV (Figure 4C). Thus, the I$^-$ displaces the OH groups on the surface. Argon ion etching of the blank, or a sample with sorbed I$^-$, readily removed the OH oxygen peak, and leaves the oxide oxygen. It is also of note that about half of the sorbed I is etched off along with the OH oxygen.

Using the computed ESCA areas of Cu $2p_{1/2}$, O 1s, and I $3d_{5/2}$ peaks, we show the I$^-$ sorption as a function of time in

Table I. ESCA Binding Energies (±0.2 eV) Relative to C 1s at 284.6 eV (*16*)

species	Cu $2p_{3/2}$	O 1s	I $3d_{5/2}$	ref
Cu blank, hydroxylated (Cu_2O)	932.3	532.0 530.1 } Figure 4B		this work and *16*
Cu_2O	932.4	~532 (shoulder) 530.4 (strong)		*16, 22, 23* and this work
I$^-$ on Cu	932.5	532.1, 530.3	619.8– 619.4 (final)	this work
CuI	932.3	532.2	619.4	this work
Cu metal	932.4			*16, 22*

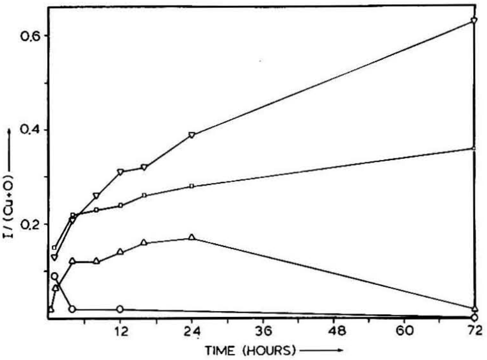

Figure 5. The intensity of the ESCA I $3d_{5/2}$ peak divided by the Cu $2p_{1/2}$ area plus the O 1s area plotted vs. time in initial I^- solutions of (○) 8×10^{-7} M; (△) 8×10^{-6} M; (□) 8×10^{-5} M; (▽) 8×10^{-4} M.

Figure 5 for initial I^- concentrations ranging from 8×10^{-7} to 8×10^{-4} M. These plots are basically characteristic of a sorption process with the amount of I^- sorbed increasing with increasing initial concentration and time. This trend is qualitatively consistent with that deduced earlier from Figure 1. There are indications of "steps" in this sorption reaction, as seen in an earlier study (*9*). Furthermore, the results for sorption from the 8×10^{-7} M solution provide additional information on the equilibrium thermodynamics of I^- uptake. Although there is some initial sorption from the 8×10^{-7} M solution (as with the powder CuO results), it falls to essentially zero after 3 days. The initial sorption may take place at surface imperfections, but as the sample ages the I^- is desorbed.

The ESCA results on the loaded samples show clearly that a hydrated and/or hydroxylated CuI complex is formed before the crystallization of CuI. The SEM and X-ray diffraction data below confirm the presence of CuI. The Cu $2p_{3/2}$ binding energies for CuI are virtually identical with those of Cu_2O (and Cu) (Table I) and thus are not informative. The measured I $3d_{5/2}$ binding energy after long sorption times is 619.4 eV—in excellent agreement with that of CuI (Table I). However, initially, the I $3d_{5/2}$ binding energies are ~0.5 eV higher than that for CuI. As mentioned previously, the OH oxygen peak decreases with sorption time and the pH of the solution increases.

The copper plates were examined by SEM and photomicrographs of three specimens are shown in Figure 6. Figure 6 (a, b) shows the surface after exposure to 10^{-3} M NaI solution for several weeks. It is covered with a thick but discontinuous layer of particulate matter, which was shown by XRD to consist of Cu_2O and CuI. Figure 6 (c, d) shows a similar copper plate which had been exposed to 10^{-5} M NaI solution for the same length of time as that shown Figure 6a. It is clear that the surface has been oxidized and that small spherical clumps of CuI are dispersed over it. The XRD pattern of this plate showed Cu metal and Cu_2O with a suggestion of a very weak CuI (111) line.

Figure 6 (e, f) shows the copper surface after exposure to 10^{-7} M NaI solution. Clearly, the surface is oxidized and deeply corroded, but there is no suggestion of CuI precipitation. This observation is completely compatible with the XRD results, which show only Cu_2O and Cu metal, and with the known solubility of CuI (vide supra).

The ESCA intensities are consistent with CuI particulate island formation on the copper surface. In our ESCA spectra of pure CuI, we found that the I $3d_{5/2}$:Cu $2p_{1/2}$ ratio was 6.5:1 compared to our maximum ratio on the sorbed samples of 1.6:1. The theoretical I $3d_{5/2}$:Cu $2p_{1/2}$ ratio for pure CuI using Equation 1 is 5.3:1.

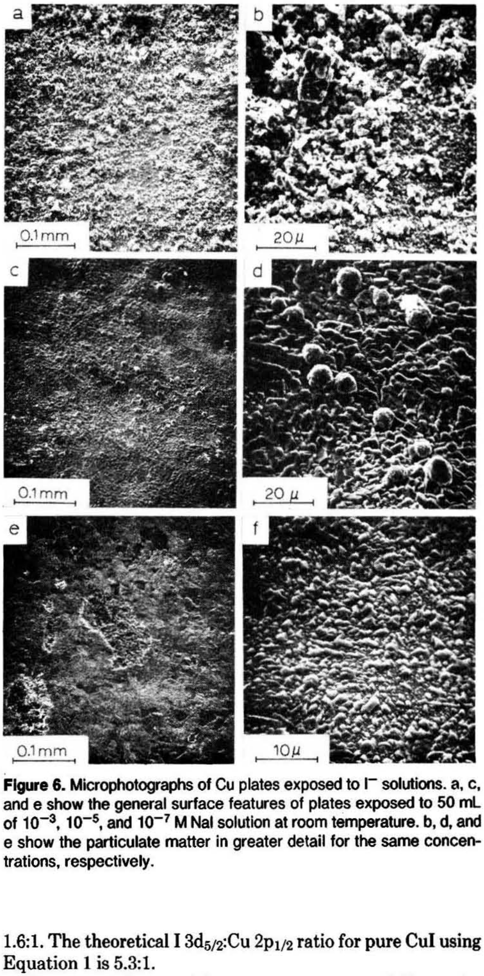

Figure 6. Microphotographs of Cu plates exposed to I^- solutions. a, c, and e show the general surface features of plates exposed to 50 mL of 10^{-3}, 10^{-5}, and 10^{-7} M NaI solution at room temperature. b, d, and e show the particulate matter in greater detail for the same concentrations, respectively.

We are now in a position to comment more fully on the mechanism of sorption and the limiting equilibrium concentration of I^- in solution after sorption by Cu or Cu_2O. We tentatively suggest that the I^- ions attach initially to the hydroxylated Cu_2O surface to form a $Cu^+(I^-)(OH^-)$ complex. The slightly higher initial I $3d_{5/2}$ binding energy (relative to CuI) is consistent with this intermediate formation, with the I^- being attached directly to copper. This direct attachment of I^- to Cu is made possible by the small primary hydration number of I^- (~1) (*24, 25*) and hence the small effective size plus higher mobility of iodide in solution (*26*).

When CuI begins to crystallize, the OH^- ions are released into the solution, raising the pH. The net effect is exchange of I^- for surface hydroxyls, a common anion sorption mechanism (*27, 28*). The ESCA spectra always show the presence of OH groups—both from the $Cu^+(I^-)(OH^-)$ intermediate and the remaining hydroxylated Cu_2O.

Figures 1 and 5 show that the sorption is not of a simple Langmuir type: the degree of sorption does not increase uniformly as the initial concentration of I^- in solution decreases. The SEM photographs show nonuniform growth of CuI on the copper surface, and there is a hint of steps (*9*) in the sorption plot (Figure 5). There may well be more than one mechanism of I^- sorption (e.g., surface sorption on a range of site types, later followed by nucleation and growth of CuI), each process

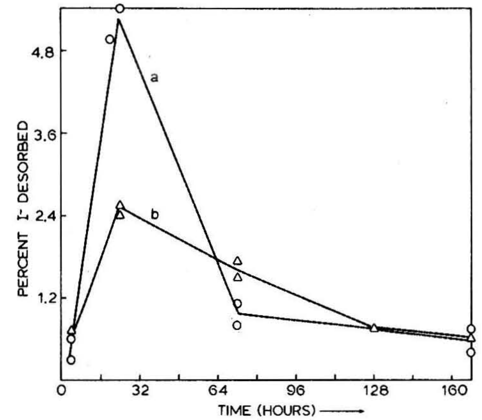

Figure 7. Desorption of I^- in 100 mL of solution from 20 g of copper powder pretreated in 200 mL of 10^{-4} M NaI solution for 72 h: (a) distilled water; (b) 10^{-7} M NaI solution.

with its own rate constant. Such processes would lead to distinct steps in the overall rate of sorption.

The lack of sorption of I^- from the 10^{-7} M solution, the final I^- concentrations, and pH in the 10^{-2} to 10^{-6} M solutions (Figure 1) are all consistent with the K_{sp} for CuI (*29*) of 1.1×10^{-12} and the K for the reaction $0.5Cu_2O + 0.5H_2O \rightleftharpoons Cu^+ + OH^-$ of 1.4×10^{-15} (*29*). Using the experimentally determined equilibrium I^- and OH^- concentrations and the equilibrium constant for Cu_2O to calculate the equilibrium Cu^+ concentration, we calculate a K_{sp} for CuI that is always within a factor of five of 10^{-13} for all concentrations—in reasonable agreement with the theoretical value of $\sim 10^{-12}$. From these two equilibrium constants, it is also apparent that at pH >6, the I^- concentration for the 10^{-7} M solution should be $>10^{-7}$ M, and I^- will not sorb permanently at this concentration.

Desorption of iodide from samples sorbed with I^- ($\sim 2 \times 10^{-5}$ mol of I^-) at 22 °C was studied at 82 °C to determine the stability of the sorbed layer (see Figure 7). For curve a of Figure 7, sample was placed in pure water. Initially, a large amount of desorption occurs (~5%), followed by resorption. In 10^{-7} M I^- (curve b) at 82 °C, the spike of desorption is reduced. Although the initial desorption spikes are not well understood, these data probably indicate that the equilibrium surface states at 22 and 82 °C are not the same, and the metastable 22 °C surface has a higher initial solubility than the states after aging. In both cases, the final 0.6% desorption ($\sim 1 \times 10^{-7}$ mol of I^- in 100 mL) is consistent with the equilibrium solubility of CuI (i.e., $\sim 10^{-6}$ M). Finally, samples loaded at 82 °C in the 10^{-4} M I^- solution, when desorbed in pure water at 22 °C, yielded approximately the same equilibrium value of I^-.

Acknowledgments

We are grateful to Dr. J. R. Brown for helpful discussions.

Literature Cited

(1) Strachan, D. M., Abstracts, International Symposium on Ceramics in Nuclear Waste Management, Meeting of American Ceramic Society, Cincinnati, May 1979, Abstracts of program.
(2) Murphy, L. P., Staples, B. A., Thomas, T. R., ICP-1135, Allied Chemical Corporation, Idaho Falls, Idaho, 1977.
(3) Yarbro, D. O., Mailen, J. C., Groenier, W. S., Proceedings of the 13th AEC Air Cleaning Conference (CONF-740807-P2), San Francisco, 1974.
(4) Wilhelm, J. G., Schuettelkopf, H., "Control of Radioiodine in the Nuclear industry", IAEA, Vienna, 1973.
(5) Mailen, J. C., Horner, D. F., *Nucl. Technol.*, **33**, 260–3 (1977).
(6) Cameron, D. J., Strathdee, G. G., Proceedings of the International Symposium on Ceramics in Nuclear Waste Management, Cincinatti, Conf 790420, 4–9 (U.S. Department of Energy, Technical Information Center, Oakridge, Tenn., 1979).
(7) "Copper as a Canister Material for Unreprocessed Nuclear Wastes—Evaluation with Respect to Corrosion", KBS-TEKNISK RAPPORT-90, 1978.
(8) Goldschmidt, V. M., "Geochemistry", Muir, A., Ed., Clarendon Press, 1958, p 603.
(9) Arnikar, H. J., Mehta, O. P., *J. Sci. Ind. Res. Sect. B*, **20**, 209–12 (1961).
(10) Siegbahn, K., Nordling, C., Fahlman, A., Nordberg, R., Hamrin, K., Hedman, J., Johannson, G., Bergmark, T., Karlsson, S., Lingren, I., Lindberg, B., *Nova Acta Regiae Soc. Sci. Ups., Ser. IV*, **20** (1967).
(11) Carlson, T. A., "Photoelectron and Auger Spectroscopy", Plenum Press, New York, 1975.
(12) Bancroft, G. M., Brown, J. R., Fyfe, W. S., *Chem. Geol.*, **19**, 131–44 (1977).
(13) Bancroft, G. M., Brown, J. R., Fyfe, W. S., *Chem. Geol.*, **25**, 227–43 (1979).
(14) Sidgwick, N. V., "The Chemical Elements and Their Compounds", Vol. 1, Clarendon Press, 1950, p 121.
(15) Bancroft, G. M., Adams, I., Coatsworth, L. L., Bennewitz, C. D., Brown, J. D., Westwood, W. D., *Anal. Chem.*, **47**, 586–9 (1975).
(16) Wagner, C. D., Gale, L. H., Raymond, R. H., *Anal. Chem.*, **51**, 466–82 (1979).
(17) Wagner, C. D., *Am. Soc. Test. Mater.*, **No. 643**, 31–46 (1978).
(18) Bancroft, G. M., Gupta, R. P., Hardin, A., Ternan, M., *Anal. Chem.*, **51**, 2102 (1979).
(19) Scofield, J. H., *J. Electron Spectrosc. Relat. Phenom.*, **8**, 129–34 (1976).
(20) Frost, D. C., Ishitani, A., MacDowell, C. A., *Mol. Phys.*, **24**, 861–70 (1972).
(21) Norton, P. R., *J. Catal.*, **36**, 211–23 (1975).
(22) Kim, K. S., Winograd, N., *Surf. Sci.*, **43**, 625–43 (1974).
(23) Schön, G., *Surf. Sci.*, **35**, 96–108 (1973).
(24) Bockris, J. O'M., *Q. Rev. Chem. Soc.*, **3**, 173–80 (1949).
(25) Davies, C. W., "Ion Association", Butterworths, London, 1962, p 151.
(26) Buijs, K., Choppin, G. R., *J. Chem. Phys.*, **39**, 2042–50 (1963).
(27) Yates, D. E., Healy, J. W., *J. Colloid Interfac. Sci.*, **52**, 222–8 (1975).
(28) Ryden, J. C., McLaughlin, J. R., Syers, J. K., *J. Soil Sci.*, **28**, 72–92 (1977).
(29) Latimer, W. M., "The Oxidation Stages of the Elements and Their Potentials in Aqueous Solutions", 2nd ed., Prentice-Hall, Englewood Cliffs, N.J., 1964, p 186.

Received for review November 5, 1979. Accepted May 6, 1980. Atomic Energy of Canada Limited and the Natural Sciences and Engineering Research Council of Canada provided financial support.

Elemental Distribution in Coal Fly Ash Particles

Lee D. Hansen[1]* and Gerald L. Fisher[2]

Laboratory for Energy-Related Health Research, University of California, Davis, Calif. 95616

■ Methods are developed for determining quantitative relative concentrations of elements in the aluminosilicate matrix and in nonmatrix or surface material of coal fly ash. The dependence of total element concentration on particle size and the solubility of elements in solutions of HCl and HF are discussed. The results indicate greater than 70% of the Ti, Na, K, Mg, Hf, Th, and Fe is associated with the aluminosilicate matrix. More than 70% of the Ca, Sc, Sr, La, the rare earth elements, and probably Ni appears to be associated with an acid-soluble phase, which has the same particle size distribution as the aluminosilicate phases. More than 70% of the As, Se, Mo, Zn, Cd, W, V, U, and Sb are associated with surface material on the ash particles. The elements Mn, Be, Cr, Cu, Co, Ga, Ba, and Pb are intermediate in behavior, i.e., distributed about equally between matrix and nonmatrix material.

A detailed knowledge of the spatial distribution of elements and compounds in the particles of fly ash resulting from coal combusion is of interest for several reasons. Such knowledge is required for assessing the bioenvironmental significance of fly ash, for designing emission control systems for coal-fired plants, and for searching for new uses for the vast amounts of fly ash that are being generated.

There are basically four methods for determining the distribution of an element within or among small particles: (a) the total concentration of the element can be determined as a function of particle size. If the concentration increases as particle size decreases, it is often assumed that the element is located on the surface of the particles (*1*). In order to obtain quantitative information such as the areal concentration or thickness of the surface layer, a deposition model or theory with several assumptions must be adopted (*2, 3*). (b) The surface of the particles can be studied directly by the use of ESCA, AES, SIMS, or other spectroscopic methods (*4–6*). These methods are also not without pitfalls, however. Depth profiles are semiquantitative, artifacts and interferences must be carefully guarded against, and these methods require expensive equipment and are generally slow and tedious. (c) Solvent leaching can also provide data on the distribution of elements and compounds within the particulate matter (*6–9*). These data give information on the soluble and insoluble phases that are present, however, and are not necessarily directly comparable to the other "surface" analysis methods. In particular, solvent leaching studies are subject to misinterpretation because dissolution and precipitation can form new phases during the leaching process. Proper attention must also be paid to the pH, volume of the leachate, and equilibrium vs. nonequilibrium conditions. (d) Analysis of single particles by X-ray fluorescence using either a SEM or an electron microprobe can identify differences in the matrix composition between individual particles. Matrix heterogeneity has been identified by these methods in the samples used in this study (*10, 11*).

When applied to coal fly ash, all four of the methods for determining elemental distribution are qualitatively in agreement. Points of agreement are (a) that certain elements (e.g., As and Se) are present quantitatively on the surface of the particles, (b) that the interior or matrix of most of the particles is predominantly an aluminosilicate material, and (c) that many elements are intermediate in their behavior, thus suggesting a distribution of these elements between the matrix and the surface of the particles. Quantitative agreement among the various methods is difficult to assess, however. Although several long lists of enrichment factors and related data have been published (*2–6, 12–14*), samples have rarely been studied by more than one of the above methods, and then only for a few selected elements. It is the purpose of this paper to quantitatively compare the results of element distributions as determined from solution leaching studies with those determined from bulk analysis of size-classified fly ash fractions.

The results of elemental analyses of a set of four size fractions of a coal fly ash have been previously reported (*13–15*). The particle size dependence of the bulk concentrations was discussed in terms of enrichment factors in the earlier communications. A more meaningful and quantitative method of treating the data is developed in this paper.

The results of leaching the finest size fraction of fly ash with water and a series of matched HCl and HF solutions are also reported. The HCl solutions dissolve predominantly nonmatrix materials, while the HF solutions dissolve both nonmatrix materials and the aluminosilicate matrix. Thus, by determining the solubility of an element in the ash as a function of acid concentration, the amount of the element associated with the aluminosilicate matrix can be determined. The finest (volume median diameter = 2.2 μm) size-classified, stack-collected fly ash sample (*16*) was chosen for this study because this fine fly ash is collected with minimal efficiency by the electrostatic precipitators of conventional power plants. Upon release to the environment, this fraction of the ash forms stable aerosols and becomes widely distributed in the atmosphere.

Materials

Many properties of the fly ash fractions used in this study have previously been described (*13–16, 18*). The samples of aerodynamically sized stack fly ash were obtained from a large Western coal-fired power plant that burns low-sulfur (0.5%), high-ash (20%) coal. Kilogram quantities of four size fractions of fly ash were collected for a 30-day period at 30 ft^3/min (cfm) and at 95°C by a specially designed fractionator mounted downstream from a cold-side ESP as reported by McFarland et al. (*16*). The volume median diameters (VMD) of the fractions were 20, 6.3, 3.2, and 2.2 μm. Only the finest size fraction (2.2 μm VMD) was used in the acid differential solubility studies.

Water was distilled, deionized, and redistilled in an all-glass still. Analytical reagent grade HF, redistilled 6 M HCl (G. F. Smith Chemical Co., Columbus, Ohio), and boric acid purified of sodium (*15*) were used. Reagent blanks were carried through all steps of the leaching and analysis procedures.

Particle Size Dependence of Total Element Concentrations

The total mass of an element in the ash may be divided into that which is in the matrix and that which is in the nonmatrix material as shown in Equation 1:

$$m_T = m_M + m_N \qquad (1)$$

---

[1] On leave from the Department of Chemistry and the Thermochemical Institute of Brigham Young University, Provo, Utah 84602.

[2] Current address, Battelle Columbus Laboratories, Toxicology/Pharmacology, Section, 505 King Ave., Columbus, Ohio 43201.

0013-936X/80/0914-1111$01.00/0 © 1980 American Chemical Society

where m_T is the total mass of the element, m_M is the mass of the element in the matrix, and m_N is the mass of the element associated with nonmatrix or surface material. Normalizing to the mass of the ash (Equation 2) results in the relationship between C_T, the total concentration of the element in the ash, and C_M and C_N, the concentrations in the matrix and in the nonmatrix, respectively.

$$C_T = C_M + C_N \tag{2}$$

Further derivation is necessary to obtain a relation between C_T and particle size. We begin by assuming that nonmatrix material is all on the surface of particles of matrix material. Then, since C_N is equal to the areal concentration, C_A, multiplied by the specific surface area, A, we obtain Equation 3:

$$C_T = C_M + C_A A \tag{3}$$

which is similar to an equation obtained by Davison et al. (*3*). The surface area, which is a function of particle size, may, of course, be obtained directly by a variety of methods. There are, however, significant differences in the values obtained for fly ash by different methods. Thus, we prefer to go one step further and substitute the function $6/D_V\rho$ for the surface area as shown in Equation 4:

$$C_T = C_M + C_A(6/D_V\rho) \tag{4}$$

where D_V is the diameter of average volume (*17*) as calculated from data taken with a Coulter counter and ρ is the density of the particles as measured by fluid displacement (*16*). The factor of 6, the ratio of surface area to volume for a sphere, is used because the particles are assumed to have the same surface to volume ratio as a sphere. Light microscopic studies support the use of this assumption, in that more than 90% of the particles in these ash samples have been classified as having spherical morphology (*18*). By plotting C_T vs. $(6/D_V\rho)$ and extrapolating to infinite diameter, a linear plot will result for constant C_M and C_A, and these parameters can then be obtained from the intercept and slope, respectively. Only the value of C_A, and not C_M, will be significantly affected if our assumption of spherical surface to volume ratio is incorrect or if our choice of D_V values is in error.

Because the matrix concentration, C_M, is, by definition, invariant with particle size, the nonmatrix concentration, C_N, may be calculated for each of the fly ash fractions. To provide comparison with results of the HCl and HF studies, C_N values were calculated for cut 4 using the appropriate C_T values.

Linear, least-squares analyses of the data indicated significant ($r > 0.90$; $p < 0.10$) correlations of elemental concentrations with the inverse of the diameters of average volume of the four size-classified fly ash fractions for all elements except Al, Ce, Dy, Eu, Hf, K, La, Na, Ni, Sc, Tb, Ti, and Yb. For those elements with concentrations displaying a significant dependence on particle size, the intercept of the regression line at $(6/D_V\rho) = 0$ was used to calculate the matrix concentration, C_M, and subsequently the fraction of element in the nonmatrix, f_N, as described in Equation 5:

$$f_N = C_N/C_T = (C_T - C_M)/C_T \tag{5}$$

For elemental concentrations that did not correlate ($r < 0.90$) with particle size, f_N was calculated from the average concentration, C_{av}, of all four fractions (Equation 6). Equation 6 is mathematically equivalent to 5 when the slope is zero, i.e., for those cases where $r < 0.90$.

$$f_N = (C_T - C_{av})/C_T \tag{6}$$

Plots of C_T vs. $(6/D_V\rho)$ gave points which appeared to fall on a straight line for most of the elements determined. Values of C_T were obtained from previously reported data (*13, 14*) and values of D_V and ρ are from Fisher et al. (*18*). Representative plots of this type are given in Figure 1. Figure 2 shows representative plots for those elements that did not show significant correlation with particle size.

Table I gives the results of linear least-squares analyses of the data for all elements studied together with values of C_N

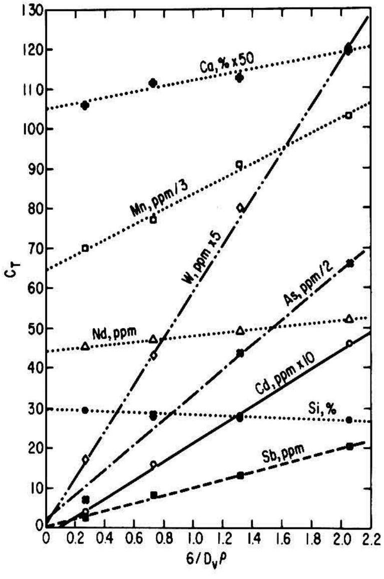

Figure 1. Representative plots of the total concentration of an element, C_T, vs. the surface area function, $6/D_V\rho$. Lines represent the linear least-squares fit of the data. Appropriate scale factors are presented after the element designation; e.g., Ca, % × 50 indicates that the actual concentration in % is equal to $C_T/50$; and Mn, ppm/3 indicates the actual concentration in μg/g is equal to $C_T \times 3$

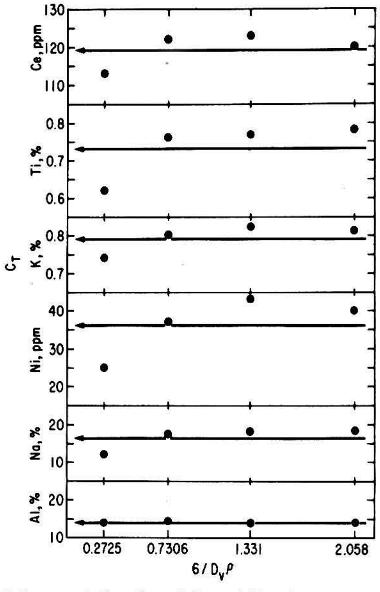

Figure 2. Representative plots of C_T vs. $6/D_V\rho$ for elements that did not show a significant correlation with particle size. Horizontal arrows are drawn through the average value of C_T

Table I. Spatial Concentrations of Elements Calculated from the Dependence of the Total Concentration on Particle Size

element	C_M[a] from intercept, μg/g unless % indicated	C_A[b] from slope, μg/cm^2 unless cg/cm^2 indicated	C_N[c] from $C_T - C_M$, μg/g unless % indicated	f_N,[d] %
Al	14.0 (%)	0.090 (cg/cm^2)	0.1 (%)	0[e]
As	1.7	64	130	98
Ba	0.14 (%)	0.13 (cg/cm^2)	0.27 (%)	66
Be	6.3	2.1	4.0	39
Ca	2.10 (%)	0.14 (cg/cm^2)	0.28 (%)	12
Cd	−0.19	2.23	4.8	104
Ce	116	3.2	4	0[e]
Co	9.4	6.3	12	56
Cr	30	23	41	58
Cu	50	43	87	64
Dy	7.3	0.69	1.2	6[e]
Eu	1.0	0.15	0.3	10[e]
Fe	2.5 (%)	0.36 (cg/cm^2)	0.7 (%)	22
Ga	42	70	136	76
Hf	9.9	0.30	0.4	1[e]
K	0.75 (%)	0.036 (cg/cm^2)	0.06 (%)	2[e]
La	63	3.2	6	4[e]
Mg	0.47 (%)	0.084 (cg/cm^2)	0.16 (%)	25
Mn	193	57	116	38
Mo	7.6	22	42	85
Na	1.3 (%)	0.32 (cg/cm^2)	0.55 (%)	11[e]
Nd	44	3.9	8	15
Ni	28	7.9	12	9[e]
Pb	66	110	212	76
Sb	0.34	9.8	20	99
Sc	13	1.7	3.0	7[e]
Se	−16	95	214	93
Si	29.6 (%)	−1.44 (cg/cm^2)	−2.8 (%)	−10
Sm	8.2	0.75	1.5	15
Sr	482	124	232	32
Tb	0.92	0.12	0.21	7[e]
Th	26	2.2	4	13
Ti	0.65 (%)	0.077 (cg/cm^2)	0.13 (%)	6[e]
U	6.8	11.1	22	76
V	65	131	262	80
W	0.25	11.6	24	100
Yb	3.5	0.36	0.7	7[e]
Zn	−7.5	262	558	101

[a] Matrix concentration. [b] Areal concentration. [c] Nonmatrix concentration. [d] Fraction (%) of element associated with nonmatrix component calculated from Equation 5 or 6. [e] Calculation from Equation 6.

and the fraction of the total concentration in the nonmatrix material (f_N). The results of this analysis indicate that Si, Al, Ti, Ca, Mg, Na, K, Ni, Sc, Hf, Th, Fe, and the rare earth elements are predominantly matrix associated ($f_N < 0.3$), while As, Cd, Ga, Mo, Pb, Sb, Se, U, V, W, and Zn are predominantly in a nonmatrix component ($f_N > 0.7$). Intermediate behavior, i.e., relatively even distribution between matrix and nonmatrix material, was observed for Ba, Be, Co, Cr, Cu, Mn, and Sr.

Acid Leaching Studies

Leaching studies were performed by weighing 0.5-g samples of fly ash into 100-mL polypropylene volumetric flasks, adding 50.0 mL of water, HCl solution, or HF solution, and shaking for 24 h at room temperature. Fifty milliliters of water was then added to the HCl solutions and a duplicate water solution to bring their volume to 100.0 mL. Fifty milliliters of saturated boric acid was added to the HF solutions and a duplicate water solution to bring their volumes to 100.0 mL. The solutions were shaken with the ash for an additional hour and then filtered through tared, acid-washed, 0.1-μm Nuclepore filters, since previous studies have demonstrated quantitative removal of fly ash particles with ≤0.2-μm pore filters, but not with ≥0.4 μm filters (*19*). The filtrate was analyzed by atomic absorption spectroscopy and instrumental neutron activation analysis as previously described (*13–15, 20*). The undissolved residue was rinsed with water and dried to a constant weight at 110 °C.

The results of the acid leaching experiments are given in Tables II and III for HCl and HF, respectively. Figures 3 and 4 illustrate the approach used to determine values of f_N from the HCl and HF leaching data. The values of f_N from the HCl solubility data were determined from the intercept of a linear least-squares fit of the percentage of element dissolved vs. the HCl molarity from 0.21 to 0.57 M HCl (see Figure 3). By extrapolation to zero HCl concentration, the data are corrected for any leaching of elements from the matrix that takes place at the higher HCl concentrations. Below an HCl concentration of 0.21 M, it is clear from the curvature of the plots that not

Table II. Percent of the Element Dissolved by Indicated Concentration of HCl

element–method	H_2O	0.029 M	0.057 M	0.086 M	0.14 M	0.21 M	0.29 M	0.43 M	0.57 M	f_N[a]
Al–AAS	0.7	12.0	16.0	18.0	20.0	21.0	22.0	23.0	27.0	17
As–INAA	1.8	6.3	43.3	71.9	101.1	100.6	99.2	100.8	91.6	98[b]
Ba–AAS	0.9	4.5	7.3	8.8	12.0	16.0	21.0	29.0	32.0	8
Be–AAS	0.0	19.0	26.0	26.0	32.0	37.0	41.0	39.0	41.0	40[b]
Ca–AAS	25.0	62.0	66.0	67.0	69.0	72.0	74.0	75.0	75.0	74[b]
Cd–AAS	35.0	46.0	43.0	52.0	65.0	50.0	54.0	52.0	59.0	54[b]
Ce–INAA	0.0	24.7	30.9	32.8	42.4	42.6	47.6	50.5	47.6	47[b]
Co–INAA	0.0	10.7	16.9	18.7	21.4	25.9	30.4	32.9	33.5	23
Cr–AAS	0.0	39.0	47.0	50.0	55.0	57.0	60.0	63.0	65.0	53
Cu–AAS	3.6	44.0	47.0	49.0	51.0	52.0	54.0	56.0	62.0	46
Dy–INAA	0.9	37.6	51.1	55.4	62.6	40.5[c]	65.1	80.1	70.0	72[b]
Eu–INAA	0.0	44.6	51.2	54.3	78.3	81.9	77.3	84.7	75.9	80[b]
Fe–AAS	0.0	3.8	14.0	18.0	22.0	26.0	28.0	30.0	32.0	23
Ga–INAA	0.0	15.8	29.9	25.5	32.8	33.6	34.5	36.9	36.5	35[b]
K–AAS	1.2	5.6	7.9	8.8	9.9	11.0	12.0	14.0	15.0	9
La–INAA	0.0	42.3	81.7	51.9	57.7	52.7	71.7	84.8	91.3	37
Mg–AAS	3.1	21.0	25.0	27.0	29.0	32.0	33.0	35.0	37.0	29
Mn–AAS	3.3	18.0	23.0	25.0	27.0	30.0	32.0	35.0	36.0	27
Mo–INAA	44.0	28.5	51.0	73.4	93.1	85.2	91.9	88.6	78.1	86[b]
Na–AAS	7.6	13.0	16.0	16.0	17.0	20.0	21.0	23.0	24.0	18
Nd–INAA	0.0	37.9	41.9	48.7	61.4	70.5	72.9	65.5[c]	72.3	70
Ni–AAS	0.0	12.0	16.0	16.0	17.0	37.0	38.0	29.0	44.0	40[b]
Pb–AAS	0.0	3.9	9.8	13.0	16.0	20.0	25.0	28.0	34.0	13
Sb–INAA	14.6	2.6	1.6	0.0	3.8	0.0	0.0	0.0	0.0	
Sc–INAA	0.0	2.7	13.9	23.6	39.9	43.9	47.1	51.8	51.0	48[b]
Se–INAA	19.9	21.3	72.4	115.1	156.1	153.6	153.9	156.1	142.3	100[d]
Si–AAS	0.2	3.1	3.5	3.7	3.9	4.0	4.1	4.2	4.3	4
Sm–INAA	0.0	29.2	35.3	37.1	47.7	46.9	49.6	52.5	48.5	49[b]
Sr–INAA	8.6	26.2	27.9	49.4	52.4	40.1	42.6	54.2	81[c]	48
Tb–INAA	0.0	30.1	32.1	30.6	42.9	41.6	48.2	49.9	50.2	47[b]
Th–INAA	0.0	0.0	2.1	10.2	28.1	27.9	32.2	57.4	59.1	8
Ti–AAS	0.0	0.0	2.1	9.4	17.0	23.0	25.0	29.0	30.0	19
U–INAA	0.0	33.6	41.0	43.0	52.0	50.7	52.7	54.3	53.1	53[b]
V–INAA	0.0	52.7	ND[e]	58.8	68.5	ND[e]	71.0	ND[e]	79.2	75[b]
W–INAA	10.7	0.0	0.0	14.0	35.3	43.7	48.7	54.9	50.0	49[b]
Yb–INAA	0.0	34.8	40.6	46.5	60.8	65.0	60.6	63.3	67.3	64[b]
Zn–AAS	49.0	50.0	88.0	70.0	78.0	74.0	79.0	66.0	91.0	78[b]
% mass dissolved	4.0	10.1	12.4	13.5	14.5	15.4	16.3	17.0	18.0	
final pH[f]	4.23	2.60	1.95	1.65	1.38	1.20	1.08	0.85	0.70	

[a] Fraction (%) of element associated with nonmatrix component. [b] f_N calculated using mean of four highest HCl concentrations. [c] Datum omitted in calculation of f_N. [d] Determined as the apparent maximum value. [e] Not detected. [f] After addition of 50 mL of H_2O to the extract solution at the indicated initial HCl concentration.

all of the surface-associated materials have dissolved. In those cases where the correlation coefficient was not significant ($p > 0.10$), the average percent element dissolved at the four highest HCl concentrations was taken as the measure of f_N.

The fraction of silicon that dissolved at each of the HF concentrations can be used to indicate the amount of matrix material which dissolved. Thus, for the HF data, the percent of an element dissolved was plotted against the percent of silicon dissolved (Figure 4). The intercept of a linear least-squares fit of the five points at the highest HF concentrations was taken as f_N for this case. As indicated in Table III, experimental difficulties (due to precipitation of silica) were encountered in the determination of the amount of Si dissolved after matrix dissolution at the two highest HF concentrations. However, because Si and K are linearly correlated ($r = 0.99$) at the lowest three values and because 98% of the K in size-classified fly ash fractions was determined to be matrix associated (Table I), the K data were used to obtain corrected values of the percent Si dissolved at the two highest points. As described for the HCl data, if the fraction of element dissolved was not significantly correlated with the fraction of Si dissolved, the average of the four data points between 0.14 and 0.43 M HF was taken as a measure of f_N.

The acid leaching curves for three elements, Sb in HCl and Ba and Pb in both HCl and HF, clearly show that the solubility is limited by an insoluble phase either present in the ash or formed during the extraction and not by association with the silicate matrix. The solubility of Sb actually decreases as the HCl concentration increases. The Ba and Pb solubilities increase with acid concentration, but there is no change in slope as observed for the other elements.

Comparison of Size Dependence with Solubility Results

In order to directly compare the results of the dissolution studies with those obtained from the analysis of the particle size dependence, regression analyses were performed. Figures 5–7 show the correlation of the results obtained for the fraction of element in the nonmatrix material by the three methods, i.e., particle size dependence of total concentrations

Table III. Percent of the Element Dissolved by Indicated Concentration of HF

element–method	satd ^{a} H_3BO_3	0.029 M	0.057 M	0.086 M	0.14 M	0.21 M	0.29 M	0.43 M	0.57 M	f_N ^{b}
Al–AAS	0.9	14.0	27.0	34.0	41.0	50.0	59.0	74.0	84.0^{c}	30
As–INAA	12.9	0.0	0.0	20.2	59.5^{c}	95.7	89.1	77.5	111.3	87^{d}
Ba–AAS	1.2	12.0	10.0	12.0	42.0	55.0	56.0	55.0	68.0	43
Be–AAS	4.9	25.0	41.0	46.0	58.0	71.0	78.0	95.0	100.0	48
Ca–AAS	25.0	35.0	26.0	73.0	80.0	86.0	88.0	96.0	103.0	77
Cd–AAS	34.0	46.0	58.0	59.0	75.0	74.0	84.0	94.0	86.0	82^{d}
Ce–INAA	0.0	1.3	2.4	9.1	46.6	71.2	68.5	69.8	111.8	41
Co–INAA	2.2	14.6	37.8	45.6	54.4	60.0	54.6	62.0	101.1	40
Cr–AAS	3.6	6.1	34.0	55.0	61.0	66.0	73.0	79.0	84.0	59
Cu–AAS	9.0	20.0	50.0	58.0	65.0	72.0	79.0	94.0	102.0	59
Dy–INAA	0.0	2.8	2.1	26.1	67.9	82.8	79.6	80.1	120.4	59
Eu–INAA	0.0	0.0	0.0	15.8	61.3	74.5	72.1	76.5	113.2	52
Fe–AAS	0.0	0.1	5.5	23.0	36.0	52.0	63.0	78.0	90.0	32
Ga–INAA	0.0	0.0	0.0	40.7	54.7	66.4	63.6	63.1	103.5	45
Hf–INAA	0.0	0.0	44.2	57.5	63.1	82.5	67.4	63.7	104.8	69^{d}
K–AAS	1.3	5.9	15.0	21.0	29.0	40.0	50.0	72.0	97.0	16
La–INAA	0.0	0.9	27.7	8.6	52.6	48.5	54.6	38.9	63.9	49^{d}
Mg–AAS	3.5	23.0	38.0	43.0	50.0	59.0	69.0	86.0	98.0	43
Mn–AAS	3.5	22.0	39.0	46.0	54.0	59.0	59.0	64.0	100.0	41
Mo–INAA	85.8	26.3	12.9	67.8	84.3	97.8	84.5	70.3	123.7	84^{d}
Na–AAS	7.8	14.0	26.0	31.0	38.0	49.0	60.0	79.0	99.0	28
Nd–INAA	0.0	0.0	0.0	0.0	64.9	113.2	84.8	80.8	134.9	86^{d}
Ni–AAS	0.0	19.0	38.0	42.0	40.0	61.0	88.0	109.0	104.0	41
Pb–AAS	0.0	0.0	1.7	2.8	20.0	57.0	75.0	94.0	97.0	26
Sb–INAA	30.9	33.4	36.8	82.5	81.4	86.3	72.5	76.4	95.5	79^{d}
Sc–INAA	0.0	28.2	54.3	58.9	66.0	78.6	70.4	69.8	106.2	71^{d}
Se–INAA	103.1	27.0	6.8	79.4	113.7	147.0	130.5	115.0	158.3	100^{e}
Si–AAS	0.3	5.4	7.0	10.0	16.0	29.0	41.0	53.0^{f}	18.0^{f}	0^{g}
Sm–INAA	0.0	0.7	0.0	11.6	52.8	69.8	65.6	66.6	102.6	46
Sr–INAA	19.5	29.8	29.1	61.2	66.7	88.2	83.0	75.8	110.4	78^{d}
Tb–INAA	0.0	0.0	0.0	0.0	55.3	80.3	82.4	63.2	110.7	70^{d}
Th–INAA	0.0	0.0	0.0	0.0	22.8	53.5	61.5	74.4	131.5	9
Ti–AAS	0.0	0.0	5.1	24.0	34.0	49.0	59.0	65.0	75.0	34
U–INAA	0.0	25.8	66.4	77.5	92.3	89.3	76.1	71.5	104.2	82^{d}
V–INAA	21.7	8.9	0.0	85.6	83.7	88.3	84.4	73.5	110.9	82^{d}
W–INAA	13.8	0.0	0.0	0.0	0.0^{c}	40.7	77.3	62.6	92.9	60^{d}
Yb–INAA	0.0	0.0	0.0	31.3	77.0	104.1	91.4	90.3	139.5	91^{d}
Zn–AAS	51.0	92.0	87.0	117.0	115.0	71.0	113.0	107.0	104.0	101^{d}
% mass dissolved	4.3	12.2	16.5	22.6	29.8	41.4	52.0	71.3^{f}	49.3^{f}	
final pH^{h}	4.93	4.80	4.10	3.25	2.60	2.25	2.00	1.75	1.60	

[a] Saturated boric acid without HF addition. [b] Fraction (%) of element associated with nonmatrix component. [c] Datum omitted in calculation of f_N. [d] f_N calculated using mean of four HF concentrations from 0.14 to 0.43. [e] Determined as apparent maximum. [f] Value low due to SiO_2 precipitation during filtration of dissolved silicate. [g] Reference zero value. [h] After addition of 50 mL of saturated H_3BO_3 to the extract solution at the indicated initial HF concentration.

compared to leaching by HCl and leaching HF. Many elements display consistent behavior in the three methods.

Regression analysis of the elemental fraction in the nonmatrix component determined by the HF method against that determined by the HCl method (omitting the Sb data) indicates a highly significant correlation ($r = 0.87, p \ll 0.001$) with a calculated slope of 0.89 in close agreement with the theoretical expectation of unity (see Figure 5). Omission of the data for Ba and Pb and for those elements displaying anomalous behavior in Figures 6 and 7, i.e., Ca, Sc, La, and the rare earth elements, results in a correlation coefficient of 0.93 ($p \ll 0.001$) and a calculated slope of 0.91.

Comparison of the results from the size-dependence method with the results of the HCl method (omitting Sb) and the HF method gave correlation coefficients of 0.40 ($p < 0.01$) for HCl and 0.51 ($p < 0.001$) for HF. The rather poor agreement results from inclusion of the data on the insoluble elements Ba and Pb and those elements (Ca, Sc, La, and the rare earths) displaying anomalous behavior. Omission of these elements results in excellent agreement of the solubility data with the size-dependence data. Specifically, correlation coefficients of 0.84 ($p \ll 0.001$) and 0.87 ($p \ll 0.001$) with slopes of 1.1 and 1.2 were obtained for comparison of the HCl and HF data, respectively, with the results of analysis by size dependence.

Discussion

In order to further evaluate the spatial distribution of elements in coal fly ash particles, differential solubility studies with HCl and HF have been performed. The results of these analyses are compared to estimates of the relative matrix and nonmatrix distributions from bulk elemental analyses of size-classified, stack-collected coal fly ash fractions.

Apparent solubility limitations were observed for Sb in HCl consistent with the formation of insoluble oxychlorides of Sb(III) (e.g., SbOCl and $Sb_4O_5Cl_2$) (*21*). The apparent insol-

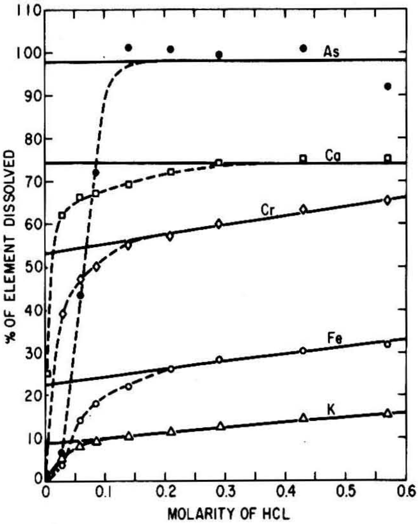

Figure 3. Percent of element dissolved vs. HCl concentration. Solid lines represent the linear least-squares fit of the last four data points for K, Fe, and Cr and are drawn through the average of the last four data points for Ca and As, elements not exhibiting a significant dependence on HCl concentration in the range considered

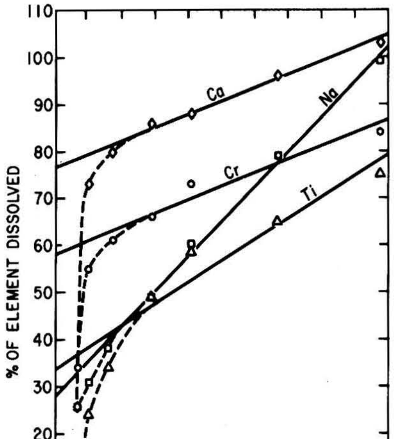

Figure 4. Percent of element dissolved vs. the percent of Si dissolved. Solid lines represent the linear least-squares fit of the last five data points

ubility of Ba is consistent with either the presence of $BaSO_4$ in the ash or its formation during dissolution. In this regard, previous analyses of water- and 0.1 M HCl-soluble sulfate indicated extractable concentrations of about 200 μmol of sulfate per g of the finest fraction of the ash (*22*). The sulfate concentration is not sufficient to limit Pb solubility, however, unless the Pb is coprecipitated with $BaSO_4$.

Anomalous behavior was observed for Ca, Sr, Sc, La, and the rare earth elements in that the HCl and HF solubility data resulted in estimates of nonmatrix components markedly greater than those derived from the size-dependent concentration data. Similarly, previous studies by other workers (*3, 6, 12*) using different ash samples indicated no dependence of the concentration of these elements on particle size. The HCl and HF solubility data can be explained if it is assumed that these elements are present in a compound that is relatively equally distributed among the size fractions but more soluble in HCl and HF than the aluminosilicate matrix. The presence of an apatite phase containing these elements has been suggested by Campbell et al. (*12*).

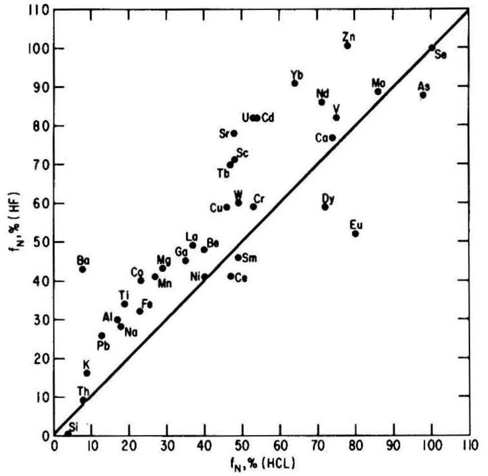

Figure 5. The fraction of an element associated with fly ash nonmatrix material calculated from HCl dissolution data, f_N(HCl), compared to the fraction calculated from HF dissolution data, f_N(HF)

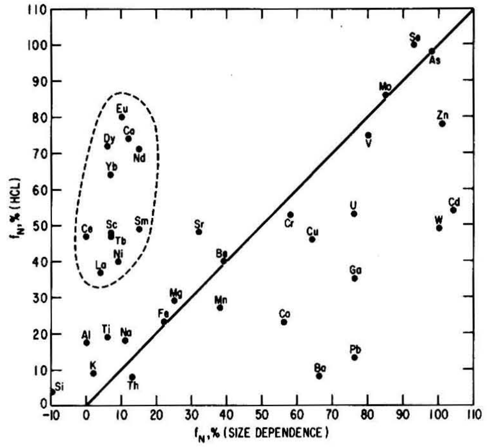

Figure 6. The fraction of an element associated with fly ash nonmatrix material calculated from HCl dissolution data, f_N(HCl), compared to the fraction calculated from particle size dependence, f_N(size dependence)

Major differences between the nonmatrix concentrations determined by the different methods remain for Ni, W, and Ga between both the HCl and HF methods and the size dependency methods (Figures 6 and 7), for Co and Cd between the HCl and the size-dependency methods (Figure 6), and for Al and Ti between the HF and size-dependency methods (Figure 7). Of these elements, Ni, Ga, and Co show a significant degree of curvature in the $6/D_V\rho$ plots, thus violating the

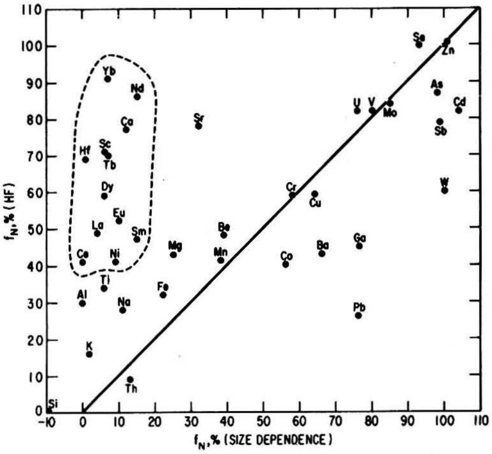

Figure 7. The fraction of an element associated with fly ash nonmatrix material calculated from HF dissolution data, f_N(HF), compared to the fraction calculated from particle size dependence, f_N(size dependence)

assumption of constant slope. It is not surprising that the values for Al and Ti, as determined by HF leaching, are high, since HF would be expected to selectively leach these elements at a higher rate than Si. The results for W show good agreement between the HCl and HF methods (Figure 5), but a large disagreement with the size dependency method (Figures 6 and 7). The behavior of W in the HF and HCl could be explained by assuming that the W is present as the oxide WO_3. Because of the insolubility of this oxide in the acid solutions used in this study (except the most concentrated HF solution (*23*)), low values would be obtained by the HF and HCl methods.

The results of the size-dependence analysis, which indicate marked matrix association for Si, K, Al, Th, Ti, Na, Ca, Sc, La, and the rare earth elements and marked nonmatrix association for V, Zn, Mo, Se, As, Cd, Pb, Sb, and W, are in agreement with previous studies of the dependence of elemental concentration on particle size. As reviewed by Fisher and Natusch (*1*), a number of investigators have presented mathematical models relating the concentrations of relatively volatile elements to geometric parameters associated with fly ash particles. Assuming a volatilization–condensation mechanism, Davison et al. (*3*) proposed a simple mathematical model for elemental concentration as a function of inverse particle size. Kaakinen et al. (*24*) presented a similar mathematical dependence based on the specific surface area (square meters per gram) of fly ash. If the specific surface area is proportional to the surface area:volume ratio and if particle sphericity is assumed, then elemental concentration is inversely proportional to particle size. Biermann and Ondov (*25*) have proposed a model with an inverse square dependence and an asymptotic maximum for concentration as a function of surface thickness. Their results indicated that the thickness of surface-deposited materials is inversely proportional to particle size and that total elemental composition is proportional to l/d^2, where l is the thickness of the surface layer and d the diameter of the particle.

Conclusions

Our unique modification of the Davison et al. (*3*) approach allowed us to calculate relative matrix and nonmatrix contributions for the $1/D$ dependence without the necessity of estimating the thickness of the surface layer as required by earlier modifications.

Good consistency for many elements has been demonstrated between two different acid-leaching methods and between either of these methods and a particle size dependent method of determining the distribution of an element within coal fly ash particles. The results show that those elements that are volatile or form volatile oxides tend to be completely nonmatrix and, hence, surface-associated, but many elements display intermediate behavior and are quantifiably distributed between the matrix and the surface of fly ash particles.

Acknowledgments

We thank David Silberman for his assistance in performing much of the experimental work and Drs. Robert Heft and John Ondov for performing the INAA analyses.

Literature Cited

(1) Fisher, G. L., Natusch, D. F. S., in "Analytical Methods for Coal and Coal Products," Vol. III, Kar, C., Ed., Academic Press, New York, 1979, pp 489–541.
(2) Smith, R. D., Campbell, J. A., Nielson, K. K., *Atmos. Environ.*, **13,** 607 (1979).
(3) Davison, R. L., Natusch, D. F. S., Wallace, J. R., *Environ. Sci. Technol.*, **8,** 1107 (1974).
(4) Linton, R. W., Williams, P., Evans, C. A., Jr., Natusch, D. F. S., *Anal. Chem.*, **49,** 1514 (1977).
(5) Linton, R. W., Lok, A., Natusch, D. F. S., Evans, C. A., Jr., Williams, P., *Science,* **191,** 852 (1976).
(6) Natusch, D. F. S., Bauer, C. F., Matusiewicz, H., Evans, C. A., Baker, J., Lok, A., Linton, R. W., in "International Conference on Heavy Metals in the Environment," Toronto, Canada, Oct. 27–31, 1975, pp. 553–76.
(7) Theis, T. L., Wirth, J. L., *Environ. Sci. Technol.*, **11,** 1096 (1977).
(8) James, W. D., Janghorbani, M., Baxter, T., *Anal. Chem.*, **49,** 1994 (1977).
(9) Green, J. B., Manahan, S. E., *Anal. Chem.*, **50,** 1975 (1978).
(10) Pawley, J. B., Fisher, G. L., *J. Micros,* **110,** 87 (1977).
(11) Huges, T. L., Pawley, J. B., Fisher, G. L., in "Scanning Electron Microscopy," Vol. I, Johari, D., Ed., SEM, Inc., O'Hare, Ill., 1978, pp 239–44.
(12) Campbell, J. A., Laul, J. C., Nielson, K. K., Smith, R. D., *Anal. Chem.*, **50,** 1032 (1978).
(13) Coles, D. G., Ragaini, R. C., Ondov, J. M., Fisher, G. L., Silberman, D., Prentice, B. A., *Environ. Sci. Technol.* **13,** 455 (1979).
(14) Fisher, G. L., Prentice, B. A., Silberman, D., Ondov, J. M., Ragaini, R. C., Biermann, A. H., McFarland, A. R., Pawley, J. B., in Proceedings of the Division of Fuel Chemistry Symposium on Properties of Coal Ash, 2nd Joint Chemical Institute of Canada/American Chemical Society Meeting, Montreal, Canada, May, 1977 (available from G. L. Fisher).
(15) Silberman, D., Fisher, G. L., *Anal. Chim. Acta,* **106,** 299 (1979).
(16) McFarland, A. R., Bertch, R. W., Fisher, G. L., Prentice, B. A., *Environ. Sci. Technol.*, **11,** 781 (1977).
(17) Raabe, O. G., *J. Aerosol Sci.*, **2,** 289 (1971).
(18) Fisher, G. L., Prentice, B. A., Silberman, D., Ondov, J. M., Biermann, A. H., Ragaini, R. C., McFarland, A. R., *Environ. Sci. Technol.*, **12,** 447 (1978).
(19) Fisher, G. L., Silberman, D., Prentice, B. A., Heft, R. E., Ondov, J. M., *Environ. Sci. Technol.* **13,** 689 (1979)
(20) Ondov, J. H., Ragaini, R. C., Heft, R. E., Fisher, G. L., Silberman, D., Prentice, B. A., *Natl. Bur. Stand. Spec. Publ.* **No. 464,** 565–71 (1977).
(21) Cotton, F. A., Wilkinson, G., "Advanced Inorganic Chemistry", Interscience, New York, 1972, p. 376.
(22) Hansen, L. D., Eatough, D. J., Fisher, G. L., in "Proceedings of a Symposium on Characterization of Coal Combustion Products at the Electrochemical Society, Inc. Meeting", Boston, Mass. May 6–11, 1979, Paper No. 229.
(23) Latimer, W. M., Hildebrand, J. H., "Reference Book of Inorganic Chemistry", 3rd ed., MacMillan, New York, 1965, p 383.
(24) Kaakinen, J. W., Jorden, R. M., Lawasani, M. H., West, R. E., *Environ. Sci. Technol.*, **9,** 862 (1975).
(25) Biermann, A. H., Ondov, J. M., *Atmos. Environ.*, **14,** 289 (1980).

Received for review December 14, 1979. Accepted May 12, 1980. This work was supported by the U.S. Department of Energy. L.D.H. thanks the Associated Western Universities for a fellowship in support of this work.

Sulfate in Diesel Exhaust

Timothy J. Truex, William R. Pierson*, and Douglas E. McKee[1]
Engineering and Research Staff, Research, Ford Motor Company, Dearborn, Mich. 48121

■ A study of sulfate emissions from diesel-powered light-duty vehicles has been conducted. The applicability of a controlled-condensation sampling procedure for determining the chemical speciation of vehicle sulfate emissions has been demonstrated and used to determine that sulfuric acid is the major sulfate species present in diesel exhaust. Diesel sulfate emissions were found not to be proportional to fuel sulfur level, the percent S → SO_4^{2-} conversion increasing as fuel sulfur level decreases. An Opel diesel vehicle was equipped with an experimental oxidation catalyst to determine the effect on diesel sulfate emissions.

Diesel fuel contains on the average 0.2 wt % sulfur (*1*), or almost an order of magnitude more than gasoline (*2*). About 2% of the fuel sulfur burned in diesel engines is emitted as sulfate (SO_4^{2-}) (*3–14*), more or less independently of engine type or operating mode. SO_4^{2-} usually comprises several percent, by mass, of the total airborne exhaust particulate matter (*3, 5, 8, 10–14*) from a diesel system.

The approximate 2% S → SO_4^{2-} conversion in diesels is higher than is observed in noncatalyst spark-ignition vehicles (*14–19*) and less than in oxidation-catalyst-equipped spark-ignition systems (*3, 4, 6, 9, 13*). Because of the amount of sulfur in diesel fuel, however, the SO_4^{2-} emission rate from a diesel system is comparable to that from an oxidation-catalyst-equipped spark-ignition system. Nationwide, diesels log ~5% of the total vehicle miles (*20*) and, judging from recent roadway results (*14*), should be responsible for about one third of the SO_4^{2-} produced by vehicles.

The SO_4^{2-} generated by oxidation-catalyst-equipped spark-ignition systems is known to be sulfuric acid (H_2SO_4) (*4, 15–19*), and the mechanism of SO_4^{2-} formation in these systems is now well understood (*19*). In contrast, the chemical speciation of diesel SO_4^{2-} has not been previously determined, nor is much known about its formation mechanism. This paper describes our experiments to determine the chemical form of diesel SO_4^{2-} and the effect of diesel fuel sulfur level on SO_4^{2-} emission levels. In addition, results are presented on the effect of an oxidation catalyst on diesel SO_4^{2-} emissions.

Experimental Methods

General. The vehicle measurements were made with a dilution tube, into which exhaust was injected from a vehicle running on a chassis dynamometer. The dilution tube/dynamometer system has been described in detail previously (*21*). All experiments were run at a dilution tube flow rate of 17 m^3/min (600 cfm).

Diesel SO_4^{2-} Speciation Experiments. The usual method for vehicle SO_4^{2-} determination involves Teflon membrane or quartz fiber filter collection of vehicle particulate matter, while sampling from a dilution tube, followed by SO_4^{2-} analysis of the water extract from the particulate matter. Although this method has been used successfully to determine SO_4^{2-} emissions from both gasoline- and diesel-powered vehicles, it does not provide information about SO_4^{2-} speciation in the vehicle exhaust, specifically the ratio of H_2SO_4 to other soluble SO_4^{2-} salts. A modification of the controlled condensation procedure, which has been extensively used for the determination of H_2SO_4 in flue gases (*22–24*), can be used to separate the contribution of H_2SO_4 from other soluble SO_4^{2-} salts in vehicle SO_4^{2-} emission studies. In this system, the diluted exhaust gases are heated above the dew point of sulfuric acid and passed through a filter that removes nonvolatile SO_4^{2-} salts and other particulate matter. The H_2SO_4 vapor is selectively condensed in a Goksøyr–Ross coil, which is located behind the heated filter.

The sampling systems used for the SO_4^{2-} speciation experiments are shown schematically in Figure 1. The standard SO_4^{2-} sampling system, shown at the top of Figure 1, includes a Teflon probe, which is connected to a stainless steel holder for 142-mm diameter filters; the sample is pulled through the filter by a bellows-type pump and the sample volume is determined with a dry gas meter on the pump outlet. A 3% hydrogen peroxide (H_2O_2) impinger, with a 47-mm filter upstream to remove particulate matter, comprises the sulfur dioxide (SO_2) sampling system.

The controlled condensation sampling apparatus for SO_4^{2-} speciation (bottom of Figure 1) consists of a stainless steel sampling probe followed by a prefilter for removing particulate matter and nonvolatile SO_4^{2-} salts, a Goksøyr–Ross (*22, 23*) condensation coil for collection of H_2SO_4, and a 3% H_2O_2 impinger for SO_2 collection. A bellows-type pump is used to pull samples through the system and a dry gas meter is used to measure sample volume. The sampling probe and prefilter are heated with a heating tape and resistance heater, respectively.

The procedure for conducting the sulfate speciation experiments involved first heating the controlled condensation sampling probe, prefilter, and Goksøyr–Ross coil to the desired temperatures. The Goksøyr–Ross coil was maintained at ~65 °C during all experiments to allow H_2SO_4 condensation in the coil but prevent water condensation; the effect of probe and prefilter temperature on the speciation experiments is discussed under Results. Sampling was conducted simultaneously in the controlled condensation and standard SO_4^{2-} and SO_2 sampling systems. At the end of the experiment the filters, hydrogen peroxide solutions, and deionized water rinses of the Goksøyr–Ross coil and sampling probe were analyzed for SO_4^{2-} (see below). Unstrengthened quartz-fiber filters were used in all experiments, and isokinetic sampling conditions were employed.

In two experiments samples were collected in the controlled condensation sampling system with the sampling probe and prefilter *unheated.* (In this arrangement all SO_4^{2-}, including H_2SO_4, is in the condensed phase and is collected by the prefilter.) At the end of sampling, the prefilter was disconnected from the sampling probe. Dry air was then pulled through the filter while it was heated to ~350 °C (200 °C air temperature) to desorb H_2SO_4, and the desorbed H_2SO_4 was collected in the Goksøyr–Ross coil. The prefilter and deionized water rinse of the Goksøyr–Ross coil were then analyzed for SO_4^{2-}. The purpose of these desorption experiments was to learn whether or not the emitted H_2SO_4 is neutralized by, or otherwise reacts with, the particulate matter or the filter surface during collection.

Four vehicles were used in the sulfate speciation studies: a 1977 6.6-L (400 CID) Ford LTD equipped with conventional oxidation catalysts and air pump, operating on Indolene Clear gasoline with di-*tert*-butyl disulfide added to increase the

---

[1] Present address, Department of Obstetrics and Gynecology, University of New Mexico School of Medicine, Albuquerque, N.Mex. 87131.

0013-936X/80/0914-1118$01.00/0

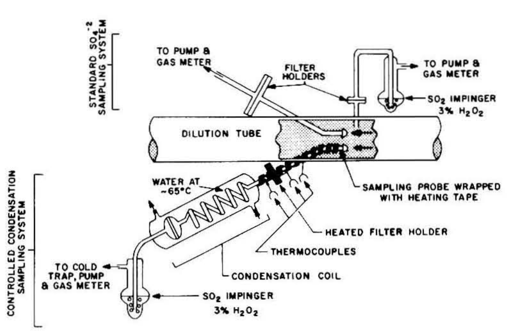

Figure 1. Schematic of the dilution tube SO_4^{2-} sampling systems

sulfur content to 0.03 wt %; a 1974 Mercedes 240 Diesel; a 1978 Oldsmobile 350 Diesel; and a 1978 Mercedes 300 Diesel. The diesel vehicles were operated on no. 2 diesel fuel that had a sulfur content of 0.315 wt %. All tests were conducted with the vehicles operating at 80 kph (50 mph).

Diesel Fuel Sulfur Level Experiments. The effect of fuel sulfur level on diesel SO_4^{2-} emissions was determined with the 1974 Mercedes 240 Diesel operating on specially blended no. 2 diesel fuel that had been doped with di-*tert*-butyl disulfide to three different fuel sulfur levels: 0.009, 0.110, and 0.190 wt % S. The SO_4^{2-} emission rates were determined at each fuel sulfur level after the vehicle had been preconditioned with the specified fuel by operation with that fuel for 1 h at 80-kph (50 mph) cruise. SO_4^{2-} emission rates were determined while the vehicle operated over the 1974 FTP (Federal Test Procedure)-hot start driving cycle, with SO_4^{2-} sampling being conducted from the dilution tube using the standard 142-mm quartz fiber filter system. SO_2 was not sampled.

Effect of Catalysts on Diesel SO_4^{2-} Emissions. An experimental noble-metal oxidation catalyst, fitted with thermocouples to monitor catalyst temperature, was installed immediately behind the exhaust manifold of a 2.1-L Opel diesel engine. Gaseous and SO_4^{2-} emissions were determined while the vehicle operated over the congested freeway driving schedule (CFDS). In another experiment, in an attempt to maximize SO_4^{2-} emissions, the exhaust manifold and catalyst were insulated with asbestos tape, and the vehicle was tested while operating at 88 kph (55 mph). Base-line tests without the catalyst installed were performed in each case. The vehicle was operated on no. 2 diesel fuel which contained 0.20 wt % S.

SO_4^{2-} Analyses. Filter samples were leached in water on either a steam bath or ultrasonically. The leaching was done in the presence of a cation exchange resin to remove potentially interfering ions. The SO_4^{2-} in the Goksøyr–Ross coil and impingers (SO_2 is oxidized to SO_4^{2-} in the 3% H_2O_2 impinger solution) was removed by rinsing with deionized water. SO_4^{2-} was determined by barium perchlorate titration to the Thorin dye indicator end point (*25, 26*) with photometric end-point detection (*27*).

Results and Discussion

Diesel SO_4^{2-} Speciation Experiments. Several experiments to validate the controlled condensation sampling system were performed using the gasoline engine 1977 Ford equipped with conventional oxidation catalysts (COC). The initial experiment involved measuring the SO_4^{2-} emission rate from the COC-equipped vehicle simultaneously with the standard 142-mm filter system and the unheated controlled condensation system. The results are shown as run 1 in Table I and indicate that the two sampling systems give equivalent SO_4^{2-} emission results. Runs 2–4 (Table I) show the effects of probe, prefilter, and exhaust gas sample (measured between the prefilter and condensation coil) temperatures on measured SO_4^{2-} emission rate and percent of total soluble SO_4^{2-} found in the condensation coil as H_2SO_4. The dew point of H_2SO_4 in the diluted exhaust should be ~120 °C (*23*). In order to assure that all the H_2SO_4 in the diluted exhaust enters the controlled condensation sampling system as a vapor, the sampling probe and prefilter holder were maintained at temperatures that assured that the exhaust gas entering the condensation coil was ≥170 °C. In run 2 the sample probe was maintained at ~200 °C and a significant amount of SO_4^{2-} was found on the inside of the probe walls. Since it was felt that this may result from interaction of H_2SO_4 vapor with the stainless steel sample probe, subsequent runs 3 and 4 were made with much lower probe temperatures and resulted in significant reductions in losses of SO_4^{2-} to the probe surfaces. SO_4^{2-} analyses of probe rinses from the Teflon probe used in the standard SO_4^{2-} sampling system indicate minimal SO_4^{2-} loss on the Teflon surface. All experiments with the diesel vehicles, described below, were run under the conditions of run 4 of Table I. The results from runs 2–4 (Table I) show that the controlled condensation sampling system can be used to distinguish between total soluble SO_4^{2-} and H_2SO_4 in vehicle exhaust, and that SO_4^{2-} emissions from oxidation-catalyst-equipped gasoline-powered vehicles are H_2SO_4 as is already known (*4, 15–19*). The total SO_4^{2-} found in the controlled condensation sampling system generally amounted to 80–90% of that found in the standard sampling system (Table I). Possibly the missing 10–20% results from interaction of H_2SO_4 vapor with the heated stainless steel filter holder. Use of a quartz or Vycor filter holder perhaps could have eliminated this problem, but it was felt that the resulting system would be too fragile for this experimental application.

Results of the diesel sulfate speciation experiments are presented in Table II. $SO_2 \rightarrow SO_4^{2-}$ conversions range between 1.2 and 1.6% for the three vehicles tested and are comparable to results reported by other workers (*3–14*). In all cases

Table I. Results of Validation Experiments on Controlled Condensation Sulfate Sampling System; 1977 Ford Gasoline-Powered, COC-Equipped Vehicle at 80 kph (50 mph) Cruise [a]

				standard 142-mm filter SO_4^{2-} sampling system		controlled condensation sampling system, mg/km			
run no.	probe [b] temp, °C	filter [b] temp, °C	exhaust [c] gas sample temp, °C	% $SO_2 \rightarrow SO_4^{2-}$ conv	total SO_4^{2-} emission rate, mg/km	SO_4^{2-} on prefilter	H_2SO_4 in cond. coil	SO_4^{2-} [d] in probe rinse	% H_2SO_4 [e] in total SO_4^{2-}
1	room temp	room temp	room temp	33	30.1	27.7	-	1.0	-
2	200	240	190	32	29.2	1.3	20.4	4.3	94
3	80	300	170	30	23.6	1.8	16.3	1.3	90
4	70	370	200	33	28.5	0.7	22.1	0.6	97

[a] All emission results normalized to 0.03 wt % S in fuel. [b] Temperatures measured with thermocouples attached to the exterior of the probe and filter holder. [c] Exhaust gas sample temperature measured with a thermocouple inserted in gas sample stream between heated filter and condensation coil. [d] Probe rinsed with distilled H_2O at end of experiment and analyzed for SO_4^{2-}. [e] [(SO_4^{2-} in cond. coil)/(SO_4^{2-} in cond. coil + SO_4^{2-} on prefilter)] × 100.

Table II. Diesel SO_4^{2-} Speciation Results at 80 kph (50 mph) [a]

vehicle	standard 142-mm filter SO_4^{2-} sampling system: % $SO_2 \rightarrow SO_4^{2-}$ conv.	standard 142-mm filter SO_4^{2-} sampling system: total SO_4^{2-} emission rate, mg/km	controlled condensation sampling system, mg/km: SO_4^{2-} on prefilter	controlled condensation sampling system, mg/km: H_2SO_4 in cond. coil	% H_2SO_4 [b] in total SO_4^{2-}
1974 Mercedes 240D	1.4	4.5	1.2	2.2	64
1974 Mercedes 240D [c]	1.6	4.8	0.3	5.4	95
1978 Oldsmobile 350D	1.4	4.3	0.8	3.8	82
1978 Oldsmobile 350D [c]	1.2	4.1	0.3	3.4	92
1978 Mercedes 300D	1.5	4.8	0.2	2.9	92

[a] All emission results normalized to 0.20 wt % S in fuel. [b] [(SO_4^{2-} in cond. coil)/(SO_4^{2-} in cond. coil + SO_4^{2-} on prefilter)] × 100. [c] Desorption experiment.

most of the SO_4^{2-} was found in the condensation coil in the form of H_2SO_4, three of the five experiments indicating >90% of the total soluble SO_4^{2-} in diesel exhaust is H_2SO_4. The results of the two desorption experiments, performed to determine if H_2SO_4 is neutralized or reacts with the particulate or filter surface during collection, are included in Table II. The results show not only that H_2SO_4 is the major SO_4^{2-} species present in diesel exhaust but also that there is little, if any, neutralization or other reaction between H_2SO_4 and the filter or particulate deposits.

Effect of Fuel Sulfur Level on Diesel SO_4^{2-} Emissions. Table III presents results on the effect of fuel sulfur level on diesel SO_4^{2-} emissions. The changes in the fuel sulfur level had a minimal effect on total particulate mass emissions, as would be expected since SO_4^{2-} represents only several percent of the total particulate.

Whereas the SO_4^{2-} emission rate in general increased with increasing fuel sulfur level, the increase was not proportional to the fuel sulfur level. The percent $S \rightarrow SO_4^{2-}$ conversion decreases with increasing fuel sulfur level.

Although there are no previous reports in the literature of the effect of fuel sulfur level alone on diesel SO_4^{2-} emissions, there are several reports of SO_4^{2-} emission levels as a function of different fuels that contained differing sulfur levels (*5, 10, 28*). Although the authors of these reports interpret their results as indicating that the SO_4^{2-} emission rates are proportional to fuel sulfur levels, in every case plots of SO_4^{2-} emission rate vs. fuel sulfur level give positive intercepts. The results appear to support those presented here in that percent $S \rightarrow SO_4^{2-}$ conversion decreases with increasing fuel sulfur level. These results indicate that diesel SO_4^{2-} formation is not controlled by thermodynamic equilibrium, but must be kinetically limited. The mechanism of SO_4^{2-} formation in diesel engines still remains unknown, but the behavior just described would be consistent with oxidation of SO_2 on the surface of carbonaceous diesel particulate. Such a mechanism would explain the absence of SO_4^{2-} formation in noncatalyst gasoline engine systems.

The rapid and extensive SO_2 oxidation to SO_4^{2-} previously reported (*29, 30*) on laboratory-generated combustion carbonaceous particles is not observed in diesel exhaust. A recent laboratory measurement (*31*), contrary to these earlier claims of extensive SO_2 oxidation on carbonaceous particulate, shows only modest SO_4^{2-} formation amounting to several weight percent SO_4^{2-} in the carbonaceous particulate.

Table III. Effect of Fuel Sulfur Level on Diesel Sulfate Emissions; Mercedes 240D Operating on 1974 FTP-Hot Start Cycle

fuel S, [a] wt %	total particulate mass emission rate (*M*), mg/km	SO_4^{2-} emission rate, mg/km	$S \rightarrow SO_4^{2-}$ conversion, [b] %	SO_4^{2-}/M, [c] %
0.009	399	2.2	8.6	0.6
0.110	385	5.8	1.8	1.5
0.190	362	4.7	0.96	1.3

[a] No. 2 diesel fuel; di-*tert*-butyl disulfide was added to obtain the 0.110 and 0.190 wt % sulfur levels. [b] Percent of fuel sulfur emitted as sulfate. [c] Sulfate as a percent of total particulate mass.

Effect of Oxidation Catalysts on Diesel SO_4^{2-} Emissions. One recent concern with diesel SO_4^{2-} emissions is that attempts to use oxidation catalysts to reduce hydrocarbon and particulate emissions of diesels may result in high SO_4^{2-} emissions due to the high sulfur content of diesel fuel. Several experiments were conducted with a 2.1-L Opel diesel vehicle equipped with an experimental noble-metal oxidation catalyst. On the congested freeway driving schedule (CFDS), installation of the catalyst reduced the hydrocarbon and carbon monoxide emissions by about 75% and increased the SO_4^{2-} emissions from 2.4 to 3.6 mg/km with the catalyst in place. In tests where the exhaust system was insulated to increase heat retention and catalyst efficiency, an approximate 60% reduction in hydrocarbon and carbon monoxide was observed while the vehicle was operating at 88 kph with the catalyst installed, whereas the SO_4^{2-} emissions were the same with and without the catalyst—5 mg/km. Although there was an increase in SO_4^{2-} emission rate in the CFDS test, it is not nearly as large as one would expect if there were significant catalytic SO_2 oxidation activity. The maximum catalyst temperature achieved during the CFDS was 420 °C, with an average of 208 °C; 245 °C was the catalyst temperature during the 88-kph cruise. Previous work (*18, 32*) on SO_2 oxidation over automotive catalysts has shown that the reaction is kinetically controlled in this temperature range with negligible oxidation below ~400 °C. Thus, although the diesel exhaust temperatures observed in these experiments were high enough to result in hydrocarbon and carbon monoxide oxidation, they are not high enough to cause significant oxidation of SO_2. It must be pointed out that systems with more active catalysts and/or higher exhaust temperatures can result in large increases in sulfate emissions, as has been reported elsewhere (*33*). In addition, the present study does not address the overall feasibility of using oxidation catalysts to reduce hydrocarbon and particulate emissions in diesel exhaust. Catalyst plugging and deactivation due to caking may result in oxidation catalysts not being suitable for treatment of diesel exhaust and will have to be investigated.

Conclusions

The results presented in this diesel sulfate emission study lead to the following conclusions.

- The controlled-condensation sampling procedure can be used to determine the chemical speciation of vehicle SO_4^{2-} emissions.
- H_2SO_4 is the major soluble SO_4^{2-} species present in diesel exhaust.
- Diesel SO_4^{2-} emissions are not proportional to fuel sulfur level; the percent $S \rightarrow SO_4^{2-}$ conversion increases as fuel sulfur level decreases.

- Little or no increase in SO_4^{2-} emissions occurred when an Opel diesel vehicle was equipped with an oxidation catalyst. This is consistent with the low exhaust gas temperatures and already existing knowledge of the temperature dependence of SO_2 oxidation rate over automotive catalysts. (The overall feasibility of catalytic treatment of diesel exhaust has not been addressed.)

Acknowledgments

The authors wish to thank F. C. Ferris for technical assistance and the Chemical Analysis Laboratory of the Ford Research Staff for performing the SO_4^{2-} analyses.

Literature Cited

(1) Shelton, E. M. "Diesel Fuel Oils, 1977", Petroleum Products Survey BERC/PPS-77/5, U.S. Energy Research and Development Administration, Bartlesville Energy Research Center, Nov 1977, and previous publications of the same series.
(2) Shelton, E. M. "Motor Gasolines, Summer 1977", Petroleum Products Survey BERC/PPS-78/1, Jan 1978, and previous publications of the same series.
(3) Begeman, C. R.; Jackson, M. W.; Nebel, G. J. *SAE Tech. Pap.* **1974**, *741060*.
(4) Bradow, R. L.; Moran, J. B. *SAE Tech. Pap.* **1975**, *750090; SAE Trans.* **1975**, *84*, 451.
(5) Braddock, J. N.; Bradow, R. L. *SAE Tech. Pap.* **1975**, *750682; SAE Trans.* **1975**, *84*, 1603.
(6) Holt, E. L.; Bachman, K. C.; Leppard, W. R.; Wigg, E. E.; Somers, J. H. *SAE Tech. Pap.* **1975**, *750683; SAE Trans.* **1975**, *84*, 1620.
(7) Ingalls, M. N.; Springer, K. J. "Measurement of Sulfate and Sulfur Dioxide in Automotive Exhaust", EPA-460/3-76-015, Southwest Research Institute, Aug 1976.
(8) General Motors "Advanced Emission Control System Development Progress", annual status report submitted to EPA, Dec 16, 1976.
(9) Somers, J. H.; Garbe, R. J.; Lawrence, R. D.; Baines, T. M. *SAE Tech. Pap.* **1977**, *770166*.
(10) Braddock, J. N.; Gabele, P. A. *SAE Tech. Pap.* **1977**, *770168*.
(11) Springer, K. J.; Stahman, R. C. *SAE Tech. Pap.* **1977**, *770254*.
(12) Springer, K. J.; Stahman, R. C. *SAE Tech. Pap.* **1977**, *770258*.
(13) Springer, K. J.; Baines, T. M. *SAE Tech. Pap.* **1977**, *770818*.
(14) Pierson, W. R.; Brachaczek, W. W.; Hammerle, R. H.; McKee, D. E.; Butler, J. W. *J. Air Pollut. Control Assoc.* **1978**, *28*, 123.
(15) Pierson, W. R.; Hammerle, R. H.; Kummer, J. T. *SAE Tech. Pap.* **1974**, *740287; SAE Trans.* **1974**, *83*, 1233.
(16) Trayser, D. A.; Blosser, E. R.; Creswick, F. A.; Pierson, W. R. *SAE Tech. Pap.* **1975**, *750091; SAE Trans.* **1975**, *84*, 462.
(17) Creswick, F. A.; Blosser, E. R.; Trayser, D. A.; Foster, J. F. *SAE Tech. Pap.* **1975**, *750411*.
(18) Griffing, M. E.; Gilbert, L. F.; Ter Haar, G. L.; Immethun, P. A.; Zutaut, D. W. *SAE Tech. Pap.* **1975**, *750697; SAE Trans.* **1975**, *84*, 1715.
(19) Pierson, W. R. *Chem. Tech.* **1976**, *6*, 332.
(20) Motor Vehicle Manufacturers' Association, "Motor Vehicle Facts & Figures '76", tables on pp 32, 68.
(21) McKee, D. E. *SAE Tech. Pap.* **1977**, *770167*.
(22) Goksøyr, H.; Ross, K. *J. Inst. Fuel* **1962**, *35*, 177.
(23) Lisle, E. S.; Sensenbaugh, J. D. *Combustion* **1965**, *36*, 12.
(24) Maddalone, R. F.; Newton, S. F.; Rhudy, R. G.; Statnick, R. M. *J. Air Pollut. Control. Assoc.* **1979**, *29*, 626.
(25) Fritz, J. S.; Yamamura, S. S. *Anal. Chem.* **1955**, *27*, 1461.
(26) Fielder, R. S.; Morgan, C. H. *Anal. Chim. Acta* **1960**, *23*, 538.
(27) Butler, J. W.; Locke, D. N. *J. Environ. Sci. Health–Environ. Sci. Eng. Ser. A* **1976**, *11*(1), 79.
(28) Hare, C. T.; Baines, T. M. *SAE Tech. Pap.* **1979**, *790424*.
(29) Novakov, T.; Chang, S.-G.; Harker, A. B. *Science* **1974**, *186*, 259.
(30) Barbaray, B.; Contour, J. P.; Mouvier, G. *Atmos. Environ.* **1977**, *11*, 351.
(31) Appel, B. R. Discussion in Proceedings of the NSF/LBL Conference on Carbonaceous Particles in the Atmosphere, Berkeley, Calif., March 20–22, 1978; June 1979, Lawrence Berkeley Laboratory Report LBL-9037 (Novakov, T., Ed.) p 163.
(32) Truex, T. J.; Hammerle, R. H.; Mikkor, M. *Ind. Eng. Chem., Prod. Res. Dev.* **1977**, *16*, 217.
(33) Marshall, W. F.; Seizinger, D. E.; Freedman, R. W. *U.S. Bur. Mines Tech. Prog. Rep.* **1978**, *105*.

Received for review January 23, 1980. Accepted May 12, 1980.

Effects of Barium Fuel Additive and Fuel Sulfur Level on Diesel Particulate Emissions

Timothy J. Truex, William R. Pierson*, Douglas E. McKee,[1] Mordecai Shelef, and Richard E. Baker
Engineering and Research Staff, Research, Ford Motor Company, Dearborn, Mich. 48121

A number of workers have investigated the effect of barium (Ba) fuel additives on carbonaceous particulate (soot) emissions. Barium has been shown to be the most effective of 40 metals tested in reducing carbonaceous particulate emissions from a propane/oxygen diffusion flame (*1, 2*). Various investigators have reported 20–75% reductions in visible smoke emissions (measured with the Hartridge or Bosch smokemeters) from diesel exhaust using Ba fuel additives (*3–6*). Literature reports on the effect of Ba additives on total mass particulate emissions of diesel systems have been conflicting. Several investigators report a general reduction in total mass particulate emissions with the use of a Ba additive (*6–8*), although the efficiency is dependent upon engine speed and load. Engine speed was the most important parameter, with the Ba additive having little or no effect on total mass particulate emissions at intermediate speeds (1800 to 2000 rpm), but resulting in 15–55% reductions in particulate emissions at higher or lower speeds (*6, 8*). In contrast, recent tests with a barium/calcium additive in two different diesel engines indicated that the total particulate mass emission rate actually increased when the additive was used (*9*). Smokemeter readings were reduced by approximately 50% with the use of the Ba/Ca additive (*9*).

Limited results on the effect of Ba fuel additives on the chemical composition of diesel particulate emissions and the form of the emitted Ba indicate that 85 to 95% of the consumed Ba is emitted as particulate in the exhaust (*5, 9*), chiefly (>75%) as insoluble species (*4–7*), identified (*4*) as $BaSO_4$. Some work (*10*), however, indicates as much as 80% of the emitted Ba is soluble in 0.1 N HCl, at least at high additive levels (*7*); the inference is drawn (*10*) that the Ba is *not* chiefly $BaSO_4$. The ratio between insoluble $BaSO_4$ and Ba compounds soluble in 0.1 N HCl (said (*4*) to be mostly $BaCO_3$) in the exhaust particulate is reported to increase with increasing fuel sulfur level (*6*) and to decline with increasing Ba content in the fuel (*6, 7*). Elemental analyses of diesel particulate generated with and without the use of a Ba/Ca fuel additive (*9*) show (a) that the additive increases the sulfur content and decreases the carbon and hydrogen content of the diesel particulate in comparison to levels found without the additive; and (b) that the emitted SO_4^{2-} tends to be ap-

---

[1] Present address, Department of Obstetrics and Gynecology, University of New Mexico School of Medicine, Albuquerque, N. Mex. 87131.

■ The effects of a barium fuel additive and of fuel sulfur level on diesel particulate emissions have been investigated. The Ba fuel additive results in a 30–40% decrease in exhaust opacity as measured by a smokemeter. The opacity reduction does not result from a reduction in total particulate mass emission rate, which is relatively unaffected by the Ba additive. There is, however, an ~30% reduction in the mass emission rate of carbonaceous material. More than 90% of the Ba introduced with the fuel can be accounted for in the vehicle exhaust. In the presence of the Ba additive, the amount of emitted SO_4^{2-} is approximately equimolar with the Ba, and electron spectroscopy shows that both the Ba and the SO_4^{2-} are wholly in the form of $BaSO_4$—provided that the amount of sulfur in the fuel is sufficient to react with all of the Ba. This $BaSO_4$ represents a substantial increase in diesel particulate SO_4^{2-} emission rate compared to that observed without the Ba additive. The level of fuel sulfur does not have a significant effect on total particulate mass emission rate. In the absence of the Ba additive, the diesel SO_4^{2-} emission rate is related to fuel sulfur level, but not linearly; the percent of sulfur converted to sulfate decreases as the fuel sulfur level is increased.

proximately stoichiometric with the sum of the Ba + Ca whenever there is enough fuel sulfur.

In this paper we present results on the effect of a Ba fuel additive on particulate mass emission rate and particulate chemical composition using a passenger car. The effect of fuel sulfur level on total particulate and sulfate emissions has been investigated as well.

Experimental Methods

A 1974 Mercedes 240D diesel-powered passenger car was used for all testing. The fuel used was a specially blended low-sulfur no. 2 diesel fuel. The base stock, which contained 0.0087 wt % S, was doped with di-*tert*-butyl disulfide to two additional fuel sulfur levels: 0.110 and 0.190 wt % S. Each fuel sulfur level was tested with and without the additive manufacturer's recommended level of 0.25 vol % of Lubrizol 556 (which, by fuel analysis, gave 0.058 wt % Ba in the fuel) to give the following six fuel sulfur/barium additive combinations:

fuel S level, wt %	**fuel Ba level, wt %**
0.0087	0.0
0.0087	0.058
0.110	0.0
0.110	0.058
0.190	0.0
0.190	0.058

All measurements were made using the chassis dynamometer/dilution tube system previously described (*11, 12*). The dilution tube flow rate was approximately 17 m^3/min (600 cfm) for all experiments. Particulate samples were collected under isokinetic sampling conditions on 20 × 25 cm quartz fiber filters. Vehicle preconditioning for each experiment consisted of 1-h driving at 80 km/h followed by an overnight soak. Testing with each fuel included a 1974 FTP-cold start followed by two 1974 FTP-hot start tests. For the cold start and the first hot start test, the vehicle exhaust was passed through a Celesco Model 107 smokemeter for measurement of opacity prior to injection into the dilution tube. During the second hot start, the exhaust was injected directly into the dilution tube.

Total mass particulate emissions were determined by filter weighing at constant temperature and humidity. Barium analyses were done by inductively coupled argon plasma atomic emission spectroscopy after leaching the samples in HCl/HNO_3. Sulfate (SO_4^{2-}) analyses of samples not containing Ba were done by $Ba(ClO_4)_2$ titrimetry and ion chromatography of water-leached samples. The SO_4^{2-} in the Ba-containing samples, where incomplete leaching of SO_4^{2-} precluded SO_4^{2-} analysis by titrimetry or ion chromatography, was determined by combustion analyses for total sulfur. Carbon (C), hydrogen (H), and nitrogen (N) analyses were performed by Spang Microanalytical Laboratories, Eagle Harbor, Mich.

Results and Discussion

The effects of fuel S level and Ba fuel additive on particulate mass emission rate and opacity of the vehicle exhaust are shown in Table I. The effect of fuel S level on both particulate mass emissions and opacity appears to be small; there is perhaps a slight decrease in particulate emissions and opacity with increasing fuel S level in the tests without Ba additive and the opposite effect in the presence of the Ba additive. If

Table I. Effect of Fuel S and Ba Levels on Total Particulate Mass Emission and Opacity; 1974 Mercedes 240D

test type	fuel S, wt %	fuel Ba, wt %	particulate mass emission rate (*M*), mg/km	% opacity [a]
cold start-FTP	0.0087	0.0	518	17
hot start-FTP	0.0087	0.0	361	15
hot start-FTP	0.0087	0.0	399	*b*
cold start-FTP	0.110	0.0	453	14
hot start-FTP	0.110	0.0	348	13
hot start-FTP	0.110	0.0	385	*b*
cold start-FTP	0.190	0.0	440	14
hot start-FTP	0.190	0.0	320	13
hot start-FTP	0.190	0.0	362	*b*
cold start-FTP	0.0087	0.058	472	9.5
hot start-FTP	0.0087	0.058	242	7.8
hot start-FTP	0.0087	0.058	339	*b*
cold start-FTP	0.110	0.058	794 [c]	15 [c]
hot start-FTP	0.110	0.058	286	7.1
hot start-FTP	0.110	0.058	454	*b*
cold start-FTP	0.190	0.058	469	11
hot start-FTP	0.190	0.058	283	10
hot start-FTP	0.190	0.058	355	*b*

[a] Average percent opacity of peak heights in smokemeter traces. [b] Smokemeter measurements not taken; exhaust injected directly into dilution tube. [c] Modal analysis of the test showed a disproportionate level of particulate emissions during the early stages of the run, indicating a possible engine malfunction or sudden release of stored particulate.

fuel S level does not affect the combustion process, one should not expect a significant change in mass particulate emissions with changes in fuel S level since SO_4^{2-} is the only significant particulate species derived from fuel S and it represents only a few percent of the total particulate mass (see below).

The Ba fuel additive caused a substantial reduction in the opacity of the diesel exhaust—on the average, 30–40% of the reading. The Ba effect on particulate mass emission rate was much smaller—only ~2% for the cold-start tests (the anomalous results with the 0.110 wt % S/0.058 wt % Ba fuel were not included in this average) and ~10% for the hot-start tests. These reductions in mass particulate are obviously not large enough to account for the observed reductions in opacity. The smoke suppression by Ba therefore must result from changes in chemical composition and/or size distribution (and/or other optical properties) of the particulate emissions.

Samples collected during those hot start-FTP tests in which the exhaust was injected directly into the dilution tube were subjected to detailed chemical analyses. Chemical analyses were not performed on samples collected downstream of the smokemeter, since it was noted that the measured particulate mass emission rates (Table I) were consistently lower when the exhaust was passed through the smokemeter—indicating particulate loss in the smokemeter that might influence the chemical composition.

Results of Ba and SO_4^{2-} analyses on the particulate emissions are given in Table II. The SO_4^{2-} emissions, both with and without the Ba fuel additive, increased with increasing fuel S levels, though not linearly in either case, so that the % $S \rightarrow SO_4^{2-}$ conversion declined as the fuel S level was increased.

When the Ba additive was present, the SO_4^{2-} emission rate increased with increasing fuel S level until the amount of emitted SO_4^{2-} was equimolar with the emitted Ba. Photoelectron spectroscopy (ESCA) analysis showed that the Ba and S lines in the particulate samples were identical with those of $BaSO_4$. At the lowest fuel S level (0.0087 wt %), the fuel Ba/S molar ratio was 1.56 and most (63%) of the fuel S was converted to SO_4^{2-}, yielding an exhaust-particulate Ba/SO_4^{2-} molar ratio of 2.6 (Table II); the excess Ba is presumably the soluble form(s) of Ba described by previous workers (*4–7*). The fact that the particulate Ba/SO_4^{2-} ratio stops at ~1.0 as the fuel S level is increased implies that the driving force for SO_4^{2-} formation in the presence of the Ba additive is the formation of $BaSO_4$.

The notable comparison of Table II is the five- to eightfold increase in SO_4^{2-} emission rate or % $S \rightarrow SO_4^{2-}$ conversion with the use of the Ba fuel additive. The increase is a consequence of $BaSO_4$ formation which, as already stated, is evidently the driving force for SO_4^{2-} formation when the additive is present. Not explained, but certainly worth pointing out, is the curious fact that the multiplication factor between the emission rate or % $S \rightarrow SO_4^{2-}$ conversion without Ba and that with Ba is essentially constant at $6.9 \pm 1.0(\sigma)$-fold.

It should be mentioned that the formation of SO_4^{2-} in the presence of the Ba additive and that in its absence probably are unrelated processes. The $S \rightarrow SO_4^{2-}$ conversion in the absence of Ba is far short of the thermodynamic equilibrium value. Since equilibrium is not attained, the Ba cannot be acting simply by shifting the equilibrium to the right by removing product.

The Ba emission rates in Table II account for >90% of the Ba consumed in the fuel. This is consistent with previously published work (*5, 9*).

Carbon, hydrogen, and nitrogen analyses presented in Table III reveal some substantial effects of Ba fuel additive. The additive brought about an average 28% reduction in carbon content, 190% increase in hydrogen content, and 42% reduction in nitrogen content of the particulate matter. (Use of a Ba/Ca-containing fuel additive is reported (*9*) to have given a similar decrease in carbon *but* a decrease in H as well.) The average C/H mole ratios from Table III are 3.6 without Ba additive and 0.95 with it. These results suggest a significant effect of the Ba additive during the carbonaceous particulate formation process. This deduction, which also was advanced by other investigators (*8*), suggests that it is worthwhile to pursue the mechanism of the involvement of Ba in the formation of particulates on a more fundamental level.

The reduction in carbonaceous content of the particulate emissions through the use of the Ba additive is enough to make plausible the large reduction in exhaust opacity in the face of negligible effect on total particulate mass emission rate. The

Table II. Ba and SO_4^{2-} Analyses of Particulate Emissions [a]

fuel S, wt %	fuel Ba, wt %	particulate mass emission rate (M), mg/km	emission rate, mg/km		% $S \rightarrow SO_4^{2-}$ conversion [b]	Ba/SO_4^{2-} mole ratio
			Ba	SO_4^{2-}		
0.0087	0	399		1.9	8.6	
0.110	0	385		5.4	1.8	
0.190	0	362		5.0	0.96	
0.0087	0.058	339	53	14.5	62.7	2.6
0.110	0.058	454	44	29.5	10.5	1.0
0.190	0.058	355	56	36.5	7.3	1.1

[a] Analyses performed on samples collected during hot start-FTP tests where the vehicle exhaust was injected directly into the dilution tube. [b] Percent of fuel S emitted as SO_4^{2-}.

Table III. Carbon, Hydrogen, and Nitrogen Analyses of Particulate Emissions [a]

fuel S, wt %	fuel Ba, wt %	particulate mass emission rate (M), mg/km	elemental analyses					
			carbon		hydrogen		nitrogen	
			mg/km	% of M[b]	mg/km	% of M[b]	mg/km	% of M[b]
0.0087	0	399	311	78	7.9	2.0		
0.110	0	385	278	72	7.4	1.9		
0.190	0	362	336	93	6.2	1.7	4.3	1.2
0.0087	0.058	339	204	60	22.2	6.5		
0.110	0.058	454	263	58	18.6	4.1		
0.190	0.058	355	201	57	18.8	5.3	2.3	0.7

[a] Analyses performed on samples collected during hot start-FTP tests where the vehicle exhaust was injected directly into the dilution tube. [b] Weight percent of total particulate mass emissions.

lack of change in total mass comes about because the carbon decrease caused by the Ba additive is offset by the additional Ba and SO_4^{2-}.

As indicated earlier, the exhaust opacity should be a function of the total particulate concentration in the exhaust, the chemical composition of the particulate, and the particulate size distribution. Particulate size distributions were not measured in this study, but Kittelson et al. (*13*) report that use of a Ba fuel additive results in a decrease in particle size, which may also be influencing the opacity.

Conclusions

The Ba fuel additive caused a 30–40% decrease in opacity and a commensurate (~30%) decrease in the concentration of carbonaceous particulate in the diesel exhaust. However, this decrease in carbon was offset by $BaSO_4$ emissions deriving from the additive Ba and its reaction with fuel-derived sulfur, so that the total particulate mass emission rate was essentially unaffected by the additive. Therefore, the reduction in exhaust opacity was not a consequence of any reduction in total particulate mass, but rather may have been related to compositional change from highly absorbing carbonaceous particulate matter to relatively nonabsorbing $BaSO_4$ particles.

Fuel S level had no significant effect on the total particulate mass emission rate. Fuel S level did affect the SO_4^{2-} emission rate, but the effect was not linear. In the no-additive case, the % S → SO_4^{2-} conversion of the fuel S was highest at low levels of fuel S and declined steadily with increasing fuel S level.

In the presence of the Ba additive, the SO_4^{2-} emission rate (and % S → SO_4^{2-} conversion) was many times larger, and all in the form of $BaSO_4$. The Ba, through $BaSO_4$ formation, governed the SO_4^{2-} emission rate; the Ba/SO_4^{2-} molar ratio was approximately 1.0 when the amount of fuel S was adequate to permit it. In all cases, better than 90% of the fuel-additive Ba consumed was emitted.

The Ba additive caused a great increase in particulate H content and in particulate H/C ratio. This, and the reduction in carbonaceous particulate emissions, suggests a significant effect by the additive during the carbonaceous particulate formation process. Whatever the mechanism for the action of the Ba fuel additive, it must account for the compositional changes, including the prominence of $BaSO_4$.

Acknowledgments

We wish to thank Fred C. Ferris for technical assistance in conducting the vehicle experiments, William Okamoto and E. H. Schanerberger for preparation of the fuels, and John S. Hammond for conducting the ESCA experiments. The Ba and SO_4^{2-} analyses were performed by the Chemical Analysis Laboratory of the Ford Research Staff.

Literature Cited

(1) Cotton, D. H.; Friswell, N. J.; Jenkins, D. R. *Combust. Flame* **1971,** *17,* 87.
(2) Jenkins, D. R. *Combust. Sci. Technol.* **1972,** 5, 245.
(3) Glover, I. *J. Inst. Petrol.* **1966,** 52, 137.
(4) Miller, C. O. *SAE Tech. Pap.* **1967,** *670093.*
(5) Saito, T.; Nabetani, M. *SAE Tech. Pap.* **1973,** *730170.*
(6) Golothan, D. W. *SAE Tech. Pap.* **1967,** *670092.*
(7) Turley, C. D.; Brenchley, D. L.; Landolt, R. R. *J. Air Pollut. Control Assoc.* **1973,** *23,* 783.
(8) Apostolescu, N. D.; Matthew, R. D.; Sawyer, R. F. *SAE Tech. Pap.* **1977,** *770828.*
(9) Hare, C. T.; Springer, K. J.; Bradow, R. L. *SAE Tech. Pap.* **1976,** *760130.*
(10) Gutwein, E. E.; Landolt, R. R.; Brenchley, D. L. *J. Air Pollut. Control Assoc.,* **1974,** *24,* 40.
(11) McKee, D. E. *SAE Tech. Pap.* **1977,** *770167.*
(12) McKee, D. E.; Ferris, F. C.; Goeboro, R. E. *SAE Tech. Pap.* **1978,** *780592.*
(13) Kittelson, D. B.; Dolan, D. F.; Diver, R. B.; Aufderheide, E. *SAE Tech. Pap.* **1978,** *780789.*

Received for review January 23, 1980. Accepted May 12, 1980.

Fate of Selected Herbicides in a Terrestrial Laboratory Microcosm

Jay D. Gile,* James C. Collins, and James W. Gillett

Terrestrial Division, Corvallis Environmental Research Laboratory, U.S. Environmental Protection Agency,
Corvallis, Oregon 97330

■ The transport and metabolism of ^{14}C-labeled herbicides (simazine, bromacil, trifluralin, and 2,4,5-T) applied as a foliar spray (0.28 kg/ha) was examined in a terrestrial microcosm chamber (TMC). These chemicals were compared to a reference compound, the insecticide dieldrin. The TMC contained a synthetic soil medium, Douglas fir and red alder seedlings, rye grass, numerous invertebrates, and a gravid gray-tailed vole (*Microtus canicaudus*). By 20 days posttreatment, total soil residues (parent and metabolites and bound residues) averaged 0.14 ppm for all chemicals. Except for dieldrin little extractable parent material was detected for any of the chemicals in the soil. Concentrations of ^{14}C material in the rye grass shoots ranged from an average of 2.5 ppm for 2,4,5-T to 16.8 ppm for simazine. 2,4,5-T and trifluralin were more rapidly degraded than the other chemicals with 2,4,5-T present primarily as extractable metabolites. ^{14}C material of dieldrin was accumulated to a much greater extent than any of the herbicides in the invertebrates. While concentrations of all chemicals in the vole were low, ^{14}C material from dieldrin and simazine was present at levels approximately twice those of the other chemicals. None of the chemicals could be detected in the ground water.

Introduction

This is the third in a series of experiments in which representatives from broad categories of pesticides were examined in a terrestrial microcosm chamber (TMC) developed at the U.S. EPA's Corvallis Environmental Research Laboratory (CERL), as described earlier (*1,2*). Microcosms allow the investigator to examine materials that may be environmentally harmful with little risk to the environment and at a much reduced cost in comparison to field studies. The utility of a microcosm rests on its adaptability to studying a wide variety of chemicals in different types of ecosystems. The TMC has previously been used to study insecticides and fungicides in an agricultural ecosystem. In this study herbicide application in a nonagricultural system is examined.

Douglas fir reforestation practices have dictated the widespread use of selective herbicides to control red alder and other deciduous trees in new growth areas. Such practices have recently generated widespread controversy about the possible adverse impacts of these chemicals primarily in relation to human health. The chemicals used in this study were herbicides commonly used in "conifer release", "right-of-way" control, or as general purpose (noncrop) herbicides. The specific chemicals selected were simazine (2-chloro-4,6-*bis*(ethylamino)-*s*-triazine), bromacil (5-bromo-3-*sec*-butyl-6-methyluracil), trifluralin (α,α,α-trifluoro-2,6-dinitro-*N*,*N*-dipropyl-*p*-toluidine), and the isooctyl ester of 2,4,5-T (isooctyl 2,4,5-trichlorophenoxyacetate). These were compared with the insecticide dieldrin (HEOD; 1,2,3,4,10,10-hexachloro-6,7-epoxy-1,4,4a,5,6,7,8,8a-octahydro-1,4:5,8-*endo*,*exo*-dimethanonaphthalene), which serves as a reference compound in our system.

The primary objective of this experiment was to show that the fate and effects of chemicals applied to a "forest ecosystem" microcosm could be followed in the same manner and by the same techniques as an "agroecosystem" microcosm (*3*,*4*). The secondary objective was to determine the disposition of the various herbicides within the system and compare this information with that of the reference chemical.

Methods and Materials

Chamber. The terrestrial microcosm chamber (TMC) utilized in this study consisted of a glass box 1.0 × 0.75 × 0.60 m with a Plexiglass lid (*2*). The chamber received 2500 ft cd of light at the soil surface with a 16-h daily photoperiod. Temperatures ranged from 25 °C during the day to 15 °C at night. The airflow rate was 50 L/min. The soil medium consisted of 40% 20-grit washed sea sand, 40% illite clay, and 20% Jiffy Mix Plus (George Ball Pacific Incorp., Sunny Vale, CA).

Flora and Fauna. Plants consisted of a Douglas fir seedling (*Pseudotsuga menziesii*) in each quadrant surrounded by red alder seedlings (*Alnus rubra*) and perennial ryegrass (*Lolium perenne*). The fir were approximately 1 yr old (20 cm high) at the time of planting while the red alder were 2 months old (6 cm high).

Invertebrates were represented by bacteriophagic nematodes (*Pristionchos inheriteiri*), earthworms (*Lumbricus* spp.), pillbugs (*Armadillarium* and *Porcellia* spp.), mealworm larvae (*Tenebrio molitar*), gray crickets (*Achetus domesticus*), and garden snails (*Helix pomata*). The lone vertebrate was a gravid female gray-tailed vole (*Microtus canicaudus*).

Radiolabeled Material. The ^{14}C-dieldrin (labeled in positions 1, 2, 3, 4, and 10) was technical grade (>85% HEOD) obtained from Amersham Searle (Arlington Heights, IL). It was purified by preparative thin-layer chromatography to >98%. Bromacil (2-^{14}C, >96%), simazine (ring-^{14}C, >96%), trifluralin (ring-^{14}C, >97%), and the isooctyl ester of 2,4,5-T (ring-^{14}C, >94%) were obtained from New England Nuclear (Boston, MA) and used without further purification.

Procedure (3,4). The soil was added to each of the six chambers in three 40-kg portions. Following the addition of each layer, 6 L of water was added and the layer allowed to compact overnight. When all three layers had been added, the boxes were warmed to 30–35 °C for 1 week, after which time airflow was started; the temperature was adjusted to operational levels (15–25 °C) and a 16-h light cycle was initiated. One Douglas fir seedling was planted in the center of each quadrant and surrounded by four red alder seedlings. Forty grams of rye grass seed were scattered over the surface and covered with approximately 1 cm of soil mixture. Water was added to each TMC via an overhead sprinkler system three times a week (15 L total/week). After rye grass growth was observed, populations of earthworms and mealworm larvae were added, followed by snails and crickets. Twenty-six days after planting, five microcosms were treated with one of the test chemicals with the sixth chamber serving as a control. Application was by foliar spray at a rate of 0.28 kg/ha (0.25 lb/a). Thus each TMC was treated with 20 mg of material containing 4.0 × 10^7 dpm of ^{14}C. Treatment solutions were made by dissolving the agents in small amounts of acetone, adding the carrier normally used with the pesticide, and mixing thoroughly. The control was treated with xylene only (which served as the carrier for the dieldrin treatment). Eight days after treatment the vole was introduced.

A census of visible animal species was conducted daily. Dead animals were removed as found. Polyurethane air filters were changed and analyzed three times on the day of treatment and daily thereafter. Rye grass was sampled for analysis on days 2, 3, 6, and 13 posttreatment and at termination. The termination days for bromacil, simazine, trifluralin, 2,4,5-T, and HEOD were 22, 26, 19, 20, and 20 days after treatment, respectively.

At termination, the macrobiota (flora and fauna) were removed, counted, weighed, and frozen until analysis. A grid was created on the soil surface which comprised 50 10 × 15 cm units. From this grid 26 designated units were removed from the first 5-cm layer for individual residue analysis. This same pattern was applied to the second 5-cm layer. Sampling in levels 3 and 4 involved pooling of the units so that 13 and 6 samples were obtained, respectively. Following removal of all soil samples, the interior surfaces of the chambers were cleaned extensively with acetone and ethanol to remove all residual radioactivity.

Analysis. Water samples were extracted in a separatory funnel with acetone; soil samples were extracted by blending with hexane/isopropyl alcohol (3:2); plant tissue was extracted by blending with acetone; and animal tissue was extracted by blending with hexane/isopropyl alcohol and then acetone. Extract was separated from sample residue by using a Büchner funnel under vaccum. Following extraction all sample residues (except water) were combusted on a Packard sample oxidizer. All extracts and residues were analyzed for ^{14}C with a Packard Tri-Carb liquid scintillation spectrometer using commercially available counting cocktails. The ^{14}C activity of any sample was assumed to be the sum of the activities for all extracts plus combusted residue. If an organic extract of soil, plant, or animal tissue contained in excess of 10^3 dpm, the sample was further analyzed by thin-layer chromatography (TLC) and autoradiography. TLC was used to identify the presence of metabolites; however, identification of specific metabolites was not attempted.

Results

Mass Balance. Table I shows the total ^{14}C recovered for each chemical. Recovery values ranged from 69% for bromacil to 100+% for dieldrin. Overall recoveries were improved from previous tests of the TMC.

Recovery of HEOD exceeded even that of seed treatment (99%) (*4*). Figure 1 illustrates the comparative distribution within each TMC at termination of the experiment. Previously the soil was the major repository for ^{14}C (*3*,*4*); however, the plants generally contained greater amounts of ^{14}C in comparison to the soil in this study.

Residue Distribution. Soil. Concentrations of ^{14}C materials in the upper 5 cm of soil (Figure 2) averaged 0.14 ppm equivalents (bromacil, 0.12; simazine, 0.18; trifluralin, 0.08; 2,4,5-T, 0.19; HEOD, 0.12). In an earlier test with HEOD (0.25 lb/acre) applied as a seed coating, the average concentration of ^{14}C material in the upper layer exceeded 1 ppm (*4*). Except for HEOD, comparatively little extractable parent material was detected for any of the chemicals in the soil. HEOD, the least soluble of the chemicals examined, exhibited the greatest vertical distribution within the soil column.

Table I. Mass Balance ^{14}C (10^6 dpm) at Termination of TMC

	bromacil	simazine	trifluralin	2,4,5-T	HEOD
amount applied	39.9	39.4	43.4	37.3	40.5
amount recovered	27.6	31.3	31.4	34.1	41.8
% recovered	69	79	72	91.0	103.2
unaccounted dpm [a]	12.3	8.1	12.6	3.2	0

[a] May reflect the conversion of the ^{14}C-labeled material to $^{14}CO_2$, which was not detectable by the filtering apparatus.

Plants. Concentrations of ^{14}C material in the rye grass shoots ranged from an average of 2.5 ppm for 2,4,5-T to 16.8 ppm with simazine (Figure 3). Only 2,4,5-T was detected in the roots. The ^{14}C material of bromacil and simazine was present mainly as extractable parent, with some extractable metabolites. More extractable metabolites were found in the trifluralin treatment. 2,4,5-T was present almost exclusively as extractable metabolites, whereas HEOD was present as extractable parent. The red alders were not analyzed for either ^{14}C or pesticide residues because of extensive herbivory by both the vole and the crickets. Although the fir did receive some damage, sufficient plant material was present to permit analysis.

The fir trees accumulated relatively little of the ^{14}C material, although a proportionally greater amount was detected in their root system in comparison to the rye grass root system. The ^{14}C material from bromacil was found primarily as parent in the root, whereas it was generally present as extractable metabolite in the shoot. Extractable parent was not present for any of the other chemicals, with HEOD present only as a bound residue (material unextractable by solvent extraction; Figure 4).

Invertebrates. The ^{14}C material of HEOD was accumulated to a much greater extent in crickets, snails, and pillbugs than any of the herbicides (Table II). The snails generally exhibited greater concentrations of all chemicals compared to the other invertebrates, with the ^{14}C material of simazine and trifluralin being accumulated to the greatest extent. Extractable parent was detected for bromacil, trifluralin, and HEOD in the snail and for bromacil only in the cricket. ^{14}C-simazine material was present primarily as bound residues; the other chemicals were mainly aqueous metabolites. Snail feces collected from the glass sidewalls of the microcosm contained high concentrations of all chemicals. The vast majority of this material was detected as bound residues for all chemicals except dieldrin where parent material predominated. While condensate frequently occurred on the sidewall, relatively little ^{14}C activity was detected from wall swipes, thus minimizing the possibility of condensate adding to the feces ^{14}C activity. The high concentrations in the snail feces probably reflects intense foraging on the rye grass at night followed by prolonged stationary periods on the sidewalls during the day were the feces were concentrated.

Vole. Residues of ^{14}C in the vole ranged from 0.18 ppm equivalents for bromacil to 0.59 ppm for simazine (Table III). Extractable parent was detected only for HEOD. The other chemicals were present primarily as bound residues with the exception of 2,4,5-T which occurred primarily as extractable metabolites. Of the tissues examined (GI, heart, lung, liver, kidney, brain, and carcass), the gastrointestinal (GI) tract contained the vast majority of ^{14}C material for bromacil, trifluralin, and 2,4,5-T. Although ^{14}C simazine material was found primarily in the GI tract, the liver contained in excess of 2 ppm, mainly as bound residue. HEOD was found as extractable parent, metabolites, and bound residue in the liver and kidney, with the parent predominating. Total HEOD in the liver reached a level of 15.7 ppm, and 14 ppm in the kidney. The effects of the chemicals on the vole and the crickets and their interaction will be discussed elsewhere.

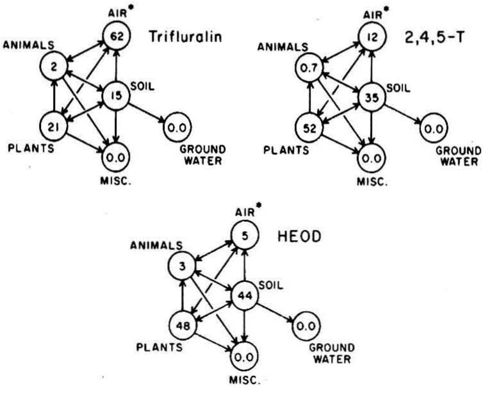

Figure 1. ^{14}C Mass balance (% of applied) in TMC at termination. *Amount measured plus estimated loss as $^{14}CO_2$.

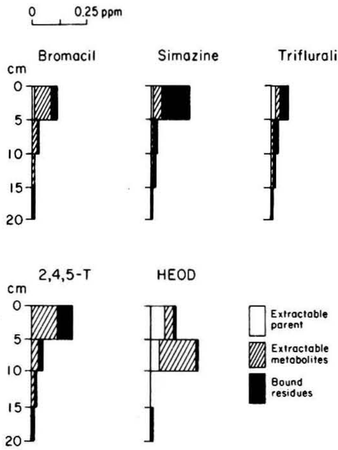

Figure 2. Vertical profile of terminal ^{14}C distribution in soil.

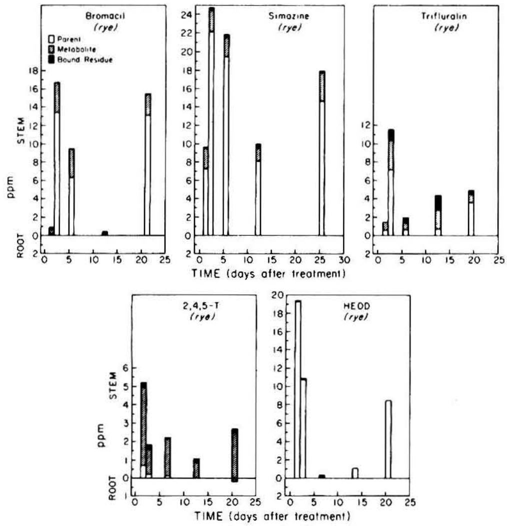

Figure 3. Profile of ^{14}C materials in rye grass.

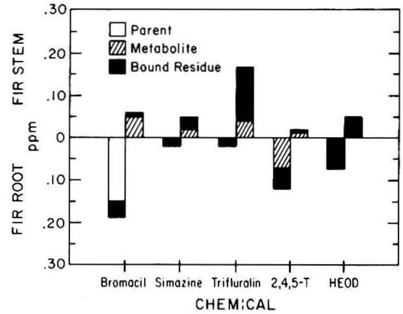

Figure 4. Profile of ^{14}C materials in Douglas fir seedlings at termination (bromacil = 22; simazine = 26; trifluralin = 19; 2,4,5-T = 20; HEOD = 20 days after treatment).

Air. Figure 5 represents only the ^{14}C trapped on the polyurethane foam air filters. Initial volatility losses of trifluralin greatly exceeded those of the other chemicals, with HEOD having the second highest loss rate followed by 2,4,5-T and a much more variable bromacil and simazine. By day 7 HEOD loss rate was relatively stable, whereas the others continued to decline. At termination, 5×10^5 dpm of ^{14}C from HEOD was still being trapped daily in the airstream.

Discussion

This study provides additional evidence that a simulated ecosystem such as the TMC can be used to indicate distribution trends of a wide variety of chemicals. In addition, comparisons between sets of experiments are possible even though conditions may differ. The recovery of ^{14}C-HEOD exceeded that of previous foliar treatments (*3*), because of improved air trapping capability with the polyurethane foam filters. The distribution of HEOD in this experiment is consistent with results from earlier work (*3,4*), with HEOD remaining at the site of application. With respect to HEOD metabolism in the soil, specifically low levels of extractable parent, we offer the following suggestions. Comparisons between microcosm and field studies cited in the literature are frequently difficult because of the minimal information available on the environmental conditions (e.g., temperature, light cycle, humidity, wind velocity) of the field studies. It is also possible that the relatively low airflow in combination with high temperature and humidity could accelerate metabolism. Furthermore, because of the conditions described above plus the organic matter content of the soil (5 wt %), the soil could be very active.

Recovery of bromacil, simazine, trifluralin, and 2,4,5-T was within an acceptable range in comparison to previous TMC experiments. Distribution of bromacil was complicated by placing the ^{14}C label in the second carbon position which is readily converted to $^{14}CO_2$. ^{14}C-bromacil material appeared to be evenly distributed between soil, plant, and air (Figure 1); however, the ^{14}C in the air probably reflects $^{14}CO_2$ rather then parent or volatile metabolite. Contrary to the findings of Hill (*5*) and Helling et al. (*6*), bromacil was relatively immobile in the soil, with the majority of the ^{14}C material residing in the upper 6 cm.

Based on a low vapor pressure (6×10^{-9} mmHg at 20 °C) and a solubility of 2 ppm, simazine should remain in the soil and the plant foliage (*7*). In a warm, moist climate such as existed in the microcosm, simazine could be expected to be less persistant in the soil, perhaps accounting for the relatively high ^{14}C levels in the air (*8*). In comparison to Metcalf's system (*9*), substantially more ^{14}C material from simazine was detected in the plant tissue, presumably due to the greater relative abundance of plants.

Trifluralin [vapor pressure of 1.99×10^{-4} mmHg at 29.5 °C (*7*)] would be expected to volatilize to a greater extent then the other chemicals tested, as was the case within the TMC. Trifluralin loss rates from the TMC appear substantially

Table II. Total[a] Pesticide Residue in Macroinvertebrates

		chemical, ppm				
species[e]	sample day[b]	bromacil	simazine	trifluralin	2,4,5-T	HEOD
cricket	7	0.67	0.96	0.41	1.30	1.42
	termination[c]	*d*	*d*	*d*	0.13	0.14
snail	8	0.52	2.40	1.70	0.88	2.41
	15	0.20	1.62	2.38	0.78	2.64
	termination	0.14	1.97	1.54	0.57	2.43
snail feces	termination	23.77	9.70	61.72	34.67	21.34
pillbug	termination	0.18	0.66	0.61	0.55	1.57
tenebrio	termination	0.11	1.04		0.23	*d*
earthworm	termination				0.32	0.09

[a] Total residue includes extractable parent, metabolites, and bound residue as ^{14}C equivalents of parent (μg/g fresh wt). [b] Number of days after treatment. [c] Termination day for bromacil = 22; simazine = 26; trifluralin = 19; 2,4,5-T = 20; HEOD = 20 after treatment. [d] No sample available. [e] Pillbugs, *Tenebrio*, snails, and earthworms were added prior to treatment; crickets were added prior to treatment, on the treatment day, and thereafter as needed.

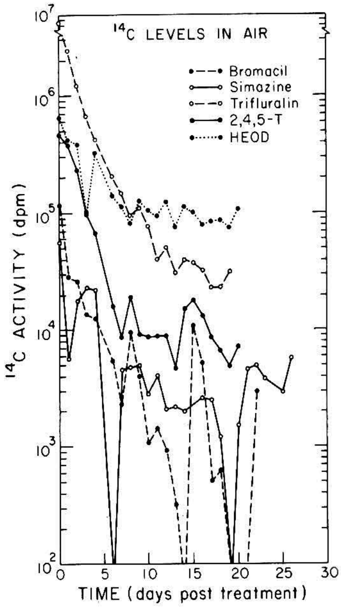

Figure 5. ^{14}C concentration in air.

greater than those observed in the field from a soil treatment (*10*), where 80–85% remained in the soil after 4 weeks in comparison to 15% in the TMC. Presumably the difference is due to the method of application.

The isooctyl ester of 2,4,5-T behaved as expected in the TMC with the majority of the ^{14}C material residing in the plants; however it was quickly degraded (Figure 3). The second most important repository was the soil, wherein again 2,4,5-T appears to be rapidly degraded (Figure 2), corresponding to results observed by McCall et al. (*11*). Metcalf et al. (*9*) observed similar results with respect to the plant/soil portion of his microcosm, although the plant material in the TMC contained substantially more ^{14}C materials from 2,4,5-T.

Conclusions

The following conclusions are based on the data from this experiment:

(1) The terrestrial microcosm chamber can be used to study the mass balance of herbicides in a terrestrial ecosystem (Figure 1).

(2) In general, distribution patterns observed in the TMC are comparable to those observed in other systems and field observations. However, insufficient information on the environmental conditions of the field studies can make comparisons difficult.

Table III. Whole Body Residues in Vole

	parent,[a] ppm	metabolites[b]	bound residue[c]	total
bromacil	nd[d]	0.08	0.11	0.18
simazine	nd	0.06	0.53	0.59
trifluralin	nd	0.06	0.20	0.26
2,4,5-T	nd	0.13	0.07	0.20
HEOD	0.4	0.06	0.01	0.47

[a] Extractable parent. [b] Polar metabolite(s), aqueous soluble material, and TLC origin material. [c] Bound residue as ^{14}C equivalents of parent (mg/g fresh wt). [d] None detected (<0.01 ppm).

(3) In comparison to the reference compound (HEOD) all of the herbicides were less persistant in the TMC (Table I).

Acknowledgment

We express appreciation to Steven Whitfield, Carol Bickford, William Albrecht, Elizabeth Frolander, Wesley Lashbrook, and Loren Russell. The voles were supplied by L. G. Forslund, Oregon State University.

Literature Cited

(1) Gillett, J. W.; Gile, J. D. In *Substitute Chem. Program: First Year Prog., Proc. Symp., 1975, v3.*

(2) Gillett, J. W.; Gile, J. D. *Int. J. Environ. Stud.* **1976,** *10,* 15–22.

(3) Gile, J. D.; Gillett, J. W. *Arch. Environ. Contam. Toxicol.* **1979,** *8,* 107.

(4) Gile, J. D.; Gillett, J. W. *J. Agric. Food Chem.* **1979,** *27,* 1159–64.

(5) Hill, G. D. "Characteristics of Herbicides by Chemical Groups. II. Hyvar X Bromacil"; California Weed Conference Proceedings, 1971; Vol. 23, pp 171–4.

(6) Helling, C. S.; Kearney, P. C.; Alexander, M. *Adv. Argon.* **1971,** *23,* 147–240.

(7) Spencer, E. Y. "Guide to Chemicals Used in Crop Protection", 6th ed.; The University of Western Ontario: London, Ontario, 1973; Canada Department of Agriculture Publication 1093.

(8) U.S. Environmental Protection Agency "Initial Scientific and Minieconomic Review of Simazine"; working draft submitted Sept 17, 1975.

(9) Metcalf, R. L.; Cole, L K.; Wood, S. G.; Mandel, D. J.; Milbrath, M. L. "Design and Evaluation of a Terrestrial Model Ecosystem for Evaluation of Substitute Pesticide Chemicals"; Ecological Research Series EPA-600/013-79-004, U.S. Environmental Protection Agency, Corvallis, OR, 1979.

(10) Golab, T.; Althaus, W. A.; Wooten, H. L. *J. Agric. Food Chem.* **1979,** *27,* 163–79.

(11) McCall, P. J.; Vrona, S. A.; Kelley, S. S. Presented at the National Meeting of the American Chemical Society, Pesticide Section, Washington, D.C., 1979.

Received for review November 1, 1979. Accepted June 3, 1980.

Partitioning of No. 2 Fuel Oil in Controlled Estuarine Ecosystems. Sediments and Suspended Particulate Matter

Patrick J. Gearing*, Juanita N. Gearing, Richard J. Pruell, Terry L. Wade[1], and James G. Quinn

Graduate School of Oceanography, University of Rhode Island, Kingston, R.I. 02881

■ To investigate the transport and incorporation of waterborne oil to sediments, no. 2 fuel oil was added as a dispersion in semiweekly doses to three controlled estuarine ecosystems. Samples of suspended particulate matter and sediments were analyzed by gas chromatography for saturated and aromatic hydrocarbons. Fractionation of the oil in the water column by adsorption to particulate matter resulted in the sedimentation of about 50% of the insoluble, saturated hydrocarbons, but less than 20% of the more soluble, aromatic hydrocarbons. The oil-derived hydrocarbons were slowly mixed down through the bioturbation zone. Biodegradation and other processes effected the removal of most of the hydrocarbons soon after the additions ended, but a residue of 10–20% in the form of branched alkanes, cycloalkanes, and aromatics in an unresolved complex mixture persisted more than 1 year later.

Oil first became an important fuel for industrialized societies toward the end of the nineteenth century (*1*). Its anthropogenic input to the marine environment probably began about the same time (*2–8*) and probably will continue in the foreseeable future. In order to minimize the effects of such pollution, it is necessary to understand the environmental behavior of the complex and variable mixture that is oil. This subject may be studied in scales ranging "between beakers and bays" (*9*). In the past decade or so, research has begun on an intermediate scale, with large, enclosed ecosystems such as those of the Controlled Ecosystems Pollution Experiment (CEPEX) (*10, 11*) and the Marine Ecosystems Research Laboratory (MERL) (*12–17*). These systems provide many of the experimental advantages associated with laboratory studies (control of environmental parameters, encapsulated populations, ease of sampling) along with a biological assemblage functioning in a manner similar to that in nature.

One such experiment, an investigation of the fate and effects of chronic inputs of no. 2 fuel oil in an estuarine environment, was conducted in 1977 using the microcosms of MERL at the University of Rhode Island. The results of that experiment which pertain to the sediments of the ecosystems have been published (*13, 14*). Some conclusions drawn from those data may be summarized as follows.

- The sediments appeared to be a relatively minor hydrocarbon reservoir: only 7–16% of the oil added to the water column in the form of a dispersion was eventually found in the sediments.
- The proportion of aromatics to saturates was much lower in the sediments than in the dosing dispersion.
- The settling of hydrocarbons in association with suspended particulate matter may have been an important route for oil in the water column to reach the sediments (although no mass balance was given for saturated and aromatic hydrocarbons between suspended particulate matter and sediments).
- Oil-derived saturated hydrocarbons had a certain stability in the sediments: they were detected in varying amounts up to the end of the experiment, 6 months after oil dosing had ended.

Another oil experiment was performed at MERL in 1978–1979, partly in order to check and elaborate the previous year's conclusions. This paper presents the results from the second experiment on the interaction of oil hydrocarbons with suspended particulate matter and sediments. An additional part of this experiment, partitioning of hydrocarbons between the ecosystem water, surface microlayer, and atmosphere, is the subject of other papers (*15, 16*).

Experimental Procedures

Setting. The MERL ecosystems are fiberglass tanks 5.5 m in height and 1.8 m in diameter. For the experiment they contained 13 m^3 of flowing seawater and 0.8 m^3 of silty clay sediment from mid-Narragansett Bay along with their associated biota. Detailed accounts of the workings of the ecosystems have been published (*12, 17*). In order to obtain a more representative population of zooplankton, the continuous, slow flow of seawater (330 mL/min added 25 cm above the sediments) used in 1977 was changed to a pulsed, fast flow (10 L/min for 12 min every 6 h, added 10 cm below the water surface) in 1978–1979.

Oil. The same locally purchased no. 2 fuel oil used in the previous experiments (density = 0.838 g/mL) was added in the form of an oil-seawater dispersion to the water column of three of the ecosystems (no.'s 2, 7, and 9) semiweekly from March 6, 1978 to July 6, 1978. During this period the average concentration of oil-derived hydrocarbons in the water column was 93 μg/L. The total dose of oil to each tank was 40.25 g. In the 1977 MERL experiment, dosing also began in late winter and ended in summer, but the addition period was slightly longer (February 14–August 1, 1977), more oil was added (108 g), and the average concentration in the water was higher (181 μg/L). Detailed descriptions of dispersion preparation and tank dosing procedures in both experiments may be found in Gearing et al. (*13*).

Figure 1 shows chromatograms of the no. 2 fuel oil (A) and the saturated hydrocarbon or F_1 fraction (B) and aromatic hydrocarbon or F_2 fraction (C) of the dosing dispersion made from that oil. Because of the high mixing energy imparted in their preparation, the dispersions were very similar to the whole oil in hydrocarbon composition, with little fractionation due to differences in the aqueous solubilities of the hydrocarbons (*17–19*). The oil, dispersion, and ecosystem water column immediately after dosing all contained 70–75% saturated hydrocarbons and 25–30% aromatic hydrocarbons. The F_1 fractions had, as major features, *n*-alkanes from about n-C_{10} to n-C_{22}; a series of isoprenoids including farnesane, pristane, and phytane; other branched alkanes; and an unresolved complex mixture (UCM) containing branched and cycloalkanes which was not separated even by the capillary columns used (Figure 1B). The F_2 fractions contained naphthalene and alkyl-substituted naphthalenes together with aromatic hydrocarbons from benzene to alkyl-substituted phenanthrenes, and a complex mixture of unresolved aromatic components (Figure 1C).

Sampling. There is evidence (*18*) that coring devices not completely open during penetration (such as the corer used in 1977) may not sample quantitatively the uppermost layer of sediment because they create shock waves that can blow away that layer. Since the highest oil concentrations in the

---

[1] Present address, Institute of Oceanography, Old Dominion University, Norfolk, Va. 23508.

0013-936X/80/0914-1129$01.00/0

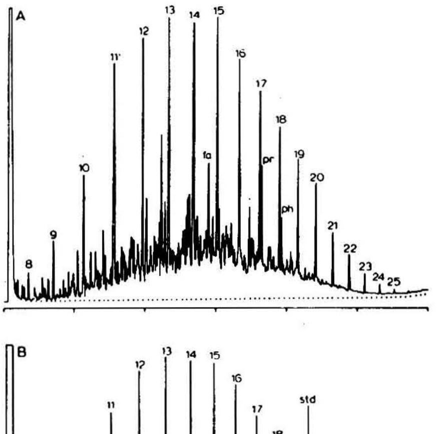

Figure 1. Gas chromatograms (SE-52, capillary column, programmed from 40 to 260 °C at 4 °C/min after a 4-min initial hold) of hydrocarbons in the no. 2 fuel oil (A) and in the F_1 (B) and F_2 (C) fractions of the oil–water dispersion. fa, pr, and ph are farnesane, pristane, and phytane; the numbers are *n*-alkanes of that carbon number; C_3-B, C_4-B, N, C_1-N, C_2-N, and C_3-N show the approximate elution ranges of alkyl-substituted benzenes, naphthalene, and alkyl-substituted naphthalenes with the indicated number of substituted carbon atoms; std. is the internal standard (3-methylnonadecane in part B; phenanthrene in part C). The dotted lines show the column bleed signal

1977 experiment were found in samples of a flocculent layer at the sediment–water interface (*13, 14*), it was felt that the old corer might not have quantitatively sampled this layer, and thereby might have caused an underestimation of the amount of oil in the sediments. For this reason, the corer design was changed from a one-way ball valve to a spring-action lid with an inner liner of Teflon for the 1978–1979 experiment. The corer was attached to a pipe 6 m long, and was manually forced into the sediments, withdrawn, and removed from the tank.

To estimate the average oil content of the sediments and to minimize the effect of an irregular areal distribution of hydrocarbons in the sediments, from two to four (usually three) cores were collected on each sampling date. The cores were extruded, with care taken to collect all of the surface layer, and cut at the desired depth intervals. Sediments from the same depth interval and tank were pooled and analyzed as one sample. Of the three oiled tanks, samples were routinely collected and analyzed only from no.'s 2 and 7.

Samples of suspended particulate matter were collected from the tanks in traps consisting of plastic graduated cylinders held below the water surface with nylon fishing line. To measure the concentration of particulates, a known volume of water was collected while the tanks were being mixed (*12, 13*). The water was filtered through a weighed Nuclepore pad (nominal pore size 0.4 μm), and the pad was washed with distilled water, dried, and reweighed.

Sample Analysis. The tank 7 sediment samples were analyzed in one laboratory, and all other samples in another. The analytical procedures used in the two laboratories were generally similar and most have been published (*13, 14, 19*). Internal standards (3-methylnonadecane or n-C_{20} or n-C_{22}, and anthracene or phenanthrene) were added before extraction of hydrocarbons. They were extracted from particulate matter by refluxing with 0.5 N KOH in CH_3OH plus 10% v/v H_2O. Sediments were refluxed with the same KOH solution, with the solution plus toluene, or with CH_3OH alone. All techniques were similar in their ability to extract hydrocarbons (*20*). After refluxing, the hydrocarbons were partitioned into petroleum ether and concentrated on a rotary evaporator. Thin-layer chromatography (silica gel) or column chromatography (silica gel or silica gel and alumina) was used to purify and split this isolate into two fractions: F_1, which contained saturated and olefinic hydrocarbons with one or two double bonds, and F_2, which contained aromatic hydrocarbons.

The hydrocarbon fractions were analyzed by gas chromatography. The extracts of suspended particulates and sediments from tank 2 were analyzed on a Perkin-Elmer Model 3920B gas–liquid chromatograph (GLC) equipped with flame ionization detectors. The early sediment extracts were run using two matched, stainless steel (2 m × 3.2 mm) packed columns containing 4% FFAP on Gas-Chrom Z (80–100 mesh) from Applied Science Laboratories, Inc., which were temperature programmed from 90 to 230 °C at 8 °C/min after a 4-min initial hold. The rest of these samples were run using a wall-coated, open tubular (WCOT) glass capillary column (SE-52, 25 m × 0.25 mm, from Applied Science Laboratories, Inc.), programmed from 40 to 260 °C at 4 °C/min after a 4-min initial hold. The extracts of sediment samples from tank 7 were analyzed on a Hewlett-Packard Model 5710A GLC with a flame ionization detector and a WCOT glass capillary column (either OV-101, 15 m × 0.25 mm, from Applied Science Laboratories, Inc., or SE-52, 20 m × 0.25 mm, J & W Scientific Co. from Supelco, Inc.), programmed from 40 to 270 °C at 4 °C/min. Quantification was made by comparing the area of the internal standard to the area of the resolved components and unresolved complex mixture using triangulation, planimetry, or cutting and weighing. An Infotronics (Columbia Scientific Industries) Model 3 Supergrator and a Hewlett-Packard Model 3385A calculating integrator were also used for measurement of resolved components.

The precision of analysis of hydrocarbons in the sediment was estimated from a well-homogenized sample from Narragansett Bay. Relative standard deviations of 5 and 8% were obtained by the two laboratories (*14*).

Results

Sediments. Samples were collected from the experimental tanks before oil additions began and from control tanks throughout the experiment. The distribution of hydrocarbons in them was essentially the same as that reported for sediments from the collection site in Narragansett Bay (*8, 19, 21*). Within the elution range of no. 2 fuel oil (Kovats Index 1200 to 2200) the mean concentrations of F_1 and F_2 hydrocarbons were 39 ± 7 and 6 ± 1 μg/g, respectively.

The concentration of no. 2 fuel oil hydrocarbons in sediments from the oiled tanks was calculated by subtracting from the measured hydrocarbon concentration (in the proper elution range) the appropriate mean concentration of the control sediments. The amount of oil at each depth in the entire tank was then estimated by extrapolation, using the formula:

$$\text{(oil in tank sediments)} = \text{(oil in sample)} \times \text{(total sediment area)}/\text{(sampled area)}$$

To estimate the precision of the grams/tank values for no. 2 fuel oil hydrocarbons, cores collected from a tank were not pooled but were analyzed separately on several occasions. The relative standard deviations were ±33% (three samples from tank 9 on July 14, 1978), ±40% (four samples from tank 7 on May 2, 1979), and ±73% (five samples from tank 2 on May 2, 1979). These values suggest that oil may have been unevenly distributed across the sediments.

A plot of the amount of no. 2 fuel oil hydrocarbons (grams/tank) added to the water column and found in pooled cores from the sediments is shown in Figure 2. The cumulative amount of oil added to the ecosystems increased at a steady rate. The amount found in the sediments increased at a much slower rate for the first 10 weeks of dosing; a similar lag was found in the 1977 experiment. The sedimentary oil climbed quickly from the 10th week until dosing ended. The maximum amounts found in the sediments (7 days after the last oil addition) represented 48% (tank 2) and 56% (tank 7) of the F_1 hydrocarbons introduced to the ecosystems, and 17% (tank 2) and 9% (tank 7) of the F_2 hydrocarbons. The concentrations (μg/g) of F_1 oil were (tank 2/tank 7): 0–1 cm, 805/1120; 1–2 cm, 427/365; 2–3 cm, 23/121. The corresponding values for F_2 oil were: 0–1 cm, 129/58; 1–2 cm, 55/22; 2–3 cm, 4/5.

The decline in sedimentary oil after dosing ended was as abrupt as the increase. Over the next 6–10 weeks following the high point, the levels in both tanks' sediments decreased to about 14% (4 g/tank) of the F_1 dose and 8% (1 g/tank) of the F_2 dose added to the tanks. The values measured in the 1978–1979 experiment were generally much higher than those found in 1977, but it appears that the actual trend in 1977 was similar to that of the later experiment. The differences are probably attributable to the change in corer design, because the final tank 2 sample from the 1977 experiment, collected with an open-barrel corer, had an oil content which, when extrapolated, was 15.8 g/tank, or 19% of the F_1 dose. Samples collected in 1978 at a similar 2-month period after additions ended gave values of 14% (tank 2) and 31% (tank 7) of the F_1 dose in that experiment. In a direct comparison in 1978, an order of magnitude more oil was found in the top centimeter of cores collected with the new corer than in sediment from the old ball valve corer. These data suggest that the sedimentary oil contents reported from the 1977 experiment (*13, 14*) are erroneously low.

Except for one higher value for the F_2 fraction, the oil concentrations in tank 2 did not change significantly in the last 10 months of the 1978–1979 experiment. In tank 7 on three late sampling dates (352, 367, and 422 days after the experiment began), the levels of F_1 oil in the sediments were considerably above the low point reached earlier. To check the results from days 352 and 367, the 0–1-cm sections of the four cores taken on day 422 were analyzed separately. They contained F_1 oil derived hydrocarbons which extrapolated to grams/tank values of 3.1, 7.3, 7.6, and 4.3, for a relative standard deviation of 40%, suggesting that the earlier analyses had not been in error. By the final sampling (day 504), the F_1 concentration in tank 7 was down to 3.5 g/tank.

The distribution of no. 2 fuel oil hydrocarbons with depth in the sediment was generally similar to that reported for the 1977 experiment (*14*). The 1978–1979 results for fuel oil derived saturates in tanks 2 and 7 are shown in Figure 3. The greatest amounts of oil were found initially in an unconsolidated floccule at the sediment–water interface. This yellowish brown, watery layer, which was clearly distinguishable from

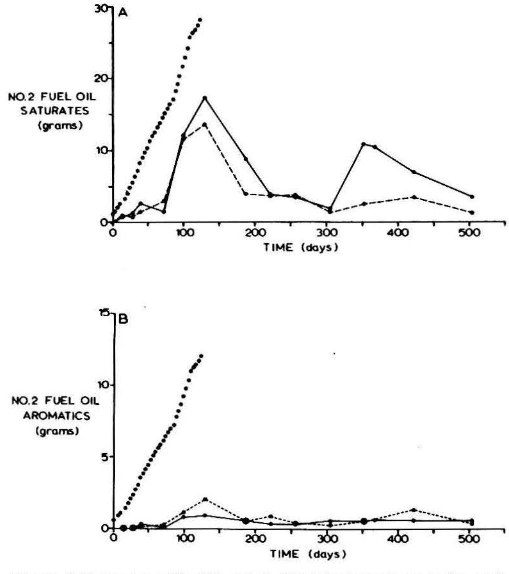

Figure 2. Estimates of F_1 (A) and F_2 (B) oil hydrocarbons in the sediments of tank 2 (dashed line) and tank 7 (solid line) with time after oil additions began. The line of unconnected dots shows the cumulative amount of each oil fraction added to the ecosystems

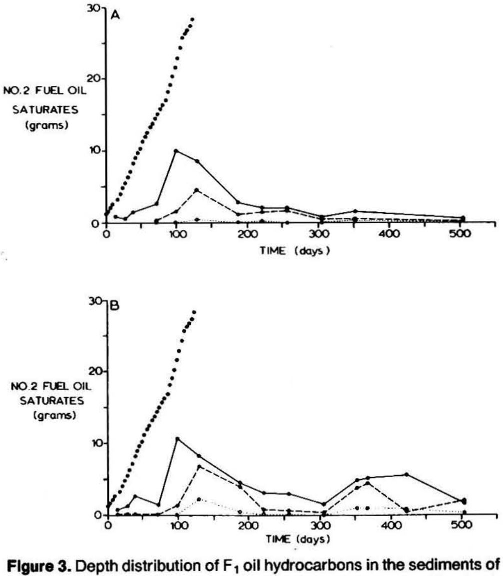

Figure 3. Depth distribution of F_1 oil hydrocarbons in the sediments of tank 2 (A) and tank 7 (B) with time after oil additions began. The depth intervals are: solid line, 0–1 cm; line of long dashes, 1–2 cm; line of short dashes, 2–3 cm. The line of unconnected dots shows the cumulative amount of F_1 oil added to the ecosystems

the gray, consolidated sediments below, was found in all cores collected from the oiled tanks after dosing began. It increased in thickness from an initial 1–2 mm to nearly 1 cm in cores taken 6 months after the last oil addition. An analogous layer in cores from the control tanks was not always present, and was never more than 2 mm thick. This feature was the most obvious visual difference between oil and control tank cores.

As in the previous oil experiment (*14*), the maximum depth of penetration of oil hydrocarbons, in greater than trace amounts, was 3 cm, the estimated depth to which sediments are mixed in mid-Narragansett Bay (*22*). Both in tank 2 and in tank 7, the highest oil contents were found throughout the experiment at depths of 1 cm or above, with lesser amounts in the 1–2-cm interval and still less at 2–3 cm (Figure 3). The unexpectedly high levels of oil that occurred in tank 7 three times late in the experiment were not related to the variation of the concentration of oil with sediment depth. All three depth intervals were relatively rich in F_1 oil on two of the three dates, whereas on the other date only the 0–1-cm layer was especially high in fuel oil hydrocarbons.

In addition to the changes with time detailed above, the sedimentary oil also altered in chemical composition during the experiment (Figures 4 and 5). In the first samples of the surface flocculent layer from tank 2, collected 2 weeks after oil additions began, we found an almost unweathered oil with a total hydrocarbon ($F_1 + F_2$) distribution (Figure 4A) very similar to that of the F_1 fraction of the dosing dispersion. Figure 4B is a gas chromatogram of the total hydrocarbons ($F_1 + F_2$) from a sample of the surface flocculent layer of tank 2 which was collected 39 days after dosing started, or about 3 weeks after the sample whose chromatogram is shown in Figure 4A. The oil was quite weathered, with all resolved components decreased in comparison to those of the unresolved complex mixture. This trend continued with time. Figures 5A and 5B show the patterns of F_1 and F_2 hydrocarbons in the 0–1-cm depth interval of sediment from tank 7 (the dotted lines show the profile of the same fractions from sediment in a control tank). These samples were collected 9 weeks after oil additions had ended, or 27 weeks after they had begun. The chromatograms are fairly typical for sediments taken after the early part of the experiment. They show for both fractions a few resolved components (including isoprenoids but no obvious n-alkanes in the F_1 fraction) overlying a large, unresolved envelope.

The progress of weathering of the F_1 oil fraction in the 0–1-cm sediment depth interval is represented in Figure 6, in which the value of the ratio of n-C_{18} to phytane is plotted logarithmically vs. time after dosings began. Since n-alkanes are microbially degraded more quickly than highly branched hydrocarbons such as the isoprenoids (see, e.g., ref *23*), ratios like the above have been used as a relative measure of the degree of biodegradation of petroleum (*24*). In the sediments of both tanks the values followed an exponential decay pattern more closely than they did a linear one, with correlation coefficients (r^2) of 0.825 for tank 2 and 0.939 for tank 7. The calculated intercept for the tank 7 samples was closer than that for tank 2 to the actual value of n-C_{18}/phytane in the dosing oil, but the slopes or decay rates of the two lines were virtually the same. The half-life of the ratio for the sediments of each tank was calculated to be about 58 days.

Much higher concentrations of fuel oil derived hydrocarbons were found in the F_1 fractions of sedimentary extracts than in the F_2 fractions (Figure 2). As in the previous MERL experiment (*13*), the bulk of the oil that reached the sediments was paraffinic rather than aromatic in character. The concentrations of oil hydrocarbons in the two fractions from tank samples could be fitted to a linear regression of the form:

$$(F_2) = m(F_1) + b$$

with the following results: for tank 2 sediments, $m = 0.13$, $b = 1.1$ μg/g; for tank 7, $m = 0.05$, $b = 3.5$ μg/g. Since the ratio of F_2 to F_1 for the dosing dispersions (analogous to the m in

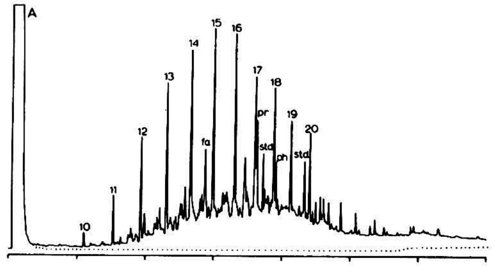

Figure 4. Gas chromatograms (SE-52, capillary column) of total hydrocarbons ($F_1 + F_2$) in samples of the surface flocculent layer of sediment from tank 2, collected 14 days (A) and 39 days (B) after oil additions began. The chromatographic conditions and labels are as described in the caption for Figure 1. The internal standards are phenanthrene (eluting at ~37 min) and 3-methylnonadecane (eluting at ~43 min). The dotted lines show the column bleed signal

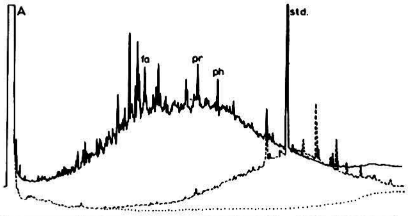

Figure 5. Gas chromatograms of F_1 (A, OV-101, capillary column, programmed from 40 to 270 °C at 4 °C/min) and F_2 (B, SE-52, capillary column) hydrocarbons in samples of the 0–1-cm layer from tank 7 (solid lines) and control tank 4 (dashed lines), collected 187 days after oil additions began. The labels are as described in the caption for Figure 1. The internal standards are n-C_{22} (A) and anthracene (B). The dotted lines show the column bleed signal

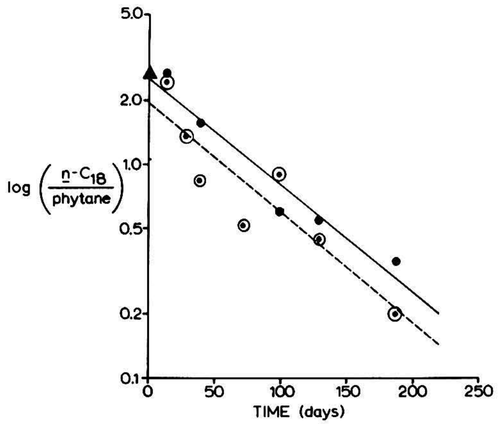

Figure 6. Relationship between value of log n-C_{18}/phytane ratio in extracts of the 0–1-cm sediment depth interval and time after oil additions began. For tank 2 (open circles, dashed line) exponential regression gave a slope (k) of −0.0120 day^{-1} and correlation coefficient (r^2) of 0.825; for tank 7 (solid circles and line) the slope was −0.0117 day^{-1} with r^2 of 0.939. The triangle shows the value of n-C_{18}/phytane (2.68) in the original oil

the equation above) was about 0.38, it can be seen that the ratio of aromatics to saturates was considerably lower in the sediments than in the original oil. The coefficients of determination (r^2) for tanks 2 and 7 were 0.92 and 0.79, indicating that, once in the sediment, the two oil fractions remained in about the same proportions.

Another difference was noted between the two fractions of sedimentary oil. While the complete boiling range of saturated hydrocarbons from the oil was found, the aromatic components were chiefly the higher molecular weight hydrocarbons. This difference cannot be attributed to evaporative losses during the analyses because saturated compounds of low volatility were carried through the same procedures, but it may be related to differences in aqueous solubility. Compounds in the aromatic fraction of no. 2 fuel oil, especially the lower molecular weight species, are generally more soluble in water than their saturated counterparts (*25–29*). A fractionation of oil according to the degree of aqueous solubility of its component compounds, as found in the ecosystem sediments, has been shown in laboratory experiments on the adsorption of individual hydrocarbons and no. 2 fuel oil to clay particles and natural sediments (*30–32*). Highly insoluble hydrocarbons such as the medium and high molecular weight n-alkanes are adsorbed in preference to slightly soluble compounds such as naphthalene. Meyers and Oas (*31*) suggested that the eventual settling of such suspended solids could bring a fractionated suite of oil hydrocarbons to the sediments.

Suspended Particulate Matter. Samples from control tanks had hydrocarbon concentrations of 100–200 μg/g (F_1) and 10–50 μg/g (F_2). These values are at the low end of the range reported by Schultz and Quinn (*33*) for total hydrocarbons ($F_1 + F_2$) in suspended matter from mid-Narragansett Bay. The distribution of hydrocarbons associated with particulates from control tanks was similar to that in sediment from those tanks, the chief characteristic being a high molecular weight unresolved envelope. The concentrations of hydrocarbons in the boiling range of no. 2 fuel oil were 15–60 μg/g (F_1) and 2–15 μg/g (F_2).

Table I lists the concentrations of F_1 and F_2 hydrocarbons in the no. 2 fuel oil range which were associated with suspended matter collected during the periods of oil addition in 1977 and 1978. The values are not corrected for the concentrations found in samples from control tanks. The level of fuel oil saturates varied from 3400 to 17 700 μg/g and was always much higher than the concentration of aromatics (150–3100 μg/g). Wade and Quinn (*14*) found a total of 9000 μg/g no. 2 fuel oil saturated hydrocarbons in a sedimentary trap sample from the 1977 MERL experiment. The total hydrocarbon concentrations reported here are in the same range as those for particulates from the Providence River (*33*), and from the Baltic Sea after the *Tsesis* oil spill (*34*).

In the oiled MERL tanks the hydrocarbons associated with suspended matter averaged 89% in the F_1 fraction and 11% in the F_2, for a mean F_2/F_1 value of 0.12. This is similar to the values calculated for sediments in tank 2 (0.13) and tank 7 (0.05), and much lower than in the dosing dispersion (~0.38). Like F_2 hydrocarbons in the sediments, the aromatics in particulate matter were skewed to the higher molecular weight end, with a depletion of benzenes and naphthalenes compared to larger compounds. The hydrocarbons associated with particulates resembled other oil in the water column in their degree of biodegradation, as measured by n-alkane to isoprenoid ratio values. When the tanks became microbially acclimated to oil, the preferential loss of n-alkanes and other quickly degraded hydrocarbons could be followed in particulate and water samples in the days between oil additions (*13*). The sedimentation of such partially degraded hydrocarbon assemblages may help to account for the rapid appearance of weathered oil in the sediments.

Table II presents a budget for fuel oil hydrocarbons in the water column, both associated with particulate material and

Table I. No. 2 Fuel Oil Hydrocarbons Associated with Suspended Particulate Matter (SPM)

date	days after oil addition	F_1 hydrocarbons concn [a]	F_1 hydrocarbons % [b,c]	F_2 hydrocarbons concn [a]	F_2 hydrocarbons % [b,d]
2/28/77	4	5 020	91.4	470	8.6
3/7/77	5	4 060	87	610	13
3/14/77	7	9 060	93.2	700	6.8
5/16/77	1	8 480	96.1	340	3.9
5/18/77	3	17 700	85	3100	15
5/20/77	5	3 400	95.8	150	4.2
3/8/78 [e]	2	12 100	97.4	320	2.6
3/18/78 [e]	12	3 590	70	1560	30
7/7/78	1	7 770	87	1190	13
7/8/78	2	5 800	87	860	13
			av 89		av 11

[a] Micrograms of hydrocarbons/gram of SPM. [b] Percent of total oil associated with SPM in this hydrocarbon fraction. [c] In the dosing dispersion this percentage was 70–75. [d] In the dosing dispersion this percentage was 25–30. [e] Samples taken from a prototype microcosm (see ref *15* for details).

Table II. Budget for No. 2 Fuel Oil Hydrocarbons in MERL Water Column

date	days after oil addition	total water column [a]		associated with suspended particulates		
		concn [b]	g/tank [c]	concn [d]	g/tank [c]	%
			F_1 Hydrocarbons			
3/8/78	2	104	1.35	12 100	0.63	46
3/18/78	12	30	0.39	3 590	0.19	49
7/7/78	1	76	0.99	7 770	0.39	39
7/8/78	2	50	0.65	5 800	0.24	37
			F_2 Hydrocarbons			
3/8/78	2	44	0.57	320	0.0165	2.9
3/18/78	12	30	0.39	1 560	0.081	21
7/7/78	1	32	0.42	1 190	0.0595	14
7/8/78	2	20	0.26	860	0.0356	13

[a] Volume = 13 000 L. [b] μg of oil/L of water. [c] g of oil/tank. [d] μg of oil/g of SPM.

dissolved or accommodated, on four occasions during the 1978 oil addition period. The March set was taken after the first dosing to a prototype microcosm (*15*), and the July pair was collected from tank 7 after the last of 35 semiweekly dosings. The concentration of hydrocarbons in the water column was determined by extracting unfiltered water samples with petroleum ether, followed by column chromatography and gas chromatography. The levels of hydrocarbons associated with samples of particulate matter were extrapolated to grams of oil per tank using the concentration of the suspended load in the water. The data indicate that 37–49% of the saturated hydrocarbons in the water, but only 2.9–21% of the aromatics, could be accounted for in suspended matter. The good agreement between these values and the percentages of F_1 and F_2 oil found in the sediments (up to 48–56 and 9–17%, respectively) suggests that the transport of hydrocarbons in association with particulates was a major route to the sediments for the oil.

Discussion

These results suggest to us the following conclusions. No. 2 fuel oil hydrocarbons are transported from the water column of a MERL ecosystem according to their physical and chemical properties. Hydrocarbons in the water associate with suspended particulate matter in inverse proportion to their degree of aqueous solubility. This process fractionates the oil, and the eventual settling of the particulate material carries to the sediment about 50% of the relatively insoluble, saturated hydrocarbons, but less than 20% of the relatively more soluble, aromatic hydrocarbons. Once in the sediments these compounds are slowly mixed down through the zone of bioturbation. The biodegradation of oil-derived hydrocarbons begins in unacclimated ecosystems almost immediately after they reach the sediments, and begins in acclimated ecosystems even earlier, on the suspended particulates en route to the sediments. Biodegradation and other weathering processes remove many of these hydrocarbons soon after the source of the oil is removed, but a residue of branched alkanes, cycloalkanes, and aromatics in an unresolved complex mixture, comprising 10–20% of the hydrocarbons originally present in the sediments, persists for at least 1 year after the end of oil addition.

A major difference between the results presented in this paper and those of the 1977 MERL experiment is the relative importance of the ecosystem sediments as an oil reservoir. We attribute the apparent difference between the two experiments primarily to a change in the design of the corer used in sampling rather than to a change in the behavior of the oil. The investigators of the spill by the tanker *Tsesis* found oil-derived hydrocarbons in suspended matter but were unable to measure such hydrocarbons in their sediment samples; they suggested that their sampling technique (gravity corer) may not have collected the uppermost layer of sediments (*34*). Whether the change in the system of seawater delivery to the MERL tanks had an effect on the behavior of the oil is unknown. The inputs in 1977 near the sediment surface may have caused resuspension of surface floc containing oil-derived hydrocarbons, but the flow rate was probably too low to disturb the sediments greatly.

The no. 2 fuel oil added to the ecosystems was not dense enough to sink unaided to the sediments. We have suggested its sedimentation in association with particles sinking through the water because of the similarity of hydrocarbon compositions between suspended particulate matter and sediment, with aromatics being deficient in both, and because of the approximate mass balance for oil hydrocarbons between the two. An exact mass balance would include factors for the fraction of particulate material which is consumed before reaching the sediment and for the resuspension of sediment back into the water, but data are available for neither of these.

The sorption behavior of hydrocarbons and other organic compounds with low aqueous solubilities has been the subject of laboratory studies. The extent of sorption appears to be inversely proportional to the solubility of the compound (*31*, *35*) and the size of the sorbent particles (*36*), and directly proportional to the percentage of organic matter in the particles (*36–38*), although Meyers and Quinn (*30*) found that adsorption of no. 2 fuel oil hydrocarbons to natural sediments was increased when the organic matter in the sediments was removed. Suspended particulate matter in the MERL ecosystems was quite rich in organic carbon (3.5 to 10.5%, averaging about 7%; *39*), so according to most studies adsorption of insoluble hydrocarbons should have been extensive.

The extent of sorption also appears to depend on the physical state of the organic compound in the water. When oil is found as droplets (in the milligrams/liter to grams/liter range), physical agglomeration of oil and particles occurs (*32*, *40*), and there is little chemical fractionation of the hydrocarbons (*32*). At low concentrations of hydrocarbons dissolved in the water, adsorption to sediments low in organic carbon appears to be insignificant (*41*). The results presented here are intermediate between these two. In the MERL water column, most of the aromatic hydrocarbons passed through a glass fiber filter with a pore size of 0.3 μm, and thus were either dissolved or solubilized, whereas more than 90% of the saturated hydrocarbons were retained on such a filter (*15*). Sorption of these saturated hydrocarbons could be expected to be much greater than sorption of dissolved or solubilized compounds. Zurcher and Thuer (*32*) found a fractionation onto particulate material at low oil concentrations similar to that in the MERL tanks, and Lee et al. (*11*) observed preferential adsorption to suspended matter of high molecular weight aromatics over smaller aromatics in a CEPEX ecosystem experiment.

If suspended matter was a major carrier of oil to the tanks' sediments, the number of particles as well as their character would affect the buildup of oil in the benthos. At the start of the experiment, the suspended loads decreased following a diatom bloom and remained fairly low (~2 mg/L) for approximately 2 months (*42*). Both sedimentary oil and suspended load began rising in May, although while the former increased by 5–6 times, the latter was increasing by only a factor of 2–3.

The end of the 10-week lag period also coincided approximately with increases in temperature and, presumably, bioturbation (*43*). In the warmer (>15 °C) weather, a greater proportion of the oil reaching the sediments may have been preserved (at least temporarily) by burial.

Other postulated mechanisms which could make oil heavy enough to sink to the sediments include weathering and ingestion by zooplankton. During its short residence in the bulk water column of the ecosystems, the no. 2 fuel oil was only slightly fractionated by evaporative weathering (*15*). Oil ingested by zooplankton could be made heavier, when excreted, by incorporation with the organisms' feces (*44*). There was oil associated with the zooplankton in the ecosystems in 1977 (*45*), but the relative importance of this mechanism in the MERL experiments can only be estimated. On the bases of filtering rates and numbers of zooplankton present, Vargo (*46*) calculated that zooplankton filtered only 0.2–0.5% of the water in the oil tanks per day. If the efficiency of oil extraction by the organisms were 100%, and all of the oil excreted as sinkable particles, the amount transported to the sediments by this pathway would still be small compared to that associated with suspended particulate matter in general, assuming equal settling rates for zooplankton feces and other particulate material.

During most of the experiment the sedimentary oil findings for tanks 2 and 7 were very close, in grams of oil per tank, composition of the hydrocarbons, depth of penetration into the sediment, and rate and degree of biodegradation. The similarities extended to the pattern of buildup and decay, including an initial lag period during the early part of dosing and a quick decrease immediately after dosing ended (Figure 1). The similarity of agreement of these results obtained by separate laboratories lends credence to the data. The results from the two laboratories diverged for samples collected in 1979 at 352, 367, and 422 days after the start of the experiment. On those dates the samples from tank 7 had concentrations of weathered no. 2 fuel oil derived hydrocarbons that extrapolated to considerably more oil than was found for tank 2. Since no oil was added to tank 7 after the general dosing period ended in July 1978, we may a priori assume that the large amounts of hydrocarbons in those samples were due to the unevenness in the distribution of oil in the sediments. Inhomogeneity of the oil across the sediment is shown by the high relative standard deviations of oil content in separately analyzed cores from tanks 2 (73%), 7 (40%), and 9 (33%). The increase in sedimentary oil in tank 7 during the later stages of the experiment points out the usefulness and importance of experimental duplication, and also the difficulties likely to be found in estimating accurately the amount of oil in the sediments after spills in the ocean.

The rapid qualitative and quantitative changes attributed to biodegradation of the low molecular weight, no. 2 fuel oil hydrocarbons occurred while the higher molecular weight unresolved mixture which was indigenous to the sediments remained unaltered. The reason for the difference in stability may be related to the physical or chemical binding to the sediment of each hydrocarbon suite, or to a difference, based on molecular weight, in the potential for biodegradation (*23*). A similar change in hydrocarbon composition has been noted for sediments between the Providence River and upper Narragansett Bay (*46, 47*).

The pattern of a quick initial disappearance of oil-derived hydrocarbons from the ecosystem sediments once the source of oil was removed, followed by a much slower decrease over the next 300 days, has been found on a longer time scale after a no. 2 fuel oil spill in the field (*48*). The slow, incremental additions to the ecosystems may have allowed bacterial populations more time for adjustment than a sudden, large, potentially toxic spill.

The results of the second ecosystem experiment indicate that the sediments are a quantitatively important reservoir for hydrocarbons from even a light distillate cut such as no. 2 fuel oil. In contrast to the water column, from which the oil hydrocarbons disappeared within 2 weeks after dosing ended (*15*), the sediments still contained hydrocarbons from the oil at the end of the experiment, over 1 year later. These data are in agreement with findings from field studies (*48–51*) that the residence time for petroleum hydrocarbons in sediments is, at the least, on the order of years. Most of the experiments on the toxicological effects of hydrocarbons on organisms have been conducted with low to medium molecular weight aromatics such as naphthalenes. There is a need for information on the long-term effects on the benthos of hydrocarbons which have proved to be refractory in sediments, including the medium and high molecular weight components of chromatographically unresolved mixtures, both saturated and aromatic.

Acknowledgment

We thank John Farrington and Richard Lee for their advice and assistance throughout this work, and Harry McCarty for help with the oil additions and the collection of some of the sediment samples.

Literature Cited

(1) Hottel, H. C., Howard, J. B., "New Energy Technology—Some Facts and Assessments", Massachusetts Institute of Technology, 1971.
(2) Walker, J. D., Colwell, R. R., Hamming, M. C., Ford, H. T., *Environ. Pollut.*, **9**, 231–8 (1975).
(3) Wakeham, S. G., Carpenter, R., *Limnol. Oceanogr.*, **21**, 711–23 (1976).
(4) Farrington, J. W., Frew, N. M., Gschwend, P. M., Tripp, B. W., *Estuarine Coastal Mar. Sci.*, **5**, 793–808 (1977).
(5) Boehm, P. D., Quinn, J. G., *Estuarine Coastal Mar. Sci.*, **6**, 471–94 (1978).
(6) Van Vleet, E. S., Quinn, J. G., *J. Fish. Res. Board Can.*, **35**, 536–43 (1978).
(7) Hurtt, A. C., Quinn, J. G., *Environ. Sci. Technol.*, **13**, 829–36 (1979).
(8) Wade, T. L., Quinn, J. G., *Org. Geochem.*, **1**, 157–67 (1979).
(9) Strickland, J. D. H., *New Sci.*, 276–8 (Feb 2, 1967).
(10) Lee, R. F., Anderson, J. W., *Bull. Mar. Sci.*, 127–34 (1977).
(11) Lee, R. F., Gardner, W. S., Anderson, J. W., Blaylock, J. W., Barwell-Clarke, J., *Environ. Sci. Technol.*, **12**, 832–8 (1978).
(12) Pilson, M. E. Q., Vargo, G. A., Gearing, P., Gearing, J. N., "Proceedings of the Second National Conference on Interagency Energy/Environment R and D Program", Environmental Protection Agency, Washington, D.C., 1977, pp 513–6.
(13) Gearing, J. N., Gearing, P. J., Wade, T., Quinn, J. G., McCarty, H. B., Farrington, J., Lee, R. F., "Proceedings of 1979 Oil Spill Conference (Prevention, Behavior, Control, Cleanup)", American Petroleum Institute, Environmental Protection Agency, and United States Coast Guard, Los Angeles, Calif., 1979, pp 555–64.
(14) Wade, T. L., Quinn, J. G., *Mar. Environ. Res.*, **3**, 15–33 (1980).
(15) Gearing, P. J., Gearing, J. N., unpublished results.
(16) Gearing, P. J., Gearing, J. N., unpublished results.
(17) Pilson, M. E. Q., Oviatt, C. A., Vargo, G. A., Vargo, S. L., "Proceedings of Symposium on State of Marine Environmental Re-

search", Environmental Protection Agency, Washington, D.C., EPA-600/9-79-035, 1979, pp 359–81.
(18) Elmgren, R., *Oikos Suppl.*, **15**, 112–20 (1973).
(19) Gearing, J. N., Gearing, P. J., Lytle, T. F., Lytle, J. S., *Anal. Chem.*, **50**, 1833–6 (1978).
(20) Hoffmann, E. J., Quinn, J. G., Graduate School of Oceanography, University of Rhode Island, Kingston, R.I., 1980, unpublished data.
(21) Farrington, J. W., Quinn, J. G., *Estuarine Coastal Mar. Sci.*, **1**, 71–9 (1973).
(22) Santschi, P. H., Li, Y. H., Carson, S., *Estuarine Coastal Mar. Sci.*, in press.
(23) Mechalas, B. J., Meyers, T. J., Kolpack, R. L., in "The Microbial Degradation of Oil Pollutants", Ahern, D. G., Meyers, S. P., Eds., Louisiana State University Publication No. LSU-GG-73-01, 1973, pp 67–79.
(24) Ehrhardt, M., Blumer, M., *Environ. Pollut.*, **3**, 179–94 (1972).
(25) Anderson, J. W., Neff, J. M., Cox, B. A., Tatem, H. D., Hightower, G. M., *Mar. Biol.*, **27**, 75–88 (1974).
(26) Boylan, D. B., Tripp, B. W., *Nature (London)*, **230**, 44–7 (1971).
(27) McAuliffe, C., *J. Phys. Chem.*, **70**, 1267–75 (1966).
(28) Peake, E., Hodgson, G. W., *J. Am. Oil Chem. Soc.*, **43**, 215–22 (1966).
(29) Eganhouse, R. P., Calder, J. A., *Geochim. Cosmochim. Acta*, **40**, 555–61 (1976).
(30) Meyers, P. A., Quinn, J. G., *Nature (London)*, **244**, 23–4 (1973).
(31) Meyers, P. A., Oas, T. G., *Environ. Sci. Technol.*, **12**, 934–7 (1978).
(32) Zurcher, F., Thuer, M., *Environ. Sci. Technol.*, **12**, 838–43 (1978).
(33) Schultz, D. M., Quinn, J. G., *Org. Geochem.*, **1**, 27–36 (1977).
(34) Boehm, P. D., in "The *Tsesis* Oil Spill: A Cooperative International Investigation", Asko Laboratory, Sweden, 1979.
(35) Boucher, F. R., Lee, G. F., *Environ. Sci. Technol.*, **6**, 538–43 (1972).
(36) Lotse, E. G., Graitz, D. A., Chesters, G., Lee, G. B., Newland, L. W., *Environ. Sci. Technol.*, **2**, 353–7 (1968).
(37) Herbes, S. E., *Water Res.*, **11**, 493–6 (1977).
(38) Pierce, R. H., Jr., Olney, C. D., Felbeck, G. T., Jr., *Geochim. Cosmochim. Acta*, **38**, 1061–73 (1974).
(39) Kopchynski, K., Hunt, C., Graduate School of Oceanography, University of Rhode Island, Kingston, R.I., 1980, unpublished data.
(40) Bassin, N. J., Ichiye, T., *J. Sediment. Petrol.*, **47**, 671–7 (1977).
(41) Malinky, G., Shaw, D. G., "Proceedings of 1979 Oil Spill Conference (Prevention, Behavior, Control, Cleanup)", American Petroleum Institute, Environmental Protection Agency, and United States Coast Guard, Los Angeles, Calif., 1979, pp 621–3.
(42) Hunt, C., Vargo, G. A., Graduate School of Oceanography, University of Rhode Island, Kingston, R.I., 1980, unpublished data.
(43) Myers, A. C., *J. Mar. Res.*, **35**, 609–32 (1977).
(44) Conover, R. J., *J. Fish. Res. Board Can.*, **28**, 1327–30 (1971).
(45) Gearing, P. J., Gearing, J. N., Graduate School of Oceanography, University of Rhode Island, Kingston, R. I., 1980, unpublished data.
(46) Vargo, G. A., Graduate School of Oceanography, University of Rhode Island, Kingston, R. I., 1980, unpublished data.
(47) Van Vleet, E. S., Quinn, J. G., *Environ. Sci. Technol.*, **11**, 1086–92 (1977).
(48) Farrington, J. W., Quinn, J. G., *J. Water Pollut. Control Fed.*, **45**, 704–12 (1973).
(49) Blumer, M., Sass, J., *Science*, **176**, 1120–2 (1972).
(50) Keizer, P. D., Ahern, T. P., Dale, J., Vandermeulen, J. H., *J. Fish. Res. Board Can.*, **35**, 528–35 (1978).
(51) Mayo, D. W., Page, D. S., Cooley, J., Sorenson, E., Bradley, F., Gilfillan, E. S., Hanson, S. A., *J. Fish. Res. Board Can.*, **35**, 552–67 (1978).
(52) Teal, J. M., Burns, K., Farrington, J. W., *J. Fish. Res. Board Can.*, **35**, 510–20 (1978).

Received for review November 13, 1979. Accepted April 7, 1980. Research supported by Environmental Protection Agency Grant No. R803902020.

Biogeochemistry of Benzanthracene in an Enclosed Marine Ecosystem

Kenneth R. Hinga[1]* **and Michael E. Q. Pilson**
Marine Ecosystems Research Laboratory, Graduate School of Oceanography, University of Rhode Island, Kingston, R.I. 02881
Richard F. Lee
Skidaway Institute of Oceanography, Savannah, Ga. 31406
John W. Farrington, Kjell Tjessem,[2] **and Alan C. Davis**
Department of Chemistry, Woods Hole Oceanographic Institution, Woods Hole, Mass. 02543

■ Carbon-14 labeled benz[*a*]anthracene was introduced into a large-scale marine microcosm containing an ecosystem functioning in a manner that was in many respects typical of the shallow coastal waters of the northeastern United States. The radiotracer label made it possible to follow the removal of benz[*a*]anthracene and labeled metabolites from the water column, their appearance and mixing into the sediments, and the production of $^{14}CO_2$ for 230 days. At the end of the experiment, 29% had been respired to CO_2, while the remaining extractable activity (43%) was evenly divided between parent compound and intermediate metabolic products.

The biogeochemistry of polycyclic aromatic hydrocarbons (PAHs) in coastal and estuarine ecosystems is important because of the deleterious effects some of these compounds may have on natural resources and human health (*1–3*). PAHs are released to the environment by a variety of processes such as oil spills, combustion of fossil fuels, forest and grass fires, and industrial effluents (*4–8*). Analyses of cores containing a historical record of near-shore marine and lake sediments (*9–13*) indicate increases in concentrations of PAHs by as much as an order of magnitude from ca. 1850 to the present. We can expect that fossil fuel combustion as currently practiced will continue to cause increasing levels of PAHs in the marine environment, especially if there is increased coal combustion in the next century (*4, 5*). Thus, it is important to understand the biogeochemistry of polycyclic aromatic hydrocarbons in coastal and estuarine areas in order to provide a basis for an evaluation of their long-term effects on these ecosystems.

The approach utilized in this experiment was to introduce a ^{14}C-labeled PAH, benz[*a*]anthracene, into a large marine microcosm. The concentrations of labeled parent compound, some of its metabolites, and $^{14}CO_2$ generated from the breakdown of the labeled compounds were measured in various compartments of the ecosystem in the microcosm tank. Since these microcosms contain functioning marine ecosystems (*14–17*), the study was conducted under reasonably natural conditions, with natural populations, for a period of

---

[1] Present address, Lamont-Doherty Geological Observatory, Columbia University, Palisades, N.Y. 10964.

[2] Present address, University of Bergen, Department of Chemistry, N-5014 Bergen, Norway.

0013-936X/80/0914-1136$01.00/0

time approaching 1 year. It was possible to account for essentially all the labeled compound added to the system. Benz[*a*]anthracene was chosen because it occurs in many crude oils and refined products, is a major constituent of PAH in combustion products, and is on the Environmental Protection Agency's list of unambiguous pollutants (*6, 8*).

Experimental

A large microcosm, one of 12 maintained by the Marine Ecosystems Research Laboratory (MERL) of the University of Rhode Island, was used for this study. Each microcosm is a fiberglass tank 1.8 m in diameter and 5.5 m in height, containing 13 m^3 of water and a 30-cm layer of sediment (*15*). The sediment in the tanks came from central Narragansett Bay and included a soft bottom community dominated by the polychaete *Mediomastis ambesita* and the bivalve *Nucula anulata*. During normal operation, approximately 120 L of water from adjacent Narragansett Bay (28–32 ‰ salinity) was pumped by a diaphragm pump into each tank four times daily, resulting in a washout rate of 3.7% per day. (This is a procedural improvement over the continuous flow regime noted in ref *15*. Flow rates were checked weekly.) The tanks were mixed for 2 h, four times a day, to simulate tidal currents and the turbulence regime in Narragansett Bay.

The MERL microcosms have, over several annual cycles, simulated adjacent Narragansett Bay with respect to biotic structure and chemical concentrations, processes, and rates (*14–17*). The enclosed ecosystems are large enough to allow many samples to be taken without noticeable depletion, and containment of the ecosystem makes it possible to identify the fate of nearly all the added material.

On May 29, 1978, approximately 200 μCi of 12-[^{14}C]benz[*a*]anthracene (Amersham Corporation, 49 mCi/mmol) was introduced into a MERL tank within an oil–water mixture. This mixture was prepared by shaking 20 mL of no. 2 fuel oil with 17 L of bay water. After 30 min of settling, the bottom 15 L was transferred to another bottle, and ~0.93 mg of [^{14}C]benz[*a*]anthracene in 19 mL of acetone was added to the oil–water mixture. The bottle was shaken and the mixture introduced into the tank at a depth of 2 m during a mixing cycle. Absorption of benz[*a*]anthracene onto the surfaces of the containers used during the spike resulted in some loss prior to addition into the tank; therefore, the estimate of the amount introduced was obtained by extrapolating concentrations in the tank water back to the time of addition. An identical oil addition except for the [^{14}C]benz[*a*]anthracene–acetone mixture was made in another MERL tank. Gas chromatographic analysis (*18*) of the water in this tank 1 h after the addition of the oil–water mixture indicated that ~1 g of oil had been added.

Sample Collection and Direct Counts. All samples except cores were taken during a mixing cycle, to ensure that the water column was homogeneous during sampling. Four liters of water was siphoned into glass bottles and 20 mL of hexane was added; the mixture was stirred for 5 h and then allowed to sit overnight. After the hexane layer was drawn off with a pipet, 50 mL of chloroform was added, the mixture was stirred for 4 h and allowed to settle overnight, and the chloroform layer was removed. Aliquots (1–2 mL) of the hexane extract samples were placed in 10 mL of scintillation cocktail (Aquasol, New England Nuclear) and counted for ^{14}C activity in a Beckman Model LS-3150T liquid scintillation counter at MERL. Duplicate samples were counted at Woods Hole Oceanographic Institution (WHOI) by adding appropriate aliquots of the extract to Aquasol scintillation cocktail and counting in a Beckman Model LS-100C liquid scintillation counter. Chloroform samples were also counted at WHOI by the same procedure. Counting efficiencies in all cases were 90% or better. MERL samples were prepared immediately after collection. WHOI hexane samples were stored at −15 °C, while chloroform samples were kept refrigerated.

Samples of particulate material were obtained by filtering 1 or 2 L of water through a 47-mm diameter Gelman A/E glass fiber filter. The filter was placed into 10 mL of cocktail and counted. Phytoplankton samples were obtained by a reverse flow concentration (*19, 20*) of 2 L of water down to 3 mL through a 10-μm nylon screen. One milliliter of the reverse flow concentrate was placed directly in Aquasol and counted. Zooplankton samples from 350 L of water were obtained by taking a single vertical tow the height of the tank with a 30-cm diameter no. 20 net (80 μm mesh). The volume of the sample was measured and an aliquot (approximately 30%) was filtered through a glass fiber filter and counted. Samples were prepared immediately for counting or stored frozen until processed at WHOI.

Half-liter samples of water were transferred to a bottle fitted with two suspended wells and acidified to a pH of <2 with 5 mL of 0.2 M sulfuric acid. Evolved CO_2 was collected on two filters, one in each well, soaked with 0.2 mL of phenethylamine (New England Nuclear), while the sample was gently shaken. After 6 h the filters were replaced with fresh filters and the sample was extracted an additional 10–18 h. Both pairs of filter pads were then counted.

Cores were taken in 11-mm diameter polyethylene core liners and then immediately frozen while still in the liners.

Separation of Intermediate Breakdown Products. Procedures to separate and identify intermediate breakdown products (including products of metabolism and chemical and photooxidation) from the parent [^{14}C]benz[*a*]anthracene were conducted both at MERL and at WHOI. At MERL, aliquots of the hexane sample were taken to dryness using a nitrogen jet at room temperature and then made up to 0.2 to 0.4 mL with benzene. One aliquot of the benzene concentrate was counted; another was applied to silica gel thin-layer plates (Merck Co.) and run in a solvent system (benzene–hexane, 3:7 v/v) to separate polar metabolites from benz[*a*]anthracene. After we ran the sample on thin-layer plates, the benz[*a*]anthracene layer was identified by UV fluorescence of standard benz[*a*]anthracene. Three areas were marked, one corresponding to benz[*a*]anthracene (identified by the standard), one to a region containing highly polar metabolites (near the origin on the thin-layer plate), and the remaining middle region of the plate corresponding to hydroxybenz[*a*] anthracenes (9-hydroxybenz[*a*]anthracene, and *cis*-5,6-dihydro-5,6-dihydroxybenz[*a*]anthracene standards provided by A. R. Patel through the National Cancer Institute, Carcinogenic Research Program) and some quinones run with this solvent system. The silica gel from each area was scraped from the plates, added to scintillation fluid, and counted. Aliquots of the zooplankton samples, phytoplankton (reverse flow) samples, and duplicate samples of total particulate material were each placed in a separatory funnel and extracted overnight with chloroform–methanol (*21*). The chloroform layer was removed, taken to dryness, and brought up to 0.2 or 0.4 mL with benzene. Aliquots of the benzene concentrate were counted and separated by thin-layer chromatography (TLC) as above.

Cores processed at MERL were extruded while frozen and sliced horizontally at 1-cm intervals. The 1-cm sections of the cores were placed in a round-bottomed flask with 5 mL of benzene and 5 mL of 0.5 N potassium hydroxide in methanol. Each sample was boiled with refluxing for 5 h. After cooling, the mixture was centrifuged to separate the sediment from the liquid. Aliquots of both the benzene and the methanol–water layers were counted. For selected cores, benzene and methanol–water aliquots were dried and used for thin-layer chromatography.

To determine the efficiency of the counting process, samples were counted, a known activity of [^{14}C]toluene was added, and the samples were recounted. Efficiencies for most samples were over 95%, except for those of the sediment extracts, which were 55 to 95%.

Duplicate samples were processed at WHOI using different procedures. Hexane and chloroform extracts were evaporated to 2–10 mL, extracted three times with 2–5 mL of warm tetrahydrofuran (THF)–2-propranol (1:1), and then passed through a Sephadex LH-20 cleanup procedure. Both the chromatography and the extractions were carried out with only red light present, in order to minimize photooxidation of benz[*a*]anthracene metabolites. Sephadex LH-20 was allowed to swell overnight in 2-propanol, packed into a 58 cm × 2.54 cm glass column, and equilibrated for 12 h with a constant flow of 24 mL/min before a sample was loaded onto the column. A flow rate of 24 mL/min was found to be a good compromise between elution time and separation efficiency for this column. 2-Propanol as the mobile phase elutes aromatic hydrocarbons from Sephadex LH-20 by increasing ring number, while more polar compounds like quinones, alcohols, and acids are retained on the column. The elution time for benz[*a*]anthracene was established in 2-propanol, and all hydrocarbons up to benz[*a*]anthracene were eluted with 2-propanol. Benz[*a*]anthracene and the more polar metabolites were then eluted with THF at a flow rate of 80 mL/min. Substitution of THF for 2-propanol did not cause any problem as the gel beads swell the same in both solvents. The column was then reequilibrated with 2-propanol before introduction of the next sample. Standards used to establish LH-20 and high-pressure liquid chromatography elution conditions were benz[*a*]anthracene-*cis*-5,6-diol, 10,11-epoxybenz[*a*]anthracene-*trans*-8,9-diol (anti), 10,11-epoxybenz[*a*]anthracene-*trans*-8,9-diol (syn), and benz[*a*]anthracene provided by IIT Research Institute with support from the National Cancer Institute.

Particulate matter and no. 20 mesh net zooplankton samples at WHOI were extracted three times with 50 mL of warm THF–2-propanol (1:1) and three times with 50 mL of warm ethyl acetate, and the extracts were subjected to the cleanup procedure described above. Sediment samples were extracted three times with 50 mL of cold THF–2-propanol (1:1), three times with 50 mL of warm THF–2-propanol (1:1), and three times with 50 mL of warm ethyl acetate. The extracts were then evaporated to a small volume, centrifuged to remove small sediment particles not removed by decantation in previous steps, and subjected to cleanup on Bio-Beads SX-12 by eluting with acetone and toluene. Acetone as the mobile phase elutes the aromatics from Bio-Beads SX-12 by increasing ring number. The retention times for selected standards [including benz[*a*]anthracene, 9-hydroxybenz[*a*]anthracene, and 8,9-dihydrodiolbenz[*a*]anthracene] were measured in acetone, and the isolation and collection of benz[*a*]anthracene and metabolites in the sample extracts were based on these retention times. The flow rate was maintained at 30 mL/h. Elementary sulfur and other materials sticking to the gel bed were eluted with toluene, and the columns were reequilibrated with acetone before the next run. Elution with toluene was at a rate of 74 mL/min.

Table I. Extraction Efficiencies, during Preparation for TLC or HPLC, from Samples of Particulate Matter, and the Retention of Labeled Material during Evaporation of Hexane from the Hexane Extract of the Water

sample day	% recovery		sample day	% recovery	
	MERL	WHOI		MERL	WHOI
	Total Particulates			Zooplankton	
1	82	75	1	63	20
2	56	70	3	53	24
3	75	33	5	37	22
4	60	87	7	56	
5	66	72	12	27	61
7	56	90	18	49	114
9	45				
	Phytoplankton			Hexane	
1	60	80	2	89	
2	62	81	3	82	
3	60		4	86	
4	74		5	87	
			7	79	
			9	91	

The hydrocarbon and metabolite isolates were analyzed on a DuPont LC-850 high-pressure liquid chromatograph (HPLC) equipped with a Zorbac ODS column and a filter photometer UV detector operating at 254 nm. Approximately 40 μL was loaded into a 50-μL loop. The elution of benz[*a*]anthracene and its metabolites was accomplished by running a gradient from 40 to 90% acetonitrile in water buffered to pH 4.0 with formic acid. The solvent gradient changed in a linear fashion at 2%/min. The flow rate was maintained at 2.0 mL/min and the temperature kept at 25 ± 1 °C. The elution times of the various groups of metabolites were established through the retention indexes of selected standard compounds. Only a few benz[*a*]anthracene standards are available, so the retention times of the quinone group were established by using benz[*a*]pyrenequinone standards. Various groups of peaks were collected from HPLC, and the activities were measured by scintillation counting as described above.

The background concentration of benz[*a*]anthracene originally present in the microcosm sediments was measured by quantitative gas chromatography–mass spectrometry as previously described (*18, 22*).

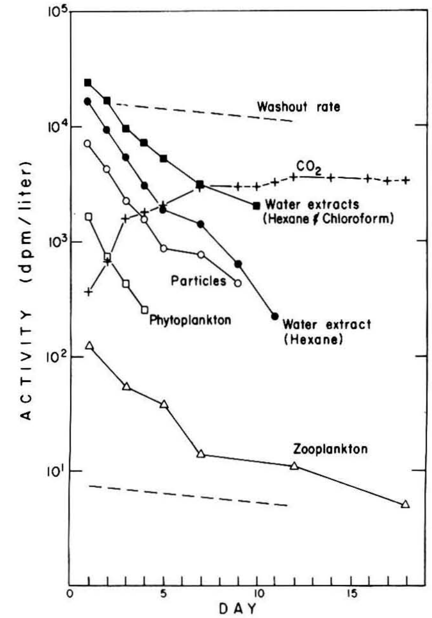

Figure 1. Observed ^{14}C activity in extracts from the water column obtained by direct counting of various kinds of particulate materials during the first 18 days. The washout rate, shown by dashed lines, is the rate that ^{14}C activity in the various samples would decrease as a result of water replacement in the tank

Results

The efficiency of the extraction techniques may be determined for total particulate, phytoplankton, and zooplankton samples by comparing direct counts (of subsamples in scintillation fluid without extraction) to the counts of the extracts from duplicates of samples to be used for TLC or HPLC. The extractions from total particulates and phytoplankton were generally 60–80% efficient, while the extractions from zooplankton were less efficient, about 20–60% (Table I). A check of the methanol–water phase and of fractions of the solid residue from methanol–chloroform extractions of the particles, phytoplankton, and zooplankton showed that the remainder of the activity could be accounted for in those portions. Hexane samples after drying were found to have 85% of their original activity (Table I). There was good agreement for direct count determinations on duplicate hexane samples when the results for the same day obtained by two different laboratories were compared.

Water Column. One day after the spike all samples from the water column had significant amounts of ^{14}C activity (Figure 1). The ^{14}C activity of the total (hexane + chloroform) water extract decreased during the first few days with a half-life of about 50 h, while that of the particulates, phytoplankton, and zooplankton decreased with a half-life of about 35 h for the first 5 days and then more slowly until the activity in the samples became too low for counting. The decrease in ^{14}C activity in these samples was much greater than would be expected from the washout of the tank. During the same interval the ^{14}C activity present as dissolved carbon dioxide (ΣCO_2) increased. Measurements of the mass of particulates, phytoplankton, and zooplankton were made for the same time period in other MERL microcosms; comparison with these data suggests that the specific activities of the three fractions (^{14}C activity/gram dry weight) were approximately equal.

Thin-layer chromatography and HPLC analysis of water extracts, particulates, phytoplankton, and zooplankton showed that the fraction of total ^{14}C activity in these extracts attributable to [^{14}C]benz[*a*]anthracene decreased with time (Figures 2 and 3). The TLC analysis showed that [^{14}C]-benz[*a*]anthracene decreased from 70% of the ^{14}C activity on day 1 to 20% by day 9, while polar metabolites increased in percentage during the same interval. HPLC analysis of both hexane- and chloroform–water extracts showed a similar decrease in [^{14}C]benz[*a*]anthracene. Although this trend is clear, it should be noted that the extraction procedures did not recover all the ^{14}C activity measured in the samples by direct counts (Table I). The unextracted ^{14}C activity is likely to be in highly polar metabolites. The relative amount of [^{14}C]benz[*a*]anthracene shown in Figure 2 is based on ^{14}C in the lipid fraction. The THF extractions and cleanup procedures select primarily benz[*a*]anthracene and its alcohol and quinone metabolites. The HPLC analysis of the cleaned hexane- and chloroform–water extracts missed 30–40% of the ^{14}C activity present in the extracts. This again indicates that some of the ^{14}C activity from the labeled benz[*a*]anthracene had been incorporated into relatively polar organic compounds as a result of the metabolism of benz[*a*]anthracene.

Chloroform extracted labeled compounds remaining in the water after hexane extraction (Figure 1). After day 3 the hexane extracted less than half of the total materials extractable by hexane followed by chloroform. HPLC analyses of the chloroform extracts also showed that the hexane procedure missed a substantial portion of the benz[*a*]anthracene.

The ^{14}C activity present in the water as ΣCO_2 reached a maximum on day 12 (Figure 4). Thereafter, the concentration of $\Sigma^{14}CO_2$ decreased, indicating that the production of $^{14}CO_2$ became less than the sum of losses from washout, escape of gaseous $^{14}CO_2$ to the atmosphere, and biological fixation. From day 63 to day 77, the water flow to the tank was stopped. During this period of batch operation there was no washout of $\Sigma^{14}CO_2$, and the concentration of $^{14}CO_2$ in the tank increased. This increase clearly demonstrated that $^{14}CO_2$ was

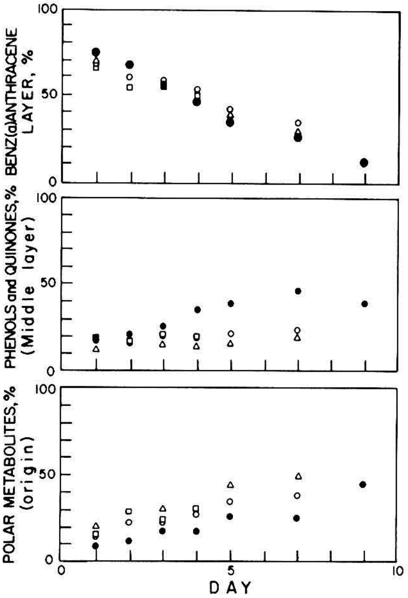

Figure 2. Distribution of radiolabeled benz[*a*]anthracene and metabolites determined by thin-layer chromatography of hexane extracts of the water (●), and on particulate samples (○), zooplankton (△), and phytoplankton (□)

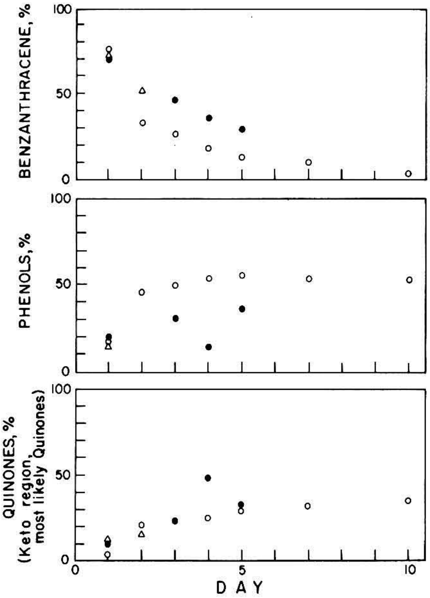

Figure 3. Distribution of radiolabeled benz[*a*]anthracene, phenols, and quinones determined by high-pressure liquid chromatography of hexane (●) and chloroform (○) extracts from the whole water samples and extracts from filtered samples of particulate material (△).

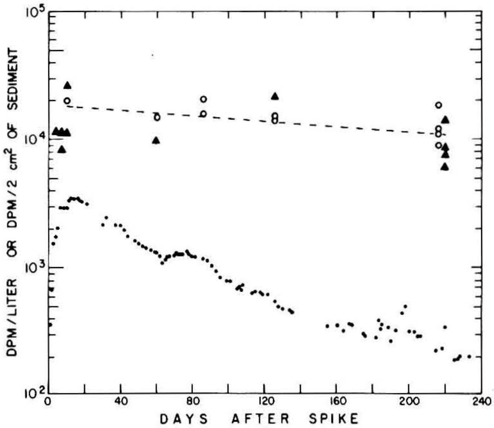

Figure 4. Concentration of $^{14}CO_2$ in water (●) and total ^{14}C activity extracted from sediment cores at MERL (O) or at WHOI (▲). The dashed line is a linear regression of data from the measured cores from day 10 to 220. On this scale the curvature associated with plotting in a semilog graph is not visible

still being produced, though at a rate much slower than during the first few days of the experiment.

The washout rate from the tank is known, and the sum of the rates of $\Sigma^{14}CO_2$ loss to the atmosphere and biological fixation in a MERL tank is 1% of the total $\Sigma^{14}CO_2$ each day (*23*). Biological fixation as used here refers to labeled carbon incorporated into the biota and not regenerated by respiration to CO_2 during the course of the experiment. Thus, it is possible to calculate the $^{14}CO_2$ production for each day of the experiment using the equation:

$$P = (D_2 - D_1) + \text{washout} + (0.010D_1)$$

where P is the $^{14}CO_2$ production, D_1 is the $\Sigma^{14}CO_2$ in the tank on any day, and D_2 is the $\Sigma^{14}CO_2$ in the tank on the following day. Washout is calculated from flow records, and the final term is a calculation of $\Sigma^{14}CO_2$ lost to the atmosphere and biological fixation. The rate of $\Sigma^{14}CO_2$ loss to biological fixation is probably variable but certainly small compared to the $\Sigma^{14}CO_2$ loss to the atmosphere, so the combined loss appears to be relatively constant over time. The $^{14}CO_2$ production (plotted in 10-day intervals to smooth the data, Figure 5) decreased during the first 40–60 days of the experiment and remained at a low but measurable level until the experiment was terminated at day 230.

Sediment. Labeled benz[*a*]anthracene and its labeled metabolites, excepting CO_2, disappeared from the water column after a few days. The major portion of the ^{14}C activity was found in the sediment with a lesser portion appearing as ΣCO_2 (Figure 4). The total activity in quadruplicate cores taken the same day showed variability by a factor of 2, but the data sets from the two laboratories were not distinguishable (Figure 4). Activities in cores are reported as disintegrations per minute under each 2 cm². The geometry of the tanks results in each 2 cm² of the sediment lying under exactly 1 L of water. Most of the ^{14}C activity was initially associated with the top centimeter of sediment (Figure 6). As time progressed the labeled compounds were found deeper, a result expected from studies of particle transport (*24, 25*) and benthic ecology (*26, 27*). There was substantial variability or patchiness in the distribution of these compounds both vertically and horizontally. Once incorporated into the sediment, the labeled compounds survived for at least 220 days and were lost slowly. The TLC analyses of extracts from a few selected cores showed that the

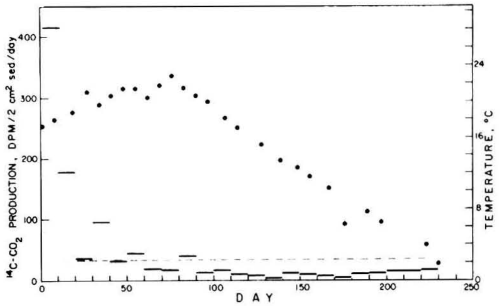

Figure 5. Solid lines are 10-day averages of the production of $^{14}CO_2$ calculated from $\Sigma^{14}CO_2$ concentrations in water. Dashed line is production of $^{14}CO_2$ determined by the decrease in ^{14}C activity in measured cores, using the linear regression from Figure 4. Closed circles are temperature of the tank water during the experiment

fraction of total activity present as benz[*a*]anthracene was about 40–60% in surface sections and about 5–15% in sections 4 to 5 cm down the core (Figure 6). Table II lists the fractions of the ^{14}C activity that were present as CO_2, benz[*a*]anthracene, or intermediate metabolites on various days.

Mass Balance. An attempt was made to identify the fate of all the ^{14}C activity that was introduced into the tank. At any one time the total ^{14}C activity must equal the sum of that in the water, in the sediment (or on the walls of the tank), washed out of the tank, and lost as a gas to the atmosphere. If the total obtained by adding all results from measurements of ^{14}C activity is close to the amount added to the tank, a reasonable assurance is provided that the sampling and analytical procedures used were not severely deficient. For calculation of the mass balance the following equation was used:

$$\text{total} = [^{14}C]\text{sediment} + [^{14}C]\text{water} + \Sigma[^{14}C]\text{washout} + \Sigma[^{14}C]\text{atmosphere}$$

The spike ^{14}C activity (31 000 dpm/L) was obtained by ex-

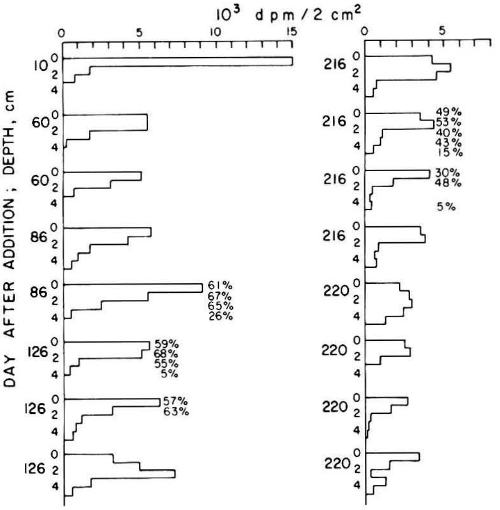

Figure 6. Distribution of ^{14}C activity with depth in sediment cores taken at intervals through the experiment from day 10 to 220. The numbers given in some cases to the right of the profiles at 1-cm intervals show the percentage of the ^{14}C activity in each interval which ran with benz[*a*]anthracene during thin-layer chromatography

Table II. Percentage of the Total ^{14}C Activity Added to a MERL Tank as [^{14}C]Benz[*a*]anthracene and Recovered as Parent Compound, $^{14}CO_2$, and Intermediate Metabolic Products

day	benz[*a*]anthracene [a]	CO_2 [b]	intermediate products [a]	total accounted for [c]
1		1		
86	34	26	23	94
126	29	28	23	91
216	21	29	22	83

[a] Includes, after day 86, data from sediments only, as water column values were then negligible. [b] All CO_2 was in the water column. Values include estimate of CO_2 washed out and CO_2 lost to atmosphere by air–water exchange. [c] Includes the amount of [^{14}C]benz[*a*]anthracene and intermediate metabolic products, estimated at 11% of total initial activity, washed out of the tank during approximately the first 20 days of the experiment.

Table III. Mass Balance of ^{14}C Activity Added as [^{14}C]Benz[*a*]anthracene to One MERL Tank [a]

day	found in water column	calcd cumulative loss through washout and gas exchange	found in sediment (range)	total accounted for
4	29	8	38	75
7	20	10	32 (26–37)	62
10	15	12	62 (37–86)	89
60	4	31	40 (31–48)	75
86	4	33	58 (50–65)	95
126	2	37	52 (45–65)	91
216	1	40	39 (27–56)	80
220	1	40	28 (19–44)	69
			mean	80

[a] All values expressed as a percent of the initial estimated value of 31 000 dpm/L.

trapolating the hexane + chloroform extract line from Figure 1 to the time of the spike. The [^{14}C]water is the summation of ^{14}C activity in the hexane + chloroform extracts plus the $\Sigma^{14}CO_2$. The washout for each day is the ^{14}C activity in the water times the portion of the water removed by washout. The Σ[^{14}C]washout is the summation of the calculated daily washouts. The $^{14}CO_2$ loss to the atmosphere (and to biological fixation) was calculated daily in the same manner as was done to estimate the $^{14}CO_2$ production. Benz[*a*]anthracene lost to the atmosphere is thought to be negligible (*28*). The results of these calculations (Table III) indicate that the mean total estimated recovery was 80% of the amount added, and there was no evident trend in this value with time. The 5 to 40% of the ^{14}C activity that was apparently missed during the various samplings was probably in the form of benz[*a*]anthracene or its metabolites not extracted from the sediments or, in the early days of the experiment, from the water column. No absolute calibration of the extraction efficiencies from either medium was attained in these experiments. However, the mean extraction efficiency from water column particulate material was 63% (Table I). Some activity may also have been adsorbed on the tank walls, although in experiments with other hydrocarbons this has not been a significant factor (*18*). At present we cannot evaluate these possible sources of error.

Discussion

Both the microbial and benthic animal populations of the microcosm originated from a coastal site near populated areas; therefore, they must have had prior exposure to benz[*a*]anthracene (*8, 10*). Quantitative gas chromatography–mass spectrometry measurements of benz[*a*]anthracene in control MERL sediments gave concentrations of 200–300 ng/g dry weight. Most of the benz[*a*]anthracene and other PAHs in the sediment likely originate from a combination of low-level chronic inputs of petroleum hydrocarbons and fossil fuel combustion products (*8, 10*). Thus, these systems have probably received anthropogenically enhanced inputs of benz[*a*]anthracene for more than 100 years, in addition to lower level inputs from natural fires since the estuary was formed (*7, 8, 10*). If all the approximately 0.93 mg of benz[*a*]anthracene added during the experiment described above had been incorporated into the sediment, the increase in concentration would have been 27 ng/cm^3 in the top 1 cm of sediment, about one-sixth of the existing concentration. Thus, the added benz[*a*]anthracene did not greatly change the prior concentration.

The total ^{14}C activity, including both the parent benz[*a*]anthracene and labeled breakdown products, was removed from the water with a half-life of about 52 h, while the [^{14}C]benz[*a*]anthracene itself had a half-life of 24 h, a behavior similar to that of benz[*a*]anthracene in another microcosm experiment (*29*). Based on knowledge of the general microbial and animal metabolism of aromatic hydrocarbons and photochemical reaction of benz[*a*]anthracene, it seems likely that a combination of microbial and photochemical processes gave rise to the labeled products which were found in the water and in the sediments. After a few days, animal metabolism and excretion might also have produced some metabolites (*30–34*). The presence of phenol and quinone metabolites in the sediment and in the water during the early stages of the experiment demonstrates that the metabolism of benz[*a*]anthracene to CO_2 was not rate limited by the initial conversion to quinones or phenols. Once they were formed they survived long enough to be detected in substantial quantities, up to 23% of the initial total ^{14}C activity.

Benz[*a*]anthracene, having a low water solubility and low rate of metabolism in the water column, became associated with sediments either through direct adsorption on the bottom after turbulent mixing of water to the sediment–water interface or by adsorption onto or incorporation into suspended particles and subsequent deposition. Once incorporated into surface sediments, the benz[*a*]anthracene and its metabolites were mixed deeper into the sediments by benthic animal activity. Both the removal and mixing processes took place on a time scale which was faster than the conversion rate of benz[*a*]anthracene and extractable metabolites to nonextractable metabolites and CO_2, as the total ^{14}C activity in the sediment did not decrease rapidly.

Because of the rapid transfer of the benz[*a*]anthracene to the sediment, it is not possible to specify whether the initial high rate of metabolite production was carried out in the water column on suspended particulates or in the sediment. However, studies of [^{14}C]benz[*a*]anthracene in bottle experiments (*35*) using water and sediments from both Narragansett Bay and the MERL microcosms indicated that no $^{14}CO_2$ production occurred in water, while a measurable $^{14}CO_2$ production took place in sediments. The greater percentage of ^{14}C-labeled metabolites in the top centimeter of sediment than in the 1–2-cm layer indicates that the metabolism of benz[*a*]anthracene occurred more rapidly in the top layer. For other coastal sediments it has been shown that microbial degradation of petroleum hydrocarbons is more rapid near the surface than in lower layers (*36*). In the MERL sediments this may be due in part to the reducing conditions below 1 cm, while the surface sediments are oxidized (*37*). The increased ^{14}C activity found in polar metabolites, relative to that in the parent compound, deeper in the core (4–5 cm layer) provides some insight into diagenetic processes and suggests further studies. This observation could perhaps be explained by assuming a greater diffusive mobility of the polar compounds, compared to benz[*a*]anthracene, or by the action of benthic animals ingesting and partially metabolizing the benz[*a*]anthracene and then excreting the metabolites at depth.

The variability of the depth distributions for quadruplicate cores on days 216 and 220 illustrates that, despite the passage of 200 days since the introduction of the benz[*a*]anthracene to the system, the combination of metabolic processes and biological and physical mixing of sediments had not resulted in a uniform distribution of either parent compound or extractable metabolites in the upper 4 to 5 cm of sediment. This is consistent with the view that in benthic ecosystems of this type there is a dynamic interaction of fluid and particle movements brought about by different benthic animals with varying feeding strategies and burrowing activities, resulting in local patchiness of chemical distributions.

The data do not allow an unequivocal calculation of how long it would take for the remaining ^{14}C activity to be converted to $^{14}CO_2$. The $^{14}CO_2$ production followed neither a linear nor an exponential loss rate (Figure 5). We do not know the mechanisms that control the rate of benz[*a*]anthracene breakdown, so we have no basis to choose a method of calculation. If the $^{14}CO_2$ production rate were to remain the same as during the last 100 days of the experiment (Figure 5), all the labeled benz[*a*]anthracene would be converted to $^{14}CO_2$ within 3.5 years after the spike. Since the temperature of the sediments would be greater in the summer, it may be more reasonable to use the decrease in ^{14}C activity in sediment cores from day 10 to day 216, which includes warmer temperatures, to predict 2.0 years for the complete mineralization of the benz[*a*]anthracene. Assuming an exponential loss rate and depending on the interval chosen, half-lives of 1.2 to 3 years may be calculated. The occurrence, however, of benz[*a*]anthracene at some depth in natural sediments suggests that a fraction of this compound and perhaps some of its metabolites may persist indefinitely.

Because so many of the better known chemical functions in the MERL ecosystems follow those in the adjacent bay, both in magnitude and timing, it seems reasonable to suggest that the behavior of benz[*a*]anthracene in the microcosm would be similar to that in Narragansett Bay and similar coastal bodies of water. Nevertheless, with the present state of our knowledge, it would be risky to extrapolate from these data to the situation in other environments. Temperature, water–sediment exchange processes, rates of bioturbation, physical characteristics of the sediment, and other effects may help control the benz[*a*]anthracene degradation rate. If the addition had been in the winter and then progressed to the warmer months of summer, the benz[*a*]anthracene loss through microbial and animal metabolism might have been different. During the winter when there is less rapid bioturbation, the benz[*a*]anthracene may remain for a longer period in the surface sediments. In regions of rapid sedimentation, or in areas subjected to destruction of the biota by an oil spill, benz[*a*]anthracene buried in the sediment may remain in anoxic layers and be protected to some extent from microbial attack. The persistence of metabolites and reaction products raises important questions with regard to assessing the environmental risk associated with levels of aromatic hydrocarbons in coastal ecosystems. Many of the metabolites and reaction products of aromatic hydrocarbons are thought to be mutagenic and/or carcinogenic (*31*). Measurements of the loss of aromatic hydrocarbons after a spill do not provide a measure of the metabolites which may persist. This is especially true for the heavier molecular weight phenanthrenes and naphthalenes and compounds such as benz[*a*]anthracene and benzo[*a*]pyrene, which persist longer than the lower molecular weight benzenes and naphthalenes (*22*). The persistence of these compounds suggests the presence of a hazard. However, further measurements and experiments are needed to determine to what extent these compounds are available for uptake by biota and subsequent long-term effects.

Acknowledgments

We thank Dr. Patrick Gearing, Dr. Juanita Gearing, Dr. James Quinn, Dr. Candace Oviatt, and Mr. David Johnson for helpful discussion and cooperation. Drs. J. and P. Gearing also provided the analysis of total oil, and made several editorial suggestions. We also thank the entire MERL staff for their helpfulness.

Literature Cited

(1) National Academy of Sciences, "Petroleum in the Marine Environment", Washington, D.C., 1975.

(2) "Proceedings of a Workshop on Scientific Problems Relating to Ocean Pollution", Estes Park, Colo., July 10–14, 1978, U.S. Department of Commerce, National Oceanic & Atmospheric Administration, Environmental Research Laboratories, Boulder, Colo., 1979.

(3) Anderson, J. W., Malins, D. C., *J. Fish. Res. Board Can.*, **35**, 679 (1978).

(4) Farrington, J. W., in "Proceedings of a Special Symposium of the American Chemical Society Environmental Division", in press.

(5) Wakeham, S. W., Farrington, J. W., in "Proceedings of a Special Symposium of the American Chemical Society Environmental Division", in press.

(6) National Academy of Sciences, "Particulate Polycyclic Organic Matter", Washington, D.C., 1972.

(7) Youngblood, W. W., Blumer, M., *Geochim. Cosmochim. Acta*, **39**, 1303 (1978).

(8) LaFlamme, R. E., Hites, R. A., *Geochim. Cosmochim. Acta*, **42**, 289 (1978).

(9) Farrington, J. W., Frew, N. M., Gschwend, P. M., Tripp, B. W., *Estuarine Coastal Mar. Sci.*, **5**, 793 (1977).

(10) Wakeham, S. G., Schaftner, C., Giger, W., *Geochim. Cosmochim. Acta*, **44**, 403 (1980).

(11) Hites, R. A., LaFlamme, R. E., Farrington, J. W., *Science*, **198**, 829 (1977).

(12) Grimmer, G., Boehnke, H., *Cancer Lett.*, **1**, 75 (1975).

(13) Muller, G., Grimmer, G., Bohnke, H., *Naturwissenshaften*, **64**, 427 (1977).

(14) Pilson, M. E. Q., Vargo, G. A., Gearing, P., Gearing, J. N., in "Proceedings of the 2nd National Conference Interagency Energy/Environment R&D Program", EPA-600/9-77-012, 1977, pp 513–6.

(15) Pilson, M. E. Q., Oviatt, C. A., Vargo, G. A., Vargo, S. L., in "Advances in Marine Environmental Research", Jacoff, F. S., Ed., EPA 600/9-79-035, 1979, pp 359–81.

(16) Pilson, M. E. Q., Oviatt, C. A., Nixon, S. W., in "Symposium on Microcosms in Ecological Research", Savannah River Ecology Laboratory, 1978, in press.

(17) Elmgren, R., Vargo, G. A., Grassle, J. F., Grassle, J. P., Heinle, D. R., Langlois, G., Vargo, S. L., in "Symposium on Microcosms in Ecological Research", Savannah River Ecology Laboratory, 1978, in press.

(18) Gearing, J. N., Gearing, P. J., Wade, T. L., Quinn, J. G., McCarty, H. B., Farrington, J. W., Lee, R. F., in "Proceedings of the 1979 Oil Spill Conference", American Petroleum Institute, Washington, D.C., 1979, pp 555–64.

(19) Dodson, A. N., Thomas, W. H., *Limnol. Oceanogr.*, **9**, 455 (1964).

(20) Hinga, K. R., Davis, P. G., Sieburth, J. McN., *Limnol. Oceanogr.*, **24**, 536 (1979).

(21) Bligh, E. G., Dyer, W. J., *Can. J. Biochem. Physiol.*, **37**, 911 (1959).

(22) Teal, J. M., Burns, K. A., Farrington, J. W., *J. Fish. Res. Board Can.*, **35**, 510 (1978).

(23) Hinga, K. R., Marine Ecosystems Research Laboratory, Graduate School of Oceanography, University of Rhode Island, unpublished data.

(24) Adler, D., Amdurer, M., Santschi, P. H., in "Symposium on Microcosms in Ecological Research", Savannah River Ecology Laboratory, 1978, in press.

(25) Santschi, P. H., Li, Y. H., Carson, S., *Estuarine Coastal Mar. Sci.*, in press.

(26) Rhoads, D. C., *Mar. Biol. Annu. Rev.*, **12**, 263 (1974).

(27) Rhoads, D. C., McCall, P. L., Yingst, J. Y., *Am. Sci.*, **66**, 577 (1978).

(28) Southworth, G. R., *Bull. Environ. Contam. Toxicol.*, **21**, 507 (1979).
(29) Lee, R. F., Gardner, W. S., Anderson, J. W., Blaylock, J. W., Barwell-Clarke, J., *Environ. Sci. Technol.*, **12**, 832 (1978).
(30) Stegeman, J. J., Binder, R. L., *Biochem. Pharmacol.*, **28**, 1686 (1979).
(31) Stegeman, J. J., *J. Fish. Res. Board Can.*, **35**, 688 (1978).
(32) Malins, D. C., in "Fate and Effects of Petroleum Hydrocarbons in Marine Organisms and Ecosystems", Wolfe, D. A., Ed., Pergamon Press, New York, 1977, Chapter 5, pp 47–59.
(33) Corner, E. D. S., *Adv. Mar. Biol.*, **15**, 289 (1978).
(34) Lee. R. F., in "Proceedings of the 1975 Conference on Prevention and Control of Oil Pollution", American Petroleum Institute, Washington, D.C., 1975, pp 549–53.
(35) Lee, R. F., Skidaway Institute of Oceanography, Savannah, Ga., 1978, unpublished data.
(36) Gardner, W. S., Lee, R. F., Tenore, K. R., Smith, L. W., *Water, Air Soil Pollut.*, **11**, 339 (1979).
(37) Pilson, M. E. Q., Marine Ecosystems Research Laboratory, Graduate School of Oceanography, University of Rhode Island, 1978, unpublished data.

Received for review January 11, 1980. Accepted April 14, 1980. This work was supported by Environmental Protection Agency Grant R 80607202. This paper is Woods Hole Oceanographic Institution Contribution No. 4513.

NOTES

Correlation of Microbial Degradation Rates with Chemical Structure

N. Lee Wolfe*, Doris F. Paris, William C. Steen, and George L. Baughman

Environmental Research Laboratory, U.S. Environmental Protection Agency, Athens, Ga. 30605

■ Structure–reactivity relationships are established for the microbial degradation of selected organic compounds. Second-order microbial degradation rate constants determined in natural water samples for six compounds correlate with the second-order alkaline hydrolysis rate constants. Also, second-order microbial degradation rate constants for four phthalate esters obtained with organisms from sediment–water samples correlate with the second-order alkaline hydrolysis rate constants. Similar correlations are demonstrated for the rates of oxidation of substituted phenols by mixed microbial cultures isolated from soils and Hammett σ constants.

Correlations between rate constants for specific chemical reactions and values for a selected physical or chemical property of the organic compounds are well established in the chemical literature (*1*). Such correlations can be used to predict rate constants required to assess the behavior of organics in aquatic environments (*2, 3*). Similar correlations of enzyme-catalyzed reactions, although often more complex, have also been demonstrated (*1, 4*). Several studies have addressed the effect of chemical structure on susceptibility to microbial breakdown using bacteria isolated from soils (*5, 6*) and natural waters (*7, 8*), but, unfortunately, the correlations have not been successful. The major difficulty with these studies has been the choice of a measurement of biological reactivity to use in the correlation.

Recent studies of the kinetics of microbial degradation of organics in natural water samples provide a data base of rate constants that can be used to examine the relationship of chemical structure to microbial degradation. In these studies, Paris and co-workers (*9–11*) applied a second-order rate expression to describe the rate of disappearance of certain organics mediated by microorganisms in natural water samples. Linear regression analysis using the second-order rate constants, k_b (L org^{-1} h^{-1}), determined in these investigations and the corresponding second-order alkaline hydrolysis rate constants, k_{OH} (M^{-1} s^{-1}), reported by Wolfe and co-workers (*11–15*) gives the correlation described by the linear equation (*16*):

$$\log k_b = m \log k_{OH} + c \qquad (1)$$

Values of m and c along with standard errors of the estimates and the correlation coefficient, r^2, are given in Figure 1. (The second-order biolysis and hydrolysis rate constants for methyl benzoate and anisate according to Wolfe and Paris (*11*) are 7.0×10^{-13} and 5.4×10^{-13} L org^{-1} h^{-1} and 5.0×10^{-3} and 1.1×10^{-2} M^{-1} s^{-1}, respectively.) For this group of compounds, 97% of the variance in the data is accounted for by alkaline hydrolysis. In addition, the F value is 141, which is significant at the greater than 99% confidence level (CL). The correlation (R^2) is improved by inclusion of a second parameter, the octanol–water partition coefficient (K_{ow}) (*17*), which has been postulated to be proportional to the binding strength of a compound at the reaction site (*4*) or proportional to biosorption by organisms (*18*). (Octanol–water partition coefficients were calculated using the transposed linear equation, $\log K_{ow} = -0.653 \log s + 0.880$, obtained by linear regression analysis of the data in ref *17*.) The resulting equation is:

$$\log k_b = m \log k_{OH} + n \log K_{ow} + c \qquad (2)$$

With the inclusion of K_{ow} as a dependent variable, the multiple linear regression coefficient, R^2, is 0.988, which accounts for an additional 2% of the variance of the data. The values of m, n, and c are 0.53 ± 0.03, 0.13 ± 0.06, and -11.8 ± 0.2, respectively. However, the F test shows that inclusion of K_{ow} as a dependent variable after K_{OH} is not significant.

A similar correlation is also shown for phthalate esters. The second-order disappearance rate constants reported by Steen et al. (*19*), for the microbial degradation of four phthalate esters by organisms from sediment samples, and the second-order alkaline hydrolysis rate constant for the corresponding esters reported by Wolfe et al. (*20*) were correlated by use of Equation 1. (Reference *19* contains the biolysis rate constant for di-*n*-butyl phthalate and a description of the experimental methodology and calculations. Second-order biolysis rate constants for the dimethyl, di-*n*-octyl, and bis(2-ethylhexyl) phthalates are 5.2×10^{-9}, 3.1×10^{-13}, and 4.2×10^{-15} L org^{-1} h^{-1}, respectively.) Linear regression analysis of the data gives the values shown in Figure 2 ($r^2 = 0.933$). In addition, the F value is 27.7, which shows that the correlation is significant at the 95% CL. Although 93% of the variance is accounted for by alkaline hydrolysis, the correlation is improved by using Equation 2 ($R^2 = 0.994$). Thus, the octanol–water partition coefficient as an independent variable accounts for an addi-

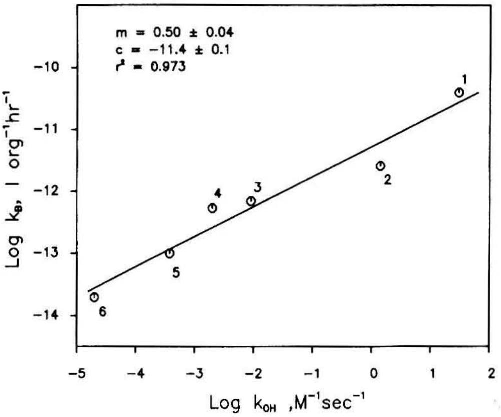

Figure 1. Correlation of second-order alkaline hydrolysis rate constants determined in distilled water at 27 °C with second-order biolysis rate constants determined in natural water samples at 25 °C. The compounds are: (1) *n*-butoxyl ethyl ester of 2,4-D; (2) malathion; (3) methyl benzoate; (4) methyl anisate; (5) methoxychlor; (6) chlorpropham

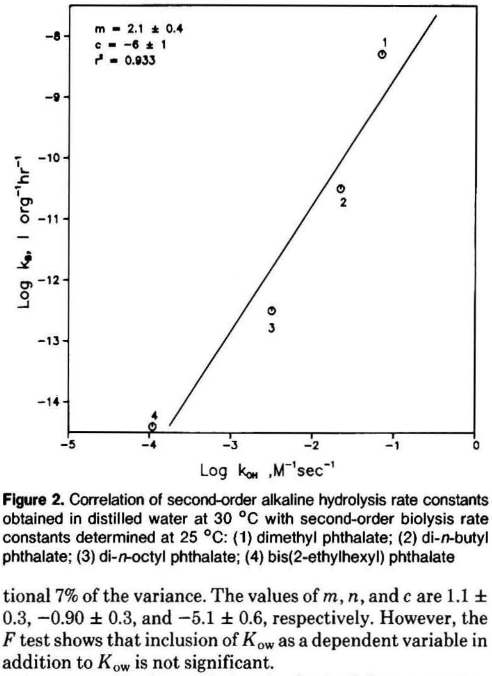

Figure 2. Correlation of second-order alkaline hydrolysis rate constants obtained in distilled water at 30 °C with second-order biolysis rate constants determined at 25 °C: (1) dimethyl phthalate; (2) di-*n*-butyl phthalate; (3) di-*n*-octyl phthalate; (4) bis(2-ethylhexyl) phthalate

tional 7% of the variance. The values of m, n, and c are 1.1 ± 0.3, −0.90 ± 0.3, and −5.1 ± 0.6, respectively. However, the F test shows that inclusion of K_{ow} as a dependent variable in addition to K_{ow} is not significant.

Support for such correlations is obtained from two other studies: the degradation of pesticides in soils and the microbial degradation of phenols in aqueous solution. In the first case, Igarashia et al. (*21*) studied the degradation of five carbamate pesticides in flooded rice soil. Although the study did not differentiate between chemical and biological processes, microbial degradation was postulated, and the authors reported a correlation between the observed first-order disappearance rate constants in the soils and the second-order alkaline hydrolysis rate constants.

Further evidence to support the feasibility of this approach is obtained by analysis of the data reported by Tabak et al. (*22*) on the microbial degradation of substituted phenols. In these studies, the authors presented data on the oxidation of substituted phenols by mixed cultures of bacteria isolated from soils. Unfortunately, kinetic expressions were not developed for the process, but, using their data for initial concentrations of 100 ppm and a 180-min time interval, rates of disappearance can be calculated. The log of these rates (v) for the ortho- and meta-substituted phenols correlated with the Hammett σ constants (Equation 3), where σ is the substituent constant, ρ the slope, and v_0 the rate of the unsubstituted phenol (*7*).

$$\log v = \rho\sigma + \log v_0 \tag{3}$$

Inspection of a plot of the data and the results from linear regression analysis suggests two separate linear relationships. One is for the methyl- and hydroxy-substituted phenols ($\rho = 0.058 \pm 0.002$, $\log v_0 = 1.99 \pm 0.01$, $r^2 = 0.836$), and the other is for chloro- and nitro-substituted phenols ($\rho = -0.50 \pm 0.05$, $\log v_0 = 1.92 \pm 0.08$, $r^2 = 0.951$).

Even though there are some obvious mechanistic implications concerning the microbial degradation process, it is important that these correlations offer some insight into a method of predicting microbial degradation rate constants in natural waters and maybe even soils. If subsequent studies confirm general applicability of such structure–reactivity relationships and the variance of these biodegradation rate constants from one natural water to another is not too large, as evidenced by recent data of Paris et al. (*11*), then the envirionmental scientist will have a powerful tool for assessing biotransformation.

Literature Cited

(1) Shorter, J., "Correlation Analysis in Organic Chemistry", Clarendon Press, Oxford, 1973, pp 1–50.
(2) Wolfe, N. L., Zepp, R. G., Paris, D. F., *Water Res.*, **12,** 561–3 (1978).
(3) Wolfe, N. L., in "Dynamics Exposure and Hazard Assessment of Toxic Chemicals in the Environment", Haque, R., Ed., Ann Arbor Press, Ann Arbor, Mich., 1980, pp 163–178.
(4) Hansch, C., Deutsch, E. W., Smith, R. N., *J. Am. Chem. Soc.*, **87,** 2738–42 (1965).
(5) Alexander, M., Lustigman, B. K., *J. Agric. Food Chem.*, **14,** 410–3 (1966).
(6) Alexander, M., Aleem, M. I. H. *J. Agric. Food Chem.*, **9,** 44–7 (1961).
(7) Lu, P.-Y., Metcalf, R. L., *Environ. Health Perspect.*, **10,** 269–84 (1975).
(8) Metcalf, R. L., Kapoor, P., Lu, P.-Y., Schuth, C. K., Sherman, P., *Environ. Health Perspect.*, **4,** 35–44 (1973).
(9) Paris, D. F., Lewis, D. L., Barnett, J. T., Jr., Baughman, G. L., "Microbial Degradation and Accumulation of Pesticides in Aquatic Systems", U.S. Environmental Protection Agency, Report No. EPA-660/3-75-007, 1975.
(10) Paris, D. F., Steen, W. C., Baughman, G. L., paper presented at the 175th National Meeting of the American Chemical Society, Anaheim, Calif., March 1978.
(11) Wolfe, N. L., Paris, D. F., unpublished data.
(12) Wolfe, N. L., Zepp, R. G., Gordon, J. A., Baughman, G. L., Cline, D. M., *Environ. Sci. Technol.*, **11,** 88–93 (1977).
(13) Wolfe, N. L., Zepp, R. G., Paris, D. F., Baughman, G. L., Hollis, R. C., *Environ. Sci. Technol.*, **11,** 1077–81 (1977).
(14) Zepp, R. G., Wolfe, N. L., Gordon, J. A., Baughman, G. L., *Environ. Sci. Technol.*, **9,** 1144–50 (1975).
(15) Wolfe, N. L., Zepp, R. G., Paris, D. F., *Water Res.*, **12,** 565–71 (1978).
(16) Kleinbaum, D. G., Kupper, L. L., "Applied Regression Analysis and Other Multivariable Methods", Duxbury Press, North Scituate, Mass., 1978, pp 37–83.
(17) Hansch, C., Quinlan, J. E., Lawrence, G. L., *J. Org. Chem.*, **33,** 347–50 (1968).
(18) Ware, G. W., Roan, C. C., *Res. Rev.*, **33,** 15–45 (1970).
(19) Steen, W. C., Paris, D. F., Baughman, G. L., paper presented at the 177th National Meeting of the American Chemical Society, Honolulu, April 1979.
(20) Wolfe, N. L., Steen, W. C., Burns, L. A., *Chemosphere*, in press.
(21) Igarashi, M., Kawahara, T., Nakamura, H., *Noyaku Kensasho Hokoku*, **15,** 48–52 (1975).
(22) Tabak, H. H., Chambers, C. W., Kabler, P. W., *J. Bacteriol.*, **87,** 910–8 (1964).

Received for review October 17, 1979. Accepted March 17, 1980.

Mutagenicity of Textile Dyes

Mendel Friedman,* Martin J. Diamond, and James T. MacGregor

Western Regional Research Center, Science and Education Administration, U.S. Department of Agriculture,
Berkeley, California 94710

■ Nine of twenty-eight textile dyes tested for mutagenicity in an Ames *Salmonella typhimurium* bacterial test have been found to be mutagenic. These findings suggest that further testing is appropriate to establish possible mutagenic hazards associated with dye production and use.

The safety of dyeing and other finishing treatments for wool, cotton, and other natural and synthetic fibers needs careful study before the safety of large-scale use can be assured (*1–3*). Although dyeing is an ancient art developed and extensively practiced in both the Old World and the New (*4–7*), the synthesis and use of synthetic dyes is only about a hundred years old. Fiber-reactive dyes form a major class of synthetic dyes developed in the last 20 years (*4*). Because these dyes have reactive side chains that can combine covalently with fibers during dyeing, exposure of living cells to fiber-reactive dyes could result in alkylation of amino and other functional groups in nucleic acids. They may, therefore, be mutagenic. Consequently, we have evaluated 28 dye formulations of 5 subclasses of fiber-reactive dyes as well as 3 non-fiber-reactive acid dyes for mutagenicity in an Ames *Salmonella typhimurium* test (*8,9*). Quantitative top agar assays were carried out as described by Ames (*8*) by using an Aroclor 1254-induced rat liver metabolizing system. The spot tests were carried out

Table I. Mutagenicity of Fiber-Reactive Dyes and an Acid Dye in *Salmonella typhimurium* Strains TA100, TA98, and TA1537

Quantitative Plate Tests of Fiber-Reactive Dyes

	revertants/μg dye added[a]					
	TA100		TA99		TA1537	
compd tested	no S-9	with S-9	no S-9	with S-9	no S-9	with S-9
bromoacrylamide dyes[b]						
1. Lanasol Blue 3R (C.I. Reactive Blue 50; Lot 965G-Ciba)	442/40	181/1000	473/200	223/5000	28/1000	1/1000[c]
2. Intracron Blue 3R (Lot 301612-3-2-Intracolor)	468/40	185/1000	465/200	339/5000	52/40	28/5000
3. Intracron Blue 3G (Lot 320611K-15-Intracolor)	755/200	245/1000	261/200	278/5000	125/200	157/5000
4. Lanasol Red G (C.I. Reactive Red 37; Lot 15767-3-Ciba)	1165/5000	1003/5000	53/5000	52/5000	1/5000[c]	0/5000[c]
5. Lanasol Red 6G (C.I. Reactive Red 84)	343/5000	230/5000	88/5000	53/5000	6/5000[c]	2/5000[c]
6. Lanasol Scarlet 2R (C.I. Reactive Red 78; Lot 964G-Ciba)	60/5000	93/5000	8/5000[c]	0/5000[c]	3/5000[c]	0/5000[c]
7. Lanasol Yellow 4G (C.I. Reactive Yellow 39; Lot 960G-Ciba)	85/1000	118/5000	27/5000	12/5000[c]	0/5000[c]	0/5000[c]
vinyl sulfone dye						
8. Remalan Brilliant Blue-B (C.I. Reactive Blue 36; Lot MO 5941-Hoechst).	3/5000[c]	175/1000	19/1000[c]	0/5000[c]	0/5000[c]	0/5000[c]

Spot Test of a Non-Fiber-Reactive Acid Dye

	revertant density surrounding dye spot, revertants/cm^2					
	TA100		TA98		TA1537	
compd tested	no S-9	with S-9	no S-9	with S-9	no S-9	with S-9
9. Acid Green 58	27.6	19.8	0.64	0.94[c]	0.17[c]	0.33
10. control (Me_2SO) (±1 std dev)	2.6 ± 0.26	2.4 ± 0.19	0.45 ± 0.06	0.80 ± 0.13	0.12 ± 0.04	0.14 ± 0.05
11. positive controls:						
aflatoxin B_1 (1.0 μg spot test)		17.9		18.0		
9-aminoacridine (100 μg spot test)					>50.0	

[a] Revertants/plate after subtracting the spontaneous control value. The quantity of dye per plate is given in the denominator. Thus, the first number in the second column denotes that 40 μg dye induced 442 revertants. Spontaneous control value (±1 std dev) for the five experiments from which the data are derived, without and with S-9 metabolizing system, respectively, were as follows: TA100, 170 ± 26; 164 ± 22; TA98, 43 ± 24; 41 ± 17; TA1537, 9.2 ± 3.6; 10.6 ± 3.6. The least significant differences (*19*) at a confidence level of 0.001 were as follows: TA100/(no S-9), 56; TA100/(with S-9), 62; TA98/(no S-9), 25; TA98/(with S-9), 34; TA1537/(no S-9), 10; TA1537/(with S-9), 15. All tabular values exceed these least significant differences except those marked with a superscript *c*. Positive controls were carried out with each test as follows: TA98, 0.5 μg/plate of aflatoxin B_1; TA100, 1.0 μg/plate of aflatoxin B_1; TA1537, 100 μg/plate of 9-aminoacridine. The revertants per plate ranged from 950 to 1575 for the aflatoxin B_1 and from 2400 to 3200 for 9-aminoacridine. [b] Color index names, lot numbers, and manufacturers in parentheses when available.

by placing 1.0 mg of the test compound at the center of the plate. A statistical treatment of the data is given in footnote *a*, Table I.

The reactive sites of these dyes comprise bromoacrylamide (e.g., Lanasol, Intracron), chloroacrylamide (e.g., Lanasyn), vinyl sulfone (e.g., Remalan, Remazol, Levafix), chlorotriazine (e.g., Cibacron), and dichlorotriazine (e.g., Procion) side chains. Dyes were tested by using spot tests (*8*). Those exhibiting mutagenicity, bacterial growth inhibition, or questionable increases in bacterial revertant frequencies were retested by the quantitative overlay technique.

Of the 28 products tested, 7 of 11 bromoacrylamide dyes, 1 of 4 vinyl sulfone dyes, and 1 of 3 acid dyes were mutagenic. No mutagenicity was observed among 4 dichlorotriazine, 1 chlorotriazine, 1 chloroacrylamide, or 4 vinyl sulfone dyes that were spot tested. Table I illustrates representative data from all dyes that gave positive findings. The complete experimental results, including dose-response data, will be published elsewhere.

The activities observed were usually less than those reported for better-known mutagens and carcinogens similarly tested (*9*). Intracron Blue 3G, Lanasol Blue 3R, and Intracron Blue 3R (C.I. Reactive Blue 50) (Table I), however, were approximately as mutagenic as the well-known mutagens and carcinogens nitrogen mustard and uracil mustard (*9*).

Since we made no attempt to isolate and purify the active dye from commercial formulations, we do not know whether the dyes themselves or additives in the dye products are in fact responsible for the mutagenicity. The mutagenic components in the commercial samples obviously must be identified to evaluate the significance of exposure to the active ingredients. In one case (Acid Green 58), the test shows that a component of the dye formulation other than the dye itself may be responsible for the mutagenicity. Since the bacteria are fixed on the agar plate and the dyes are not, and since the ring of revertants on the petri plate was found outside the dye spot, the activity is evidently due not to the dye but to a more rapidly diffusing constituent(s) in the formulation. Bacterial growth on the plate was not inhibited.

To determine whether residual mutagenic activity remains after dyeing, we tested the spent dye after test-dyeing a wool fabric with Intracron Blue 3G, one of the most mutagenic dye samples listed in Table I. Wool fabric (50 g) was added to 2 L of a solution consisting of 1 g of dye, 5 g of Na_2SO_4, 5 cm^3 of acetic acid, and 0.5 cm^3 of Albegal B (a dispersing agent). One hundred cm^3 of this solution was removed for a control, and, after the remaining sample was boiled for 30 min, both the original and the remaining spent dye liquor were evaporated to dryness in vacuo under sterile conditions. An identical experiment in which dye was omitted was carried out as a control. No mutagenicity was observed in strains TA100, TA98, or TA1537, either with or without an in vitro metabolic activation system, when water or dimethyl sulfoxide extracts of the residue obtained after dyeing were tested. The activity expected from a sample of the original solid dye was confirmed in a sample of the dyebath removed before dyeing. The conditions of the mutagenicity test were such that 2% of the activity originally present would have been detected in strain TA100 in the sample taken after dyeing. Thus, at least 98% of the initial mutagenicity in the dyebath disappeared from the dyebath liquor during dyeing. Spectral measurement of the spent dyebath solution indicated that 97% of the dye is taken up by wool under these conditions.

Thus, though no generalizations should be made from data obtained with one dye, and though we believe that the spent dye liquors, freshly dyed fabrics, and finished fabrics should be further tested, the present results suggest that in one case where nearly all of the dye is absorbed by the wool not only do additional mutagens appear not to be formed during dyeing, but most, if not all, of the mutagenic constituent(s) originally present either decomposed or was taken up by the wool fabric during dyeing.

Although our findings are at present limited, they raise significant questions about possible mutagenic hazards associated with dye production and use. About one-third of the dyes tested contained measurable mutagenic constituents. Consequently, exposure to these dyes probably should be minimized until any actual hazards from their use can be accurately defined.

Exhaustion of dyes (*4,10–16*) and flameproofing (*17*) and mothproofing (*18*) agents in the dyeing process are often less complete than in the one case we tested. If the dye or mutagenic impurities were to escape hydrolysis or decomposition during dyeing and remain in the spent dye liquor effluents, they could present a mutagenic hazard. More likely, unbound dye in the fabric or in the effluent is in the hydrolyzed form and may have been inactivated. Similarly, dye bound to the fabric is no longer in its original reactive form. Nevertheless, possible mutagenicity associated with the final dyed textile product to be worn by the consumer deserves further study. Finally, epidemiological studies of dye-exposed workers may also help define the importance of this problem.

Acknowledgment

It is a pleasure to thank Dorris P. Frederick and John F. Ash for excellent technical assistance.

Literature Cited

(1) Kay, K. *Text. Chem. Color.* **1977**, *9*, 275.

(2) Kay, K. *Text. Chem. Color.* **1978**, *10*, 47.

(3) Tesoro, G. C., presented at Symposium on "Recent Advances in Textile Dyeing and Finishing," American Chemical Society Meeting, Miami, FL, September 1978, Abstracts CELL 30.

(4) Peters, R. H. "Textile Chemistry"; Elsevier: Amsterdam, 1975; pp 582–648.

(5) Beech, F. W. "Fiber-Reactive Dyes"; SAF International: New York, 1970.

(6) Elliott, R. L. *J. Soc. Dyers Colour.* **1976**, *92*, 303–5 and references cited there.

(7) Kashwigi, K. M. *Bull. Chem. Soc. Jpn.* **1976**, *49*, 1236–9.

(8) Ames, B. N.; McCann, J.; Yamasaki, E. *Mutat. Res.* **1975**, *31*, 347–64.

(9) McCann, J.; Choi, E.; Yamasaki, E.; Ames, B. N. *Proc. Natl. Acad. Sci. U.S.A.* **1975**, *72*, 5135–9.

(10) Baumgarte, U. *Melliand Textilber.* **1962**, *43*, 1297–303.

(11) Bühler, A.; Hurter, R.; Mäusezahl, D.; Petipierre, J. C. *Proc.—Int. Wool Text. Res. Conf., 5th, 1975* **1976**, *5*, 263–72.

(12) Lewis, D. M. *Wool Sci. Rev.* **1974**, *49*, 13–31.

(13) Mäusezahl, D. *Textilveredlung* **1970**, *5*, 839–45.

(14) Mosimann, W. *Text. Chem. Color.* **1969**, *1*, 182–9.

(15) Rouette, H. K.; Wilshire, J. F. K.; Yamase, I.; Zollinger, H. *Text. Res. J.* **1971**, *41*, 518–25.

(16) Venkataraman, K. "The Chemistry of Synthetic Dyes"; Academic Press: New York, 1972; Vol. VI.

(17) Friedman, M. In "Flame-Retardant Polymeric Materials"; Lewin, M., Atlas, S. M., Pierce, E. M., Eds.; Plenum Press: New York, 1977; Vol. 2, 229–84.

(18) Friedman, M.; Ash, J. F.; Bry, R. E.; Simonaitis, R. A. *J. Agric. Food Chem.* **1979**, *27*, 331–6.

(19) Snedecor, G. W.; Cochran, W. G. "Statistical Methods"; 6th ed.; The Iowa State University Press: Ames, IA, 1967.

Received for review November 26, 1979. Accepted May 30, 1980.

Aromatic Amines in and near the Buffalo River

Charles R. Nelson and Ronald A. Hites*

School of Public and Environmental Affairs and Department of Chemistry, Indiana University, 400 East Seventh Street, Bloomington, Indiana 47405

■ Three sediment samples taken from the Buffalo River and two soil samples taken near its bank have been analyzed for 2-propanol-extractable, basic organic compounds by using GC/MS. Eleven aromatic amines related to the commercial production of malachite green and crystal violet were identified in both the sediment and soil samples. Apparently a dye manufacturing plant used this part of the river bank as a dump, and several of its waste chemicals were leached into the river. It is possible that the compounds reported here are, at least partially, responsible for tumors observed in fish taken from this river.

The Buffalo River in Buffalo, NY, has had many pollution problems resulting, at least in part, from the discharge of wastes by several industries located on the river. As a consequence of both chemical and domestic sewage pollution, this river has been classified as one of the most heavily polluted bodies of water in the United States (*1*). Recently, it was reported that several bottom-feeding species of fish obtained from the Buffalo River exhibited a high incidence of proliferative tissue lesions (*2*) and that sediments from the Buffalo River contained highly mutagenic compounds (*2, 3*). These latter data, which were the result of Ames bacterial mutagenesis assays, revealed a strong correlation between the level of mutagenic activity of sediment extracts and the proximity of the sampling sites to a dye manufacturing plant (*2, 3*). In addition, several aromatic amines (including 1-naphthylamine) which were formerly produced by this dyestuff manufacturer have been detected in fish obtained from the Buffalo River (*4*).

Although these data suggest a possible link between the activities of the dyestuff manufacturer and the mutagenic materials present in the river sediment, the specific identities and origins of the mutagenic compounds in the sediment remain points of considerable uncertainty and interest. This paper describes the identification of the 2-propanol-extractable, basic organic compounds present in soil and river sediment obtained near this dye manufacturing plant and discusses the environmental implications of the results.

Experimental Section

Sampling Procedure and Storage. Sediment samples were collected in midchannel by using an Eckman dredge during June 1979 at the sampling locations shown in Figure 1. One-quart, precleaned, glass jars were used for the sediment samples. The jars were covered with aluminum foil before replacement of the screwcap lids and were refrigerated until analyzed. Soil samples were collected in 1978 and were kept frozen until analyzed.

Extraction. The sediment samples (140–150 g) and defrosted soil samples (15–20 g) were Soxhlet extracted with 2-propanol (500 mL) for 24 h. The extracting solvent was removed under vacuum, and the residue was redissolved in methylene chloride. Preliminary studies revealed that the sediment extracts were heavily contaminated with aliphatic hydrocarbons. Consequently, the basic compounds were separated by extracting the methylene chloride solution (150 mL) with 1.0 N H_2SO_4 (100 mL). The acidic extract was made basic (pH 12) with aqueous NaOH and extracted with ethyl acetate (2 × 100 mL). The combined ethyl acetate extracts were dried over anhydrous $MgSO_4$ and concentrated under reduced pressure. All solvents were of nanograde quality purchased from Mallinckrodt.

Instrumentation and Analysis. Preliminary gas-chromatographic analysis of the sample extracts was performed on a 2-mm i.d., 0.25-in. o.d., 6-ft glass column packed with 3% OV-17 on 80/100 mesh Supelcoport. The column was temperature programed from 70 to 310 °C at 8 °C/min in a Hewlett-Packard 5720A gas chromatograph equipped with a flame ionization detector. Gas-chromatographic mass spectrometry was performed on a Hewlett-Packard 5982A quadrupole mass spectrometer operated under computer control. Electron-impact mass spectra were obtained at 70 eV ionizing energy by continuously scanning a mass range of 50–600 amu every 4 s. The GC conditions described above were also used for packed column GC/MS. A 10-m, high-resolution, glass capillary column coated with SP 2100 (0.25-mm i.d.) and directly interfaced to the mass spectrometer was also utilized in the analyses. The capillary column was temperature programmed from 70 to 260 °C at 4 °C/min.

Results and Discussion

Since it is very difficult to show all of the chromatographic and mass spectral data on which the identifications are based, example data only will be presented here. Figure 2 is the mass spectrum of the most abundant of the identified compounds, bis(4-dimethylaminophenyl)phenylmethane (see Figure 3, compound 8 for its structure). This spectrum is typical of most compounds seen in this study. The major mass spectral features are (a) intense singly and doubly charged molecular ions at *m/e* 330 and 165, (b) ions due to the loss of the unsubsti-

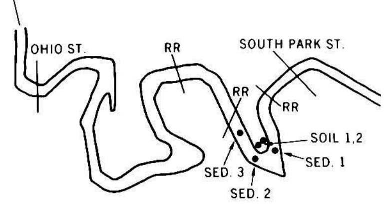

Figure 1. Map of the Buffalo River (New York, USA) showing the sampling sites. The locations of the Ohio and South Park Street bridges and three railroad bridges are marked.

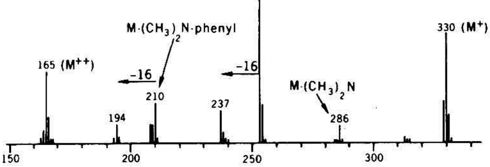

Figure 2. Mass spectrum of a major component of the 2-propanol-extractable, basic compounds isolated from a sediment sample. It was subsequently identified as that of bis(4-dimethylaminophenyl)phenylmethane (see compound **8**, Figure 3 for its structure).

0013-936X/80/0914-1147$01.00/0 © 1980 American Chemical Society

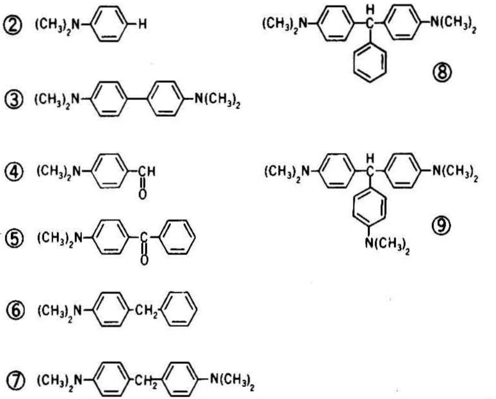

Figure 3. Structures of some of the compounds found in and near the Buffalo River. Compound numbers refer to Table I.

tuted phenyl ring (M − 77 at *m/e* 253) and the *N,N*-dimethylamino substituted phenyl ring (M − 120 at *m/e* 210), and (c) ions due to the loss of 16 amu (presumably CH_3 and H) from the M − 77 and M − 120 ions to give ions at *m/e* 237 and 194.

The positions of substituents on ring systems cannot always be assigned on the basis of mass spectrometry alone. In this case, we have assigned the position of the *N,N*-dimethylamino groups to the 4 position in all structures (see Table I). We have based this assignment not on mass spectral features but rather on the known synthetic chemistry of the dye-manufacturing industry.

The compounds identified in the sediment and soil samples are listed in Table I along with their approximate concentrations which are not corrected for extraction efficiencies and, thus, represent minimum values. All compound identifications were confirmed by comparison of the mass spectra and exact gas-chromatographic retention times with those of authentic reference compounds. The structures of several of the compounds listed in Table I are given in Figure 3. Since the Buffalo River is dredged annually (the previous dredging took place during the fall of 1978), the concentration data in Table I reflect only the accumulation of these chemicals during the 7–8-month period following the dredging.

Most of the compounds found in these soil and river sediment samples are either starting materials, intermediates, byproducts, or products associated with the commerical synthesis of two dyes: malachite green and crystal violet. Compound **9** is the leuco base of crystal violet, and compound **8** is the leuco base of malachite green. Both of these leuco bases are produced by the condensation, under acidic conditions, of *N,N*-dimethylaniline with compounds of the form

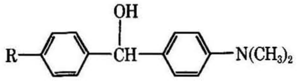

R = H or $(CH_3)_2N$

These are, in turn, formed from the reaction of *N,N*-dimethylaniline with the appropriately substituted benzaldehyde. Although these diphenyl carbinols were not observed in the soil or sediment samples, compounds formed by both their reduction (compounds **6** and **7**) and their oxidation (compound **5**) were identified. Of the other compounds, clearly compounds **1**, **2**, **4**, and **12** are starting materials for this synthesis. The remaining compounds are either other products of the dyestuff plant (1-naphthylamine and *N*-ethyl-*N*-phenylbenzylamine) or common industrial chemicals (compounds **13** to **16**).

The high concentrations and close structural similarity of the various aromatic amines present in the soil samples suggest that this particular site may have been used as a chemical dump by the dyestuff manufacturer. In fact, production information indicates that a variety of triarylmethane dyes and leuco dyes bases were produced by this plant (*5*). The close proximity of the soil sampling sites to the Buffalo River and the similarity in structure and concentration ratios of several of the aromatic amines present in both the soil and sediment samples suggest that these compounds may have entered the water and sediment of the Buffalo River via leaching from the chemical dump. We should point out that both 1-naphthylamine and *N*-ethyl-*N*-phenylbenzylamine

Table I. Compounds Found in Soil and Sediment from Buffalo River, New York

compd no.	compd name	concn,ᵃ ppm: sediment 1	sediment 2	sediment 3	soil 1	soil 2
	Aromatic Amines					
1	aniline	ND	ND	ND	5	ND
2	*N,N*-dimethylaniline	ND	ND	ND	10	40
3	4,4′-bis(dimethylamino)biphenyl	0.004	ND	0.01	200	400
4	4-(dimethylamino)benzaldehyde	ND	ND	ND	ND	20
5	4-(dimethylamino)benzophenone	ND	ND	0.02	300	300
6	4-(dimethylamino)diphenylmethane	ND	ND	ND	20	20
7	bis(4-dimethylaminophenyl)methane	0.1	0.2	0.1	ND	20
8	bis-(4-dimethylaminophenyl)phenylmethane	0.1	0.1	0.1	1000	2000
9	tris(4-dimethylaminophenyl)methane	ND	ND	ND	ND	2000
10	1-naphthylamine	0.08	0.06	0.007	ND	ND
11	*N*-ethyl-*N*-phenylbenzylamine	0.07	ND	ND	ND	ND
	Other Compounds					
12	benzaldehyde	ND	ND	ND	4	ND
13	nitrobenzene	ND	ND	ND	8	ND
14	2,4-dinitrotoluene	ND	ND	ND	ND	50
15	2,6-dinitrotoluene	ND	ND	ND	ND	50
16	trichlorobenzenes	ND	ND	ND	10	40

[a] ND = not detected.

Table II. Dose-Dependent Mutagenicity of Two Compounds Found in the Buffalo River

	concn, μg/mL	10^5 × IMF[a]
4-(dimethylamino)benzophenone	25	18
	50	22
	75	41
	100	49
4-(dimethylamino)benzaldehyde	100	31
	300	40
	1000	79
background		13 ± 1
benzo[*a*]pyrene	20	200 ± 50

[a] IMF = induced mutant fraction; see ref *6* for details. All compounds were assayed in the presence of Aroclor-induced postmitochondrial supernatant.

are present in substantial amounts in the sediment (see Table I) and that both have previously been detected in fish obtained from the Buffalo River (*4*).

Compounds **3, 4, 5,** and **8** were bioassayed to determine their individual mutagenic activity by using a quantitative forward bacterial mutagenesis assay described elsewhere (*6, 7*). Benzo[*a*]pyrene was run as a positive control in each mutation assay. Only compounds producing an induced mutant fraction at least twice background were considered to give a positive mutagenic test. Both 4-(dimethylamino)benzophenone and 4-(dimethylamino)benzaldehyde induced significant mutation to 8-azaquanine resistance in *S. typhimurium* (see Table II). These two compounds have up to 5% of the activity of benzo[*a*]pyrene on a weight basis.

The following scenario emerges from these chemical and biological data. Over several years, this dyestuff manufacturing plant used the Buffalo river bank as a dump for experimental or failed dye production batches. Leaching and runoff from this dump have transferred many of the dye-related chemicals into the Buffalo River and its sediment. In the river, fish have been exposed to these compounds by direct contact with contaminated sediment. Since some of these compounds could be mutagenic or carcinogenic, it is not unreasonable to assume that the chemicals originally derived from the dyestuff manufacturer's dump are at least partially responsible for the tumors observed in fish taken from this river.

Acknowledgment

We thank W. Zapisek (Canisius College) for providing the soil samples and J. Spagnoli (New York State Department of Environmental Conservation) for help in obtaining the sediment samples. We also thank W. G. Thilly and B. M. Andon for the bioassay experiments.

Literature Cited

(1) Kraybill, H. F. *Prog. Exp. Tumor Res.* **1976,** *20,* 34.
(2) Black, J. J.; Holmes, M.; Dymerski, P. P.; Zapisek, W. F. In "Hydrocarbons and Halogenated Hydrocarbons in the Aquatic Environment", Afghan, B. K., Mackay, D., Eds.; Plenum Press: New York, 1980; p 559.
(3) Paigen, B.; Braun, M.; Steenland, K.; Holmes, E.; Cohen, H., Roswell Park Memorial Institute, Buffalo, NY, private communication, 1980.
(4) Diachenko, G. W. *Environ. Sci. Technol.* **1979,** *13,* 329.
(5) "1974 Directory of Chemical Producers, United States"; Stanford Research Institute: Menlo Park, CA, 1974.
(6) Skopek, T. R.; Liber, H. L.; Kaden, D. A.; Thilly, W. G. *Proc. Natl. Acad. Sci. U.S.A.* **1978,** *75,* 4465.
(7) Krishnan, S.; Kaden, D. A.; Thilly, W. G.; Hites, R. A. *Environ. Sci. Technol.* **1979,** *13,* 1532.

Received for review January 4, 1980. Accepted June 16 1980. This work has been supported by the U.S. Environmental Protection Agency (Grant No. 806350).

CORRESPONDENCE

SIR: The work of Rollins and Homolya (*1*) has been noted with great interest. The levels of chlorides that were found come as no surprise, as I had personally been involved in the early studies of Carotti and Kaiser (*2*).

Rollins and Homolya have estimated ambient levels of HCl aerosol and suggest a secondary transformation possibility in which some of the HCl might be transformed into ammonium chloride. The presence of the latter species has been previously reported by Cunningham et al. (*3*) and Hindman et al. (*4*). Each of these studies found the presence of ammonium chloride concurrent with ammonium sulfate. Hindman et al. (*4*) found relatively few particles that were only sodium chloride; most of the particles consisted of many elements and compounds, including sulfur forms.

For the most part, the role of HCl in the atmosphere has all but been ignored. Most investigators discount the direct emission of HCl associated with the burning of fossil fuels, although in oil the amount of available chloride for emission can be linked not only to that inherent in the fuel but also to the amount of excess water in the fuel. The latter is related to sea water, most probably the residual of tanker ballast or wash water, and can be highly variable.

The creation of HCl in the atmosphere is generally assumed to be a breakdown of sea salt (NaCl) by photooxidation with nitrogen dioxide (*5, 6*) along with aldehydes (*12*) or through sulfate reactions (*6, 7*). A more complex relationship is projected by Yue and Mohnen (*8*) for the production of HCl in clouds. They show that the amount of HCl released from an aqueous system depends, in part, on the ambient concentrations of SO_2, NH_3, and H_2SO_4, as well as the liquid water content available in the cloud. The production of HCl increases with the amount of SO_2 available but is limited by the increase of NH_3. This suggests a competition between HCl and sulfate for the available NH_3 as is also implied by Cunningham et al. (*3*) and Brosset et al. (*7*).

The production of HCl in an aqueous acidic system is based on the fact that SO_2 can be absorbed and converted to SO_4^{2-}. As the concentration of SO_4^{2-} increases either through production or evaporation, the solution vapor pressure will approach that of sulfuric acid. Since the vapor pressure of sulfuric acid is less than that of hydrochloric acid, as the reduction proceeds past the equilibrium point between the two, HCl will be driven from the system (followed by nitric acids, if present). Whether or not the system is driven to total HCl depletion is not now relevant. However, the important question to be answered is what happens to the HCl aerosol so produced in accordance with the scenario or by direct emission from combustion sources.

Rollins and Homoloya (*1*) have suggested a transformation of HCl into ammonium chloride. This suggests a complex role for HCl that relates directly to the creation of strong acid aerosols and aqueous sites suitable for the conversion of SO_2

to sulfates and sulfuric acid premised on the fact that most chlorides are deliquescent.

Twomey (*9*) and Orr et al. (*10, 11*) have investigated changes that occur with various deliquescent compounds. They developed a methodology to predict the relative humidity necessary to change a dry particle into a liquid aerosol and the size changes that will result. They also predicted the point at which such liquid aerosols would revert to solids. Hindman et al. (*4*) have observed growth and aerosol size distribution alterations, which they attributed to deliquescent particles. Fenton and Ranade (*13*) indicated that aerosol growth promoted by the presence of HCl in a humid system may be attributable to the hygroscopic properties of HCl vapor.

With deliquescence as a key, a cycle is hypothesized as follows:

$$\begin{gathered}\text{nondeliq. metallic oxide} + \mathrm{HCl} \rightarrow \\ \text{deliq. metallic chloride} + \mathrm{H_2O} \rightarrow \\ \text{deliq. metallic chloride} + \mathrm{H_2O} + \mathrm{SO_2} + \mathrm{O_2} \rightarrow \\ \text{metallic ion} + \mathrm{H_2SO_4} + \mathrm{SO_4}^{2-} + \mathrm{HCl} + \mathrm{H_2O} \rightarrow \\ \text{metallic sulfate} + \mathrm{H_2SO_4} + \mathrm{HCl} + \mathrm{H_2O}\uparrow \rightarrow \\ \text{metallic sulfate} + \mathrm{H_2SO_4} + \mathrm{HCl}\uparrow \rightarrow \\ \downarrow \mathrm{HCl} + \text{nondeliq. metallic oxide} \rightarrow\end{gathered}$$

A number of statements can be made relative to this hypothesis and its implications:

- The creation of mixed acid solutions with significantly low vapor pressure will result in the effervescence of free hydrochloric and possibly nitric acids.
- Chlorides through their deliquescent property will generate acidic liquid film particulates and liquid aerosols in all size ranges that are conducive to the absorption of SO_2 with subsequent conversion of sulfites to sulfuric acid, which may in due course lead to the effervescence of HCl.
- Hydrochloric acid absorbed in sufficient abundance in a metallic solution can create a deliquescent droplet that can, upon absorbing atmospheric water vapor, provide sites conducive to later formation of strong low vapor pressure acids.
- Hydrochloric acid impinging on the surface of dry particulate can begin to dissolve its substrate, convert to a deliquescent particle, absorb water vapor, and provide an environment conducive to the formation of strong low vapor pressure acids.
- The atmospheric recyclability role hypothesized for HCl gave it characteristics of a catalyst for the formation of atmospheric sulfuric acid and sulfate compounds.

Since the recycling of HCl is an ongoing process requiring moisture and excess SO_2, it is not restricted by distance from a single known source. It may reach an equilibrium at any time and begin again when the equilibrium is upset. Thus, by the hypothesized role of recyclability, a relatively small amount of chloride or HCl would have a disproportionate effect. Perhaps HCl may be the missing link in the formation of sulfate species in the atmosphere. It is an aspect that should be considered.

Response to this hypothesis would be appreciated.

Literature Cited

(1) Rollins, R., Homolya, J. B., *Environ. Sci. Technol.*, **13**, 1380–3 (1979).
(2) Carotti, A. A., Kaiser, E. R., *J. Air Pollut. Control Assoc.*, **22**(4), 248–53 (1972).
(3) Cunningham, P. T., Johnson, S. A., Yang, R. T., *Environ. Sci. Technol.*, **8**, 131–4 (1974).
(4) Hindman, E. E., Hobbs, P. V., Radke, L. F., *J. Air Pollut. Control Assoc.*, **27**(3), 224–9 (1977).
(5) Robbins, R. C., Cadle, R. D., Eckhardt, D. L., *J. Meteor.*, **16**(1), 53–6 (1959).
(6) Cadle, R. D., *J. Colloid Interface Sci.*, **39**(1), 25–31 (1972).
(7) Brosset, C., Andreasson, K., Ferm, M., *Atmos. Environ.*, **9**(6/7), 631–42 (1975).
(8) Yue, G. K., Mohnen, V. A., "Proceedings of the 1st International Symposium on Acid Precipitation and the Forest Ecosystem," USDA, Forest Service, General T.R. NE-23, 1976, PB 258 645, pp 181–203.
(9) Twomey, S., *J. Meteor.*, 11(4), 334–8 (1954).
(10) Orr, C., Hurd, F. K., Corbett, W. J., *J. Colloid Sci.*, **13**, 472–82 (1958).
(11) Orr, C., Hurd, F. K., Hendrix, W. P., Junge, C., *J. Meteor.*, **15**(2), 240–2 (1958).
(12) Hanst, P. L., Gay, B. W., *Environ. Sci. Technol.*, **11**, 1105–9 (1977).
(13) Fenton, D. L., Ranade, M. B., *Environ. Sci. Technol.*, **10**, 1160–2 (1976).

Edward J. Kaplin

York Research Corporation
One Research Drive
Stamford, Conn. 06906

☐ True, or
☐ False:

Computers have a definite place in your laboratory.

TRUE. And the American Chemical Society helps to answer your questions on choosing the right computer system for your laboratory.

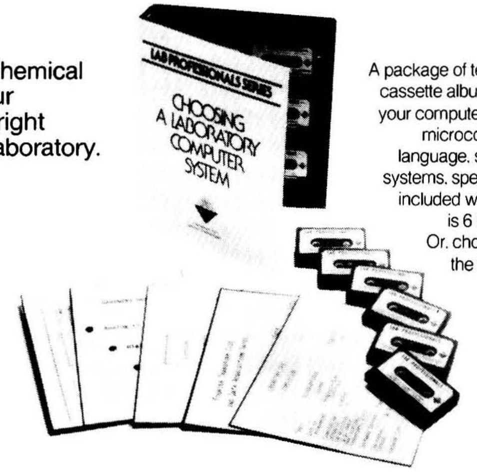

A package of ten tape recordings bound in a handsome cassette album provides information for you to analyze your computer needs in the lab. Lab pros discuss both microcomputer and minicomputer capabilities in language, storage, ability to communicate with other systems, speed, and costs. Nearly 200 illustrations are included with the full cassette package. Playing time is 6 hours. Total package price is only $99.95. Or, choose one tape for $11.95. **To order,** fill out the form below or call toll free **800-424-6747.**

Here are the 10 tapes included in the **Choosing a Laboratory Computer System** symposium collection:

☐ **Networks and Languages,** R.E. Dessy, Virginia Polytechnic Institute and State University. Architecture, physical and logical interconnect for a small computer network based on minicomputers communicating to one or more host computers is described. 49 Illustrations. $11.95

☐ **Minicomputer Based Lab Data Systems,** Charles L. Wilkins, University of Nebraska-Lincoln. Minicomputers versus microcomputers: factors for making the choice, advantages and trade-offs. 17 Illustrations. $11.95

☐ **Microcomputers as Components For Instrument Construction,** J.T. Arnold, Varian Associates, Inc. Examples of packaged microcomputers in terms of specification, interconnection, and programming protocols. 21 Illustrations. $11.95

☐ **Data System For a Separations Group,** P. Riggio, Hoffman-LaRoche, Inc. 33 Illustrations. $11.95

☐ **Microcomputer Systems in the Lab,** Daniel J. Macero, Syracuse University. Microcomputers ranging from single to sophisticated general purpose systems. 9 Illustrations. $11.95

☐ **Personal Computers in the Lab,** G.S. Owen, Atlanta University. Apple II microcomputer system for data acquisition interfaced to several instruments. 20 Illustrations. $11.95

☐ **Desirable Properties of Real Time Lab Languages,** T.H. Ridgway, University of Cincinnati. 21 Illustrations. $11.95

☐ **Development of a Distributed Lab Data Reduction Network Using Desktop Computers,** W.C. Fischer, CIBA-GEIGY Corporation. 22 Illustrations. $11.95

☐ **Criteria for Selecting a Lab Microcomputer System,** E.B. Buchanan, Jr., University of Iowa. Attention is given to small user groups with limited electronic support facilities. 7 Illustrations. $11.95

☐ **Planning for Growth In Choosing a Lab Computer System,** Jackson B. Sosebee, Jr., Environmental Science and Engineering, Inc. Check list includes: language, storage capacity, ability to communicate with other systems, number of input ports, printer capabilities, lab personnel and data coding procedures. 6 Illustrations. $11.95

To order entire symposium including cassette album and illustrations for $99.95, check the box below. Or, check the individual tapes of your choice. Send payment along with this ad to: **American Chemical Society,** *Department 722,* 1155 Sixteenth Street, N.W., Washington, D.C 20036. A 10% discount is given if payment accompanies order. VISA and Mastercharge are accepted. California residents add 6% state use tax. Prices include postage and handling.

☐ **Entire Symposium** ☐ **Payment Enclosed** ☐ **Invoice Me**

☐ Invoice Company/Purchase Order # ____________
☐ Master Charge Interbank Code ____________
☐ Visa Account Number ____________
Expiration Date ____________

Signature ____________
Name ____________
Company ____________
Address ____________
Billing Address ____________
City ____________ State ____________ Zip ____________

(Allow 3-5 weeks for delivery) **(Released 1980)**

Air Quality Services

In Service North of the Arctic Circle

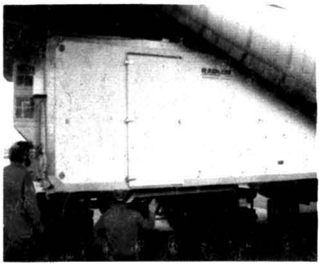

Loading onto a C-130 Hercules for Shipment Overseas

Radian air and meteorological monitoring systems have faced a broad spectrum of climatological and operational challenges. Only meticulous planning based on seven years of monitoring experience could have produced continuous data acquisition under these trying conditions. For example, it would have been impossible to conduct a successful air quality monitoring program on the Alaskan North Slope without innovative approaches to design, delivery and operation.

Continuous Monitoring During Spring Floods on the Upper Mississippi

Radian is an experienced professional services firm with the resources to provide a wide range of air quality services and the flexibility to meet specific client needs. The full range of Radian's air quality services includes:

- Monitoring
- Data Management
- Quality Assurance
- Dispersion Modeling
- Permit Acquisition Assistance
- Control Technology Assessment

Radian Corporation offers a variety of systems and services which permits clients to choose the most cost-effective monitoring approach.

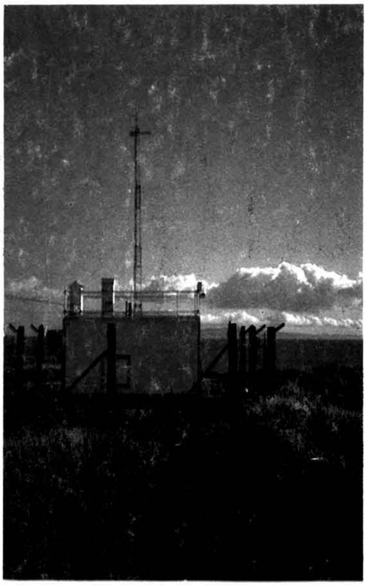

Monitoring for Utility on Maui, Hawaii

Remote Inquiry for Data Reporting

Louisiana Gulf Coast Installation

Meteorological Monitoring in Iowa

The Radian DART is a proven computer system which offers real-time data processing, remote inquiry and instrument calibration.

Echosonde® - Acoustic Sounding at High Noon in Prudhoe Bay, Alaska

Radian Corporation now enters its twelfth year of responsive service to its clients. To discuss your requirements and the ability of the Radian staff to meet your needs, please call or write: Mr. Lou Fowler
P.O. Box 9948
Austin, Texas 78766
512/454-4797

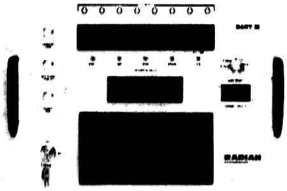

DART II Computer System

RADIAN CORPORATION

8500 Shoal Creek Blvd.. Austin, Texas 78766

Austin / Washington, D.C. / Research Triangle Park /
Salt Lake City / Houston / Sacramento

CIRCLE 16 ON READER SERVICE CARD